GASIFICATION OF BIOMASS AND SOLID RECOVERED FUELS (SRFS) FOR THE SYNTHESIS OF LIQUID FUELS

Javier Recari Ansa

Javier Recari Ansa

Gasification of biomass and solid recovered fuels (SRFs) for the synthesis of liquid fuels

DOCTORAL THESIS

UNIVERSITAT ROVIRA i VIRGILI
2017

Javier Recari Ansa

Gasification of biomass and solid recovered fuels (SRFs) for the synthesis of liquid fuels

DOCTORAL THESIS

Supervised by

Dr. Xavier Farriol Roigés

Dr. César Berrueco Moreno

UNIVERSITAT ROVIRA i VIRGILI
2017

UNIVERSITAT ROVIRA i VIRGILI

Departament d'Enginyeria Química

Av. Països Catalans, 26

43007 Tarragona, Spain

I STATE that the present study, entitled "Gasification of biomass and solid recovered fuels (SRFs) for the synthesis of liquid fuels", presented by Javier Recari Ansa for the award of the degree of Doctor, has been carried out under my supervision at the Department of Chemical Engineering of this university.

Tarragona, 2nd June 2017

Doctoral Thesis Supervisors

Dr. Xavier Farriol Roigés

Dr. César Berrueco Moreno

AGRADECIMIENTOS

Por fin puedo escribir estas palabras. Después de varios años trabajando en esta tesis, no puedo hacer otra cosa que dar las gracias a todas las personas que se han interesado por mí y por este proyecto.

Primero de todo, como no, agradecer a mis dos directores de tesis, Xavier Farriol y César Berrueco, su apoyo y disponibilidad siempre que lo he necesitado. En especial a César, con quien he compartido tantas horas y me ha enseñado tanto (de verdad, vaya paciencia tienes). Gracias por todo, con vosotros este camino ha sido menos complicado.

A Daniel Montané, por darme la oportunidad de participar en el proyecto de SYN3 y, por lo tanto, acabar haciendo el doctorado y conocer a todas las personas que han formado parte de IREC Tarragona. Grandes investigadores y currantes como vosotros: Sònia Abelló, Carles Torras, Joan Salvadó, Ester Clavero, Esther Lorente... siempre me acordaré de los congresos en los que hemos estado y de esas comidas dentro y fuera del horario laboral (*visca el kebab de la Ribera!*). Gracias también al resto de compañeros que han pasado por el N5, como Claudia Nurra, Maria Rey, Marlene Barrera, Detta, David Waddicor, Lídia Arce, etc. Y a los que siguen, como Francesc Valls y Elena Fuentes. Espero no olvidarme a alguien, pero si lo he hecho, lo siento, también estás incluido en el etcétera anterior.

Thank you a todos los que he conocido a lo largo de estos años, compañeros de clase, de congresos y de doctorado. Ánimo, Monika Haponska y Jordi Plana, ¡vosotros sois los siguientes en defender la tesis!

Por último, a los que siempre han estado allí. Mi familia y mis amigos, que tanto se han preocupado por cómo llevaba la tesis y siempre me han dado ánimos y deseado lo mejor.

Esta tesis se la dedico a mis padres, por muchas cosas, pero también porque han sufrido a su manera la espera de que acabara el doctorado.

Mit freundlichen Grüßen,

Javier

TABLE OF CONTENTS

LIST OF FIGURES IX

LIST OF TABLES XIII

NOMENCLATURE XV

SUMMARY XVII

1. Introduction and scope 1

1.1 Introduction 1

1.2 General objectives 2

1.3 Biomass and waste 3

1.4 Conversion processes 4

1.5 Thermochemical conversion 5

1.5.1 Pyrolysis 6

1.5.2 Torrefaction 8

1.5.3 Combustion 9

1.5.4 Gasification 9

1.5.4.1 Gasification reactors 11

1.5.4.2 Gasification reactions 13

1.5.4.3 Gasification inputs and outputs 15

1.6 An overview on biomass and waste gasification advances 21

1.6.1 Gasification plants 24

1.7 References 26

2. Materials and methods 35

2.1 Introduction 35

2.2 Feedstocks 35

2.2.1 Biomasses 35

2.2.2 Municipal solid waste fractions 36

2.3 Bed materials 38

2.4 Experimental equipment 39

2.4.1 Gasification system rig 39
2.4.1.1 Fluidized bed reactor 39
2.4.1.2 Furnace 41
2.4.1.3 Solid and gas feeding system 41
2.4.1.4 Gas cleaning system 42
2.4.2 Gas and tar analyses 43
2.4.2.1 Major gas composition 43
2.4.2.2 Minor contaminants analysis 43
2.4.2.3 Tar analysis 47
2.4.3 Other equipment 48
2.5 Experimental procedure 49
2.5.1 Operational observations and modification of the experimental setup 50
2.5.1.1 Solid feeding system 50
2.5.1.2 Fluidized bed reactor 51
2.6 Data analysis 52
2.6.1 Fluidizing velocity and gas residence time 53
2.6.2 Equivalence ratio (ER) 53
2.6.3 Mass balances 53
2.6.4 Solid fuel and gas heating value 54
2.6.5 Carbon conversion 54
2.6.6 Minor contaminants concentration 55
2.6.7 Error estimation of experimental data 56
2.7 References 56
3. Pressurized gasification of torrefied woody biomass 57
3.1 Introduction 58
3.2 Experimental 60
3.2.1 Sample characterization and preparation 60
3.2.2 Setup and procedure for torrefaction 61
3.2.3 Fluidized bed gasifier 62
3.2.3.1 Experimental procedure 62
3.2.4 Gas and tar analysis 63
3.3 Results and discussion 66

3.3.1 Fuel characterization of the raw and torrefied materials 66
3.3.1.1 Proximate analysis 66
3.3.1.2 Ultimate analysis 66
3.3.1.3 O/C and H/C ratios 67
3.3.1.4 Heating value 68
3.3.2 Bench-scale fluidized bed gasification of torrefied biomass 68
3.3.2.1 Product yields 68
3.3.2.2 Gas composition 71
3.3.2.3 Tar characterization 74
3.3.2.4 Effect of experimental parameters on gasification performance 79
3.3.2.5 Overall torrefaction-gasification efficiency: 81
3.4 Conclusions 83
3.5 References 84
4. Solid recovered fuel (SRF) gasification: effect of temperature and equivalence ratio 89
4.1 Introduction 90
4.2 Materials and methods 91
4.2.1 Sample characterization and preparation 91
4.2.2 Fluidized bed gasifier 93
4.2.3 Gas and tar analysis 93
4.3 Results and discussion 95
4.3.1 Product yields and syngas composition 95
4.3.1.1 Effect of gasification temperature 95
4.3.1.2 Effect of equivalence ratio: 97
4.3.2 Tar concentration 98
4.3.3 Evolution of HCl, HCN, NH_3 and H_2S in the producer gas 101
4.3.4 Effect of experimental parameters on gasification performance 106
4.3.4.1 H_2/CO ratio in the producer gas 106
4.3.4.2 Carbon conversion efficiency (X_C) 107
4.3.4.3 Syngas heating value 107
4.4 Conclusions 108
4.5 References 109

5. Gasification of two solid recovered fuels (SRFs): effect of experimental conditions 113

5.1 Introduction 114

5.2 Materials and methods 115

5.2.1 SRF samples preparation and characterisation 115

5.2.2 Bed materials 116

5.2.3 Experimental setup and procedure 116

5.2.4 Gas and minor contaminants analyses 118

5.3 Results and discussion 119

5.3.1 SRF characterisation and classification 119

5.3.2 Product yields 119

5.3.2.1 Effect of SRF 121

5.3.2.2 Effect of bed material 121

5.3.2.3 Effect of gasification agent 122

5.3.3 Gas composition 122

5.3.3.1 Effect of SRF 122

5.3.3.2 Effect of bed material. 123

5.3.3.3 Effect of gasification agent 124

5.3.4 Tar content 126

5.3.5 Evolution of minor contaminants (HCl, H_2S, HCN and NH_3) in the syngas 126

5.3.5.1 Effect of SRF 127

5.3.5.2 Effect of bed material. 129

5.3.5.3 Effect of fluidizing agent 130

5.4 Conclusions 131

5.5 References 132

6. Oxygen/steam gasification of two solid recovered fuels (SRFs): effect of bed material 137

6.1 Introduction 138

6.2 Experimental 139

6.2.1 SRF samples characterization and bed materials 139

6.2.2 Experimental setup and procedure 140

6.2.3 Analyses of gas composition, tar and minor contaminants....141
6.3 Results and discussion....142
6.3.1 SRFs characterization....142
6.3.2 Product yields....143
6.3.3 Gas composition....145
6.3.4 Tar characterization....147
6.3.4.1 Tar content....147
6.3.4.2 GC-FID analysis....148
6.3.5 Minor contaminants....151
6.4 Conclusions....155
6.5 References....156
7. Gasification of a torrefied solid recovered fuel (SRF)....161
7.1 Introduction....162
7.2 Experimental....164
7.2.1 SRF sample preparation and characterization....164
7.2.2 Torrefaction process....166
7.2.3 Gasification setup and procedure....167
7.2.4 Gas, tar and minor contaminants analyses....168
7.3 Results and discussion....169
7.3.1 Characterization of raw and torrefied samples....169
7.3.2 Gasification tests....170
7.3.2.1 Product yields....170
7.3.2.2 Gas composition....171
7.3.2.3 Tar characterization....174
7.3.2.4 Minor contaminants....178
7.3.3 Overall efficiency. Torrefaction combined with gasification....183
7.4 Conclusions....185
7.5 References....187
8. Techno-economic analysis of liquid fuel plants via biomass and SRF gasification....191
8.1 Introduction....192

8.2 Materials and methods 193
8.2.1 Biomass- and waste-to-liquids via gasification 194
8.2.1.1 Area 100: Pretreatment 194
8.2.1.2 Area 200: Gasification 194
8.2.1.3 Area 300: Syngas cleaning 198
8.2.1.4 Area 400: Fischer-Tropsch synthesis 198
8.2.1.5 Area 500: Hydroprocessing 199
8.2.1.6 Area 600: Air separation unit 199
8.2.1.7 Area 700: Power generation 199
8.2.2 Economic analysis 199
8.2.2.1 Assumptions made for the economic assessment 204
8.2.3 Sensitivity analysis 206
8.3 Results and discussion 206
8.3.1 Aspen model results 206
8.3.2 Economic results 207
8.3.3 Sensitivity analysis results 210
8.3.4 Comparison to other studies 212
8.4 Conclusions 214
8.5 References 216
9. Conclusions and future work 221
9.1 General conclusions 221
9.2 Future work 225
10. Appendix 227
10.1 Research articles 227
10.2 Oral presentations 228
10.3 Poster presentations 228

LIST OF FIGURES

Figure 1.1 Scheme of the conversion processes. Adapted from [5] 4
Figure 1.2 Scheme of the gasification process and routes. Source [32] 10
Figure 1.3 Gasifiers: a) Updraft fixed bed, b) Downdraft fixed bed, c) Bubbling fluidized bed, d) Circulating fluidized bed, e) Entrained flow 12
Figure 1.4 Evolution of tar compounds. Adapted from [50] 18
Figure 2.1. Norwegian spruce (particle size range of 250-500 µm): a) VW, b) VW-LT and c) VW-ST 36
Figure 2.2 Norwegian forest residues (particle size range of 250-500 µm): a) GROT, b) GROT-LT and c) GROT-ST 36
Figure 2.3 RT (particle size of 1 mm) for analytical and gasification tests 37
Figure 2.4 FL and FL derived samples: a) FL as received (particle size > 5 cm), b) FL milled and sieved to a particle size of 1 mm for analytical and gasification tests, c) FL torrefied at 290 ºC (FL290) and d) FL torrefied at 320 ºC (FL320) 38
Figure 2.5 Bed materials (particle size 150-200 µm): a) calcined silica sand, b) calcined dolomite, c) original olivine, d) calcined olivine 39
Figure 2.6 Picture of the laboratory-scale gasification system 40
Figure 2.7 Scheme of the gasification setup 40
Figure 2.8 Gas bubbling system 44
Figure 2.9 ISE analysis equipment. Adapted from Metrohm.com 45
Figure 2.10 Screw feeding calibration curve for different solid fuels 51
Figure 2.11 Modified fluidized bed reactor setup 52
Figure 3.1 Van Krevelen diagram for the raw and torrefied samples [◆ VW, ◆ VW-LT, ◇ VW-ST, ▲ GROT, ▲ GROT-LT, △ GROT-ST]. 68
Figure 3.2 Effect of pressure and torrefied level on gas yields (VW). Temperature 850 ºC, ER: 0.23, H_2O/Biomass: 1.6 72
Figure 3.3 Effect of pressure and torrefied level on gas yields (GROT). Temperature 850 ºC, ER: 0.23, H_2O/Biomass: 1.6 72
Figure 3.4 Effect of pressure and torrefied level on tar content (VW). Temperature 850 ºC, ER: 0.23, H2O/Biomass: 1.6 75
Figure 3.5 Effect of pressure and torrefied level on tar content (GROT). Temperature 850 ºC, ER: 0.23, H2O/Biomass: 1.6 75

Figure 3.6 Size exclusion analysis of VW tars obtained in a FBR, influence of pressure and torrefaction level 76
Figure 3.7 Size exclusion analysis of GROT tars obtained in a FBR, influence of pressure and torrefaction level..... 77
Figure 3.8 FTIR spectra of VW tars obtained in a FBR, influence of pressure and torrefaction level 78
Figure 3.9 FTIR spectra of GROT tars obtained in a FBR, influence of pressure and torrefaction level 78
Figure 3.10 Schematic diagram of the overall mass and energy balances for the combination of torrefaction and gasification processes..... 82
Figure 4.1 Effect of gasification temperature on producer gas composition (ER ~ 0.31) 96
Figure 4.2 Effect of ER on producer gas composition (T 750 ºC)..... 98
Figure 4.3 Effect of gasification temperature (ER 0.31) and ER (T 750 ºC) on tar content..... 99
Figure 4.4 FTIR spectra of tars obtained in a FBG: influence of: a) gasification temperature and b) ER.....100
Figure 4.5 Effect of gasification temperature on minor contaminants concentration in producer gas.....102
Figure 4.6 Effect of ER on minor contaminants concentration in producer gas 105
Figure 5.1 Gas composition. Effect of SRF (RT and FL) with gasification temperature (750 and 850 ºC).....122
Figure 5.2 Gas composition. Effect of SRF (RT and FL) with bed material (sand and dolomite).....124
Figure 5.3 Gas composition. Effect of RT with gasification agent (air or oxygen/steam) 125
Figure 5.4 Minor contaminants release. Effect of SRF (RT and FL) with: a) gasification temperature (ER 0.3 and sand as bed material), b) bed material (T 850 ºC and ER 0.3), c) gasification agent (T 850 ºC, ER 0.3 and dolomite as bed material) 128
Figure 6.1 Gas composition (dry basis) of oxygen/steam gasification experiments (T=850 C, ER ~0.3, Steam/SRF ~1; two SRFs (RT and FL) and three bed materials (sand, dolomite and olivine).....146
Figure 6.2 Example of a GC-FID tar chromatograph with detected peaks 148

Figure 6.3 Total tar and PAHs yields in oxygen/steam gasification experiments (T=850 ºC, ER ~0.3, Steam/SRF ~1) 149
Figure 6.4 Tar composition in oxygen/steam gasification experiments (T=850 ºC, ER ~0.3, Steam/SRF ~1) 150
Figure 6.5 Minor contaminants in oxygen/steam gasification experiments (T=850 ºC, ER ~0.3, Steam/SRF ~1) 152
Figure 7.1 Scheme of torrefaction process 166
Figure 7.2 Gas composition (dry basis) in air gasification experiments (T= 850 ºC, ER ~0.3) 172
Figure 7.3 Gas composition (dry basis) in oxygen/steam gasification experiments (T= 850 ºC, ER ~0.3 and Steam/SRF ~ 1) 173
Figure 7.4 Total tar and PAHs yields in: a) air and b) oxygen/steam gasification experiments. (T=850 ºC, ER ~0.3 and Steam/SRF ~ 1) 176
Figure 7.5 Tar composition of FL290 and FL320 air gasification experiments (T=850 ºC, ER 0.3 and bed materials: sand and dolomite) 177
Figure 7.6 Tar composition of FL290 and FL320 oxygen/steam gasification experiments (T= 850 ºC, ER ~0.3, bed materials: sand, dolomite and olivine) 178
Figure 7.7 Minor contaminants in air gasification experiments (T=850 C and ER~0.3). Data for FL experiments from [16] 180
Figure 7.8 Minor contaminants in oxygen/steam gasification experiments. (T=850 C, ER~0.3 and Steam/SRF~1). (T=850 C and ER~0.3). Data for FL experiments from [25] 182
Figure 7.9 Scheme of the mass and energy balances for the combination of torrefaction and gasification 184
Figure 8.1 Plant flow diagram for all scenarios 194
Figure 8.2 Aspen Plus flowsheet of gasification model 196
Figure 8.3 Annual operating costs (in million €2015) for biomass and SRF scenarios 209
Figure 8.4 PV sensitivity analysis for the scenarios: a) VW and b) VW-LT 211
Figure 8.5 PV sensitivity analysis for the scenarios: a) FL and b) FL320 211

LIST OF TABLES

Table 1.1 Most common process conditions and reaction products for pyrolysis, gasification and combustion. Adapted from [13] 6
Table 1.2 Pyrolysis types and operating conditions [5,16,17] 8
Table 1.3 Main reactions in a gasification process [38–40] 14
Table 1.4 Typical cleaning requirements in syngas applications. [44–46] 17
Table 1.5 Tar classes based on solubility and condensability [41,44] 19
Table 1.6 Typical levels of contaminants in syngas obtained from fluidized bed reactors 21
Table 1.7 Plants/projects based on gasification [94–98] 25
Table 2.1 Catalysts properties (as indicted by the supplier) 39
Table 2.2 Gas mixtures (% mol) used for micro GC calibration 43
Table 2.3 Characteristics of the ion selective electrode measurements 46
Table 2.4 Results of some ion interference tests 47
Table 2.5 Equipment used in for sample processing and analyses 49
Table 3.1 Main characteristics of feedstocks (as received basis) 65
Table 3.2 Experimental conditions and product yields for the gasification of the six biomass samples at 850 ºC. 69
Table 3.3 Influence of experimental conditions on gasification parameters. 80
Table 4.1 Main characteristics of feedstock (as received basis) 92
Table 4.2 Characteristics of the Ion Selective Electrode measurements 94
Table 5.1 Main characteristics of feedstock (as received basis) 117
Table 5.2 Ion selective electrodes characteristics 118
Table 5.3 Experimental conditions and product yields for the gasification of SRF samples 120
Table 6.1 Characterization of SRFs (as received basis) 143
Table 6.2 Product yields of oxygen/steam gasification experiments (T= 850 ºC, Equivalence Ratio (ER) ~0.3 and Steam/SRF ~ 1) 144
Table 7.1 Characterization and torrefaction yields of studied samples (as received basis) 165
Table 7.2 Product yields of torrefied SRFs gasification experiments. (T= 850 ºC and Steam/SRF ~ 1) 170
Table 7.3 Gasification parameters of experiments. (T= 850 ºC and Steam/SRF ~ 1) 175

Table 8.1 Characterization of feedstocks (as received basis) as reported by [24,26] 195
Table 8.2 Operational conditions, simulation and experimental results 197
Table 8.3 Base costs for major equipment 202
Table 8.4 Methodology for capital cost estimation 203
Table 8.5 Material costs and assumptions ($€_{2015}$) 203
Table 8.6 Power requirements for main units 203
Table 8.7 Sensitivity parameters 206
Table 8.8 Main plant process and economic results 208
Table 8.9 Capital investment breakdown costs for plant scenarios 209
Table 8.10 Capital costs for BTL plants based on gasification and FT synthesis 213

NOMENCLATURE

BFB	Bubbling fluidized bed
BTL	Biomass-to-liquid
CFB	Circulating fluidized bed
ER	Equivalence ratio
FBG	Fluidized bed gasifier
FBR	Fluidized bed reactor
FL	Fluff (a SRF sample)
FL320	FL torrefied at 320 ºC
FT	Fischer-Tropsch
FTIR	Fourier transform infrafred
GC	Gas chromatograph
GC-FID	Gas chromatograph with a flame ionization detector
GROT	Forest residues (a biomass sample)
GROT-LT	GROT lightly torrefied at 225 ºC
GROT-ST	GROT strongly torrefied at 275 ºC
HHV	Higher heating value
HPLC	High-performance liquid chromatography
IC	Ion chromatography
ICP-OES	inductively coupled plasma-optical emission spectroscopy
ISE	Ion-selective electrode
LHV	Lower heating value
MSW	Municipal solid waste
NMP	N-Methyl 2-pyrrolidinone
PAH	Polycyclic aromatic hydrocarbon
PS	Polystyrene
RDF	Refuse-derived fuel
RT	Rejects of trommel (a SRF sample)
SAOB	Sulphide Anti-Oxidant Buffer
SEC	Size-exclusion chromatography

SNG	Synthetic natural gas
SRF	Solid recovered fuel
TEA	Techno-economic assessment
TISAB	Total Ionic Strength Adjustment Buffer
VW	Virgin wood (a biomass sample)
VW-LT	Virgin wood lightly torrefied at 225 ºC
VW-ST	Virgin wood strongly torrefied at 275 ºC
VW-ST	VW strongly torrefied at 275 ºC
WTE	Waste-to-energy
WTL	Waste-to-liquid

SUMMARY

The European Union aims to meet several climate and energy targets in the near future by promoting the mitigation of CO_2 emissions and the generation of clean energy. In this framework, valorisation of biomass and some fractions of municipal solid waste can contribute to the growing needs for sustained energy supply.

Gasification is perceived as a promising technology for energy exploitation of biomass and waste-derived fuels (i.e. solid recovered fuels, SRFs), converting carbonaceous fuels into a synthesis gas (syngas) with multiple end-use applications, including the generation of electricity, chemicals and fuels. However, technical obstacles hinder the full implementation of this technology at industrial scale particularly for the production of liquid fuels through Fischer-Tropsch (FT) synthesis. Those challenges are mainly related to the syngas quality, such as a low H_2/CO ratio and the presence of impurities (tar and minor contaminants), and strongly depend on the nature of the feedstock and the operating conditions of the gasification process. The present work addresses these problems.

The overall objective of this thesis is to assess the feasibility of producing liquid fuels from the gasification of biomass and SRFs. A preliminary bibliographic review denoted the need of additional research, in particular to evaluate the release of tar and minor contaminants (HCl, H_2S, HCN and NH_3). Therefore, several studies were performed to determine the adequate operational conditions in order to improve the syngas quality. Besides evaluating several gasification operating conditions, the application of a thermal pretreatment (torrefaction) to the gasification feedstocks is proposed as a way to upgrade the feedstock properties and abate the emission of contaminants in the syngas.

This doctoral thesis is divided in two main blocks: gasification experiments of biomass and SRFs, and a techno-economic analysis for liquid fuel plants based on the obtained experimental results.

Gasification tests were carried out in a laboratory-scale fluidized bed reactor and several techniques were used for the characterization of the feedstocks and the analysis of the produced gas. The first experimental part deals with woody biomass gasification in order to study some of the least

investigated parameters: the influence of torrefaction and pressure. Torrefaction of woody biomass proved to enhance the gasification performance, increasing the gas quality (higher H_2/CO ratio and lower tar concentration). On the other hand, pressurized gasification showed a diminishment on the gas quality. The second part gathers several studies concerning waste gasification using SRFs as feedstocks. These studies evaluated key operating conditions (i.e. gasification temperature, equivalence ratio) and the use of bed materials (sand, dolomite and olivine) and gasification agents (air and a mixture of oxygen and steam) in order to improve the quality of the syngas. The selection of appropriate gasification conditions was crucial when dealing with SRFs, since these materials contain higher amounts of contaminants precursors than biomass. For this reason, a method was developed to assess the concentration of HCl, H_2S, HCN and NH_3 in the syngas by means of ion-selective potentiometry. The experimental results indicated that adequate conditions for SRFs gasification were: high gasification temperature (850 ºC), equivalence ratio ranging 0.30-0.35 and the combination of dolomite as bed material and oxygen-steam as gasification agent. Oxygen-steam gasification resulted in important improvements on the gasification performance despite a higher release of minor contaminants in the syngas. The last experimental part investigates the gasification of a SRF at two torrefaction levels and at different gasification conditions. The study revealed that the torrefaction pretreatment in the range of 290-320 ºC produces a relevant diminishment of HCl concentration, an important issue at industrial scale.

The final part of this work consists in a techno-economic analysis that estimates capital and production costs of FT liquid fuel plants based on biomass and waste gasification, using as input the experimental results obtained in the first block of the thesis. The results pointed out the benefits of including torrefaction in the process chain and suggested that waste gasification is a potential route for the generation of liquid fuels, with a cost that could be comparable to current diesel and gasoline prices for final users in Europe.

1. INTRODUCTION AND SCOPE

1.1 Introduction

The recent concerns about global warming and climate change have been extensively discussed among the scientific community and policy makers, motivating the use of clean and green energy sources to mitigate greenhouse gas emissions. Clear examples are the objectives set by the European Union (EU) to reduce CO_2 emissions systematically by 2020, 2030 and 2050. In the long term, by 2050, the EU aims to reduce greenhouse gas emissions by 80-95% compared to 1990 levels [1]. There is also a global increasing concern about depletion of fossil fuels, which meet nearly the 80% of world total primary energy [2] and furthermore release pollutants that boost climate change. In this context, the exploitation of renewable energy sources (i.e. solar, wind, biomass) is playing a major role. The EU aims to fulfil that at least 20% of its total energy comes from renewable sources by 2020. In fact, all EU countries must ensure that at least 10% of transportation fuels come from renewables [3]. Since transportation fuels are extremely bounded to CO_2 emissions, biomass has been identified as a potential renewable energy source for producing liquid fuels (i.e. biofuels).

Biomass is an abundant feedstock and available in different forms. Currently energy derived from biomass (i.e. bioenergy) accounts 10% world total primary energy but it is estimated to increase up to 27% by 2050 [4]. In Europe, the Renewable Energy Directive (2009/28/EC) promotes bioenergy production from various renewable sources. Some waste fractions derived from municipal solid waste (MSW) are included as possible sources. According to the European waste management hierarchy (i.e. Directive 2008/98/EC), only non-recyclable MSW fractions can be used for energy recovery. Nonetheless, most of those MSW fractions are landfilled or incinerated, mainly without energy recovery. Therefore waste-derived fuels (e.g. solid recovered fuels, SRFs) are presented as a potential source to reach the aforementioned targets.

There are several routes for the energy exploitation of biomass and waste. One of the most promising technologies is a versatile process called gasification. Gasification converts a carbonaceous material into a gas mixture (syngas) with

multiple end uses, one of them the synthesis of liquid fuels. However there are crucial aspects in gasification that still hinder the implementation of this technology at larger scale, particularly for biofuels production. Principal drawbacks include syngas cleaning (e.g. removal of contaminants) and high costs related to biomass transportation and investment expenditures.

Many of the problems associated to biomass, such as the low energy content and variation of seasonal supply, may be offset by waste-derived fuels (e.g. SRFs). However waste is a heterogeneous feedstock and its composition varies significantly depending on regions (e.g. economic development and waste management system). A thermal pretreatment such as torrefaction is an interesting approach aiming to enhance the fuel properties of several feedstocks and reduce technical limitations during gasification.

This thesis deals with the production of a cleaner syngas for liquid fuels production via gasification of biomass and SRFs.

The document is organized in the following way. Chapter 1 introduces the aim of this thesis, provides general background of solid fuels (biomass and waste) and thermochemical routes focusing on the gasification field. The second chapter (Chapter 2) describes the materials and equipment used during experimental sessions. Chapters 3-8 present the studies performed in this project. Gasification of torrefied biomass is discussed in Chapter 3, while Chapters 4-7 gather the work carried out on gasification of solid recovered fuels. Chapter 8 presents a techno-economic analysis for liquid fuels production based on gasification of the studied feedstocks. Finally, chapter 9 presents the general conclusions from the completion of this work together with possible future work in this field.

1.2 General objectives

The main goals of this doctoral thesis are:

- To improve the quality of the synthesis gas produced during gasification of solid fuels (biomass and waste fractions) with the final purpose of obtaining a cleaner syngas for the production of liquid fuels with a lower carbon footprint.

- To validate the selection of adequate operational conditions for gasification and the application of a thermal pretreatment (torrefaction) on biomass and waste fractions in order to improve the gasification performance and the quality of the synthesis gas, reducing the concentration of contaminants.
- To assess the techno-economic feasibility of liquid fuels production from the gasification of biomass and waste fractions, integrating the thermal pretreatment in the process chain.

1.3 Biomass and waste

Biomass include all organic materials derived from living and recently dead biological species (i.e. does not include fossil fuels like coal and petroleum), coming from botanical and biological sources [5]. Unlike fossil fuels, which take millions of years to develop, biomass is considered a renewable source. Generally biomass grows relatively fast through photosynthesis by absorbing carbon dioxide (CO_2) from the atmosphere. The release of CO_2 when biomass is burned does not add extra CO_2 to the planet, for this reason it is also considered carbon neutral.

Biomass comes from a diversity of sources, some examples are agricultural (bagasse, nutshells, switchgrass, straw), forest (trees), biological (aquatic species, animal waste) and secondary biomass sources, such as municipal (sewage sludge, domestic waste). However, these sources can be divided in two major groups: primary biomass (lignocellulosic such as wood, and carbohydrates such as cereals) and secondary biomass or waste (municipal, animal and agricultural waste).

In this work, lignocellulosic biomass and waste-derived fuels were used as feedstocks for energy production.

Lignocellulosic biomass is primarily the fibrous part of a plant, which is composed of three major constituents: cellulose, hemicellulose and lignin [6]. Currently, there is a growing interest in the cultivation of lignocellulosic materials for energy production (i.e. energy crops), as they grow fast and have a high energy yield per unit of land area [5].

Municipal solid waste (MSW) partially derives from renewable biomass waste (paper, food waste…) but also an important amount comes from non-

renewable components such as plastics and glass. Some of the MSW fractions that cannot be easily reused or recycled, may still have an important energy content that can be used for energy recovery. In the literature, any refuse waste fraction is referred as a refuse-derived fuel (RDF), however in the last years the term solid recovered fuel (SRF) has been coined [7]. This term arises after the development of European standards [CEN/TC 343]. A solid recovered fuel (SRF) is a solid fuel generated from non-hazardous waste to be used for energy recovery in thermal applications (e.g. incineration). SRFs meet a defined quality criteria laid down in CEN/TS 15359 attending to levels of certain fuel properties (net calorific, chlorine and mercury content). The production of SRFs is a potential alternative to direct combustion and to reduce our reliance on landfill [7–9].

1.4 Conversion processes

A wide range of biomass and waste can be used as feedstocks for the production of solids, liquids, and gaseous products by means of several conversion methods (Fig. 1.1).

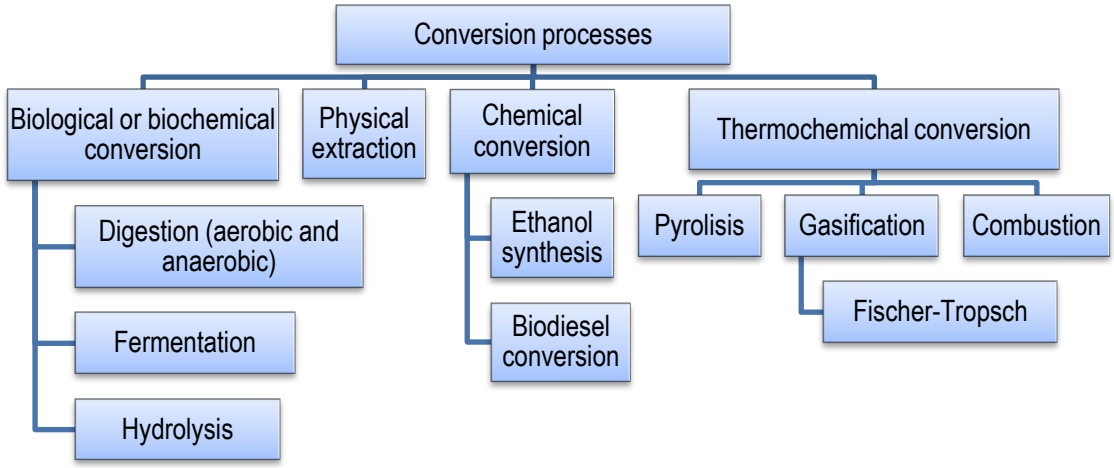

Figure 1.1 Scheme of the conversion processes. Adapted from [5]

According to how molecules are broken down there are two broad routes: biological or biochemical (by bacteria/microorganisms/enzymes) and thermochemical (by temperature).

The biological or biochemical treatment involves the chemical transformation of the feedstock by use of chemicals, catalysts, heat or a

combination thereof [10]. This conversion route is mainly based on the fermentation of sugars to produce renewable hydrocarbons (i.e. ethanol). For instance, lignocellulosic biomass is used to extract lignin (one of the constituents in the lignocellulosic matrix) by a pretreatment method followed by hydrolysis to produce sugars. These sugars are then saccharified by fermentation. The biological or biochemical conversion route is divided into three main categories: (i) digestion (aerobic and anaerobic), (ii) fermentation and (iii) acid hydrolysis or enzymatic.

The thermochemichal route is based on the chemical changes of a material occurring when heat is applied. The thermal decomposition produces solid, liquid and gas products that can be upgraded to fuels (i.e. synthetic biofuels). This approach has some advantages over the biochemical route, depending on the feedstock used and the final output. One advantage is that no pretreatment is needed to separate the feedstock components although some pretreatment can be applied to upgrade the properties of the feedstock. Another advantage is the short reaction time compared to biochemical processes and the complete or almost utilization of the feedstock. In this sense, a partially dry feedstock like biomass and waste can be treated thermochemically for the development of energy. The thermochemical route offers commonly three principal categories (i) pyrolysis, (iii) gasification and (iii) combustion. Torrefaction would be included as a pyrolysis type (see section 1.5.1).

This thesis focuses on the thermochemical route of gasification, converting biomass and waste-derived fuels into a syngas for the production of liquid fuels with a low carbon footprint.

1.5 Thermochemical conversion

Thermochemical conversion implies elevated temperature conditions (200-1500 ºC) to convert any organic matter and upgrade the outputs into a wide variety of resources, producing fuels, chemicals, electricity and heat. The reaction products include gases (hydrogen, carbon monoxide, carbon dioxide, methane...), carbon products (ash, char) and condensable liquids (water, tar). Several parameters such as the final temperature, heating rate, reactor configuration and even the feedstock affect the product ratios [5,10–12]. For

instance, low temperatures and long residence times favour the production of carbon solids, while higher temperatures increases the yield to gas.

Table 1.1 gathers typical process conditions and reaction products for the three principal thermochemical conversion processes: pyrolysis, gasification and combustion.

Table 1.1 Most common process conditions and reaction products for pyrolysis, gasification and combustion. Adapted from [13]

	Pyrolysis	**Gasification**	**Combustion**
Temperature range (ºC)	250-700	700-1300	> 750-< 1500
Pressure (bar)	1	1-45	1
Atmosphere	Inert, nitrogen	Gasification agent: air, oxygen, steam, CO_2 or mixtures of thereof	Air
Stoichometric ratio	0 (no air)	< 1 (partial air)	> 1 (excess air)
Products			
Gases	H_2, CO, H_2O, N_2, and hydrocarbons	H_2, CO, CO_2, H_2O, N_2, CH_4 and other hydrocarbons	CO_2, H_2O, O_2, N_2
Liquids	Pyrolysis oil, water	Tars, water	-
Solids	Ash, char, coke	Ash, char	Ash, slag

As observed in Table 1.1, gasification would be a combination of pyrolysis and combustion conditions. In fact, pyrolysis and combustion reactions take place during gasification, for this reason it is important to present a general overview of these thermochemical conversion pathways.

1.5.1 Pyrolysis

Pyrolysis is the thermal conversion of a feedstock in complete absence of oxidizing agent (i.e. oxygen) at temperatures ranging between 250-700 ºC or slightly higher. Three primary outputs are produced: solid (char), liquid (pyrolisis oil or tar) and gas, all of them with combustible characteristics.

The solid product is commonly referred to as char (or derivatives as charcoal, biochar, and so forth). Char is characterized to have a high content of carbon (> 70%) and low ash content (< 5%) [14]. The liquid product is formed by a dark fluid known as tar (or pyrolysis oil) with some water content. Tar is a

mixture of hydrocarbons which may evolve to larger compounds as the severity of the process increases (i.e. pyrolysis temperature, pressure, reaction time, etc.). Further details are explained in the gasification section 1.5.4.

The final gas product is a mixture of condensable gases (vapour and heavier molecular weight gases) and non-condensable gases (low molecular weight gases such as H_2, CO, CO_2, CH_4, etc.).

From a thermal point of view, the feedstock decomposition during the pyrolysis process occurs in four steps [5], which may be overlapped:

1. Drying (~ 100 ºC): The initial step corresponds to the evaporation of moisture and the release of heat (exothermic reaction).
2. Dehydratation (100-300 ºC): After the initial drying, the continuous heating favours the release of more water and low-molecular-weight gases (CO, CO_2).
3. Primary pyrolysis (> 200 ºC): Char (also referred as primary char) is produced at this stage together with condensable (vapour and precursors of pyrolysis oil) and non-condensable gases (more low-molecular-weight gases such as CH_4).
4. Secondary pyrolysis (~ 300-900 ºC): The final stage involves cracking of volatiles into additional char (or secondary char) and more non-condensable gases. Usually a high spot of hydrocarbons release is observed between 450-500 ºC [15]. Hot char particles may catalyse cracking of gases and therefore increase liquid yield.

The different types of pyrolysis processes depend on operational parameters including pyrolysis temperature and heating rate. Pyrolysis temperature (or peak or final temperature) is the maximum temperature reached and held up for a period of time until completion of the process. Temperature affects both composition and the relative amount of product yields. For instance, char production is favoured by low temperatures and slow heating rates [16].

Table 1.2 compiles the types of pyrolysis methods depending on the operating parameters.

Table 1.2 Pyrolysis types and operating conditions [5,16,17]

	Mild pyrolysis (or torrefaction)	**Slow pyrolysis (or conventional pyrolysis)**	**Fast pyrolysis**	**Flash pyrolysis**
Temperature range (ºC)	200-300	350-800	500-1250	800-1300
Heating rate	Slow (<10 ºC/min)	Slow (<10 ºC/min)	Fast (> 100 ºC/s)	Very fast (>1000 ºC/s)
Residence time	Minutes-hours	Minutes-days (for carbonization)	Seconds (0.5-10 s)	Seconds (< 0.5 s)
Particle size	5-50 mm	5-50 mm	< 1 mm	< 0.2 mm
Primary product	Stabilized friable feedstock	Char	Bio-oil, tar products	Bio-oil, tar products

1.5.2 Torrefaction

Torrefaction is a mild pyrolysis carried out at a low temperature range (200-300 ºC).

Previous research [18–21] has shown the benefits of torrefaction as a thermal pretreatment for upgrading biomass properties. The principal advantages are listed as follows:

- Increase of the energy density as a result of releasing moisture (H_2O). Despite the loss of volatiles (CO, CO_2, etc.) the torrefied material preserves most of the energy content.
- Reduction of size. Together with the increase of energy density, this is an important feature for reducing transportation costs.
- Torrefaction relatively increases the carbon content but diminishes oxygen and hydrogen. The removal of H_2O and CO_2 decreases both oxygen-to-carbon (O/C) and hydrogen-to-carbon (H/C) ratios. These low ratios improve the gasification properties of the feedstock.
- The torrefied material enhances its hydrophobic behaviour and absorbs less moisture when stored (i.e. less hydrophilic).
- Grindability also increases. For instance, after biomass torrefaction the product is more friable and hence easier for storing and for feeding purposes. A common technique for handling biomass is to form pellets, which also minimize transport and storage problems.

In this work, the effect of torrefaction as a pretreatment for gasification has been studied on woody biomass (Chapter 3) and a waste-derived fuel (Chapter 7). Recently, gasification of torrefied materials has become increasingly popular [22–25].

1.5.3 Combustion

Combustion subjects the feedstock to a total oxidation at high temperatures (750-1000 ºC) converting the fuel material into a hot flue gas and the incombustible material into stable inorganic matter (ash). This exothermic process takes place for instance in incineration plants.

Regarding treatment of waste, incineration is the most widely used method, as it can reduce waste mass (by up 75%), volume (by 90%) and hazard [17,26,27]. This technique is also able to recover energy, producing electricity [28] at an efficiency of around 20%, and reclaim some mineral and chemical content from waste. However waste incineration is associated not only with high economic and operating costs [29] but also with pollution. Air pollution must be controlled to meet environmental legislative limit values, according to the EU Waste Incineration Directive (2000/76/EC). Compounds to be monitored and measured include: particulates, NOx, SOx, COx, HCl, HF, organic traces and certain heavy metals (Cd, Hg, Pb, Sb, Cr, Ni, etc.). Organic species include several hydrocarbons: halogenated aromatic hydrocarbons, polycyclic aromatic hydrocarbons (PAHs), benzene, toluene and xylene (BTX), dioxins and furans. For instance, dioxins (polychlorinated dibenzo-para-dioxins, PCDDs) and furans (polychlorinated dibenzofurans, PCDFs) are one of those toxic chemical air pollutants considered carcinogenic and to cause immune system damage [30].

1.5.4 Gasification

Gasification is a partial oxidation of a feedstock to produce a combustible gas (also called producer gas, synthesis gas or syngas) to be used for energy purposes, which includes power generation or the manufacturing of chemicals and fuels. The process is carried out at a high temperature range (700-1300 ºC) under an oxygen-deficient environment by the addition of a gasification agent (air, oxygen, steam, carbon dioxide or combination of thereof). The feedstock reacts with the gasification agent and, if required by the reactor configuration,

in the presence of a bed material. The gasification technology exhibits a high flexibility as it can accept a variety of solid feedstocks like coal, biomass or waste [31].

This thermochemical conversion pathway produces three major outputs, similarly to the pyrolysis process: a solid residue (ash and some unconverted carbon or char), a liquid fraction (a mixture of water with hydrocarbons) and the gas (a mixture of H_2, CO, CO_2, CH_4 and other compounds); although the main desired product is the gas. The producer gas is utilized in the production of liquid fuels (diesel, gasoline), methanol, ammonia, synthetic natural gas (SNG) and energy production (heat and electricity) [11]. Fig. 1.2 shows a general scheme of the possible routes.

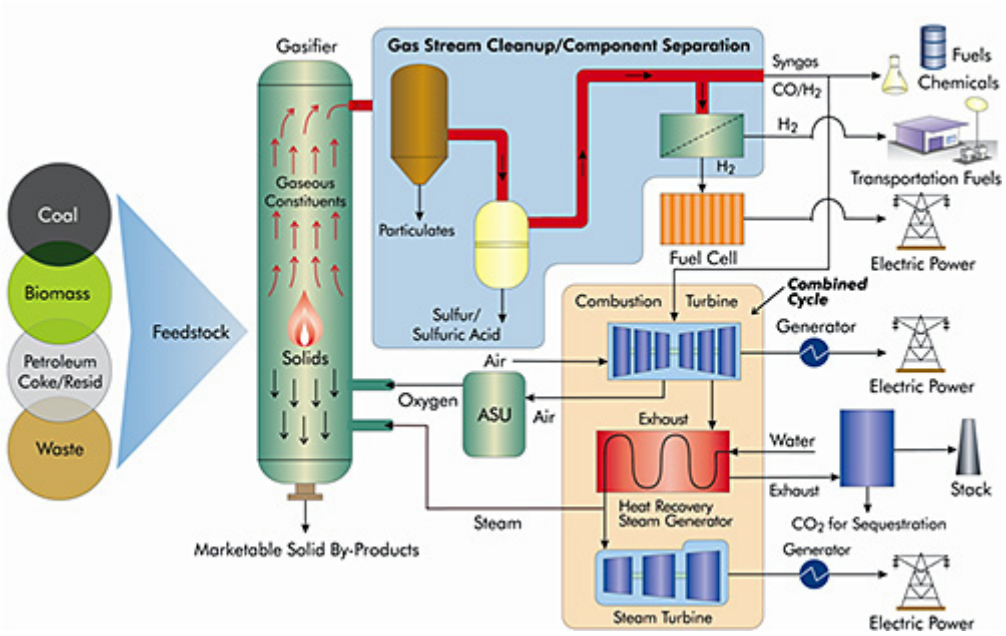

Figure 1.2 Scheme of the gasification process and routes. Source [32]

Despite the advantages of producing a combustible gas, the main drawback in gasification are operational problems related to bed sintering, slagging, corrosion, fouling and the release of impurities included in the syngas, such particulates (fly ash), condensable hydrocarbons (tar) and trace contaminants (e.g. H_2S, HCl, NH_3) [18,33,34].

1.5.4.1 Gasification reactors

The different types of gasification reactors (gasifiers) can be classified according to the fuel transport process within the gasifier [11,35–37]. An illustration of the main types is shown in Figure 1.3.

Fixed bed reactor

In this type of gasifier the reactions occur in a fixed or moving bed. The solid fuel is usually fed from the top of the gasifier but depending on the inlet position of the gasification agent, these gasifiers are divided in two generic types: updraft (or countercurrent) and downdraft (or cocurrent). In updraft gasifiers (Fig 1.3-a) the fuel is fed from the top of the reactor moving downward while the gasification agent inlet is at the bottom side. Thereby the producer gas is exhausted at the top. On the contrary, in downdraft gasifiers (Fig. 1.3-b), the gasification agent enters from the middle/bottom side, flowing in the same direction as the fuel, exhausting the gas at the bottom.

Fluidized bed reactor

In a fluidized bed reactor the fuel fed from the side enters in contact with the hot bed, fluidized by the gasification agent. Immediately there is a high heat exchange between both solid materials. The rapid drying and pyrolysis reactions produce char and gases leaving from the top of the reactor, the freeboard region. The solid products (char and ash) are usually collected in a cyclone and thereafter the gas passes through a cleaning chain. The principal types of fluidized beds are: the bubbling fluidized bed (BFB, Fig 1.3-c) and the circulating fluidized bed (CFB, Fig 1.3-d). In a BFB the entrained particles are removed from the process, while in a CFB the particles are recirculated in the bed.

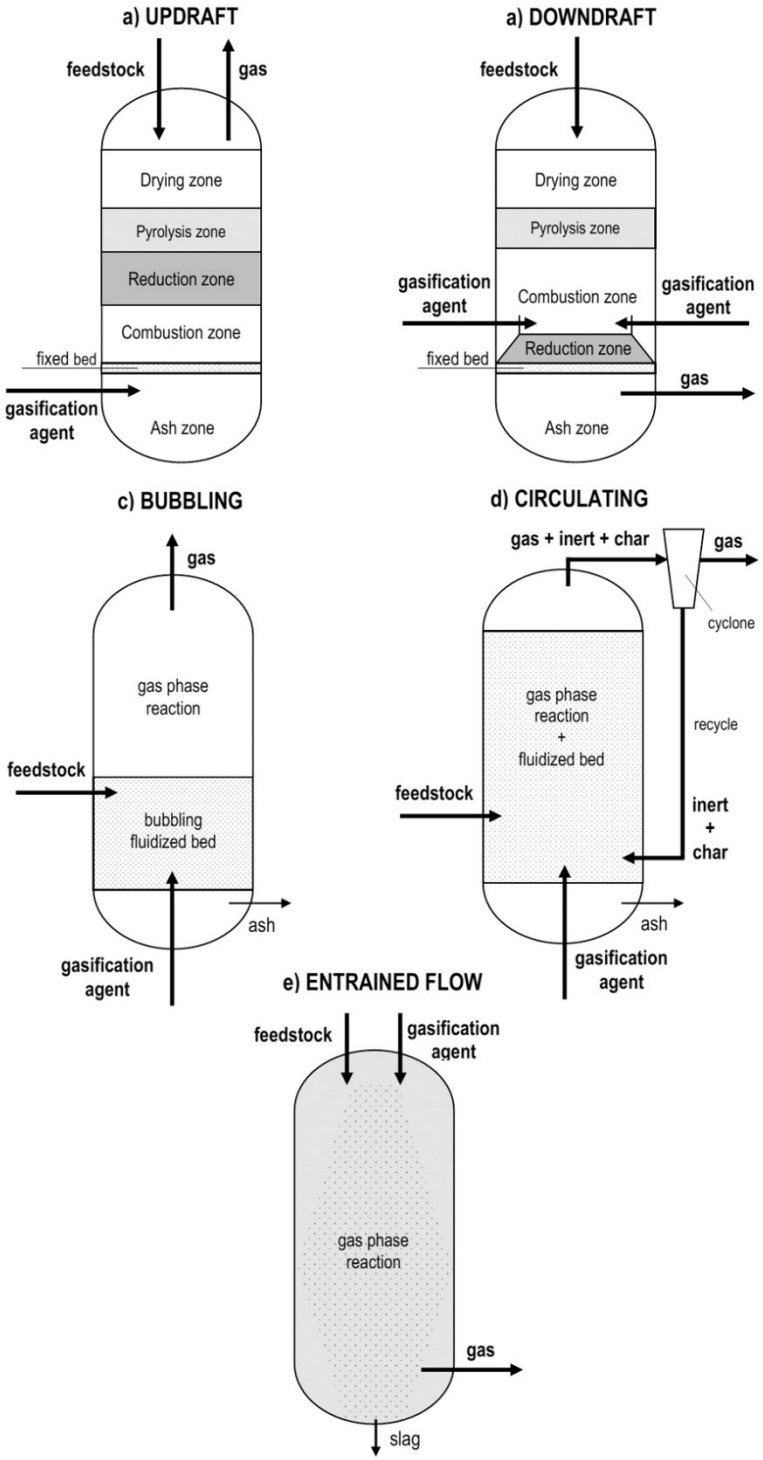

Figure 1.3 Gasifiers: a) Updraft fixed bed, b) Downdraft fixed bed, c) Bubbling fluidized bed, d) Circulating fluidized bed, e) Entrained flow

Entrained flow

An entrained flow gasifier (Fig. 1.3-e) is the most common technology for processing coal. Pulverized fuel (e.g. finely-ground coal) enters along with the gasification agent in cocurrent flow from the top or in countercorrent from the

side. The reactions occur very fast and the residence time is in the order of seconds. Entrained flow gasifiers operate at high temperatures (typically 1200-1600 ºC) and are designed for operation at large scale (>> 100 MW_{th}).

In this work a laboratory-scale bubbling fluidized bed reactor was used for gasification experiments (see Chapter 2).

1.5.4.2 Gasification reactions

The gasification process can be described as a combination of pyrolysis, gasification and combustion reactions, therefore is a complex process with multiple reactions (Table 1.3). A sequence of the phases and reactions in a typical gasification process is described as follows [5,11,36]:

- Pyrolysis: The heat inside the gasifier volatilises the fuel releasing water, low molecular-weight compounds and char (R1). For further details of this step see section 1.5.1.
- Gasification: The char produced in the pyrolysis step reacts with the gasification agent and other gases produced from the devolatiliation reactions. Apart from carbon reactions (R2-R6), further gas reactions occur, which include homogeneous and tar reactions (R7-R19).
- Combustion: This stage involves oxidation reactions (R2-R3). In oxygen-deficient conditions like gasification, reaction R3 is more likely to take place than a complete combustion (R2).

Note that these sequential steps are often overlapped.

Table 1.3 Main reactions in a gasification process [38–40]

Name(s)	**Reaction**	**ΔH^0_r (kJ/mol)**	**Number**
Devolatilization reaction			
Fuel + heat → volatiles ($CO+CO_2+H_2+CH_4+N_2$+ light hydrocarbons) + tar + char		>0	R1
Heterogeneous reactions			
Char combustion			
Oxidation	$C + O_2 \rightarrow CO_2$	-394	R2
Partial oxidation	C + ½O2 → CO	-111	R3
Char gasification			
Boudouard reaction	$C + CO_2 \rightarrow 2CO$	+172	R4
Water gas reaction	$C + H_2O \rightarrow CO + H_2$	+131	R5
Hydrogenation or hydrogasification	$C + 2H_2 \rightarrow CH_4$	-75	R6
Homogeneous reactions			
Methanation reaction	$CO_2 + 4H_2 \rightarrow CH_4 + 2H_2O$	-165	R7
Methane reforming or Steam reforming reaction	$CH_4 + H_2O \rightarrow CO + 3H_2$	+206	R8
Dry reforming reaction	$CH_4 + CO_2 \rightarrow 2CO + 2H_2$	+247	R9
Methane oxidation	$CH_4 + 2O_2 \rightarrow CO_2 + 2H_2O$	-283	R10
Methane partial oxidation	$CH_4 + ½O_2 \rightarrow CO + 2H_2$	-36	R11
Water gas-shift reaction	$CO + H_2O \leftrightarrow CO_2 + H_2$	-41	R12
Carbon monoxide oxidation	$CO + ½O_2 \rightarrow CO_2$	-284	R13
Hydrogen oxidation	$H_2 + ½O_2 \rightarrow H_2O$	-242	R14
Tar reactions (tar assumed C_nH_m)			
Tar partial oxidation	$C_nH_m + (n/2)O_2 \rightarrow nCO + (m/2)H_2$		R15
Tar dry reforming	$C_nH_m + nCO_2 \rightarrow (2n)CO + (m/2)H_2$	Highly	R16
Tar steam reforming	$C_nH_m + nH_2O \rightarrow (m/2+n)H_2 + nCO$	endothermic	R17
Tar hydrogenation	$C_nH_m + (2n-m/2)H_2 \rightarrow nCH_4$	(200-300),	R18
Thermal cracking	$C_nH_m \rightarrow (m/4)\ CH_4 + (n-m/4)C$	except R15	R19

In Table 1.3, the energy released or absorbed in each reaction is given by the standard heat of reaction (ΔH^0_r) set to a temperature of 25 ºC. Although most of gasification reactions are endothermic ($\Delta H^0_r>0$), which means that absorb heat, some of them can also release heat, the exothermic ($\Delta H^0_r<0$) reactions. Generally, the heat released in exothermic reactions may be sufficient to ensure the heat consumption of endothermic reactions. This would be the case for an autothermal gasifier, whereas a system requiring additional external heat is known as allothermal gasifier.

1.5.4.3 Gasification inputs and outputs

This section describes the main inputs (others than feedstocks like biomass and waste) as well as the obtained products in a typical gasification process.

INPUTS

Bed material

The bed material employed in fixed and fluidized bed reactors acts as heat transfer medium. The typical bed material is silica sand but the utilization of catalysts favours several reactions that influence the properties of the product gas, especially promoting the abatement of tar and the reforming of methane and higher hydrocarbons. The main catalysts for gasification can be classified in the following groups [5,41,42]:

- Natural catalysts or earth metal catalysts: dolomite ($CaMg(CO_3)_2$) and olivine $(Mg, Fe)_2SiO_4$. These earth metal catalysts are commonly used in gasification because they are cheap and easy to find in nature. Dolomite effectively reduces tar, however this material generates particulates as it is calcined in the gasifier. An alternative is to use calcined dolomite to avoid the formation of fines in the product gas. In this regard, olivine is considered a better mineral due to its resistance against attrition but it is reported to be less effective on tar removal than dolomite.
- Synthetic catalysts: alkali-based catalyst (Li, Na, K, Rb, Cs, Fr) and metal-based catalysts (Ni, Co, Fe, to name a few). In contrast to natural catalysts, synthetic catalysts are produced at a relatively high cost. Agglomeration is another of the main problems associated to alkali-based catalysts, whereas catalyst deactivation as a result of carbon deposition is the principal inconvenient for metal-based catalysts.

Gasification agent

The main gasification agents are: air, oxygen, steam and carbon dioxide, used either alone or in mixtures such as oxygen-steam. Among them, oxygen is the absolutely essential in any combustion process, however the production of pure oxygen is expensive. The preferred gasification agents are air or an oxygen-steam mixture (O_2/H_2O).

Air (approximately 71% N_2 and 29% O_2) is used due to economic advantages but the main inconvenient is that nitrogen greatly dilutes the product gas. For instance, gas heating values for air biomass gasification could range between 4-7 MJ/Nm^3 [36].

The choice of steam as gasification agent promotes the H_2 and CO production in the product gas, improving the gasification of remaining char, and produces a non-diluted gas. In biomass gasification, an average gas heating value of 12-17 MJ/Nm^3 is reached under oxygen-steam conditions [36].

OUTPUTS

Solids

The solid products produced inside the gasifier are represented by ash and char, which consist of carbon, minerals and metals not converted into gas. Depending on the amount of carbon content, the solid residue is called char (high carbon content > 75%) or ash (mainly minerals and metals, and a low carbon content).

Liquids

The liquid phase consists of condensable compounds after cooling the product gas (mainly tar and water are collected).

Gas

The main goal in gasification is the production of a synthesis gas (syngas), ideally a mixture of mainly hydrogen (H_2) and carbon monoxide (CO) but generally contains other gases and impurities (tar and minor traces). The final composition of the syngas is strongly influenced by the feedstock composition and operating conditions [12,43].

One of the main hurdles to overcome on gasification is the formation of tar and other contaminants, which must be removed to certain levels depending on the end-use and emission limits. Table 1.4 gathers the contaminant limits for the most common syngas applications.

Table 1.4 Typical cleaning requirements in syngas applications. [44–46]

Contaminant	Applications			
	Gas turbine	**Internal combustion engine**	**Methanol synthesis**	**FT synthesis**
Particulates (ash, char, soot)	< 30 mg/Nm³ (PM5)	< 50 mg/Nm³ (PM10)	< 0.02 mg/Nm³	0
Tar	< 5 mg/Nm³	< 100 mg/Nm³	< 0.1 mg/Nm³	< 0.01 mg/Nm³
Sulphur (H_2S, COS)	< 30 mg/Nm³		< 1 mg/Nm³	< 0.01 mg/Nm³
Nitrogen (NH_3, HCN)	< 50 mg/Nm³		< 0.1 mg/Nm³	< 0.02 mg/Nm³
Alkalis (Na, K)	< 0.02 mg/Nm³		-	< 0.01 mg/Nm³
Halides (HCl)	< 1.5 mg/Nm³		< 0.1 mg/Nm³	< 0.01 mg/Nm³

Particulate matter can be removed almost completely by cyclones, rigid filters or electrostatic precipitators with a collection efficiency higher than 95% [44]. Wet scrubbers can remove as well both particulates and tar compounds in the same process, although water soluble tars can reduce the removal effectiveness. More problematic are trace contaminants as even small amounts can poison catalysts used for syngas cleaning and upgrading [44]. Acid gas removal units are used to remove acid gases (H_2S and also CO_2) whereas other water soluble products (NH_3 and HCl) are generally removed by wet scrubbers. The advantage of wet processes is the removal of multiple contaminants in contrast to dry processes (i.e. filters, electrostatic precipitators, cyclones); however the main drawback is the loss in efficiency due to gas cooling. For this reason, hot gas cleanup can be carried out at temperatures above 300 ºC by using catalysts and sorbents devoted to contaminants removal. Nonetheless a challenge to overcome is the rapid catalyst deactivation [47].

Tar

Tar is defined as all organic condensable compounds with molecular weights higher than that of benzene (C_6H_6) [48,49], generally formed in the pyrolysis step and assumed to be largely aromatic.

According to molecular weight, tar can be divided in various groups. Milne et al [49] classified tar products into lumps (primary, secondary, and tertiary) as function of the reaction severity (process temperature and residence time).

Figure 1.4 shows a tar maturation scheme from oxygenated compounds to polycyclic aromatic hydrocarbons (PAHs) as function of temperature.

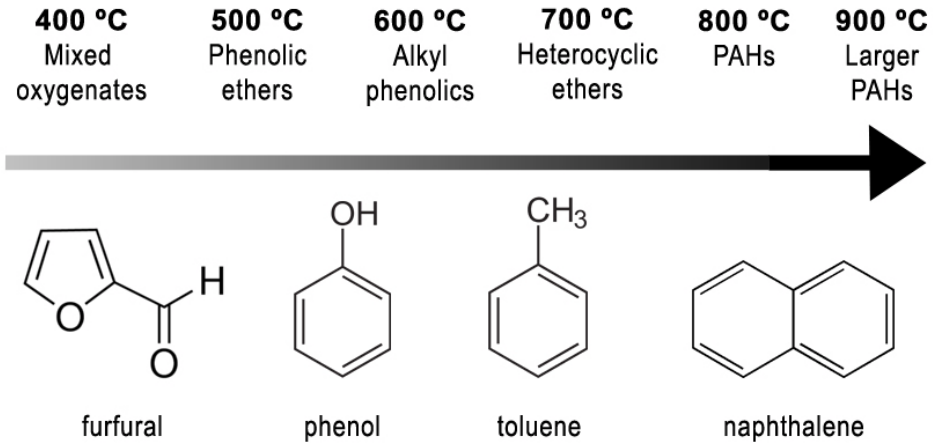

Figure 1.4 Evolution of tar compounds. Adapted from [50]

Primary tars (low molecular weight oxygenated hydrocarbons such as levoglucosan and furfural) derive from pyrolysis of biomass components (cellulose, hemicellulose and lignin) produced at a relatively low temperature (400 ºC). Secondary tars include phenolics and olefins (phenol, xylene, etc.) as temperature rises to 500 ºC. Tertiary tars comprise alkyl tertiary products and condensed tertiary aromatics. Alkyl products are mainly methyl derivatives of aromatic compounds (toluene, indene, etc.) formed at > 600 ºC. Above 700 ºC condensed tertiary tars consist of aromatic compounds, primary naphthalene, anthracene, pyrene and benzene to name a few.

Devi et al. [41] as well categorized tar in other five classes based on solubility and condensability (Table 1.5). The heaviest tars (class 1 and 5) condense even at very low concentration. This could be the main reason of the condensation problem. Class 2 tars are highly soluble in water and class 4 are either very stable even after severe catalytic treatment.

Table 1.5 Tar classes based on solubility and condensability [41,44]

Tar class	Class name	Property	Representative compounds
1	GC-undetectable	Very heavy tars, which cannot be detected by GC	-
2	Heterocyclic	Tars containing heteroatoms (atoms other than C or H). Highly water soluble compounds	Pyridine, phenol, cresols
3	Light aromatic (1 ring)	Usually light hydrocarbons with single ring. Not problematic regarding condensability and solubility	Toluene, ethylbenzene, xylenes
4	Light polyaromatic (2-3 rings)	Two and three ring compounds. Condense at low temperature	Indene, naphthalene, fluorine, phenanthrene
5	Heavy polyaromatic (4-7 rings)	Larger than three ring compounds. Condense at high temperature	Fluoranthene, pyrene, chrysene, perylene

This complex mixture of condensable compounds hinders the implementation of gasification because tar diminishes the product gas yield and causes fouling and plugging in equipment, increasing the cost associated to their cleaning. Since the temperature of the producer gas needs to be cooled down for targeted uses, tar becomes a crucial problem as it starts condensing from 300 ºC [46]. Furthermore, above 400 ºC, tar may suffer dehydration and therefore form solid coke or soot which also causes operational problems such as plugging, fouling and abrasion of turbine blades [46].

Tar removal from syngas is generally carried out by wet processes such as wet scrubbing with liquid sorbents. Water is the conventional solvent used for tar scrubbing because it is cheap however the low removal efficiency (mainly light and oxygenated compounds) and costs of wastewater treatment have promoted the utilization of organic liquids such as oils. The OLGA process developed at the Energy research Center of the Netherlands (ECN) is one of the earliest technologies using oil based scrubbers with almost complete tar removal [51]. This process is based on a multi-stage scrubber with the benefit that the scrubbing oil can be regenerated by air stripping. Despite the regeneration of oil absorbent, this type of processes is economically feasible in large scale facilities [47]. For this reason, the importance of producing a cleaner syngas becomes

relevant in order to reduce the process complexity and costs related to cleaning strategies. Several options to reduce tar have been studied providing insight under different experimental conditions [44,47,52–54]. The most common treatments are thermal and catalytic cracking, such as the use of high temperatures (1100-1300 ºC) and different bed materials (dolomite, olivine, Ni-based catalysts, etc.). These applications in biomass gasification can lead to tar levels below 50 mg/Nm^3, which are adequate for many combustion engines [44]. Nevertheless, thermal cracking may not be cost competitive due to the energy required for rising temperature to crack very stable and refractory tars.

Minor contaminants

During biomass gasification the main minor contaminants released in the syngas are sulphur and nitrogen compounds, and halides to a lesser extent. Waste-derived fuels tend to contain more chlorinated compounds derived from polymer fractions such as plastics and inorganic salts (e.g. NaCl). Relative to other contaminants, trace metals such as sodium and potassium may be present in the producer gas, although these compounds were not studied in this work.

The release of contaminants is highly dependent on the feedstock properties; consequently the concentration of inorganic compounds widely varies in the syngas. A principal problem is that even small amounts of these contaminants may be detrimental in some applications for syngas cleaning (such as acid gas removal units) and upgrading. Typically, minor contaminants poison catalysts used for syngas upgrading (i.e. FT synthesis), for this reason the presence of these contaminants must be decreased to stringent limits, as shown in Table 1.4, to abate technical and operational issues.

Sulphur contaminants occur mostly as hydrogen sulphide (H_2S) with lesser amounts of carbonyl sulphide (COS) and carbon disulphide (CS_2). In combustion processes, sulphur compounds are as well oxidized producing sulphur dioxide (SO_2). H_2S is problematic because corrodes metal surfaces and poison catalysts used to upgrade syngas. Typically H_2S is removed by absorption with zinc oxide (ZnO) [44].

Nitrogen contaminants include mainly ammonia (NH_3) and hydrogen cyanide (HCN) released at different levels regarding the nitrogen content and functionalities in the feedstock. Commonly in biomass gasification the fuel-

nitrogen is converted to NH_3 rather than to HCN and isocyanic acid (HNCO), all of them precursors of nitrogen oxides (NO_x and N_2O) under combustion processes [55]. Conventional water scrubbers are capable of removing almost complete ammonia in the syngas [47].

Hydrogen chloride (HCl) is the predominated halide in the syngas. Other species can be formed such as sodium chloride (NaCl) and ammonium chloride (NH_4Cl) which tend to precipitate producing fouling in cooler downstream stages [44]. Removal of HCl and other halides can be done by wet scrubbing systems, as they are highly water-soluble, or another option is by absorption on ZnO bed together with sulphur compounds.

Table 1.6 Typical levels of contaminants in syngas obtained from fluidized bed reactors

Contaminant	**Concentration in syngas**	
	Woody biomass [46,56,57]	**SRFs** [58–60]
Particulates (ash, char, soot)	2-16 g/Nm³	50 g/Nm³
Tar	< 10 g/Nm³	20-100 g/Nm³
H_2S	25-800 mg/Nm³	> 400 mg/Nm³
COS, CS_2	< 25 mg/Nm³	Not available
NH_3	350-2000 mg/Nm³	> 2000 mg/Nm³
HCN	< 25 mg/Nm³	Not available
Halides (HCl)	1-300 mg/Nm³ (dry basis)	> 50 mg/Nm³
Alkalis (Na, K),	0.5-5 mg/Nm³	Not available

The chemical composition of the feedstock is a key parameter, besides the gasifier configuration and process conditions, that determines the amount of impurities that will be present in the product gas. Table 1.6 compiles typical concentration values of contaminants in syngas for biomass and SRFs gasification, showing that the syngas must be thoroughly cleaned to comply the requirements for most of syngas applications.

1.6 An overview on biomass and waste gasification advances

Biomass gasification has been extensively investigated regarding syngas production under different operating conditions [61–71]. The research available denotes that gasification agent, equivalence ratio (ER), temperature and the gasification technology play an important role on gas composition. In this sense, air as gasification agent produces a low calorific gas due to dilution of nitrogen

whereas the mixture of oxygen and steam enhances hydrogen formation and gas heating value [62]. Depending on the type of feedstock, the optimal value for ER has been observed to range between 0.2-0.4 [63–65] with tar reductions about 50% within that range. Furthermore, operation at high gasification temperature favours carbon conversion and production of combustible gases together with reductions of tar content [70,71]. The main concern during biomass gasification is the presence of impurities in the syngas (Table 1.6), mostly condensable hydrocarbons referred as tar. A decrease of tar content is observed at temperatures above 750 ºC [61,68,69] and when using catalyst as bed material [65–67]. Investigations with dolomite as bed material showed tar reductions up to 50% [65,67]. The quality of the producer gas is also influenced by the choice of a particular gasification reactor. Each type of gasifier has positive and negative aspects depending on the final use of the producer gas. Several gasification reactors have been investigated (i.e. fixed bed and fluidized bed reactors) pointing out conversion efficiencies in the gasifier higher than 70% and the production of a gas with considerable high calorific value (> 4 MJ/Nm^3) [43,64]. Among fixed bed reactors, downdraft gasifiers have been identified to produce cleaner syngas than updraft gasifiers, with tar levels in the order of 6 g/Nm^3 and 50 g/Nm^3, respectively [64]. Usually updraft gasifiers report high tar contents due to incomplete reduction and thermal cracking of volatiles [43]. On the other hand, fluidized bed gasifiers offer higher thermal cracking of volatiles as a result of a better heat transfer of particles due to fluidization. Comparatively to fixed beds, the conversion efficiency of fluidized beds can be higher than 95% if the process operates at adequate conditions [43]. However, other gasification parameters such as pressure and torrefaction during biomass gasification have received limited attention [72,73]. In view of the benefits on biomass properties accomplished by torrefaction, for instance the increase of energy density and reduction of moisture content [19,20], torrefied biomass is expected to improve the gasification efficiency and diminish tar formation because of the loss of volatiles [19]. An initial part of this project aims to provide insight into these parameters, by studying the gasification of torrefied biomass and the effect of pressure on gas production.

The high versatility of gasification allow the system to operate with a wide range of feedstocks including waste [58,74–80]. Waste gasification has been

considered a promising route for waste-to-energy conversion as it can act as a solution to reduce the impact of municipal solid waste (MSW) in landfills [81]. As stated previously, during gasification the main technical limitations are the release of contaminants in the syngas, including tar, particulates, alkalis, halides, sulphur and nitrogen compounds (e.g. HCl, H_2S, NH_3, etc.), which cause troubles at several levels, both operational and environmental. Therefore the requirement of gas cleaning is essential in any gasification process especially when dealing with extremely heterogeneous materials such as waste-derived fuels (i.e. solid recovered fuels, SRFs). Thus, it is important to produce a clean syngas in order to achieve an efficient process. Some of the problems related to gasification of MSW and derived fractions may be solved, for instance, by co-gasification (e.g. SRF blended with biomass [59]) and the addition of low cost minerals like dolomite and olivine as bed materials [58]. Similarly to biomass gasification, waste gasification studies have reported high conversion efficiencies at the following operating conditions: high gasification temperatures around 850 ºC, equivalence ratio of 0.3 and the utilization of steam as gasification agent for improving gas yield and H_2 production [58,59,78]. Concerning the release of tar, air gasification of a marketed SRF called Stabilat® showed a total tar content around 15 g/Nm^3 under gasification temperatures of 700-850 ºC and ER ranging 0.25-0.3 [58]. Another study [59] led to similar tar content results around 20 g/Nm^3 for gasification of a SRF at 800 ºC, ER ~0.2 and the addition of steam (steam/feedstock ratio of 0.85), observing a tar diminishment by 50% with the use of dolomite as bed material. Tar content in air gasification of MSW is usually higher than 20 g/Nm^3 [78,82] and thus higher tar concentration compared to biomass gasification (see Table 1.6). Nevertheless, the evolution of other impurities during gasification is still scarce in the literature. Few studies [58,59] have reported the concentration of some minor contaminants (e.g. HCl, H_2S and NH_3) in the syngas, highly dependent on the feedstock properties and gasification conditions. For this reason further research is needed to understand the release of these compounds and to establish adequate gasification conditions for waste-derived fuels.

As previously commented, torrefaction has been applied to overcome some of the most relevant inconveniences of biomass (i.e. high moisture content, low calorific value and bulk density) and after that, gasification of torrefied biomass

has reported lower concentration of contaminants [24,25,83]. Thus, it is interesting to explore this thermal pretreatment with waste fractions for improving the gasification performance. Few investigations have addressed torrefaction of different wastes [28,84–86]. In the case of torrefaction of various MSW samples improved the fuel properties by increasing calorific value [28,84] and decreasing chlorine contents [28], which are positive aspects for gasification. In contrast to gasification of torrefied biomass, there is no published data of gasification using torrefied waste. This presents an opportunity to seek the integration of torrefaction and gasification processes for the production of a cleaner syngas.

A way to determine the economic feasibility of a large-scale facility is through a techno-economic analysis. Based on many parameters, such studies evaluate the process performance and cost effectiveness of the system in the long term. In recent years, techno-economic studies based on gasification plants have been carried out for several end uses of the syngas [87–92]. Precisely the syngas conversion into liquid transportation fuels (e.g. diesel, gasoline) faces up several challenges mostly related to the aforementioned technical barriers but also to commercial limitations because of high investment costs [88]. There remains an urgent need for further studies to achieve an efficient gasification process which improves the quality of the syngas that will reduce costs related to cleaning requirements in the production of liquid fuels.

1.6.1 Gasification plants

Currently, there exist more than 272 gasification plants worldwide with 686 operating gasifiers, which produce over 100,000 MW_{th} of syngas. Most of them are pilot or demonstration plants. More than 75 plants with 240 gasifiers are expected to be constructed during the following years [93] although some gasification projects have been discontinued in recent months. Table 1.7 gathers some of the gasification plants in the world.

Table 1.7 Plants/projects based on gasification [94–98]

Location	Company	Type*	Gasification technology	Size	Status
Sweeden Göteborg	Göteborg Energi	Biomass to SNG	Dual CFB	32 MWth of forest residues to produce 20 MW of bio-methane	Operating. Start-up year: 2013
Sweeden Hagfors	Varmlands Methanol	BTL	FBR (HTW™ gasifier)	111 MWth. 600 t/d forest biomass to 300 tons/d methanol and 15 MWe for local use	Project temporarily on hold
Germany Karlsruhe	Karslruthe Institute of Technology	BTL	Fast pyrolysis + High pressure entrained flow	Pilot 5 MWth (1 t/h wheat straw) to produce 150 kg/h Dimethyl ether and < 100 L/h gasoline.	Operating. Start-up year: 2013
German Freiberg	CHOREN Industries GmbH	BTL	Entrained flow 3-stage gasifier. (Choren Carbo-V®)	45 MWth. 75 kt/year wood) to produce 18 ML/yr FT diesel	Closed in 2011. Start-up year: 2008
China Jincheng	Shanxi Lanhua Coal Chemical Co., Ltd	CTL	Entrained flow	2000 t/d coal to produce 300 kt/yr ammonia and 520 kt/yr urea	Operating. Start-up year: 2015
Ireland Belfast	Belfast WTE	WTE	Plasma	180 kt/yr MSW to produce 15 MWe	Under construction
Japan Nagasaki	JFE/Thermoselect	WTE	Downdraft	300 t/d MSW to produce 8 MWe	Operating. Start-up year: 2005
USA Nevada	Fulcrum Bioenergy	WTL	Downdraft + Plasma arc	200 ktons/year MSW to produce 38 ML/yr of FT jet fuel or diesel	Under construction. To begin commercial operations early 2019
Canada Edmonton	Enerkem Alberta Biofuels	WTL	BFB	350 t/d of refuse MSW to produce 38 ML/year of ethanol	Operating. Start-up year: 2014.

*SNG: Synthetic Natural gas. BTL: Biomass-to-liquids. CTL: Coal-to-liquids. WTE: Waste-to-energy

1.7 References

[1] European Comission. Energy Strategy and Energy Union n.d. https://ec.europa.eu/energy/en/topics/energy-strategy-and-energy-union (accessed April 17, 2017).

[2] World Bank. Fossil fuel energy consumption n.d. http://data.worldbank.org/indicator/EG.USE.COMM.FO.ZS (accessed April 17, 2017).

[3] European Commission. Renewable energy directive n.d. https://ec.europa.eu/energy/en/topics/renewable-energy/renewable-energy-directive (accessed April 17, 2017).

[4] International Energy Agency. Statistics n.d. http://www.iea.org/statistics/.

[5] Basu P. Biomass Gasification and Pyrolysis: practical design and theory. Elsevier Science; 2010. doi:10.1016/B978-0-12-374988-8.00001-5.

[6] Arnsfeld S, Senk D, Gudenau HW. The qualification of torrefied wooden biomass and agricultural wastes products for gasification processes. J Anal Appl Pyrolysis 2014;107:133–41. doi:10.1016/j.jaap.2014.02.013.

[7] Rada EC, Andreottola G. RDF/SRF: Which perspective for its future in the EU. Waste Manag 2012;32:1059–60. doi:10.1016/j.wasman.2012.02.017.

[8] Rada EC. Present and future of SRF. Waste Manag 2016;47:155–6. doi:10.1016/j.wasman.2015.11.035.

[9] Rotter VS, Lehmann A, Marzi T, Möhle E, Schingnitz D, Hoffmann G. New techniques for the characterization of refuse-derived fuels and solid recovered fuels. Waste Manag Res 2011;29:229–36. doi:10.1177/0734242X10364210.

[10] Bhaskar T, Pandey A. Advances in Thermochemical Conversion of Biomass-Introduction. Recent Adv Thermochem Convers Biomass 2015:3–30. doi:10.1016/B978-0-444-63289-0.00001-6.

[11] Higman C, van der Burgt M. Gasification (Second Edition). Gasif. (Second Ed., Burlington: Gulf Professional Publishing; 2008, p. 1–9. doi:http://dx.doi.org/10.1016/B978-0-7506-8528-3.00001-8.

[12] Couto N, Rouboa A, Silva V, Monteiro E, Bouziane K. Influence of the biomass gasification processes on the final composition of syngas. Energy Procedia 2013;36:596–606. doi:10.1016/j.egypro.2013.07.068.

[13] European Commission. Reference document on the Best Available Techniques for Waste Incineration. Integr Pollut Prev Control 2006:1–638. doi:10.1002/0470012668.ch5.

[14] Antal MJJ, Croiset E, Dai X, DeAlmeida C, Mok WS-L, Norberg N, et al. High-Yield Biomass Charcoal. Energy & Fuels 1996;10:652–8. doi:10.1021/ef9501859.

[15] Recari J, Berrueco C, Abelló S, Montané D, Farriol X. Effect of temperature and pressure on characteristics and reactivity of biomass-derived chars. Bioresour Technol 2014;170:204–10. doi:10.1016/j.biortech.2014.07.080.

[16] Manyà JJ. Pyrolysis for biochar purposes: A review to establish current knowledge gaps and research needs. Environ Sci Technol 2012;46:7939–54. doi:10.1021/es301029g.

[17] Kalyani KA, Pandey KK. Waste to energy status in India: A short review. Renew Sustain Energy Rev 2014;31:113–20. doi:10.1016/j.rser.2013.11.020.

[18] Batidzirai B, Mignot APR, Schakel WB, Junginger HM, Faaij APC. Biomass torrefaction technology: Techno-economic status and future prospects. Energy 2013;62:196–214. doi:10.1016/j.energy.2013.09.035.

[19] Chew JJ, Doshi V. Recent advances in biomass pretreatment–Torrefaction fundamentals and technology. Renew Sustain Energy Rev 2011;15:4212–22. doi:http://dx.doi.org/10.1016/j.rser.2011.09.017.

[20] van der Stelt MJC, Gerhauser H, Kiel JH a, Ptasinski KJ. Biomass upgrading by torrefaction for the production of biofuels: A review. Biomass and Bioenergy 2011;35:3748–62. doi:10.1016/j.biombioe.2011.06.023.

[21] Kataki R, Chutia RS, Mishra M, Bordoloi N, Saikia R, Bhaskar T. Feedstock Suitability for Thermochemical Processes. 2015. doi:10.1016/B978-0-444-63289-0.00002-8.

[22] Kwapinska M, Xue G, Horvat A, Rabou LPLM, Dooley S, Kwapinski W, et al. Fluidized Bed Gasification of Torrefied and Raw Grassy Biomass (Miscanthus × gigantenus). the Effect of Operating Conditions on Process Performance. Energy and Fuels 2015;29:7290–300. doi:10.1021/acs.energyfuels.5b01144.

[23] Kuo PC, Wu W, Chen WH. Gasification performances of raw and torrefied biomass in a downdraft fixed bed gasifier using thermodynamic analysis. Fuel 2014;117:1231–41. doi:10.1016/j.fuel.2013.07.125.

[24] Chen W-H, Peng J, Bi XT. A state-of-the-art review of biomass torrefaction, densification and applications. Renew Sustain Energy Rev 2015;44:847–66. doi:10.1016/j.rser.2014.12.039.

[25] Dudyński M, van Dyk JC, Kwiatkowski K, Sosnowska M. Biomass gasification: Influence of torrefaction on syngas production and tar formation. Fuel Process Technol 2015;131:203–12. doi:10.1016/j.fuproc.2014.11.018.

[26] Singh RP, Tyagi V V., Allen T, Ibrahim MH, Kothari R. An overview for exploring the possibilities of energy generation from municipal solid waste (MSW) in Indian scenario. Renew Sustain Energy Rev 2011;15:4797–808. doi:10.1016/j.rser.2011.07.071.

[27] Ma W, Hoffmann G, Schirmer M, Chen G, Rotter VS. Chlorine characterization and thermal behavior in MSW and RDF. J Hazard Mater 2010;178:489–98. doi:10.1016/j.jhazmat.2010.01.108.

[28] Yuan H, Wang Y, Kobayashi N, Zhao D, Xing S. Study of Fuel Properties of Torrefied Municipal Solid Waste. Energy & Fuels 2015:150728062838002. doi:10.1021/ef502277u.

[29] Svensson Myrin E, Persson PE, Jansson S. The influence of food waste on dioxin formation during incineration of refuse-derived fuels. Fuel 2014;132:165–9. doi:10.1016/j.fuel.2014.04.083.

[30] McKay G. Dioxin characterisation, formation and minimisation during municipal solid waste (MSW) incineration: Review. Chem Eng J 2002;86:343–68. doi:10.1016/S1385-8947(01)00228-5.

[31] Zaccariello L, Mastellone M. Fluidized-Bed Gasification of Plastic Waste, Wood, and Their Blends with Coal. Energies 2015;8:8052–68. doi:10.3390/en8088052.

[32] National Energy Technology Laboratory n.d. http://www.netl.doe.gov/research/coal/energy-systems/gasification/gasifipedia/intro-to-gasification (accessed April 17, 2017).

[33] Bläsing M, Zini M, Müller M. Influence of feedstock on the release of potassium, sodium, chlorine, sulfur, and phosphorus species during gasification of wood and biomass shells. Energy and Fuels 2013;27:1439–45. doi:10.1021/ef302093r.

[34] Van Caneghem J, Brems A, Lievens P, Block C, Billen P, Vermeulen I, et al. Fluidized bed waste incinerators: Design, operational and environmental issues. Prog Energy Combust Sci 2012;38:551–82. doi:10.1016/j.pecs.2012.03.001.

[35] Quaak P, Knoef H, Stassen HE. Energy from Biomass: A Review of Combustion and Gasification Technologies. World Bank; 1999.

[36] Heidenreich S, Müller M, Foscolo PU, Heidenreich S, Müller M, Foscolo PU. Chapter 2 – Fundamental Concepts in Biomass Gasification. Adv Biomass Gasif 2016:4–10. doi:10.1016/B978-0-12-804296-0.00002-6.

[37] Zhang L, Xu C, Champagne P. Overview of recent advances in thermo-chemical conversion of biomass. Energy Convers Manag 2010;51:969–82. doi:http://dx.doi.org/10.1016/j.enconman.2009.11.038.

[38] Gómez-Barea a., Leckner B. Modeling of biomass gasification in fluidized bed. Prog Energy Combust Sci 2010;36:444–509. doi:10.1016/j.pecs.2009.12.002.

[39] Knoef HAM. Handbook biomass gasification. BTG Biomass Technology Group; 2005. doi:9081938509.

[40] Morales MP, Mun P, Ruiz J a, Jua MC. Biomass gasification for electricity generation : Review of current technology barriers. Renew Sustain Energy Rev 2013;18:174–83. doi:10.1016/j.rser.2012.10.021.

[41] Devi L, Ptasinski KJ, Janssen FJJG, Van Paasen SVB, Bergman PC a, Kiel JH a. Catalytic decomposition of biomass tars: Use of dolomite and untreated olivine. Renew Energy 2005;30:565–87. doi:10.1016/j.renene.2004.07.014.

[42] Neves D, Thunman H, Matos A, Tarelho L, Gómez-Barea A. Characterization and prediction of biomass pyrolysis products. Prog Energy Combust Sci 2011;37:611–30. doi:10.1016/j.pecs.2011.01.001.

[43] Sansaniwal SK, Pal K, Rosen MA, Tyagi SK. Recent advances in the development of biomass gasification technology: A comprehensive review 2017;72:363–84. doi:10.1016/j.rser.2017.01.038.

[44] Woolcock PJ, Brown RC. A review of cleaning technologies for biomass-derived syngas. Biomass and Bioenergy 2013;52:54–84. doi:10.1016/j.biombioe.2013.02.036.

[45] Tijmensen MJ a, Faaij a. PC, Hamelinck CN, Van Hardeveld MRM. Exploration of the possibilities for production of Fischer Tropsch liquids and power via biomass gasification. Biomass and Bioenergy 2002;23:129–52. doi:10.1016/S0961-9534(02)00037-5.

[46] Asadullah M. Biomass gasification gas cleaning for downstream applications: A comparative critical review. Renew Sustain Energy Rev 2014;40:118–32. doi:10.1016/j.rser.2014.07.132.

[47] Abdoulmoumine N, Adhikari S, Kulkarni A, Chattanathan S. A review on biomass gasification syngas cleanup. Appl Energy 2015;155:294–307. doi:10.1016/j.apenergy.2015.05.095.

[48] Abatzoglou N, Barker N, Hasler P, Knoef H. The development of a draft protocol for the sampling and analysis of particulate and organic contaminants in the gas from small biomass gasifiers. Biomass and Bioenergy 2000;18:5–17. doi:10.1016/S0961-9534(99)00065-3.

[49] Milne T a, Evans RJ. Biomass Gasifier " Tars ": Their Nature , Formation , and Conversion. National Renewable Energy Laboratory; 1998. doi:10.2172/3726.

[50] Elliott DC. Relation of Reaction Time and Temperature to Chemical Composition of Pyrolysis Oils. Pyrolysis Oils from Biomass, vol. 376, American Chemical Society; 1988, p. 6–55. doi:doi:10.1021/bk-1988-0376.ch006.

[51] Bergman P, van Paasen S, Boerrigter H. The novel "OLGA" technology for complete tar removal from biomass producer gas. Pyrolysis Gasif Biomass Waste 2002:10.

[52] Shen Y, Yoshikawa K. Recent progresses in catalytic tar elimination during biomass gasification or pyrolysis - A review. Renew Sustain Energy Rev 2013;21:371–92. doi:10.1016/j.rser.2012.12.062.

[53] Saroğlan A. Tar removal on dolomite and steam reforming catalyst: Benzene, toluene and xylene reforming. Int J Hydrogen Energy 2012;37:8133–42. doi:10.1016/j.ijhydene.2012.02.045.

[54] Blanco PH, Wu C, Onwudili JA, Williams PT. Characterization of Tar from the Pyrolysis/Gasification of Refuse Derived Fuel: Influence of Process Parameters and Catalysis. Energy & Fuels 2012;26:2107–15. doi:10.1021/ef300031j.

[55] Yu QZ, Brage C, Chen GX, Sjöström K. The fate of fuel-nitrogen during gasification of biomass in a pressurised fluidised bed gasifier. Fuel 2007;86:611–8. doi:10.1016/j.fuel.2006.08.007.

[56] Cheah S, Carpenter DL, Magrini-Bair KA. Review of mid- to high-temperature sulfur sorbents for desulfurization of biomass- and coal-derived syngas. Energy and Fuels 2009;23:5291–307. doi:10.1021/ef900714q.

[57] Boerrigter H, Uil H Den, Calis H-P. Green Diesel from Biomass via Fischer-Tropsch synthesis: New Insights in Gas Cleaning and Process Design. Pyrolysis Gasif Biomass Waste, Expert Meet 2002:1–13.

[58] Dunnu G, Panopoulos KD, Karellas S, Maier J, Touliou S, Koufodimos G, et al. The solid recovered fuel Stabilat®: Characteristics and fluidised bed gasification tests. Fuel 2012;93:273–83. doi:10.1016/j.fuel.2011.08.061.

[59] Pinto F, André RN, Carolino C, Miranda M, Abelha P, Direito D, et al. Gasification improvement of a poor quality solid recovered fuel (SRF). Effect of using natural minerals and biomass wastes blends. Fuel 2014;117:1034–44. doi:10.1016/j.fuel.2013.10.015.

[60] Belgiorno V, De Feo G, Della Rocca C, Napoli RMA. Energy from gasification of solid wastes. Waste Manag 2003;23:1–15. doi:10.1016/S0956-053X(02)00149-6.

[61] Mayerhofer M, Mitsakis P, Meng X, De Jong W, Spliethoff H, Gaderer M. Influence of pressure, temperature and steam on tar and gas in allothermal fluidized bed gasification. Fuel 2012;99:204–9. doi:10.1016/j.fuel.2012.04.022.

[62] Lv P, Yuan Z, Ma L, Wu C, Chen Y, Zhu J. Hydrogen-rich gas production from biomass air and oxygen/steam gasification in a downdraft gasifier. Renew Energy 2007;32:2173–85. doi:10.1016/j.renene.2006.11.010.

[63] Lysenko S, Sadaka S, Brown RC. Comparison of mass and energy balances for air blown and thermally ballasted fluidized bed gasifiers. Biomass and Bioenergy 2012;45:95–108. doi:10.1016/j.biombioe.2012.05.018.

[64] Gai C, Dong Y. Experimental study on non-woody biomass gasification in a downdraft gasifier. Int J Hydrogen Energy 2012;37:4935–44. doi:10.1016/j.ijhydene.2011.12.031.

[65] Narvaez I, Oro A, Aznar MP, Corella J, Narváez I, Orío A, et al. Biomass Gasification with Air in an Atmospheric Bubbling Fluidized Bed . Effect of Six Operational Variables on the Quality of. Ind Eng Chem Res 1996;35:2110–20. doi:10.1021/ie9507540.

[66] Gil J, Caballero M a., Martín J a., Aznar M-P, Corella J. Biomass Gasification with Air in a Fluidized Bed: Effect of the In-Bed Use of Dolomite under Different Operation Conditions. Ind Eng Chem Res 1999;38:4226–35. doi:10.1021/ie980802r.

[67] Miccio F, Piriou B, Ruoppolo G, Chirone R. Biomass gasification in a catalytic fluidized reactor with beds of different materials. Chem Eng J 2009;154:369–74. doi:10.1016/j.cej.2009.04.002.

[68] Qin YH, Feng J, Li WY. Formation of tar and its characterization during air-steam gasification of sawdust in a fluidized bed reactor. Fuel 2010;89:1344–7. doi:10.1016/j.fuel.2009.08.009.

[69] Rabou LPLM, Zwart RWR, Vreugdenhil BJ, Bos L. Tar in biomass producer gas, the Energy research Centre of The Netherlands (ECN) experience: An enduring challenge. Energy and Fuels 2009;23:6189–98. doi:10.1021/ef9007032.

[70] Chang ACC, Chang H-F, Lin F-J, Lin K-H, Chen C-H. Biomass gasification for hydrogen production. Int J Hydrogen Energy 2011;36:14252–60. doi:10.1016/j.ijhydene.2011.05.105.

[71] Franco C, Franco C, Pinto F, Pinto F, Gulyurtlu I, Gulyurtlu I, et al. The study of reactions influencing the biomass steam gasification process. Fuel 2003;82:835–42. doi:http://dx.doi.org/10.1016/S0016-2361(02)00313-7.

[72] Couhert C, Salvador S, Commandré JM. Impact of torrefaction on syngas production from wood. Fuel 2009;88:2286–90. doi:10.1016/j.fuel.2009.05.003.

[73] Prins MJ, Ptasinski KJ, Janssen FJJG. More efficient biomass gasification via torrefaction. Energy 2006;31:3458–70. doi:10.1016/j.energy.2006.03.008.

[74] Pinto F, Franco C, André RNN, Miranda M, Gulyurtlu I, Cabrita I. Co-gasification study of biomass mixed with plastic wastes. Fuel 2002;81:291–7. doi:10.1016/S0016-2361(01)00164-8.

[75] Tanigaki N, Manako K, Osada M. Co-gasification of municipal solid waste and material recovery in a large-scale gasification and melting system. Waste Manag 2012;32:667–75. doi:10.1016/j.wasman.2011.10.019.

[76] Tchapda AH, Pisupati S V. A review of thermal co-conversion of coal and biomass/waste. Energies 2014;7:1098–148. doi:10.3390/en7031098.

[77] Arena U, Di Gregorio F. Gasification of a solid recovered fuel in a pilot scale fluidized bed reactor. Fuel 2014;117:528–36. doi:10.1016/j.fuel.2013.09.044.

[78] Wang J, Cheng G, You Y, Xiao B, Liu S, He P, et al. Hydrogen-rich gas production by steam gasification of municipal solid waste (MSW) using NiO supported on modified dolomite. Int J Hydrogen Energy 2012;37:6503–10. doi:10.1016/j.ijhydene.2012.01.070.

[79] He M, Hu Z, Xiao B, Li J, Guo X, Luo S, et al. Hydrogen-rich gas from catalytic steam gasification of municipal solid waste (MSW): Influence of catalyst and temperature on yield and product composition. Int J Hydrogen Energy 2009;34:195–203. doi:10.1016/j.ijhydene.2008.09.070.

[80] Luo S, Zhou Y, Yi C. Syngas production by catalytic steam gasification of municipal solid waste in fixed-bed reactor. Energy 2012;44:391–5. doi:10.1016/j.energy.2012.06.016.

[81] Arena U, Zaccariello L, Mastellone ML. Fluidized bed gasification of waste-derived fuels. Waste Manag 2010;30:1212–9. doi:10.1016/j.wasman.2010.01.038.

[82] Campoy M, Gómez-Barea A, Ollero P, Nilsson S. Gasification of wastes in a pilot fluidized bed gasifier. Fuel Process Technol 2014;121:63–9. doi:10.1016/j.fuproc.2013.12.019.

[83] Berrueco C, Recari J, Güell BM, Alamo G Del. Pressurized gasification of torrefied woody biomass in a lab scale fluidized bed. Energy 2014;70:68–78. doi:10.1016/j.energy.2014.03.087.

[84] Poudel J, Ohm T-I, Oh SC. A study on torrefaction of food waste. Fuel 2015;140:275–81. doi:10.1016/j.fuel.2014.09.120.

[85] Benavente V, Fullana A. Torrefaction of olive mill waste. Biomass and Bioenergy 2015;73:186–94. doi:10.1016/j.biombioe.2014.12.020.

[86] Liu S, Qiao Y, Lu Z, Gui B, Wei M, Yu Y, et al. Release and Transformation of Sodium in Kitchen Waste during Torrefaction. Energy & Fuels 2014;28:1911–7. doi:10.1021/ef500066b.

[87] Swanson RM, Platon A, Satrio JA, Brown RC. Techno-economic analysis of biomass-to-liquids production based on gasification. Fuel 2010;89:S11–9. doi:10.1016/j.fuel.2010.07.027.

[88] Rafati M, Wang L, Dayton DC, Schimmel K, Kabadi V, Shahbazi A. Techno-economic analysis of production of Fischer-Tropsch liquids via biomass gasification: The effects of Fischer-Tropsch catalysts and natural gas co-feeding. Energy Convers Manag 2017;133:153–66. doi:10.1016/j.enconman.2016.11.051.

[89] Luz FC, Rocha MH, Lora EES, Venturini OJ, Andrade RV, Leme MMV, et al. Techno-economic analysis of municipal solid waste gasification for electricity generation in Brazil. Energy Convers Manag 2015;103:321–37. doi:10.1016/j.enconman.2015.06.074.

[90] Andersson J, Lundgren J, Marklund M. Methanol production via pressurized entrained flow biomass gasification - Techno-economic comparison of integrated vs. stand-alone production. Biomass and Bioenergy 2014;64:256–68. doi:10.1016/j.biombioe.2014.03.063.

[91] Man Y, Yang S, Xiang D, Li X, Qian Y. Environmental impact and techno-economic analysis of the coal gasification process with/without CO2 capture. J Clean Prod 2014;71:59–66. doi:10.1016/j.jclepro.2013.12.086.

[92] Yassin L, Lettieri P, Simons SJR, Germanà A. Techno-economic performance of energy-from-waste fluidized bed combustion and gasification processes in the UK context. Chem Eng J 2009;146:315–27. doi:10.1016/j.cej.2008.06.014.

[93] Gasification and Syngas Technologies Council. The Gasification Industry n.d. http://www.gasification-syngas.org/resources/the-gasification-industry (accessed May 2, 2017).

[94] National Energy Technology Laboratory. Gasification Plant Databases n.d. https://www.netl.doe.gov/research/coal/energy-systems/gasification/gasification-plant-databases (accessed May 2, 2017).

[95] Janssen R, Turhollow AF, Rutz D, Mergner R. Production facilities for second-generation biofuels in the USA and the EU - current status and future perspectives. Biofuels, Bioprod Biorefining 2013;7:647–65. doi:10.1002/bbb.1451.

[96] Arena U. Process and technological aspects of municipal solid waste gasification. A review. Waste Manag 2012;32:625–39. doi:http://dx.doi.org/10.1016/j.wasman.2011.09.025.

[97] Karltorp K. Challenges in mobilising financial resources for renewable energy - The cases of biomass gasification and offshore wind power. Environ Innov Soc Transitions 2016;19:96–110. doi:10.1016/j.eist.2015.10.002.

[98] European Biofuels Technology Platform. Biomass to Liquids (BtL) n.d. http://www.biofuelstp.eu/btl.html (accessed May 2, 2017).

Chapter 1

2. MATERIALS AND METHODS

2.1 Introduction

This chapter presents the materials and experimental setup used in this thesis. In addition, the configuration of the equipment is discussed in detail.

Sections 2.2 and 2.3 describe the gasification feedstocks and bed materials used in the fluidized bed reactor. Section 2.4 presents the main experimental equipment, while section 2.5 explains the procedure of a typical gasification test, including relevant changes in the setup during the completion of this work. Lastly, section 2.6 summarizes the calculations carried out for the analysis of the experimental data.

2.2 Feedstocks

The feedstocks used during gasification experiments can be divided in two main blocks: biomass and waste.

2.2.1 Biomasses

Two sorts of woody biomasses (Virgin wood and GROT) were obtained from local sources in Trondheim, Norway. The biomasses were used raw (original) and treated (torrefied) as feedstocks for gasification experiments. Two torrefaction levels were tested: lightly torrefied (LT), where biomass was subjected to a final torrefaction temperature of 225 ºC and strongly torrefied (ST) with a final torrefaction temperature of 275 ºC.

Virgin wood (VW) is a softwood obtained from Norwegian spruce (*Picea abies*), one of the fastest growing spruces, commonly found in northern and central Europe. Figure 2.1 shows the original VW with a typical creamy white colour and both torrefied samples, VW-LT and VW-ST, with a darker brown colour.

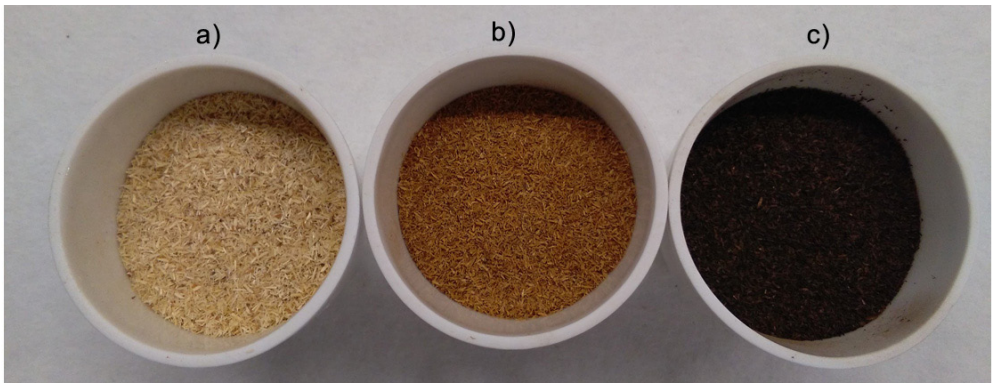

Figure 2.1. Norwegian spruce (particle size range of 250-500 µm): a) VW, b) VW-LT and c) VW-ST

The second biomass, GROT, is composed of tree-tops and branches of Norwegian forest residues. GROT stands for the Scandinavian term *Grenar och toppa,* which refers to these forest residues. Figure 2.2 depicts the original GROT and torrefied products GROT-LT and GROT-ST.

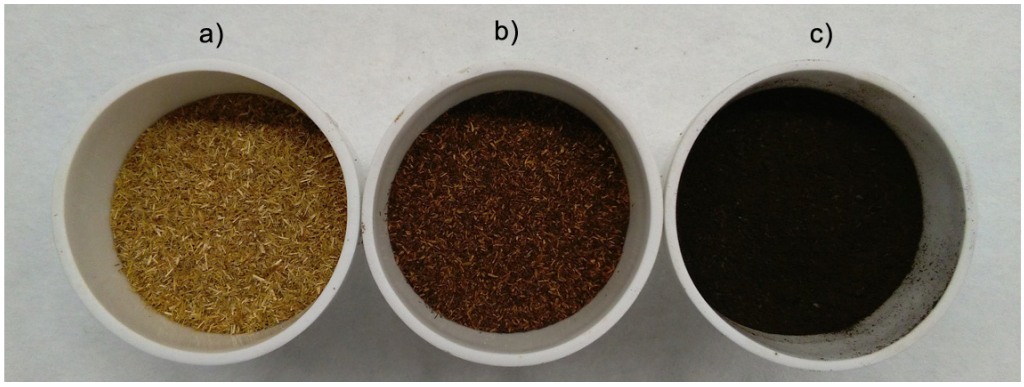

Figure 2.2 Norwegian forest residues (particle size range of 250-500 µm): a) GROT, b) GROT-LT and c) GROT-ST

2.2.2 Municipal solid waste fractions

Two products derived from municipal solid waste (MSW) were used in this project. The MSW-derived material were produced by two local MSW waste management companies aiming to produce solid recovered fuels (SRFs) for further energy recovery. Both SRFs, namely RT and FL, were obtained after different waste collection streams and mechanical treatments.

The first SRF studied in this project was a product named RT, obtained from rejects of trommel in a process from the company Ambiensys (Spain). This company produced a diversity of potential SRFs from unsorted MSW through

their process of active hyginiezation (GeiserBox®). The GeiserBox® system subjects the waste materials to high temperatures (140-165 ºC) and pressures (4-6 bar) in contact with saturated vapour for 25-45 min. The subproducts (organic fiber, metals, plastics, etc.) are separated into several fractions through a series of sorting processes, for instance by using a trommel (i.e. a rotary drum to separate materials by means of physical size separation).

RT contains a high quantity of textiles and plastics and a low content of paper and biomass. This SRF was not subjected to any additional pretreatment before the gasification experiments. Fig. 2.3 depicts the obtained RT in particle sizes of 1 mm.

Figure 2.3 RT (particle size of 1 mm) for analytical and gasification tests

Fluff (FL), the second SRF used in this work, was produced by the GRIÑÓ group (Spain) from rejected waste fractions after a sorting process from selective waste collection. Waste fractions that cannot be conveniently re-used or recycled are converted into a fluff fraction. FL is a low density SRF composed by paper, cardboard, non-recyclable plastics but also contains some fabrics and sorts of biomass such as wood. During this project, FL was subjected to a torrefaction pretreatment at two severity levels, obtaining two different subproducts. The selected final torrefaction temperatures were 290 ºC and 320 ºC, leading to the correspondent FL290 and FL320 materials. Figure 2.4 depicts FL and FL derived samples.

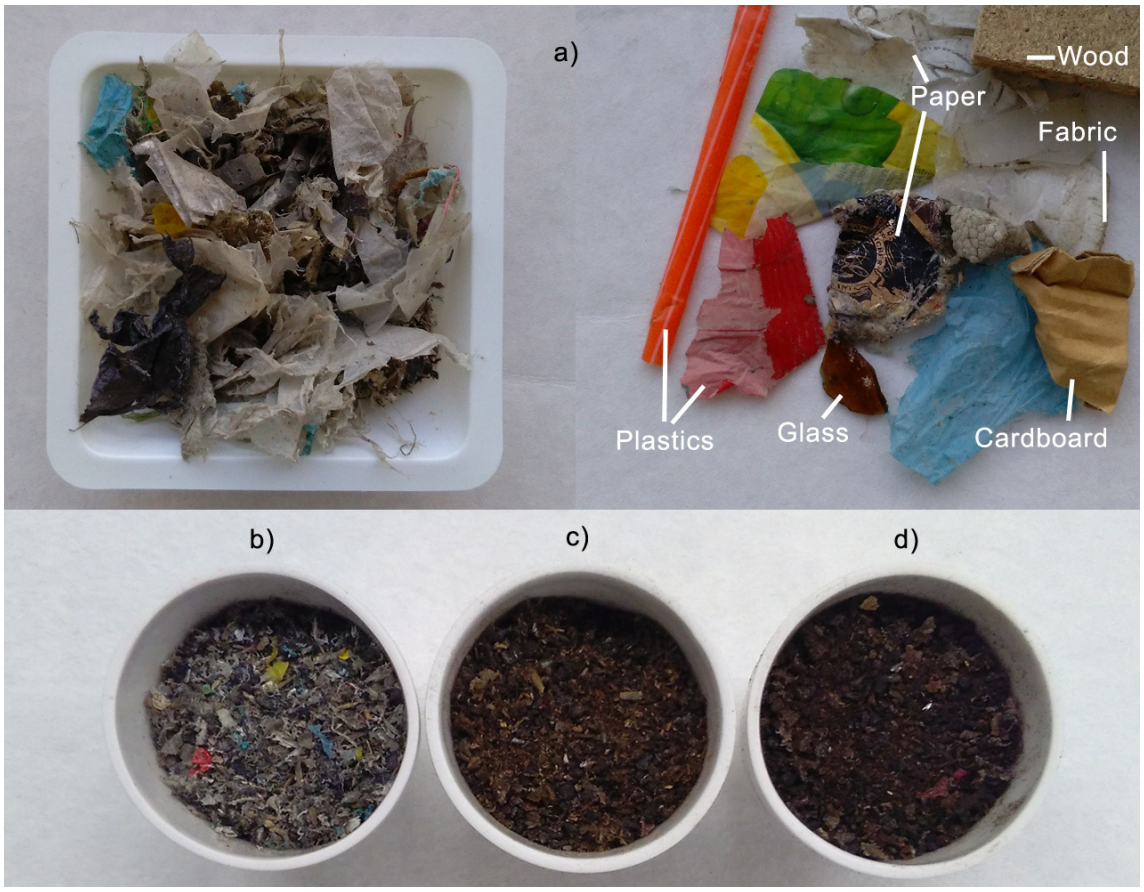

Figure 2.4 FL and FL derived samples: a) FL as received (particle size > 5 cm), b) FL milled and sieved to a particle size of 1 mm for analytical and gasification tests, c) FL torrefied at 290 ºC (FL290) and d) FL torrefied at 320 ºC (FL320)

2.3 Bed materials

Three bed materials were tested during the gasification experiments: silica sand (J.T.Baker) and two catalysts: dolomite (Minelco GmbH and Productos Dolomíticos de Málaga S.A.) and olivine (Sibelco Hispania). Previous to the gasification experiments, all bed materials were sieved to particle size range of 150-200 μm, to assure appropriate bed fluidization conditions [1], and were calcined in a furnace at 900 ºC for 4 hours. Figure 2.5 shows the pictures of the calcined bed materials. After calcination, only olivine changed its original colour from green to redish; for this reason pictures before and after calcination are included. Additional characteristics of the catalysts can be found in Table 2.1.

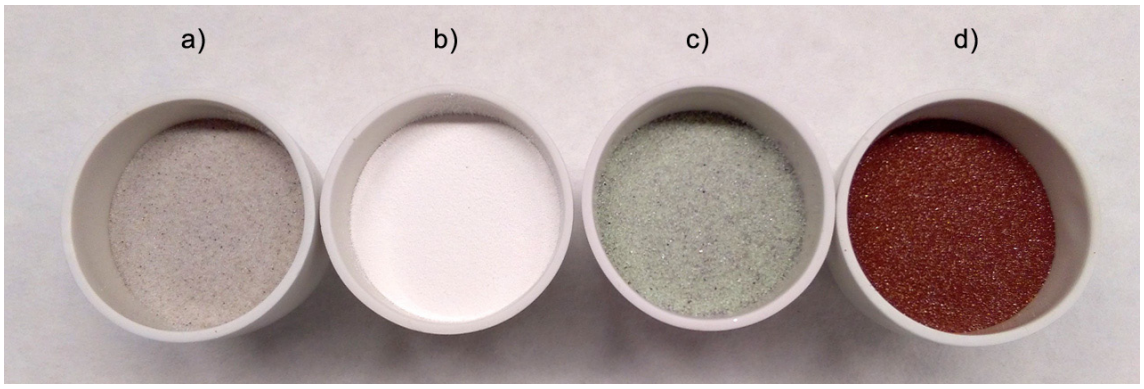

Figure 2.5 Bed materials (particle size 150-200 μm): a) calcined silica sand, b) calcined dolomite, c) original olivine, d) calcined olivine

Table 2.1 Catalysts properties (as indicted by the supplier)

Properties	Dolomite	Olivine
Chemical composition (wt.%)		
CaO	31.0	-
MgO	21.3	49.0
SiO_2	0.08	41.0
Fe_2O_3	0.02	7.0
Al_2O_3	0.04	0.5
CrO_3	-	0.3
NiO	-	0.3
Physical properties		
Specific gravity (g/cm^3)	2.85	3.30
Hardness (Moh's scale)	3	6.5-7.0

2.4 Experimental equipment

This section includes the main experimental equipment. During the completion of this thesis project, a process for the analysis and quantification of minor contaminants present in the producer gas was developed (section 2.4.2.2).

2.4.1 Gasification system rig

The gasification system consists of four main blocks: fluidized bed reactor, feeding system, gas cleaning, and gas analysis system.

2.4.1.1 Fluidized bed reactor

The laboratory-scale fluidized bed reactor was designed by PID Eng&Tech, Spain. The experimental setup was equipped with a control system

(flow, feeding, pressure and temperature control), allowing a continuous operation and data acquisition along the experiments. Temperature control included several temperature measurement points (type K thermocouples). Figure 2.6 shows a picture of the experimental rig, while Figure 2.7 depicts a schematic representation of the experimental installation.

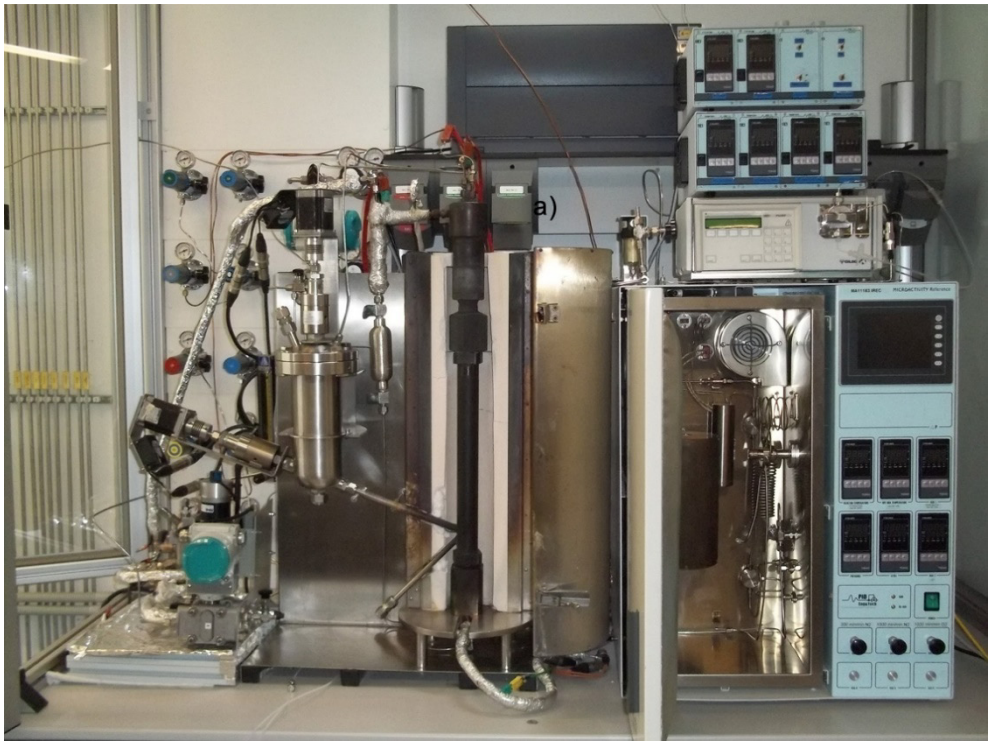

Figure 2.6 Picture of the laboratory-scale gasification system

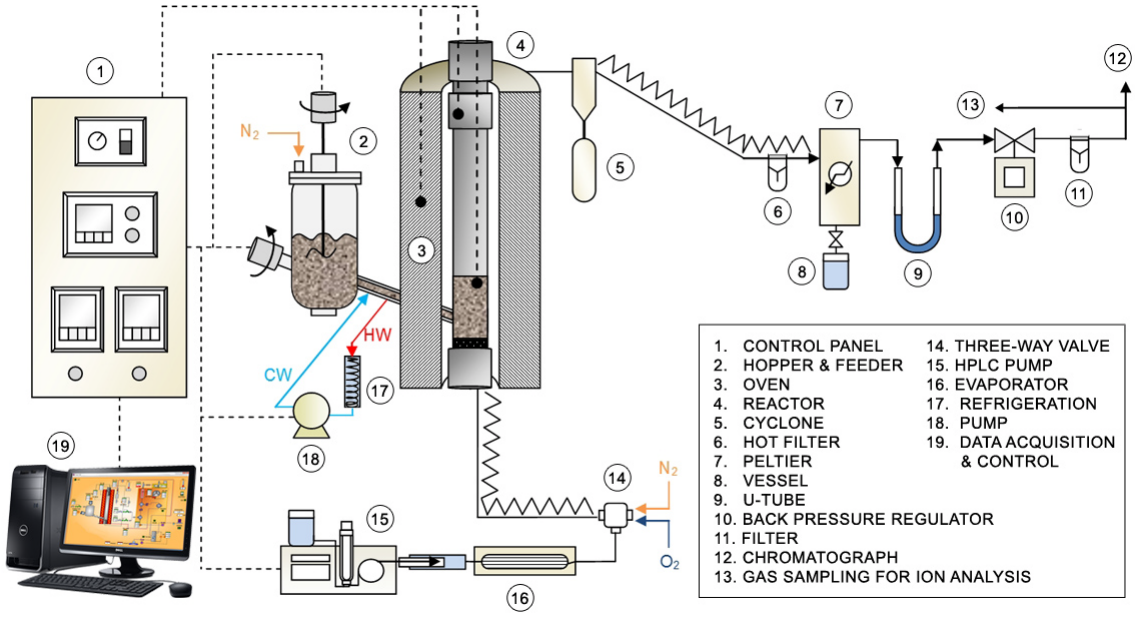

Figure 2.7 Scheme of the gasification setup

The system was able to operate at temperatures of up to 900 ºC and pressures of up to 20 bar. The body of the reactor consisted in a Hastelloy X pipe divided in two zones:

- Reactor zone: 404 mm long and 23.8 mm internal diameter
- Freeboard zone: 122 mm long and 50.8 mm internal diameter

Temperature control was carried out using K-type thermocouples placed in each zone. At the bottom of the reactor zone, a porous plate (25 µm) supported the bed material.

2.4.1.2 Furnace

The reactor was externally heated with an electrical furnace using two heating zones (Watlow ceramic fiber heaters). The maximum heating power of each zone was 2500W and 900W for the reactor and freeboard, respectively. Both zones were thermally insulated to reduce heat loss.

2.4.1.3 Solid and gas feeding system

The feeding system consisted of a hopper (with a stirrer) and a screw feeder (with a cooling water jacket).

The hopper had a volume capacity of about 1 liter and is equipped with a stirrer with two open blades that assured a continuous agitation of the material inside the hopper and a correct feeding. A small inlet of nitrogen (max. 300 NmL/min) was used to facilitate the feeding and prevent counterflow of gas from the reactor.

The screw feeder (330 mm long and 8 mm diameter) is operated with a MAE motor, which allows the variation of both the speed rate (rotational velocity) and the spin of the motor (clockwise or counterclockwise). The screw can be operate at a feeding rate up to 0.1 kg/h. In addition, the excess of heat in the screw feeder was restrained by a cooling system. The screw cooling system consisted of a capillary tubing (1/16") with a continuous flow of cold water (~5 ºC) from a LAUDA cooling bath.

The gases (O2, N2, steam) were introduced at the bottom of the reactor at a temperature of 400 ºC by means of a heating line with an electric resistance of 650W/220V. All gases were previously mixed inside a heating box set at 80 ºC.

The heating box together with other instrumentation were placed in the control panel box.

For steam gasification tests, Milli-Q water was pumped into the steam generator using a GILSON 307 HPLC pump able to work up to 5 mL/min and 140 bar. The evaporator, also inside the heating box, consisted of a cylindrical heater (800W/220VAC) able to operate up to 450 C.

2.4.1.4 Gas cleaning system

Particulates and condensable products were removed of the producer gas using a series of conditioning steps.

The solid removal system consisted of a cyclone and a filter, both instruments were heated to avoid condensation of liquids (water and tar), which were collected after the run. The cyclone (150 mm long and 21.8 mm internal diameter) was coupled to a cylindrical deposit to collect the solid products. The hot filter (40 µm stainless steel, Classic Filters Ltd.) retained the finest particles.

The liquid products were collected in two condensers or cold traps, a peltier system and a U-tube (1/2" and 200 mm long). The deposit of the peltier system, with a capacity of 75 mL, was controlled by a differential pressure level transmitter (SITRANS P). The U-tube, packed with stainless steel mesh, was cooled down using a mixture of ice and water in a dewar container. Finally, the gas flowed through a flowmeter (Bronkhorst High-Tech) for measuring the gas flow rate. Afterwards, the gas composition was analyzed by gas chromatography. Note that in some experiments, for the analysis of minor contaminants, a fraction of the syngas was collected in a 25 L Tedlar® gas sampling bag coupled after the hot filter (in air gasification runs) or after the cold trap (in oxygen/steam gasification conditions).

Other experimental conditions (i.e. gas flow rates) varied among experiments and are detailed in each particular study (Chapters 4-7).

2.4.2 Gas and tar analyses

2.4.2.1 Major gas composition

The major compounds of the produced gas were quantified by means of an online micro gas chromatograph (Agilent 490 micro GC). Some practical advantages of a micro GC are the reduction of both the instrument size and the total analysis time compared to conventional gas chromatography techniques.

The micro GC configuration included three analytical GC channels using up to two different types of carrier gas. Channel 1 was equipped with a 10 m Molecularsieve 5A column set at temperature of 100 ºC and using Ar as carrier gas. The second channel consisted on a 10 m PoraPLOT Q column operating at 80ºC, whereas Channel 3 used a 10 m Al_2O_3 column at 80 ºC. Channel 2 and 3 used He as carrier gas. Injection was carried out with a micro-machined injector (injection volumes from 1 µm to 10 µm software-selectable) and detection in each channel was performed with micro-machined thermal conductivity detectors. The injection time was 30 seconds and total analysis time was less than three minutes.

Permanent gases (H_2, O_2, N_2, CO and CH_4) except CO_2 were analysed on channel 1, CO_2 and C_1-C_3 hydrocarbons were analysed on channel 2 and hydrocarbons up to C_5 were analysed on channel 3.

The micro GC was calibrated before the beginning of each run using several certified gas standards (Table 2.2).

Table 2.2 Gas mixtures (% mol) used for micro GC calibration

Standard 1	**Standard 5**	**Standard 6**
34% N_2, 20% H_2, 5% CH_4, 15% CO, 20% CO_2, 2% C_2H_4, 3% C_2H_6, 1% C_2H_2	5% N_2, 9% H_2, 1% CH_4, 5% CO, balance He	1% C_2H_4, 1% C_2H_6, 0.5% C_2H_2, 1% C_3H_8, 1% C_3H_6, 2% C_3H_4, 2% C_4H_{10}, 0.5% N_2, balance He

2.4.2.2 Minor contaminants analysis

This section describes the methodology for the assessment of inorganic traces in the syngas, including hydrogen sulfide (H_2S), hydrogen cyanide (HCN), hydrogen chloride (HCl) and ammonia (NH_3). These minor contaminants were measured in liquid state by means of ion potentiometry through ion selective electrodes (ISEs, Metrohm). Although this method can be subjected to

interferences between ions, it is an attractive approach in comparison to other costly analytical methods [2]. Alternative approaches were evaluated such as the use of Dräger tubes or ion chromatography (IC), however the potentiometric method was chosen based on costs, detection range and the available equipment in the laboratory.

For the minor contaminants analysis, a fraction of the producer gas was collected in a tedlar bag during the gasification experiments for a certain period of time (approximately 30 minutes). As the contaminants were measured in liquid state by ISEs, the collected gas was forced to pass through a series of impingers (or bubblers) containing specific solutions (Table 2.3) to retain the respective ions (S^{2-}, CN^-, Cl^- and NH_4^+). The gas sampling system (or gas bubbling system) is depicted in Figure 2.8. Three drechsel flasks were used as impingers (HCl and NH_3 utilized the same flask and absorbing solution) inside a cooling bath containing ice and water for better ion retention. Each bubbler was connected individually to the gas sampling bag and the exit of the flask to a filter (a glass tube with cotton) to avoid downstream contamination in the flowmeter (Swagelok® VAF-GM-06M-Z) and the vacuum pump (N 86 LABOPORT®). The gas was pumped through the system at a constant flow of 1 NL/min for 5 minutes and finally it was exhausted to a fume hood.

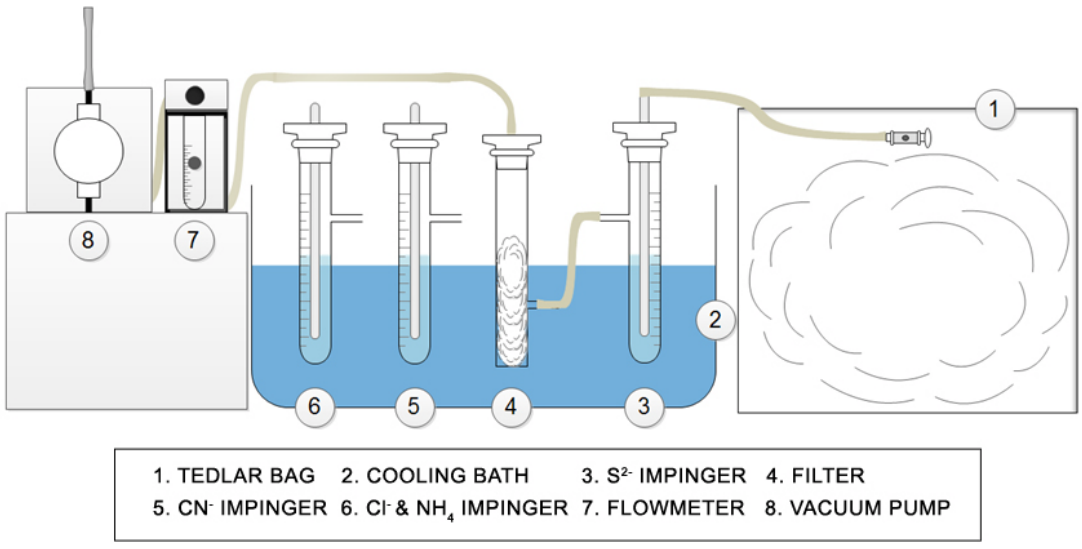

Figure 2.8 Gas bubbling system

Additionally, when steam was used as gasification agent, the liquid collected in the condensers was also analysed by ISEs since it may have retained part of the inorganic compounds of the gas. In those cases, samples of 1 mL of the liquid from the condensers were filtered with a syringe filter (CHROMAFIL® Xtra. PTFE-45/25) and diluted into 50 mL of Milli-Q water.

The ion analyses of the sample solutions were performed with a 905 Titrando and an 814 USB Sample Processor (Metrohm) equipped with *tiamo*™ software for direct potentiometry. An advantage of this equipment was the use of the sample processor controlled by PC. Several methods were developed in the control software in order analyse all samples almost fully automatically.

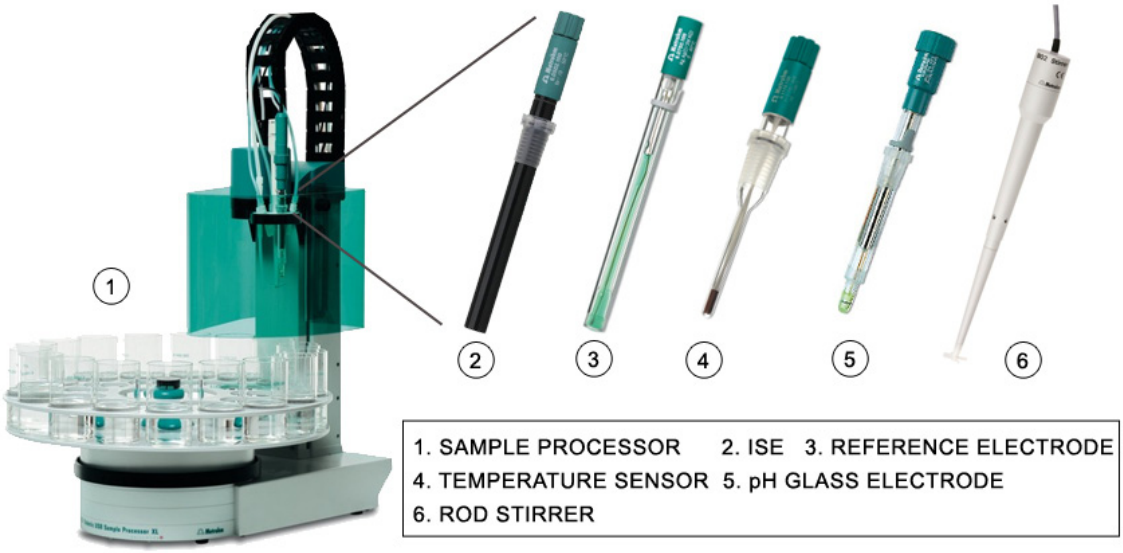

Figure 2.9 ISE analysis equipment. Adapted from Metrohm.com

The setup shown in Figure 2.9 consisted of a specific ISE and an Ag/AgCl reference electrode containing electrolyte solution (i.e. KCl 3M) connected to the sample processor. Additionally, temperature and pH were controlled with a PT1000 temperature sensor and pH glass electrode, respectively, and a rod stirrer assured a continuous stirring of the samples. Samples were placed in beakers filled up to 50 mL and each solution was analysed at least by triplicate. Table 2.3 gathers the main characteristics for the ion measurements.

Table 2.3 Characteristics of the ion selective electrode measurements

ISE	Absorbing solution (mL)	Calibration solutions (ppm)	Reference electrolyte	TISAB solution	pH range
S^{2-}	50 % Milli-Q water + 50 % SAOB	0.1, 1, 10 and 100	KCl 3 M	NaOH 10 M	2 - 12
CN^-	100 % NaOH 0.1 M	0.2, 2, 20 and 100	KCl 3 M	NaOH 10 M	10 - 14
Cl^-	100 % Milli-Q water	1.8, 10, 50 and 100	KNO_3 1 M	$NaNO_3$ 5 M	0 - 14
NH_4^+	100 % Milli-Q water	0.1, 5, 50 and 100	No needed	NaOH 10 M	11 - 14

SAOB: Sulphide Anti-Oxidant Buffer. TISAB: Total Ionic Strength Adjustment Buffer

Prior to the analyses, ISEs were calibrated and sample solutions were conditioned. The electrodes were calibrated using standard stocks of 1000 ppm in order to obtain a linear calibration curve for each ion concentration determination. The ionic strength and pH value of the samples were fixed by adding about 0.1 mL of Total Ionic Strength Adjustment Buffer (TISAB). Note that HCN and NH_3 samples must be in basic conditions (pH $\geq$10) for a correct ion determination.

Some considerations about this method are that measurements must be carried out at the same conditions of temperature and pH as the calibration standards in order to guarantee reliable results. Also ion interferences, mainly CN^- with S^{2-} and Cl^- to a lesser extent, can lead to inaccurate results. For this reason major interferences were minimized as a result of using different absorbing solutions to retain each ion. In addition, a preliminary study using several ion mixtures was carried out in order to assess the influence of these interferences, leading to errors below 10% at the studied concentration levels. Table 2.4 shows, as an example, the obtained values during one of the ion interference tests.

Table 2.4 Results of some ion interference tests

ISE	Sample matrix in 50 mL	Average concentration of analysed ion (ppm)
S^{2-}	S^{2-} (10 ppm), CN^-, Cl^- and NH_4^+ (1 ppm)	8.7 ± 0.1
CN^-	CN^- (10 ppm), S^{2-}, Cl^- and NH_4^+ (1 ppm)	10.4 ± 0.1
Cl^-	Cl^- (100 ppm) and S^{2-} (1 ppm)	108.8 ± 1.0
NH_4^+	NH_4^+ (10 ppm) and Cl^- (1 ppm)	9.0 ± 0.3

Therefore the direct potentiometric measurements based on ISEs was a reliable approach for estimating the concentration of minor contaminants.

The ion analysis of the bubbled solutions was carried out following the order showed in Table 2.3. S^{2-} bubbled solution was analysed in first place in order to avoid oxidation of sulphides, despite the addition the SAOB for this purpose. The following solution was the one containing CN^- as it was measured using the same reference electrode as the previous ISE. Cl^- and NH_4^+ solutions were analysed afterwards. Note that NH_4^+ electrode needed to be conditioned in water for 10 minutes between analyses, increasing the analysis time up to 15 minutes per sample.

2.4.2.3 Tar analysis

Tars collected during gasification were analysed by several techniques described as follows:

Gas chromatograph with a flame ionization detector (GC-FID)

Quantification of polycyclic aromatic hydrocarbons (PAHs) in tar samples was carried out in an Agilent Hewlett Packard 6850 GC-FID (gas chromatograph with a flame ionization detector) with an automatic sampler (7683B). A high-temperature capillary column (DB-5 phase, 15 m length, 0.32 mm i.d., 0.1 mm film thickness) was used with He as carrier gas at a flowrate of 1 mL/min. The injector and detector temperatures were set at 275 ºC and 325 ºC, respectively, while the oven temperature program started at 40 ºC (held for 2 min) with a posterior ramp of 10 ºC/min to 280 ºC, and a final ramp of 15 ºC/min up to 320 ºC (held for 2 min).

A standard with 16 PAHs (EPA 610 PAH Mix) was used for calibration and peak identification of the compounds present in tar samples. Each tar sample was dissolved in chloroform or dichloromethane and 1 µL of the solution was injected with a split ratio of 100:1. Three separate analyses were performed from each sample in order to check the reproducibility of the results.

Size-exclusion chromatography (SEC)

An Agilent Technologies 1100 Series HPLC system was used to perform the size exclusion analysis of tar samples. Three (300 mm long, 7.5 mm i.d.) polystyrene/polydivinylbenzene-packed columns (PL Gel 104 Å 5µm, PL Gel 500 Å 5µm and PL Gel 50 Å 5µm) were used (Polymer Laboratories, Church Stretton, UK).

The system operated at 80 °C using N-Methyl 2-pyrrolidinone (NMP) as the mobile phase at a flow rate of 0.5 mL/min. Detection was carried out using a diode array UV-absorbance detector. As NMP is opaque at 254 nm, detection of standard compounds and tar samples was performed at 270, 300, 350 and 370 nm, where NMP is partially transparent. The results obtained at 300 nm were considered representative of the main trends observed at all wavelengths.

System calibration was carried out using two sets of standards, PS standards calibration was applied to the 30-52 min time range, while PAHs calibration was used in the 52-62 min region.

Fourier transform infrared spectroscopy (FTIR):

The structural features of the tar compounds were analysed using FTIR (Fourier transform infrared) spectroscopy, performed in a Bruker Vertex 70 spectrometer equipped with Platinum diamond ATR unit. Tar spectra were collected at room temperature in the range 400-4000 cm^{-1} by co-addition of 32 scans at a nominal resolution of 4 cm^{-1}, taking the spectrum of the empty cell at ambient conditions as the background.

2.4.3 Other equipment

The gasification system rig and gas analyses setup were the principal equipment used during gasification runs. Additional equipment for processing and analysing are listed in Table 2.5.

Table 2.5 Equipment used in for sample processing and analyses

Purpose	Equipment	UNE standard method
Milling	Retsch Cutting Mill SM 100 and Retsch Ultra Centrifugal Mill ZM 200	SRF: EN-15413:2010
Sieving	Cisca Siever shaker RP 200 N	-
Ultimate analysis	LECO TruSpec Micro Elemental Serie	Biomass: CEN/TS 15104:2005 SRF: EN 15407:2011
Proximate analysis	LECO TGA701 Thermogravimetric Analyzer	Biomass: EN 14775:2009 SRF: EN 15402:2011 and EN-15403:2011
Calorific value	LECO AC600 Semi-Automatic Calorimeter	Biomass: EN 14918:2009 SRF: EN 15400:2011
Ion chromatography	Dionex ICS-1100 Ion Chromatography	Biomass and SRF: EN 15408:2011
Ash digestion	Berghof Microwave Digester Speedwave Four	SRF: EN 15410:2006 and EN 15411:2006
Ash composition	Spectro Arcos 165 spectrophotometer	-
Tar recovery	Büchi Rotavapor® R-210	-

2.5 Experimental procedure

This section describes a typical gasification experiment, although specific conditions (i.e. gas flow rates) can be found in each experimental study (Chapters 3-7).

The preparation of the gasification system to run an experiment took several hours. All parts of the experimental rig had to be well-assembled in order to avoid gas leaks. Leaks were checked by pressurizing the system with nitrogen before the experiments. Furthermore, the gas analysis equipment (micro GC and ISEs) were calibrated prior to each gasification test by using standards as previously explained (section 2.4.2).

To begin, a certain amount of feedstock (~100 g) was placed in the hopper, and both solid stirring and feeding screw were set to the desired feed rate. The gasifier was filled with ca. 50 g of bed material (sand, dolomite or olivine) fluidized on a stream of nitrogen during the heating period up to the final gasification temperature (usually 750-850 ºC). Once the desired temperature was reached, the fluidization gas flow was switched from N_2 to the chosen gasification agent. As well, a small stream of (50 NmL/min) was used in the hopper. At this point, if needed, the gasification system was pressurized. As

soon as the system was stable, the solid and gas feeds were switched on. A constant gas composition was reached after about 5 min of starting the feeding for biomass samples, whereas 7-10 minutes were needed for SRFs. This is the gas composition reported in this work. The experiment length was about 60 min for all performed tests.

Afterwards, the entire setup was disassembled and cleaned thoroughly not only to collect the liquid and solid products but also to remove all tar (condensable hydrocarbons). The setup (tubing and accessories such as cyclone, peltier, filter, u-tube, etc.) was cleaned with solvent (a 4:1 mixture in volume of chloroform:methanol or dichloromethane:methanol), rinsed with acetone and dried with air or nitrogen.

2.5.1 Operational observations and modification of the experimental setup

This section presents the main drawbacks experienced during the experimental runs and the modification carried out in the experimental setup.

2.5.1.1 Solid feeding system

The screw feeder needed to be calibrated in order to determine the screw rate (setpoint value in the control panel) for a continuous feeding rate (g/min) into the reactor. A calibration curve was obtained for each feedstock. Despite the calibration curve and given the complexity of waste-derived fuels, the feeding rate slightly varied during gasification tests. As stated, gasification of waste-derived fuels was more problematic than biomass tests due to melting of plastics or adhesive materials, which eventually clogged the screw. For this reason the experimental system was modified including a more efficient cooling jacket for the feeding screw. Due to the characteristics of biomass, biomass samples did not present any issue during the first part of the experimental program. Furthermore, it is important to remark that the accuracy of the feeding rate during the experiments is key as it determines the equivalence ratio during the gasification experiments. In fact, the amount of gasification feedstock fed into the reactor could be only determined after the experiment by weighing the quantity of feedstock left in the feeding system (hopper and screw).

Therefore the feedrate accuracy was complex to control, requiring multiple experimental runs to achieve the desired equivalence ratio.

Nonetheless, torrefaction of waste-derived fuels led to a significant improvement on the solid feeding rate, achieving higher feed rates at low setpoints of the screw feeder than those obtained with raw materials. Figure 2.10 shows an example of calibration curves obtained for biomass and SRFs.

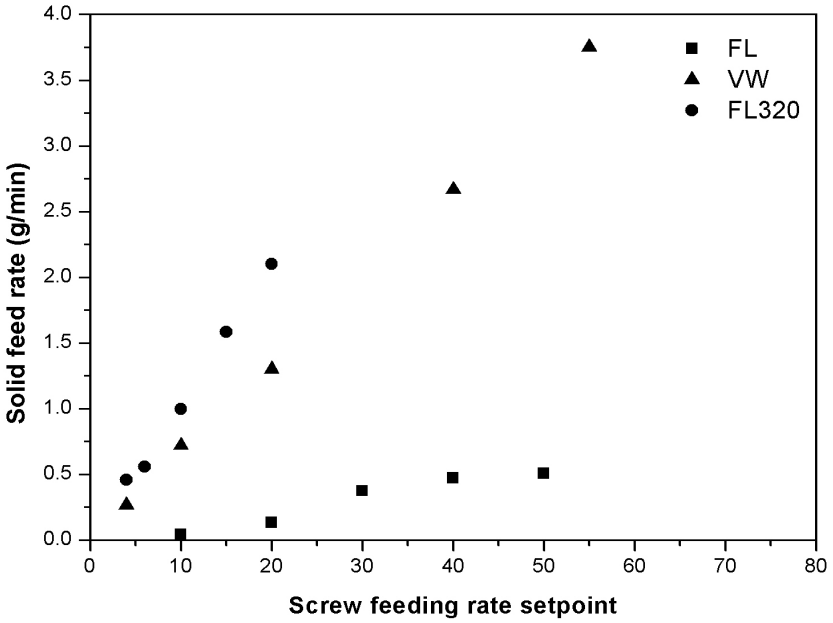

Figure 2.10 Screw feeding calibration curve for different solid fuels

Note that biomass (VW in this case), even when not pretreated, achieved an adequate solid feed rate at low screw feed rates. On the other hand, a low density SRF such as FL was more difficult to feed even at high screw feed rates, leading to an excess of heating of both screw and solid fuel during gasification tests. However, a positive effect of torrefaction, not shown in experimental results, was observed for torrefied FL. FL320 was easier to feed in the reactor by the screw feeder, increasing considerably the solid feeding rate at low screw setpoints.

2.5.1.2 Fluidized bed reactor

As stated in the previous part, the gasification setup suffered some modifications along the experiments. The first biomass and SRF experiments (Chapters 3-5) were performed with the gasifier shown in Figure 2.6, divided in

two zones (reactor and freeboard). A joint coupling ring sealed both zones, however the elevated working temperatures resulted in a deformation of the joint, provoking gas leaks. The replacement of the joint temporarily fixed the problem for a series of runs but finally the reactor suffered a severe deformation. At this point the reactor was redesigned. A new freeboard zone was welded to the reactor body, ending the top of the reactor with a flange. Additionally, the screw cooling system was improved by adding a double jacket for cooling. These modifications resulted in several months of delay, affecting the experimental schedule of this project.

The modified gasifier (Figure 2.11) had the following dimensions: 450 mm long and 23.8 mm internal diameter. The new design of the freeboard kept similar residence time of the gas than the previous reactor in order to obtain comparable data.

Figure 2.11 Modified fluidized bed reactor setup

2.6 Data analysis

This section explains the methods followed to calculate experimental data. All data were analysed in developed Microsoft Excel spreadsheets.

2.6.1 Fluidizing velocity and gas residence time

For all experiments, operation flows provided a fluidizing gas velocity between 3 and 7 times the minimum fluidizing velocity (U_{mf}) for the studied bed materials (particle sizes of 150-200 μm). An average of four times the U_{mf} is commonly applied for fluidized bed reactors [1], leading to a bubbling fluidized bed regime. In our system, the gas residence time in the reactor was between 2 and 3 seconds.

2.6.2 Equivalence ratio (ER)

The equivalence ratio (ER) is defined as the actual oxygen to fuel ratio divided by the stoichiometric oxygen to fuel ratio required for complete combustion [3]. Eq 2.1 shows the formula to calculate ER, where m represents the mass flow rate [kg/h].

$$ER = \frac{\left(m_{oxygen}/m_{fuel\,dry}\right)_{actual}}{\left(m_{oxygen}/m_{fuel\,dry}\right)_{stoichiometric}} \qquad \text{Eq. 2.1}$$

At a fixed ER and fluidizing velocity (around $4\times U_{mf}$), the oxygen and solid fuel rates were calculated to obtain the desired ER.

2.6.3 Mass balances

Material balances of experiments were calculated considering the mass of inputs (solid fuel and gases) introduced in the gasifier and the mass of outputs (solids, liquids and gas) produced during gasification.

The amount of fuel fed into the reactor was calculated from weight of solid fuel in the hopper before and after the experiment, whereas the introduction of gases was controlled and measured by volume flow controllers [NmL/min].

Mass balance of outputs was calculated taking into account the weight of collected liquids (i.e. water and tar), solids products (i.e. char and ash) and mass of gases (determined through gas composition).

Gas measurements are given on dry basis (unless stated otherwise). Gas flow rate and composition were determined using a flowmeter and a micro GC, respectively. Apart from the value obtained from the flowmeter, gas flow rate was double checked by N_2 balance.

Note that for all conducted experiments, adequate mass balance closures (> 95%) were obtained.

2.6.4 Solid fuel and gas heating value

The solid fuel heating value was calculated by means of a bomb calorimeter (Table 2.5) which directly provided the gross calorific value (or higher heating value, HHV). The calculation of net heating value (or lower heating value, LHV) was estimated with Eq. 2.2 [4], considering values obtained in the calorimeter, ultimate and proximate analyses.

$$LHV_{fuel}[kJ/kg] = HHV_{fuel} - [(9 \cdot \%H_2) + \%H_2O] \cdot 22.4 \qquad \text{Eq. 2.2}$$

HHV : higher heating value of solid fuel [kJ/kg]

$\%H_2$: weight percentage of hydrogen

$\%H_2O$: weight percentage of moisture

The LHV of producer gas was calculated using Eq. 2.3 and taking into account gas components analysed by GC. LHV values for gas compounds were obtained from [5].

$$LHV_{gas}[kJ/Nm^3] = \sum_n \frac{(m_n \cdot \frac{LHV_n}{MW_n})}{V_{gas}} \qquad \text{Eq. 2.3}$$

n :H_2, CO, CH_4 and light hydrocarbons up to C_5.

m : weight [g]

LHV: Lower heating value [kJ/mol]

MW_n : Molecular weight [g/mol]

V_{gas}: Volume of gas produced during experiment [Nm^3]

2.6.5 Carbon conversion

The conversion of carbon (X_c) in the reactor was calculated from experimental results based on gas analysis and fuel feeding rate (Eq. 2.4). Carbon conversion determines the ratio of carbon leaving the reactor in gas phase in relation to the amount of carbon introduced with the solid fuel.

$$X_c\,[\%] = 100\,\frac{C_{gas}}{C_{fuel}} \qquad \text{Eq. 2.4}$$

C_{gas}: *Carbon in the form of gaseous products in the gas [kmol/h]*

C_{feeed}: *Carbon introduced with the feedstock [kmol/h]*

2.6.6 Minor contaminants concentration

The concentration of minor contaminants in the producer gas (Eq. 2.5) is calculated from data obtained during gas sampling and ISE analyses, as stated in section 2.4.2.

$$C_i\,[mg/Nm^3] = \left(\frac{C_{ion}\cdot V_{solution}}{t\cdot F}\right)\frac{MW_i}{MW_{ion}} \qquad \text{Eq. 2.5}$$

i : H_2S, HCl, HCN and NH_3.

C: Concentration of bubbled solution [ppm]

ion: S^{2-}, Cl^-, CN^-, NH_4^+

$V_{solution}$: Volume of absorbing solution volume [mL] (i.e. 100 mL)

t: Bubbling time [min] (i.e. 5 min)

F: Bubbling flow rate [NL/min] (i.e. 1 NL/min)

MW: Molecular weight [g/mol]

For oxygen-steam gasification experiments, when liquid from condensers was analysed, the concentration of minor contaminants comprises the sum of Eq. 2.5 and Eq. 2.6.

$$C_i\,[mg/Nm^3] = \left(\frac{C_{liquid}\cdot D\cdot V_{liquid}}{V_{gas}}\right)\frac{MW_i}{MW_{ion}} \qquad \text{Eq. 2.6}$$

i : H_2S, HCl, HCN and NH_3.

ion: S^{2-}, Cl^-, CN^-, NH_4^+

C_{liquid}: Concentration of liquid sample from condenser [ppm]

D: Dilution factor (e.g. 50, for 1 mL of sample from 50 mL) [-]

V_{liquid}: Volume of liquid collected after experiment [mL] (e.g. 50 mL)

V_{gas}: Volume of gas produced during experiment [Nm^3]

MW: Molecular weight [g/mol]

2.6.7 Error estimation of experimental data

To assess the experimental repeatability, each test was performed at least by triplicate with uncertainties estimated at a 95% confidence level (Eq. 2.7) [6].

$$sample\ mean \pm z_{0.025} \cdot \frac{S}{\sqrt{N}} \qquad \text{Eq. 2.7}$$

S: Standard deviation of samples

z : critical value of the standard normal distribution

N: Number of samples

2.7 References

[1] Kunii D, Levenspiel O, Brenner H. Fluidization Engineering. Elsevier Science; 2013.

[2] Brown RC, Norton G, Suby A, Smeenk J, Cummer K, Nunez J. Biomass-Derived Hydrogen from a Thermally Ballasted Gasifier. Proc 2002 US DOE Hydrog Progr Rev 2002:1–20.

[3] Meng X, de Jong W, Fu N, Verkooijen AHM. Biomass gasification in a 100 kWth steam-oxygen blown circulating fluidized bed gasifier: Effects of operational conditions on product gas distribution and tar formation. Biomass and Bioenergy 2011;35:2910–24. doi:10.1016/j.biombioe.2011.03.028.

[4] Kreith, F. and Goswami YD. Handbook of Energy Efficiency and Renewable Energy. Change 2007:1–22. doi:10.1201/9781420003482.

[5] Higman C, van der Burgt M. Gasification (Second Edition). Gasif. (Second Ed., Burlington: Gulf Professional Publishing; 2008, p. 1–9. doi:http://dx.doi.org/10.1016/B978-0-7506-8528-3.00001-8.

[6] Devore JL, Farnum NR, Doi JA. Applied Statistics for Engineers and Scientists. Cengage Learning; 2013.

3. PRESSURIZED GASIFICATION OF TORREFIED WOODY BIOMASS

Abstract

This work reports experimental results concerning the influence of torrefaction level and pressure on product yields and composition during fluidized bed O_2/steam gasification of two different raw biomasses. The results show an increase on gas yield with pressure and torrefaction level for both types of biomass considered. Increasing pressure caused the produced gas composition to shift towards higher CH_4 and CO_2 content, while H_2 and CO levels decreased. The effect of the type of original biomass on gas composition was limited, and became less relevant as pressure and torrefaction level increased. The analysis of the tars produced during gasification also revealed that higher pressures led to the increase of tar yields. On the other hand, torrefaction level presented the opposite effect, with lower tar yields and lighter molecular weight distribution of tars as torrefaction level increased. Since torrefaction is being considered as a promising pre-treatment technique for upgrading biomass to a higher quality solid fuel more suitable for the integration of gasification into biofuels production, the results from this study are relevant for evaluating the influence of the level of torrefaction on the performance of gasification under typical operating conditions in practical applications.

This chapter is based on the following research article:

Berrueco C, Recari J, Güell BM, Alamo GD. Pressurized gasification of torrefied woody biomass in a lab scale fluidized bed. Energy 2014;70:68-78. http://dx.doi.org/10.1016/j.energy.2014.03.087.

3.1 Introduction

Nowadays, concerns about climate change effects and depletion of fossil fuels have drawn attention to find alternatives and more environmentally-friendly ways of energy supply. Some of the major issues for fossil fuels are their non-renewable nature and the problems related to the release of pollutants (mainly CO_2, NO_x and SO_x) into the atmosphere [1], enhancing the global warming effect [2]. Despite that, fossil-derived fuels are the most common energy sources used in the world, reporting over 80% of the total energy consumption [3]. However, substantial efforts are being made on the development of alternative renewable energy sources that can replace the aforementioned fossil-derived fuels. In this context, biomass is reaching more positions and becoming one of the most widely used renewable energy sources. Biomass supplies about 15-20% of the total fuel use in the world [4], being currently the fourth largest resource of energy worldwide just after coal, oil and gas [5]. One of the main advantages associated with biomass is its conventional neutral CO_2 impact, when produced in a sustainable manner. Furthermore, among all renewable energies, biomass is the only storable and transportable source and the only renewable source of carbon, hydrogen and oxygen, which makes it a prime feedstock for production of multiple bio-based products within the next 20-30 years. In this scenario, biofuels, particularly for the aviation and heavy-duty trucks, have been recognized as one of the main pieces in the bioeconomy puzzle, as these transport sectors are not likely to be electrified in the coming decades and biofuels is thus the only near-medium term alternative to fossil-derived [6, 7].

Despite the great potential of biomass, its use presents also a series of challenges. Two main limitations are the space needed to grow it and the expensive cost of transportation due to its low energy density [8]. Other drawbacks are high oxygen and water content, and hydrophilic properties [9].

A pretreatment stage prior to biomass conversion is needed in order to minimize some of the abovementioned drawbacks. In this context, torrefaction seems to be an effective option. Torrefaction is a thermochemical process that subjects the biomass at a temperature in the range of 200-320 ^{o}C in an inert atmosphere achieving a higher energy-dense product (almost moisture free) which is more feasible for transport. Besides, previous studies have shown other

advantages of this technology, i.e., the fact that not only improves energetic value but also enhances feedstock homogeneity, grindability and hydrophobicity [10-14].

Another key aspect when evaluating the use of biomass as energy source is the conversion technology. Biofuels can be produced from a broad spectrum of conversion processes (biological, thermal and physical processes). Among the thermochemical conversion technologies, gasification is perceived as the most promising pathway to improve the efficiency in the use of biomass towards liquid fuels [8, 15].

Biomass gasification has been exhaustively studied [8,16-19], particularly regarding the producer gas composition and heating value. The syngas composition can be influenced by several process parameters such as feedstock composition and particle size, gasification conditions, mainly temperature, equivalent ratio (ER), steam-to-biomass ratio and pressure [16,19], but also by the gasification reactor design.

With regards to temperature, Gil et al. [17] studied the gasification of pine chips with steam-oxygen mixtures in a fluidized bed gasifier varying the temperature from 780 to 890 ºC. The study concluded that the increase of bed temperature leads to an increase in H_2 content, H_2/CO and CO/CO_2 ratios, together with higher thermal efficiencies of the process. Other studies on fluidized bed gasification of woody biomass [20-24] also have concluded that the introduction of steam was favorable to improve gas quality and that higher temperatures favored both hydrogen production and gas yield. However, it was stated that gasification temperatures above 850 ºC decreased the gas heating value, mainly due to the reduction of CO, CH_4 and C_2 hydrocarbons in the produced gas.

Mayerhofer et al. [25] studied the gasification of wood pellets in a bubbling fluidized bed (BFB) varying several operating conditions (temperature, pressure and steam to biomass ratio (S/B)). The results showed that high temperatures (750–840 ºC) promoted the formation of H_2, while CH_4 and CO_2 content decreased. Additionally, higher S/B ratios shifted the gas composition to higher concentrations of H_2 and CO_2 and lower contents of CO and CH_4 in the produced gas, which can be explained qualitatively with the enhanced water gas shift reaction. Lastly, pressure had a significant effect on the effluent gas

composition [25]. For comparable temperatures and S/B, and increase in gasification pressure led to higher CH_4 content due to the enhancement of the methanation reaction at high pressures, together with a slight increase in H_2 content, and lower CO/CO_2 ratios.

The bibliographic revision denotes that although gasification is influenced by several other parameters, the two principal studied parameters have been temperature and ER. This fact evidences a lack of studies related to the effect of pressure and biomass feedstock properties (influenced by (i) feedstock nature and (ii) thermal pretreatments such as torrefaction level) on syngas composition.

The goal of this paper is to study the influence of pressure and biomass composition (by the gasification of two different biomasses at three different torrefaction levels: raw biomass, Lightly-torrefied and Significantly-torrefied), on product yields and composition during fluidized bed O_2/steam gasification. The obtained results will allow the evaluation of gasification performance in order to determine optimal operation conditions. Notice that the information here presented has been obtained in a lab-scale gasifier, and although the main trends and conclusions of this study can be useful to give insight to the gasification of torrefied biomass, the actual numbers could be different in an industrial scale gasifier.

3.2 Experimental

3.2.1 Sample characterization and preparation

Norwegian spruce and Norwegian forest residues (mainly tops and branches), hereby referred as VW and GROT respectively, were obtained from local sources in Trondheim, Norway. The original biomasses were treated at two different torrefaction levels: Lightly-Torrefied LT (final torrefaction temperature of 225 ºC) and Significantly-Torrefied ST (final torrefaction temperature of 275 ºC). The raw samples and torrefied products were sieved to a particle size range of 250 to 500 µm. The proximate and ultimate analyses were carried out using a LECO Thermogravimetric analyzer (TGA 701) and a LECO TruSpec CHN-S-O analyser respectively. The proximate analyses of all samples were conducted following the ASTM D7582 standard test method for moisture,

volatile matter, and fixed carbon determination. The results together with the lower heating values (LHVs) are included in Table 3.1. The determination of the heating value of the samples was performed in an isoperibol LECO Automatic calorimetric bomb (AC600), according to the ASTM D5865-07standard test method. After each measure the bomb was washed out with a 0.2 M KOH solution to recover sulphur (H_2SO_4), halogens (HCl, HF, HBr) and phosphorous (H_3PO_4), which were measured afterwards by ionic chromatography (Dionex ACS 1100) according to the EN-15408:2011 standard method.

3.2.2 Setup and procedure for torrefaction

Torrefaction experiments were performed using a bench-scale continuous reactor consisting in four independent horizontal conveyors positioned in parallel from top to bottom. Each conveyor consisted in a horizontal pipe (i.d.: 100 mm) with a screw-conveyor that allowed a precise control of temperature and residence time of the different stages. Drying, heating and cooling conveyors had a length of 700 mm, whereas the torrefaction conveyor was 1000 mm long. The reactor, capable of operating at temperatures of up to 300 ºC, had a capacity of 0.2-7.0 kg/h of biomass in size range of 1-25 mm. The feedstocks were first ground and afterwards compressed to produce pellets of 6 mm diameter without adding binders. These pellets were fed from the storage hopper to the first conveyor by a feeding screw, after that the fed material passed through the screw conveyors for drying, heating to torrefaction temperature, torrefaction and cooling and finally left by gravity to a collecting vessel. Notice that the material was transferred between conveyors using pneumatically controlled sliding valves. The conveyors were temperature controlled using electrical heating elements with the exception of the last one, where torrefied material was cooled using a water jacket. In order to ensure inert conditions and remove the volatiles, each part of the reactor (including the hopper and the collecting container) was purged with a nitrogen flow of about 8 NL/min.

Feeder and screws were driven by individual motors allowing for basically independent setting of mass flow (feeder setting) and residence time (screw

setting). However, since the filling degree of the screws was limited, the settings were not fully independent from each other.

3.2.3 Fluidized bed gasifier

Gasification experiments were conducted on a laboratory-scale pressurized fluidized bed reactor (PID Eng&Tech, Spain). The experimental rig was equipped with a complete control system including, flow control, feeding system control, pressure control, together with several temperature measurement points, temperature control inside the fluidized bed and freeboard. The body of the reactor consisted in a 404-mm-long (23.8 mm internal diameter) Hastelloy C pipe, capable of operating at pressures of up to 20 bar and temperatures of up to 900 °C. The solid fuel was continuously fed into the bed by means of a screw feeder, at feed rates from 0.2 to 5 g/min. Water flow was pumped into the steam generator using a GILSON HPLC pump (0-5 ml/min range) before it was injected in the reactor. The product gas went through a cyclone and hot filter (10 µm) to remove entrained solids. After that the gas was cooled in a condenser (5 ºC) and an ice-salt tar trap (-10 ºC). An additional trap, packed with stainless steel mesh, was installed at the outlet to ensure efficient trapping of the tars in the form of aerosol droplets. The gas composition and flow were measured by means of an online micro GC (Agilent 490) and a Bronkhorst High-Tech flowmeter respectively.

The fluidized bed reactor is commonly used for biomass gasification, and additionally it presents a series of advantages for its operation at lab scale. It allows a fast heating of the biomass particles and a quite precise temperature control in the fluidized bed (where the main char gasification reactions take place). On the other hand, the gas and tar products keep reacting along the freeboard zone with an approximately linear decay of temperature of about 50 ºC.

3.2.3.1 Experimental procedure

The required amount of feedstock was placed in the hopper, and the agitation and feeding screws were set to the desired feed rate. The reactor was filled with 50 g of sand (silica with particle size 150 - 200 µm), fluidized on a stream of N_2 (Praxair, Inc.) during the heating period up to the experiment

temperature. During the heating period, the online micro GC was calibrated, using a gas calibration mixture. Once the temperature was reached, the gas flow was switched from N_2 to O_2 (Praxair, Inc.) and the system was pressurized to the experimental final conditions. As soon as the system was stable, the solid and water feeds were switched on. A constant gas composition was reached after about 5 minutes of starting the feeding (these are the gas compositions reported in this study). The experiment length was about 60 min for all the performed tests.

At the end of the experiment, tars were recovered by washing the tar trap with a mixture of chloroform:methanol (4:1 vol:vol). The solvent was removed by rotavap and then by purging with N_2 until the tar was completely dry. The unconverted solid particles remaining in the bed, filter and cyclone were also collected after the completion of the test for characterisation.

The gasification was performed under O_2/steam atmosphere, with an equivalence ratio (ER) around 0.23 and a steam/biomass ratio of about 1.6 and three different pressure levels (0.1, 0.5 and 1.0 MPa). The operation flows provided a fluidizing gas velocity six to seven times the minimum fluidization velocity (U_{mf}), corresponding to gas residence times in the reactor of 2.0-2.4 s. Mass balances were calculated taking into account the mass of gases produced (gas balance) and the weight of tar and unconverted solid particles. Adequate mass balance closures (≥ 95 %) were obtained for all the conducted experiments.

3.2.4 Gas and tar analysis

An online micro GC (Agilent 490) was used to quantify the major components in the fuel gas during the experiments. The chromatograph configuration included three different channels: Channel 1, equipped with a 10 m MS5A (Molecular Sieve 5A), running on argon as carrier gas for the analysis of permanent gases other than carbon dioxide (H_2, O_2, N_2, CO and CH_4). Channel 2 was equipped with a 10 m PoraPlotQ and used helium as carried gas, allowing the separation of CO_2 and saturated and unsaturated C_1 to C_3 hydrocarbons. The C_3 to C_5 hydrocarbons were analyzed on the third channel (also using helium as carrier gas) with a 10 m Al_2O_3 column. Detection was carried out by means of micro-machined thermal conductivity detectors (μTCD), included in each channel.

An Agilent Technologies 1100 Series HPLC system was used to perform the size exclusion analysis of the obtained tars. Three (300 mm long, 7.5 mm i.d.) polystyrene/polydivinylbenzene-packed columns (PL Gel 10^4 Å 5µm, PL Gel 500 Å 5µm and PL Gel 50 Å 5µm) were used (Polymer Laboratories, Church Stretton, UK). The system was operated at 80 °C and a flow rate of 0.5 mL/min. N-Methyl 2-pyrrolidinone (NMP) was used as the mobile phase. Detection was carried out using a diode array UV-absorbance detector. As NMP is opaque at 254 nm, detection of standard compounds and samples was performed at 270, 300, 350 and 370 nm, where NMP is partially transparent. The results obtained at 300 nm were considered representative of the main trends observed at all wavelengths; only those results will be shown and discussed. System calibration was carried out using two sets of standards, PS standards calibration was applied to the 30-52 min time range, while polycyclic aromatic hydrocarbon (PAH) compounds calibration was used in the 52-62 min region [26-28].

The calibration used to convert elution time to mass estimates was as follows:

Elution time	Calibration equation	Basis
< 27.5 minutes	> 200000 u average mass (Mn)	
27.5–47.5 minutes	log (MM) = 8.6855-0.1232 × (time)	Polystyrene (PS)
47.5–60.0 minutes	log (MM) = 6.0797-0.0682 × (time)	PS + PAH std's
> 60.0 minutes	Approximately 100 u	PAH std's

In order to compare structural features of the tar compounds Fourier transform infrared (FT-IR) spectroscopy was carried out in a Bruker Vertex 70 spectrometer equipped with Platinum diamond ATR unit. Tar spectra were collected at room temperature in the range 400-4000 cm^{-1} by co-addition of 32 scans at a nominal resolution of 4 cm^{-1}, taking the spectrum of the empty cell at ambient conditions as the background.

Table 3.1 Main characteristics of feedstocks (as received basis)

		VW	VW-LT	VW-ST	GROT	GROT-LT	GROT-ST
Proximate analysis (wt.%)	**Moisturee**	5.03±0.01	3.45±0.01	3.79±0.01	6.26±0.03	4.79±0.01	4.17±0.01
	Volatiles	77.15±0.12	77.44±0.04	72.34±0.06	70.06±0.12	68.91±0.12	61.63±0.11
	Fixed carbon	17.46±0.12	18.70±0.05	23.41±0.05	21.50±0.18	24.13±0.17	31.47±0.11
	Ash	0.36±0.02	0.42±0.01	0.46±0.01	2.19±0.03	2.27±0.05	2.73±0.02
Ultimate analysis (wt.%)	**C**	47.20±0.17	48.86±0.48	52.72±0.29	47.58±0.28	51.13±0.46	56.84±0.08
	H	6.21±0.10	6.08±0.13	5.88±0.11	6.10±0.08	5.93±0.09	5.51±0.10
	O	46.18±0.30	44.57±0.55	40.86±0.40	43.62±0.30	40.26±0.50	34.29±0.20
	N	0.02±0.02	0.05±0.02	0.06±0.02	0.48±0.02	0.49±0.01	0.61±0.02
	S	0.03±0.002	0.03±0.002	0.03±0.002	0.07±0.002	0.07±0.005	0.06±0.004
	F	> 0.002	> 0.002	> 0.0015	> 0.0015	> 0.002	0.051±0.001
	Cl	> 0.002	> 0.002	> 0.002	0.05±0.001	0.02±0.001	0.01±0.001
	P	< 0.002	< 0.002	< 0.002	< 0.005	0.01±0.001	0.02±0.003
LHV (MJ/kg)		17.74±0.09	18.26±0.04	19.80±0.03	18.22±0.04	19.30±0.03	21.74±0.02

3.3 Results and discussion

3.3.1 Fuel characterization of the raw and torrefied materials

As stated in the experimental section, torrefaction was performed using a bench-scale continuous reactor. Both raw biomasses (VW and GROT) were torrefied at two different torrefaction levels (LT and ST), giving a total of six different feedstocks. The torrefaction temperatures were selected based on previous studies [13, 29-31]. In particular Park et al. [30], reported the highest energy yield for samples torrefied at 275 ºC when processing woody biomass under torrefaction and low-temperature carbonization conditions (250-375 ºC).

Table 3.1 presents the main characteristics of the six studied feedstocks, in terms of elemental analysis and heating value.

3.3.1.1 Proximate analysis

The obtained results indicate a general increase in fixed carbon content and a decrease in moisture and volatile content as the degree of torrefaction conditions intensified, being this effect independent on the biomass nature. Another aspect worth noting is that, independently on the biomass, the most relevant changes in fixed carbon and volatiles took place in the interval from Lightly Torrefied (LT) to Significantly Torrefied (ST) with variations of about 5-7% versus 1-2% in the interval raw to LT. On the other hand, moisture decrease was more noticeable in the interval from raw to LT (around 1.5%), and much less important from LT to ST. These results revealed that the main changes in the interval from raw to Lightly Torrefied (LT) materials were related to the decrease in moisture content, whereas variations in fixed carbon and volatile content were more significant in the temperature range from 225 to 275 °C (LT to ST).

3.3.1.2 Ultimate analysis

Table 3.1 also presents the ultimate analysis of the feedstocks. Comparing both raw biomasses, GROT presented lower levels of hydrogen and oxygen, together with higher levels of carbon and other minor components (N, S, Cl and P), usually related to contaminants emission. The ash content of GROT sample (2.2%) was about six times larger than the one observed for VW (0.4%). This

fact is directly related to the nature of GROT, this biomass consists in forest residues that contain significant larger amounts of inorganics as compared to cleaner VW.

The torrefaction process resulted in an increase in carbon, nitrogen and ash contents whereas the hydrogen and oxygen levels decreased. Sulphur content remained nearly constant.

The obtained results are in agreement with previous studies that show that the main changes derived from torrefaction process on the properties of the solid product are related to the removal of oxygen from the raw biomass [32,33]. In particular, the chemical changes due to torrefaction involve decomposition of hemicelluloses (160-200 ºC) and partial depolymerisation of cellulose (240-350 ºC) and lignin (280-500 ºC) [29,30,34]. Water is a major product released during the process, firstly during drying when moisture evaporates and secondly during dehydration reactions between organic molecules [31]. As a result, the torrefied materials become more coal like and energy dense than the original biomass [9], enhancing its fuel properties for gasification processes [35].

3.3.1.3 O/C and H/C ratios

The torrefaction effect on oxygen and hydrogen content is further illustrated in Figure 3.1 (Van Krevelen diagram). The O/C and H/C ratios were 0.73 and 1.58, respectively, for raw VW and 0.69 and 1.54 for raw GROT. These ratios decreased only marginally at a torrefaction temperature of 225 °C for both materials. However, a significant decrease was observed when torrefaction temperature increased up to the ST conditions. At 275 °C, the O/C and H/C ratios decreased up to 0.58 and 1.34 for VW and 0.45 and 1.16 for GROT, respectively, in line with the results from the proximate analysis discussed above.

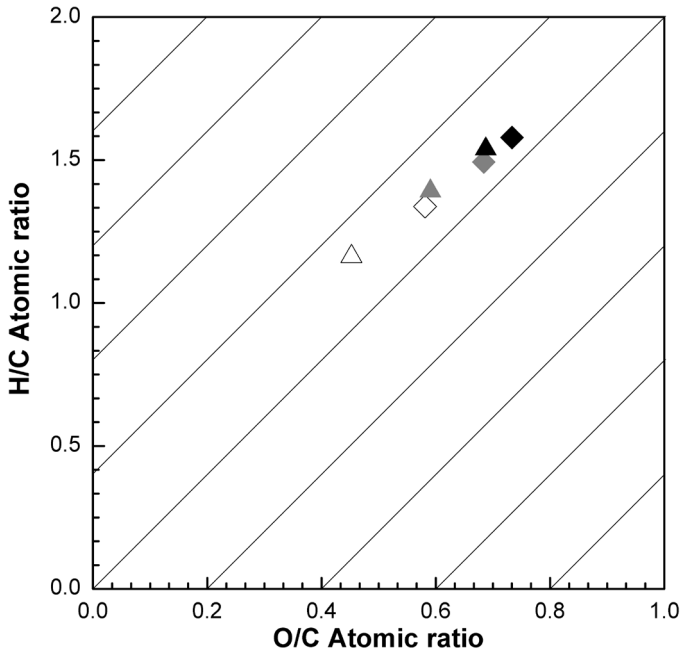

Figure 3.1 Van Krevelen diagram for the raw and torrefied samples [◆ VW, ◆ VW-LT, ◇ VW-ST, ▲ GROT, ▲ GROT-LT, △ GROT-ST].

3.3.1.4 Heating value

The loss of moisture and light oxygenated compounds also resulted in an improvement of feedstock heating value [11,36]. This effect is clearly observed in Table 3.1. Raw VW and GROT presented LHVs of 13.9 and 14.4 MJ/kg, respectively. The energy increase of the torrefied VW was similar to the one presented in previous studies for other wood samples. In particular the increase in the HHV of leucaena samples treated at 225 and 275 °C with 30 min of holdup time were reported to be 4.4% and 12.3% [37]. On the other hand, GROT samples exhibited a LHV increase similar to those reported for logging residue chips and pine chips under the same pretreatment conditions: 5.3% and 17.2% and 5.5% and 18.2%, respectively [38]. The results reflect the differences between the feedstocks, showing the higher reactivity of GROT as compared to VW under torrefaction conditions.

3.3.2 Bench-scale fluidized bed gasification of torrefied biomass

3.3.2.1 Product yields

Table 3.2 shows the results obtained in terms of variation of gas, tar and char yields during the experiments under different experimental conditions.

These yields are calculated as the percentage of mass of compound per mass of dry biomass. As a result of using this basis the sum of gas, tar and char yields results above 100%, since products are formed due to the reaction with the gasification agents (O_2 and steam).

Table 3.2 Experimental conditions and product yields for the gasification of the six biomass samples at 850 ºC.

Run	Feedstock	Pressure (MPa)	ER	Ratio g H_2O/g dry biomass	Yield (g/100 g dry biomass)		
					Gas	Tar	Char
1	VW	0.1	0.22	1.6	133.6±0.3	0.52±0.03	2.06±0.05
2	VW	0.5	0.24	1.7	139.4±0.5	0.64±0.02	2.46±0.06
3	VW	1.0	0.24	1.7	147.3±0.3	1.58±0.05	2.10±0.04
4	VW-LT	0.1	0.23	1.6	138.3±0.1	0.18±0.02	2.80±0.06
5	VW-LT	0.5	0.23	1.6	142.1±0.4	0.98±0.02	2.18±0.05
6	VW-LT	1.0	0.22	1.6	146.4±0.3	1.31±0.03	2.59±0.04
7	VW-ST	0.1	0.22	1.5	140.4±0.2	0.11±0.01	3.41±0.03
8	VW-ST	0.5	0.24	1.7	142.9±0.2	0.64±0.02	2.28±0.09
9	VW-ST	1.0	0.23	1.6	150.5±0.5	0.67±0.03	1.93±0.04
10	GROT	0.1	0.23	1.6	130.3±0.5	1.08±0.02	3.10±0.05
11	GROT	0.5	0.23	1.6	137.2±0.3	1.75±0.03	2.68±0.05
12	GROT	1.0	0.23	1.5	143.4±0.4	1.95±0.06	2.40±0.07
13	GROT-LT	0.1	0.22	1.6	131.8±0.3	0.50±0.01	4.13±0.10
14	GROT-LT	0.5	0.21	1.6	141.4±0.2	1.18±0.02	2.24±0.07
15	GROT-LT	1.0	0.23	1.7	144.0±0.5	1.54±0.02	2.22±0.05
16	GROT-ST	0.1	0.22	1.6	138.5±0.2	0.19±0.01	5.37±0.08
17	GROT-ST	0.5	0.22	1.6	148.1±0.4	0.70±0.02	4.49±0.10
18	GROT-ST	1.0	0.22	1.7	149.1±0.2	1.03±0.01	4.39±0.09

Effect of torrefaction level*:* The obtained results showed an increase in gas yield as torrefaction level increased. The cited rise was more relevant for GROT materials- experiments 10 to18- (with increases in the order of 6 – 11% comparing gasification gas yield of raw GROT and GROT-ST), than those obtained when VW materials- experiments 1 to 9- were gasified (3.2-6.9 %). Additionally, tar yield decreased for more severe torrefaction conditions. For instance, tar yield varied from 1.1 to 0.2% when GROT and GROT-ST (experiments 10 and 16) were gasified at atmospheric pressure. This decrease was slightly lower in the case of VW and VW-ST, although tar production was

always lower for this particular biomass and its torrefied products. Char yield presented an increase for both studied biomasses as the torrefaction level increased, but only at the lowest tested pressure (0.1 MPa). This increase was almost double for GROT (experiments 10, 13 and 16) in comparison to VW materials (experiments 1, 4 and 7). However the effect of torrefaction level on char yield at higher pressures was not evident (0.5 and 1.0 MPa). Different trends were observed depending on the torrefaction level and original feedstock (VW or GROT). A possible explanation for this uncertain trend is the competition between two mechanisms, on the one hand, the more relevant role of char gasification for more torrefied materials (that increases with pressure), and the effect of tar repolymerization to produce char [25,39,40].

Effect of pressure: Pressure presented a clear effect on gas yield, which increased in the whole range of torrefaction level and for both biomasses. The results showed a slightly higher gas yield for the experiments carried out using VW-derived feedstocks as compared with the GROT-derived samples. Additionally, the effect of pressure on gas yield rise differed for both biomasses. The increase in gas yield with pressure was similar for the original biomasses, however a sharper increase with pressure was observed for GROT torrefied materials in comparison to VW materials. Thus, the increase in gas yield for GROT-LT and ST in the interval from 0.1 to 0.5 MPa (experiments 14 and 17) was about 9.5 % in comparison to the 3.8 and 2.5 % obtained for VW-LT and ST, respectively (experiments 5 and 8). Tar yield increased with pressure for both biomasses, with GROT and its torrefied materials always yielding higher levels of tar than the correspondent VW materials. The tar yield rise with pressure was quite remarkable, and appeared to be more pronounced in the pressure interval from 0.1 to 0.5 MPa. Tar evolution with pressure was probably related to the formation of PAH compounds, more relevant at higher pressure [25]. Regarding char yield evolution, in general it decreased with gasification pressure (the decrease differed for the different levels of torrefaction and original feedstock). As indicated above, the two competing mechanisms can explain char evolution, and increasing pressure would favour char gasification reactions [25,39,40].

3.3.2.2 Gas composition

The main components of the gas were H_2 (30-40 $\%_{db}$ vol.), CO_2 (30-37$\%_{db}$ vol.), CO (18-24$\%_{db}$ vol.) and CH_4 (4-12$\%_{db}$ vol.), whereas O_2, C_2H_4, C_2H_6 and C_3H_8 appeared in lower concentrations. The evolution of the gas composition under different experimental conditions can be explained taking into account the initial devolatilization of the biomass, which forms light gases and primary tars, followed by their subsequent conversion through steam reforming, oxidation, methanation and water-gas shift [3,41].

Note that, in order to compare the main trends on gas product evolution under the different experimental conditions, the results are presented as weight of gas product by 100 g of dry biomass (Figures 3.2 (VW) and 3.3 (GROT)).

Effect of torrefaction level: The torrefaction level presented a positive effect on hydrogen yield, the results showed an increase in hydrogen yield of about 0.6% for VW-LT in comparison with original VW for all tested pressures, whereas the increment was more important in the case of GROT (around 1.3, 1.4 and 0.9% for 0.1, 0.5 and 1.0 MPa respectively).

The influence of torrefaction level on the rest of permanent gases was not that evident. It can be observed a reduction in both methane yield and concentration in the fuel gas for the highest torrefaction level and pressure, although this trend varied under other experimental conditions (i.e. GROT at 0.1 MPa). Influence of torrefaction level on CO and CO_2 was again limited, although a slight increase in CO and CO_2 yields could be depicted from the plots.

The significant increase of H_2 and the simultaneous increase of CO, CO_2 together with the reduction of the hydrocarbons in the product gas can be explained by evaluating the changes in feedstock composition with torrefaction. The higher the torrefaction level, the lower the contribution of devolatilization to the product gas formation, while char gasification would play a more relevant role in the process [40]. The main gas products by char gasification are H_2 and CO, so in theory their production would be favoured by more torrefied feedstocks. The lower influence of torrefaction on the CO yields is directly related to the presence of O_2 and the equilibrium CO-CO_2. Additionally, it is worth noting that the main differences between the original biomasses (VW and

GROT) and its correspondent torrefied materials were observed at atmospheric pressure (0.1 MPa). The differences became less relevant as pressure and torrefaction level increased (more severe conditions).

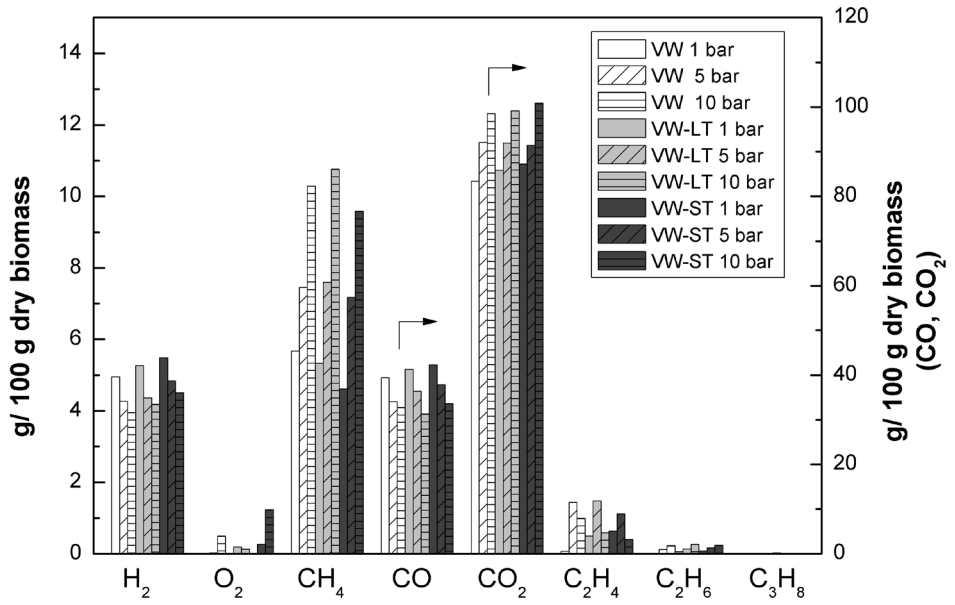

Figure 3.2 Effect of pressure and torrefied level on gas yields (VW). Temperature 850 ºC, ER: 0.23, H_2O/Biomass: 1.6

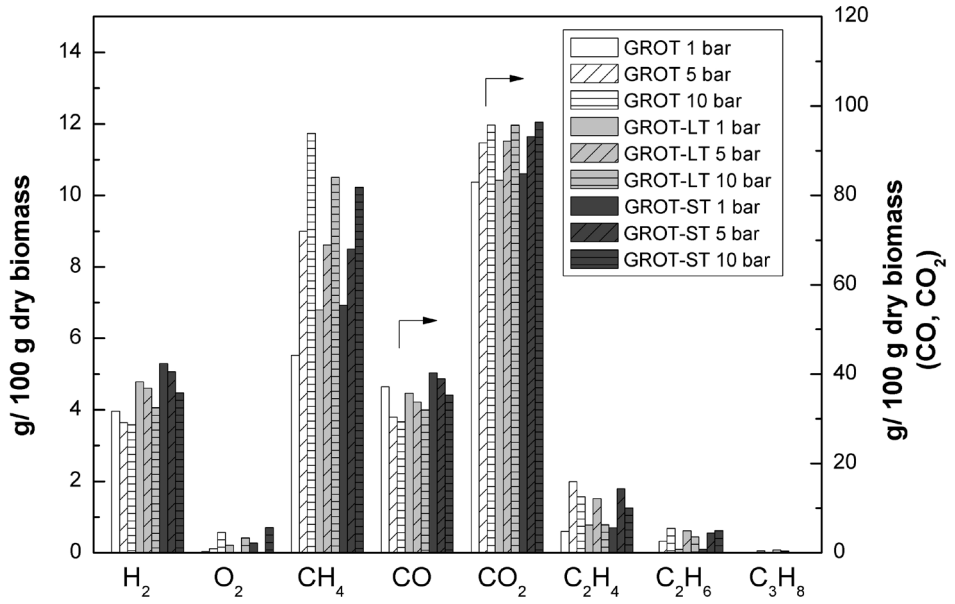

Figure 3.3 Effect of pressure and torrefied level on gas yields (GROT). Temperature 850 ºC, ER: 0.23, H_2O/Biomass: 1.6

Effect of pressure: Among the observed trends, H_2 yield decreased as pressure increased for both studied biomasses. This drop with gasification

pressure can be explained taking into account the gasification reactions [42]. At high pressure the chemical equilibrium of the hydrogen production reactions (heterogeneous water gas reaction, steam reforming reaction and hydrogenation reaction) is shifted to the reactant side.

Increasing pressure provokes also an enrichment of the producer gas with methane. This trend can be explained by the fact that pressure favours the methanation reaction, especially at moderate temperatures [43]. For instance methane yield in experiments using VW-derived samples as feedstock increased from 5.7, 5.3 and 4.6% at 0.1 MPa to 7.5, 7.6 and 7.2% at 0.5 MPa and 10.3, 10.8 and 9.6% at 1.0 MPa, respectively. Experiments using GROT and its torrefied materials as feedstock showed similar trends, however the increase in methane yield was lower when GROT-LT and GROT-ST were used as feedstock.

Regarding the evolution of CO and CO_2 yields with pressure, these compounds presented an inverse trend, mainly due to the Boudouard reaction [25,43]. Formation of CO is favoured at low pressures within the temperature and ER range used in the present study, whereas CO_2 formation is promoted at higher pressures (above 0.3 MPa). Comparing the results obtained for both biomasses, higher CO yields were obtained for gasification experiments of VW and its torrefied materials in all the range of experimental conditions, with the exception of higher pressures and torrefaction. Additionally, the drop in CO yield as pressure increased was more intense for the VW materials. CO_2 yields presented quite similar values, the most relevant differences appeared at high pressure (1.0 MPa) and torrefaction level (CO_2 yields: 99.2 and 100.8% for VW-LT and VW-ST and 95.7 and 96.4 for GROT-LT and GROT-ST, respectively).

C_2 and C_3 hydrocarbons appeared in lower level than the rest of the permanent gases for the different feedstocks in all the studied range of pressure. However, some changes were consistently observed on C_2H_4 and C_2H_6 yields. In all cases, these compounds presented a maximum yield at 0.5 MPa, with a decrease at higher pressure. This trend may be related with the mechanisms of formation of secondary tars, which are relevant under the studied conditions (850ºC and high pressure) [25,39]. Several mechanisms have been proposed to explain the growth of PAH compounds, some of them indicate the role of C_2 and C_3 hydrocarbons in the process [44-46].

3.3.2.3 Tar characterization

This section summarizes the evolution of tar content in the produced gas, together with a preliminary characterization of the tars in terms of molecular weight distribution and chemical structure.

Tar content: The results of tar content in the dry produced gas (expressed as g/Nm^3) appear displayed in Figure 3.4 and Figure 3.5 for the experiments performed with VW and GROT derived feedstocks, respectively.

The data showed an increase in tar content as pressure increased in all the studied range and for both biomasses. This increase was, in general, more marked in the interval from 0.1 to 0.5 MPa (especially for the Significantly Torrefied biomasses). The pressure effect on primary tars causes a greater resistance exerted by the sweeping gas on the escaping volatiles. This causes an increase in the material residence time resulting in repolymerization reactions and carbon reincorporation into the forming char, and a decrease on tar yields [18]. Additionally, the pressure also has an effect on the evolution of the secondary tar reactions along the reactor and freeboard. This parameter probably enhances the tar polymerization reactions towards polycyclic aromatic hydrocarbon (PAH) compounds [25]. Decrease of C_2 and C_3 hydrocarbons in gas phase at high pressure also supported this hypothesis, as these compounds can be involved on PAH growth mechanisms [44-46].

Additionally, the results evidence that torrefaction level affected the tar content in the produced gas. The tar content decreased as torrefaction level increased, being this effect more relevant for GROT derived materials in comparison to VW derived materials. It is worth noting that tar content in the fuel gas was higher for GROT and GROT torrefied materials, in comparison with VW, although this difference diminished with the torrefaction level. The effect of torrefaction level on tar content can be explained taking into account the changes in feedstock composition with torrefaction. The higher the torrefaction level, the lower the volatile content of the feedstock, parameter directly related to tar evolution.

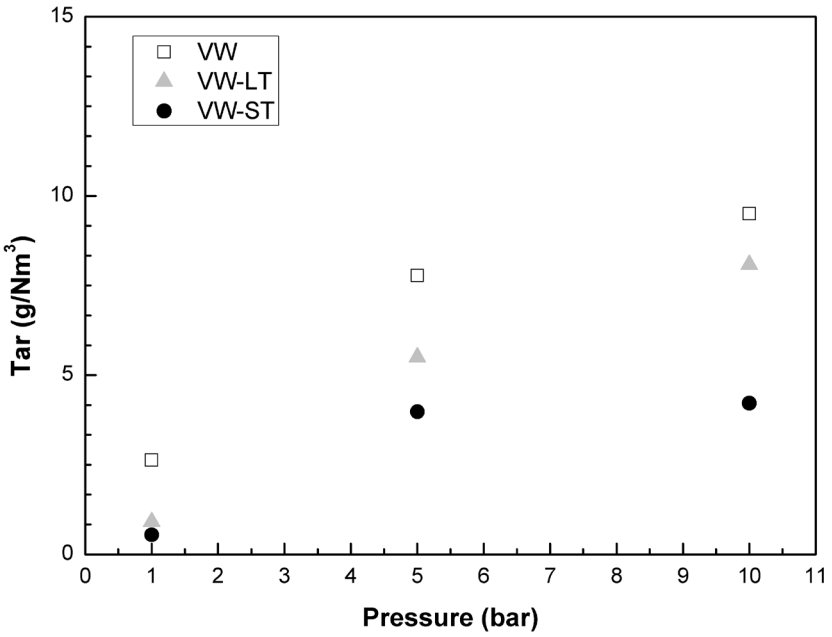

Figure 3.4 Effect of pressure and torrefied level on tar content (VW). Temperature 850 ºC, ER: 0.23, H2O/Biomass: 1.6

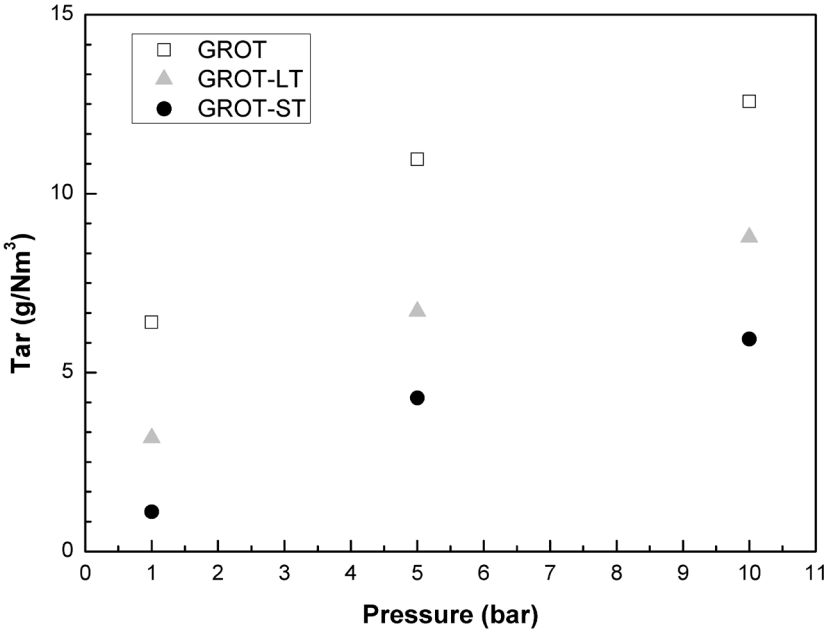

Figure 3.5 Effect of pressure and torrefied level on tar content (GROT). Temperature 850 ºC, ER: 0.23, H2O/Biomass: 1.6

Size-exclusion chromatography (SEC): The examination of the molecular weight distribution of biomass tars was carried out using the SEC system described in the experimental section. Figures 3.6 and 3.7 present some examples of the molecular weight distribution of tars obtained at different pressures and levels of torrefaction for VW and GROT respectively. All the

curves showed bimodal distributions of signal in all the cases, the earliest eluting peak corresponds to the material of molecular size unable to penetrate the porosity of the column packing, and referred to as "excluded" from the column porosity. The second eluting peak corresponds to the material able to penetrate the porosity of the column packing. The exclusion limit of the column, defined according to the standards of polystyrene behaviour, is about 200000 u. However, molecular conformation is considered to be the factor that causes molecules to become excluded from the column porosity rather than the molecular weight [26,27]. Estimates of molecular masses can be calculated from a mass calibration based on the elution times of polystyrene (PS) standards and polycyclic aromatic hydrocarbon (PAH) standards.

Comparing the results of the SEC analysis of the tars obtained from GROT at various pressures and torrefaction levels (Figure 3.7), it can be noticed that they presented similar MW distributions, although several trends can be extracted. The tars obtained at higher pressures presented slightly heavier molecular weight distribution curves (particularly remarkable for GROT-ST). The tars obtained when GROT-ST was gasified at 0.1, 0.5 and 1.0 MPa showed a distribution shifted to higher MWs with maxima at 56.3, 56.1 and 54.5 min , which correspond to a mass of about 175, 180 and 230 u respectively. The lift-off of the retained peak appeared around 44.5, 41.7 and 39.9 min, corresponding to masses of 1600, 3500 and 5900 u respectively. This fact agrees with the increase in tar yield observed at higher pressures, probably related to polymerization towards heavier PAH compounds [25].

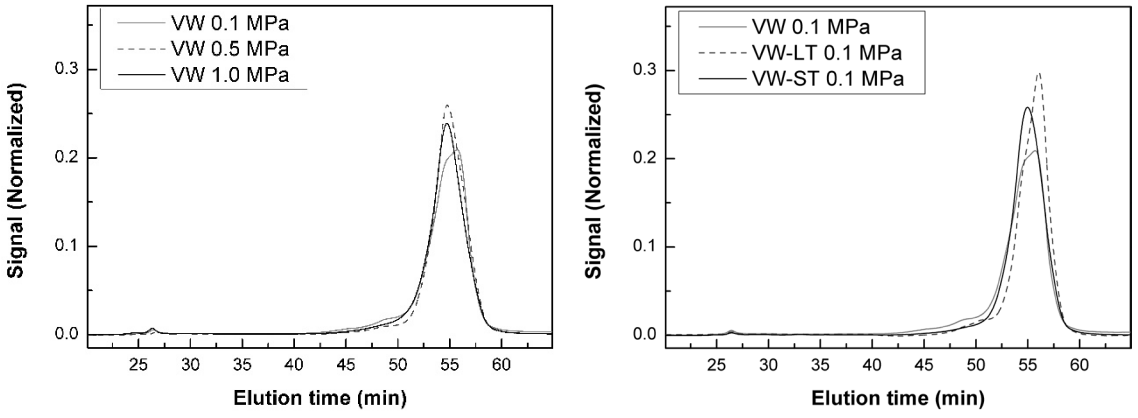

Figure 3.6 Size exclusion analysis of VW tars obtained in a FBR, influence of pressure and torrefaction level

On the other hand, the torrefaction level presented an opposite trend, the obtained results showed decreasing molecular weight distribution of tars in the order: raw biomass > LT > ST. For instance the tars obtained during the gasification of GROT, GROT-LT and GROT-ST at 0.1 MPa showed lift-off around 40.4, 41.3 and 44.5 min respectively, which correspond to a mass of about 5100, 3950 and 1600 u taking into account the calibration, and a maxima intensity that corresponded to 220, 190 and 175 u respectively. This effect declined as the gasification pressure increased, in particular at the highest evaluated pressure (1.0 MPa), the tars obtained under these conditions presented analogous molecular weight distributions. These results are comparable to those obtained for VW (Figure 3.6), however in this case, the tars obtained at pressures higher than 0.1 MPa presented resembling molecular weight distributions.

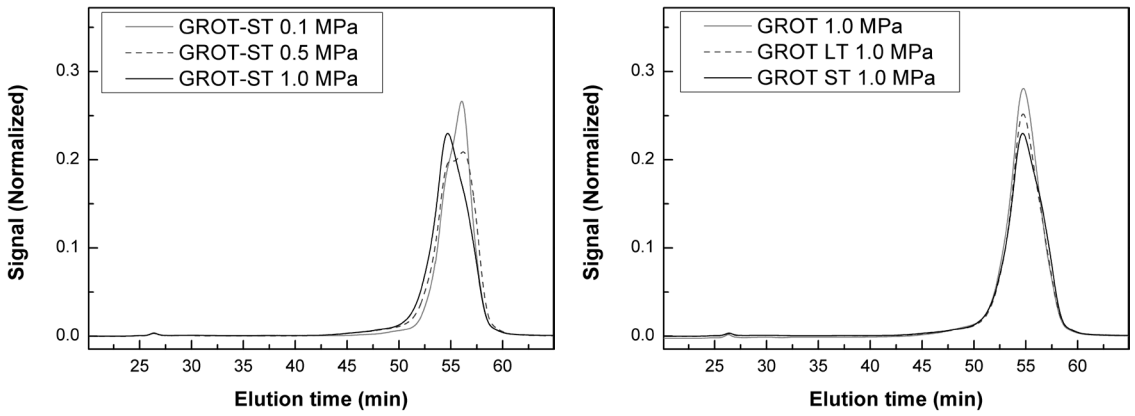

Figure 3.7 Size exclusion analysis of GROT tars obtained in a FBR, influence of pressure and torrefaction level

FT-IR analysis: Figures 3.8 and 3.9 show the FT-IR spectra of the tars obtained in the fluidized bed reactor at different pressures and torrefaction levels. The tar spectra showed in all the cases absorption bands corresponding to aromatic structures at 3050, 1600, 870, 813 and 750 cm^{-1} and aliphatic structures at 2960, 2922, 2855, 1352 and 1379 cm^{-1}. The bands in the region 900-700 cm^{-1} are usually assigned to the out-of-plane bending of aromatic CH groups. The bands in the region 1630-1470 cm^{-1} are assigned to the stretching of aromatic C = C groups and bands at 3050 and 3016 cm^{-1} to the stretching of aromatic C-H groups. The bands in the 2968-2864 and 1444-1377 cm^{-1} regions are due to the stretching and bending modes of saturated aliphatic

hydrocarbons (C-H). Additionally, peaks appearing at 1100-1300 and 1700 cm^{-1} are assigned to phenoxyl and ether stretching and carbonyl groups, respectively.

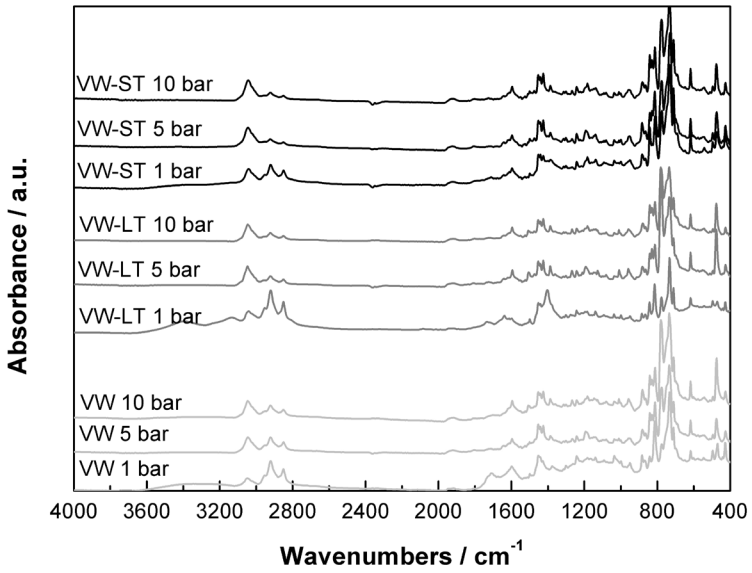

Figure 3.8 FTIR spectra of VW tars obtained in a FBR, influence of pressure and torrefaction level

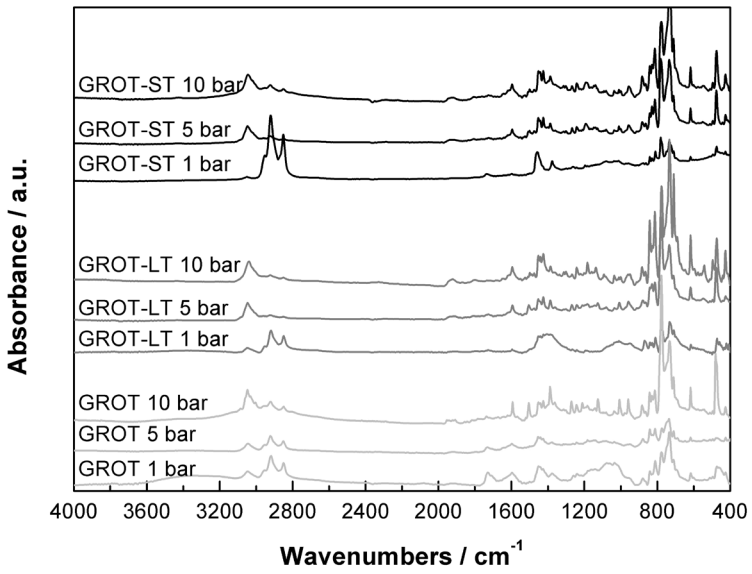

Figure 3.9 FTIR spectra of GROT tars obtained in a FBR, influence of pressure and torrefaction level

For both feedstock materials, the results showed a decrease in the aliphatic band (2990 cm^{-1}) together with an increase in the signal of the different aromatic bands as pressure increases. The signal in the oxygenated functionalities regions decreased when pressure increased (more relevant in the

range 0.1 to 0.5 MPa). These results indicate that an increase in pressure favours the formation of oxygen-poor polyaromatic compounds. Among the oxygen functional groups present in the tars, C=O structures (broad band at 1715 cm^{-1}- 1650 cm^{-1}), methoxyl groups (1265 cm^{-1}) and C-O bands (1035 cm^{-1}) could be detected. The signal of the oxygenated functionalities was also lower for the most torrefied samples (ST) as compared to the raw material, which is in good agreement with the composition of the initial feedstock.

3.3.2.4 Effect of experimental parameters on gasification performance

This section gathers a series of parameters that allow, together with the information related to syngas composition and tar content presented beforehand, the assessment of the gasification performance. It is important to notice that these parameters are presented as qualitative information and are not directly applicable to industrial gasifiers. Two aspects are key in this regard, first the different scale and secondly the type of reactor. Both aspects can strongly affect the actual numbers here shown, in particular the gasification technology would affect the devolatilization process, due to the different biomass heating profile as well as the type of contact between the biomass/products and the gasification agents. Nevertheless the main trends and conclusions can be useful for further evaluation of the integration of torrefaction and gasification processes at the temperature and pressure ranges of the study.

H_2/CO and CO/CO_2 ratios: The H_2/CO ratio in the produced gas is important for further possible end uses of the gas. Table 3.3 shows the evolution of this ratio with the gasification pressure and torrefaction levels of GROT and VW materials, respectively. The ratio ranged between 1.5 and 1.9, but mainly centred in values close to 1.8. These values are quite close to the levels required for methanol or ammonia production or Fischer-Tropsch processes, the latter being the aim of this study for biofuels production [8]. The ratio increased with the torrefaction level whereas the effect of pressure differed depending on the feedstock. Several factors affected the H_2/CO ratio, on the one hand H_2 production increased with torrefaction level and decreased as pressure rose (due to the gasification reactions), on the other hand CO yield also decreased, to a greater or lesser extent depending on the CO/CO_2 equilibrium.

The evolution of CO/CO_2 ratio also appears in Table 3.3. The value of the ratio was lower than 0.8 in all the studied range, and decreased almost linearly with pressure. The effect of torrefaction was less evident, although a slight increase with the torrefaction level could be observed (more evident in the case of GROT-derived materials).

Table 3.3 Influence of experimental conditions on gasification parameters.

Feedstock	**Pressure (MPa)**	**H_2/CO**	**CO/CO_2**	**X_C**	**CGE (LHV)**	**η_{LHV}**
VW	0.1	1.76±0.05	0.74±0.02	88.45±0.45	68.49±0.88	68.49±0.88
VW	0.5	1.75±0.05	0.58±0.01	93.66±0.48	69.73±0.90	69.73±0.90
VW	1.0	1.69±0.05	0.52±0.01	96.68±0.49	69.82±0.90	69.82±0.90
VW-LT	0.1	1.78±0.05	0.76±0.02	89.05±0.46	71.00±0.86	64.81±0.78
VW-LT	0.5	1.68±0.05	0.62±0.02	92.27±0.48	71.36±0.87	65.13±0.79
VW-LT	1.0	1.87±0.05	0.50±0.01	94.75±0.49	70.69±0.85	64.52±0.78
VW-ST	0.1	1.81±0.05	0.76±0.02	83.92±0.43	65.62±0.79	60.61±0.73
VW-ST	0.5	1.79±0.05	0.65±0.02	94.06±0.48	67.24±0.81	62.11±0.75
VW-ST	1.0	1.88±0.05	0.52±0.01	94.60±0.49	67.66±0.82	62.50±0.76
GROT	0.1	1.49±0.04	0.70±0.02	85.12±0.44	59.51±0.73	59.51±0.73
GROT	0.5	1.68±0.05	0.52±0.01	91.90±0.47	67.02±0.82	67.02±0.82
GROT	1.0	1.71±0.05	0.48±0.01	97.35±0.50	69.58±0.85	69.58±0.85
GROT-LT	0.1	1.88±0.05	0.67±0.02	81.71±0.42	64.98±0.78	61.42±0.74
GROT-LT	0.5	1.91±0.05	0.58±0.01	89.13±0.46	70.35±0.84	66.50±0.79
GROT-LT	1.0	1.78±0.05	0.53±0.01	90.84±0.47	68.86±0.83	65.09±0.78
GROT-ST	0.1	1.84±0.05	0.75±0.02	77.98±0.40	62.90±0.75	59.80±0.71
GROT-ST	0.5	1.82±0.05	0.66±0.02	84.96±0.43	67.83±0.81	64.49±0.77
GROT-ST	1.0	1.77±0.05	0.58±0.01	85.42±0.44	65.94±0.79	62.69±0.75

Carbon conversion: One parameter that gives insight into the performance of gasification process is the conversion of carbon in the gasifier to gaseous products, also known as carbon conversion. This value (see Table 3.3) was determined as the ratio of carbon leaving the gasifier in the form of gaseous products in the product gas stream to the amount of carbon introduced by the feedstock (Eq. 3.1).

$$X_C(\%) = 100\left(\frac{Carbon\ in\ producer\ gas\ [kmol/h]}{Carbon\ in\ biomass\ [kmol/h]}\right) \quad \text{Eq. 3.1}$$

The obtained results showed an increase in carbon conversion with gasification pressure in all the studied cases. This fact could be attributed to the higher CO_2 and CH_4 yields obtained under these conditions. The effect of torrefaction on carbon conversion was more significant for the experiments performed on the GROT derived materials as compared to the analogous VW samples (Table 3.3). This trend is consistent with the higher tar and char yields obtained in the experiments of GROT materials.

Gasifier cold gas efficiency: Another key figure on the gasification performance is the cold gas efficiency (CGE) (Table 3.3). This parameter is defined as the energy in the gas in relation to energy in the biomass fed (Eq. 3.2).

$$CGE_{LHV}(\%) = 100\left(\frac{LHV_{producer\ gas}\ [MW]}{LHV_{biomass}\ [MW]}\right) \quad \text{Eq. 3.2}$$

The calculated CGE values ranged between 60 to 71%, and increased with the gasification pressure in the range from 0.1 to 0.5 MPa, and remained constant or decreased at higher pressures. This trend is in agreement with the higher carbon conversion, however at higher pressures the lower heating value of the produced gas is related to the higher CO_2 yields, together with the decrease in H_2 yield. Another factor that would influence de CGE in an integrated process is the introduction of the volatiles obtained during the torrefaction process into the gasifier. In this way the efficiency of the global process would improve [31].

The calculated data also showed that the effect of torrefaction level on CGE was not relevant from the raw material to the lightly torrefied materials, however a clear decrease in CGE was noticed for the significantly torrefied materials, which could be linked with the lower carbon conversion for the ST materials.

3.3.2.5 Overall torrefaction-gasification efficiency:

This parameter is calculated taking into account the energy content of the producer gas in relation to energy content of the raw biomass (previously to the

torrefaction process) (Eq. 3.3). The Figure 3.10 presents a diagram that explains the calculation of this parameter.

$$\eta_{LHV}(\%) = 100\left(\frac{LHV_{producer\ gas}[MW]}{LHV_{raw\ biomass}\ [MW]}\right) \qquad \text{Eq. 3.3}$$

The overall efficiency values ranged between 60 to 69%. These values were lower for torrefied materials than for raw biomass, due to the energy inefficiency related to the loss of volatiles, not used in the process [30]. The results showed an increase of the efficiency with the gasification pressure in the range from 0.1 to 0.5 MPa, and remained constant or decreased at higher pressures. The data also showed a decrease of the global efficiency of the process with the torrefaction level. This reduction is related with both the energy efficiency of the torrefaction process and the lower carbon conversion for the torrefied materials.

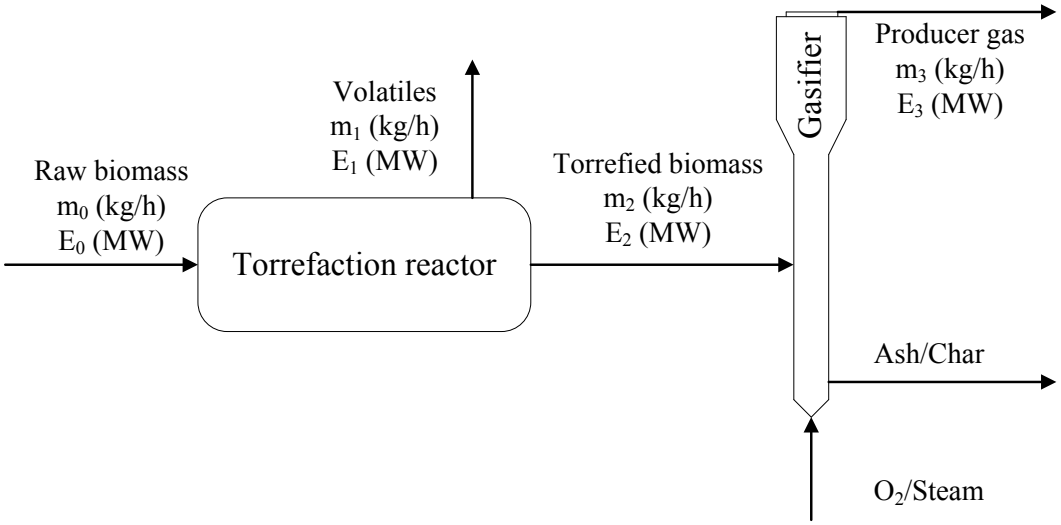

Figure 3.10 Schematic diagram of the overall mass and energy balances for the combination of torrefaction and gasification processes

3.4 Conclusions

This work reports experimental results concerning the influence of torrefaction level and pressure on product yields and composition during fluidized bed O_2/steam gasification for the production of liquid fuels.

Regarding the torrefaction process, the composition of torrefied samples was closer to that of coal, with higher carbon content and lower volatile matter content, increasing with the torrefaction severity.

Gasification experiments varying pressure and torrefaction level and using two different biomasses were performed in order to determine the effect of these parameters on gasification performance. The main trend for both biomasses was an increase on gas yield with pressure and torrefaction level. Additionally, it was noticed that tar yield increased with the experimental pressure, together with a decrease of char yield.

Pressure made the produced gas composition shift towards higher CH_4 and CO_2 content, while H_2 and CO levels decreased. Regarding the effect of the original biomass, VW derived materials (VW-LT, VW-ST) yielded higher levels of H_2 and CO, and lower levels of CH_4 than the correspondent GROT-derived materials. The differences became less relevant as pressure and torrefaction level increased (more severe conditions).

The analysis of the obtained tars through SEC and FTIR corroborated that the increase in pressure led to higher tar levels, which could be related to polymerization of the tar compounds towards heavier PAH compounds. Torrefaction level presented the opposite effect, with lower tar yields and lighter molecular weight distribution of tars in the order raw biomass, LT and ST.

This study also provides insight into the influence of pressure and torrefaction level on several key parameters of the gasification performance (H_2/CO and CO/CO_2 Ratios, carbon conversion and cold gas efficiency). The information is of great interest to determine optimal operation conditions. However, an exhaustive evaluation of the different factors is needed for that purpose, as not only technical aspects on thermal conversion or gas composition have to be taken into consideration, but also other factors as the costs associated to the whole process.

3.5 References

[1] Demirbas, A., Progress and recent trends in biofuels. Progress in Energy and Combustion Science 2007, 33 (1), 1-18.

[2] Escobar, J. C.; Lora, E. S.; Venturini, O. J.; Yáñez, E. E.; Castillo, E. F.; Almazan, O., Biofuels: Environment, technology and food security. Renewable and Sustainable Energy Reviews 2009, 13 (6-7), 1275-1287.

[3] Alauddin, Z. A. B. Z.; Lahijani, P.; Mohammadi, M.; Mohamed, A. R., Gasification of lignocellulosic biomass in fluidized beds for renewable energy development: A review. Renewable and Sustainable Energy Reviews 2010, 14 (9), 2852-2862.

[4] Basu, P., Biomass Gasification and Pyrolysis - Practical Design and Theory. Ed. Academic Press: Boston, 2010. ISBN: 978-0-12-374988-8.

[5] World Energy Outlook 2008, International Energy Agency, 2008. ISBN: 978-92-64-04560-6.

[6] Re-Thinking 2050. A 100% Renewable Energy Vision for the European Union, European Renewable Energy Council, 2010.

[7] Roadmap 2050 – A practical guide to a prosperous low-carbon Europe, European Climate Foundation, 2010.

[8] Higman, C.; van der Burgt, M., Gasification (2nd Edition). Eds. Gulf Professional Publishing: Burlington, 2008. ISBN: 978-0-7506-8528-3.

[9] van der Stelt, M. J. C.; Gerhauser, H.; Kiel, J. H. A.; Ptasinski, K. J., Biomass upgrading by torrefaction for the production of biofuels: A review. Biomass and Bioenergy 2011, 35 (9), 3748-3762.

[10] Bach, Q.V.; Pfeiffer, B.; Tran, K.-Q.; Khalil, R.; Skreiberg, Ø., Combustion kinetics of wet-torrefied Norwegian biomass fuels. 20th European Biomass Conference and Exhibition 2012 – Book of proceedings. Milan, Italy, pp. 1739-1744.

[11] Chew, J. J.; Doshi, V., Recent advances in biomass pretreatment – Torrefaction fundamentals and technology. Renewable and Sustainable Energy Reviews 2011, 15 (8), 4212-4222.

[12] Khalil, R.; Skreiberg, Ø., Stable operating conditions in bioenergy plants through utilization of torrefied biomass. International Nordic Bioenergy 2011 - Book of proceedings. FINBIO: Jyväskylä, 2011; Vol. Language: eng, pp 268-271.

[13] Tapasvi, D.; Khalil, R.; Skreiberg, Ø.; Tran, K.-Q.; Grønli, M., Torrefaction of Norwegian Birch and Spruce: An Experimental Study Using Macro-TGA. Energy & Fuels 2012, 26 (8), 5232-5240.

[14] Tapasvi, D.; Khalil, R.; Várhegyi, G.; Skreiberg, Ø.; Tran, K.-Q.; Grønli, M., Kinetic Behavior of Torrefied Biomass in an Oxidative Environment. Energy & Fuels 2013, 27 (2), 1050-1060.

[15] Matas Güell, B.; Sandquist, J.; Sørum, L., Gasification of biomass to second generation biofuels: A review. Journal of Energy Resources Technology, Transactions of the ASME 2013, 135 (1).

[16] El-Emam, R. S.; Dincer, I.; Naterer, G. F., Energy and exergy analyses of an integrated SOFC and coal gasification system. International Journal of Hydrogen Energy 2012, 37 (2), 1689-1697.

[17] Gil, J.; Aznar, M. P.; Caballero, M. A.; Francés, E.; Corella, J., Biomass Gasification in Fluidized Bed at Pilot Scale with Steam–Oxygen Mixtures. Product Distribution for Very Different Operating Conditions. Energy & Fuels 1997, 11 (6), 1109-1118.

[18] Kandiyoti, R., Herod, A., and Bartle, K., Solid Fuels and Heavy Hydrocarbon Liquids, Eds. Elsevier Science Ltd: Oxford, 2006. ISBN: 978-0-08-044486-4.

[19] Pereira, E. G.; Da Silva, J. N.; De Oliveira, J. L.; MacHado, C. S., Sustainable energy: A review of gasification technologies. Renewable and Sustainable Energy Reviews 2012, 16 (7), 4753-4762.

[20] Lv, P. M.; Xiong, Z. H.; Chang, J.; Wu, C. Z.; Chen, Y.; Zhu, J. X., An experimental study on biomass air–steam gasification in a fluidized bed. Bioresource Technology 2004, 95 (1), 95-101.

[21] González, J. F.; Román, S.; Bragado, D.; Calderón, M., Investigation on the reactions influencing biomass air and air/steam gasification for hydrogen production. Fuel Processing Technology 2008, 89 (8), 764-772.

[22] Gupta, A. K.; Cichonski, W., Ultrahigh temperature steam gasification of biomass and solid wastes. Environmental Engineering Science 2007, 24 (8), 1179-1189.

[23] Kumar, A.; Eskridge, K.; Jones, D. D.; Hanna, M. A., Steam-air fluidized bed gasification of distillers grains: Effects of steam to biomass ratio, equivalence ratio and gasification temperature. Bioresource Technology 2009, 100 (6), 2062-2068.

[24] Turn, S.; Kinoshita, C.; Zhang, Z.; Ishimura, D.; Zhou, J., An experimental investigation of hydrogen production from biomass gasification. International Journal of Hydrogen Energy 1998, 23 (8), 641-648.

[25] Mayerhofer, M.; Mitsakis, P.; Meng, X.; de Jong, W.; Spliethoff, H.; Gaderer, M., Influence of pressure, temperature and steam on tar and gas in allothermal fluidized bed gasification. Fuel 2012, 99 (0), 204-209.

[26] Berrueco, C.; Venditti, S.; Morgan, T. J.; Álvarez, P.; Millan, M.; Herod, A. A.; Kandiyoti, R., Calibration of size-exclusion chromatography columns with 1-methyl-2-pyrrolidinone (NMP)/chloroform mixtures as eluent: Applications to petroleum-derived samples. Energy and Fuels 2008, 22 (5), 3265-3274.

[27] Herod, A. A.; Bartle, K. D.; Morgan, T. J.; Kandiyoti, R., Analytical methods for characterizing high-mass complex polydisperse hydrocarbon mixtures: An overview. Chemical Reviews 2012, 112 (7), 3892-3923.

[28] Morgan, T. J.; George, A.; Alvarez, P.; Herod, A. A.; Millan, M.; Kandiyoti, R., Isolation of size exclusion chromatography elution-fractions of coal and petroleum-derived samples and analysis by laser desorption mass spectrometry. Energy and Fuels 2009, 23 (12), 6003-6014.

[29] Chen, W.-H.; Kuo, P.-C., A study on torrefaction of various biomass materials and its impact on lignocellulosic structure simulated by a thermogravimetry. Energy 2010, 35 (6), 2580-2586.

[30] Park, S.-W.; Jang, C.-H.; Baek, K.-R.; Yang, J.-K., Torrefaction and low-temperature carbonization of woody biomass: Evaluation of fuel characteristics of the products. Energy 2012, 45 (1), 676-685.

[31] Prins, M. J.; Ptasinski, K. J.; Janssen, F. J. J. G., More efficient biomass gasification via torrefaction. Energy 2006, 31 (15), 3458-3470.

[32] Deng, J.; Wang, G.-j.; Kuang, J.-h.; Zhang, Y.-l.; Luo, Y.-h., Pretreatment of agricultural residues for co-gasification via torrefaction. Journal of Analytical and Applied Pyrolysis 2009, 86 (2), 331-337.

[33] Bridgeman, T. G.; Jones, J. M.; Shield, I.; Williams, P. T., Torrefaction of reed canary grass, wheat straw and willow to enhance solid fuel qualities and combustion properties. Fuel 2008, 87 (6), 844-856.

[35] Prins, M. J.; Ptasinski, K. J.; Janssen, F. J. J. G., From coal to biomass gasification: Comparison of thermodynamic efficiency. Energy 2007, 32 (7), 1248-1259.

[36] Boateng, A. A.; Mullen, C. A., Fast pyrolysis of biomass thermally pretreated by torrefaction. Journal of Analytical and Applied Pyrolysis 2013, 100 (0), 95-102..

[37] Wannapeera, J.; Fungtammasan, B.; Worasuwannarak, N., Effects of temperature and holding time during torrefaction on the pyrolysis behaviors of woody biomass. Journal of Analytical and Applied Pyrolysis 2011, 92 (1), 99-105.

[38] Phanphanich, M.; Mani, S., Impact of torrefaction on the grindability and fuel characteristics of forest biomass. Bioresource Technology 2011, 102 (2), 1246-1253.

[39] Berrueco, C.; Mastral, E. J.; Esperanza, E.; Ceamanos, J., Production of waxes and tars from the continuous pyrolysis of high density polyethylene. Influence of operation variables. Energy and Fuels 2002, 16 (5), 1148-1153.

[40] Kern, S.; Pfeifer, C.; Hofbauer, H., Co-Gasification of Wood and Lignite in a Dual Fluidized Bed Gasifier. Energy & Fuels 2013, 27 (2), 919-931.

[41] Gómez-Barea, A.; Ollero, P.; Leckner, B., Optimization of char and tar conversion in fluidized bed biomass gasifiers. Fuel 2013, 103 (0), 42-52.

[42] Knoef H.A.M., Handbook Biomass Gasification, Eds BGT biomass technology group The Netherlands, 2005. ISBN: 978-9-08-100681-1.

[43] Kitzler, H.; Pfeifer, C.; Hofbauer, H., Pressurized gasification of woody biomass—Variation of parameter. Fuel Processing Technology 2011, 92 (5), 908-914.

[44] Mastral, J. F.; Berrueco, C.; Ceamanos, J., Pyrolysis of high-density polyethylene in free-fall reactors in series. Energy and Fuels 2006, 20 (4), 1365-1371.

[45] Mastral, J. F.; Berrueco, C.; Ceamanos, J., Theoretical prediction of product distribution of the pyrolysis of high density polyethylene. Journal of Analytical and Applied Pyrolysis 2007, 80 (2), 427-438.

[46] Richter, H.; Grieco, W. J.; Howard, J. B., Formation mechanism of polycyclic aromatic hydrocarbons and fullerenes in premixed benzene flames. Combustion and Flame 1999, 119 (1-2), 1-22.

Chapter 3

4. SOLID RECOVERED FUEL (SRF) GASIFICATION: EFFECT OF TEMPERATURE AND EQUIVALENCE RATIO

Abstract

The growing problem related to municipal solid waste generation has encouraged the development of alternative paths to convert waste to energy. Among the different options, gasification has been proposed as an interesting and efficient technology. In this study the influence of equivalence ratio (ER) and temperature on the performance of the air-gasification process during the gasification of a SRF material has been evaluated. One of the parameters to assess the gasification performance was the tracking of the evolution of some minor contaminants present in the syngas (tar, N, S and Cl compounds). The results suggest that gasification temperatures around 800-850 ºC and ER in the order of 0.30-0.35 could be appropriate conditions during SRF gasification aiming for tar and trace contaminants abatement without compromising to a large extent other gasification performance parameters.

This chapter is based on the following research article:

Berrueco C, Recari J, Abelló S, Farriol X, Montané D. Experimental Investigation of Solid Recovered Fuel (SRF) Gasification: Effect of Temperature and Equivalence Ratio on Process Performance and Release of Minor Contaminants. Energy & Fuels 2015;29:7419–27. doi:10.1021/acs.energyfuels.5b02032.

4.1 Introduction

Regardless the recent global economy recession a steady increase of municipal solid and all other kinds of waste production is patent [1]. Despite the implementation in the last decades of modern waste management systems, which combine prevention, reduction, separation, recycling, energy recovery and land filling, the amount of landfilled waste is still important [1]. In this framework, thermal treatment plants are an essential component of a sustainable waste management system, given the process attains a certain level of energy efficiency [2], and gasification has been proposed as an interesting solution for waste valorization with energy recovery [1].

Gasification presents several advantages over incineration of solid wastes: it is potentially more efficient than incineration (electric efficiency of gasification installation can be up to 50% higher than conventional WtE plants), presents similar capital cost to that of conventional WtE plants, it can be as environmentally clean as a state-of-the-art waste incinerator [3] and produces an energy carrier that can be utilized in gas engines, turbines, or synthesis of liquid fuels (i.e. biofuels) [4]. Of course, only a fraction of waste streams are 100% biogenic and would classify as "100% biofuels". Nevertheless, even if non-biogenic waste is used, the recovery of energy from non-recyclable waste is without doubt a reasonable option.[1]

Despite the promising aspects of gasification technology, there are several aspects of biomass and waste gasification that have delayed its full implementation, in particular for the production of second-generation biofuels. Those are mainly related to the highly heterogeneous nature of feeds, the limited experience under commercial conditions and the quality of the obtained syngas [2]. Some of the problems related to the heterogeneity of the wastes are partially overcome with the preparation of solid recovered fuels (SRF) from municipal solid waste (MSW). These are solid fuels obtained from non-hazardous wastes that must meet quality and classification criteria of the CEN/TS 15359:2006 technical specification.

On the other hand, the presence of impurities is the main concern for any application of the syngas, but especially in any catalytic synthesis. Crude syngas contains a series of contaminants, including tars, sulphur-, nitrogen- and chlorine-containing gases (NH_3, HCl, HCN, H_2S, COS) [5,6], volatile ash and

particulates that contain K, Na and traces of other elements which may influence catalyst performance [7,8].

Gasification of different wastes, including municipal solid wastes (MSW) and solid recovered fuels (SRF) as an energy recovery method has been studied in detail [5,9-12]. However, a limited number of studies have investigated the influence of process conditions on syngas quality and in particular on the release of minor contaminants such as HCl, NH_3, HCN or H_2S [5,11], and none of them have presented a detailed study of the evolution of N, S and Cl compounds during gasification of SRF materials.

The objective of the present study is to partially cover this gap, evaluating the influence of two crucial operating parameters, i.e. equivalence ratio (ER) and reaction temperature, on process performance and mainly on the release of minor contaminants during the air-gasification of a SRF. The final aim is to include the minor contaminant release parameter into the equation when selecting the most appropriate gasification conditions, but without compromising to a large extent other gasification performance parameters. In addition, the information reported can be useful for further development of feedstock pretreatments or gasification strategies in order to reduce the presence of these contaminants in the producer gas.

4.2 Materials and methods

4.2.1 Sample characterization and preparation

One MSW-derived mixed material, hereby referred to as RT, was used as feedstock during the gasification tests. This material is a mixed fraction produced by Ambiensys (Spain) through their process of active hygienization (GeiserBox®) of unsorted MSW and refuse materials from plants processing selective waste collection streams. This fraction was rich in plastics and textiles, with a low content of biomass and paper.

Before the characterization and gasification tests, the sample was ground and sieved to 1 mm using a low-speed rotary cutting mill (Retsch SM-300), operated at low feeding rate to avoid excessive heating of the samples.

Table 4.1 Main characteristics of feedstock (as received basis)

		RT
Proximate analysis (wt.%)	**Moisture**	1.13±0.12
	Volatiles	86.20±0.90
	Fixed carbon	2.51±0.11
	Ash	10.15±0.31
Ultimate analysis (wt.%)	**C**	66.78±1.01
	H	10.70±0.46
	O (by difference)	10.68±1.12
	N	0.76±0.12
	S	0.23±0.018
	F	<0.01
	Cl	0.70±0.0001
LHV (MJ kg^{-1})		26.99±0.69
Ash composition (mg kg^{-1}_{fuel})	**Aluminium as Al_2O_3**	18029±429
	Calcium as CaO	24453±452
	Chrome as Cr	<50
	Iron as Fe_2O_3	3051±60
	Lead as Pb	<50
	Magnesium as MgO	2359±115
	Manganese as MnO	<50
	Nickel as Ni	<50
	Phosphorus as P_2O_5	3749±116
	Potassium as K_2O	1973±80
	Silicon as SiO_2	19597±609
	Sodium as Na_2O	2881±115
	Titanium as TiO_2	3693±131
	Vanadium as V	<50
	Zinc as Zn	224±11

The proximate and ultimate (C, H, N, S) analyses of the RT sample were carried out according to the EN-15402:2011, EN-15403:2011 and EN-15407:2011 standard methods using a LECO Thermogravimetric analyser (TGA 701) and a LECO Truspec CHN-S analyser. The heating value was measured following the EN-15400:2011 standard method in an AC600 LECO isoperibol calorimeter. After each sample combustion the bomb was washed out with Mili-Q® water to recover sulphur (H_2SO_4) and halogens, which were analysed by ionic chromatography (Dionex ACS 1100) (EN-15408:2011 standard method).

The chemical composition of the feedstock ash was determined by inductively coupled plasma-optical emission spectroscopy (ICP-OES) in a Spectro Arcos 165 spectrophotometer. A batch of ash was prepared by calcining several batches of sample in a furnace, following the EN-15403:2011 standard method. The prepared ash sample was digested in a Berghof microwave, following the EN-15410:2006 and EN-15411:2006 standard methods. Table 4.1 depicts the results for the characterization of RT sample. These data are the result of at least triplicate analysis, being the uncertainties of the average values estimated at a 95% probability level.

4.2.2 Fluidized bed gasifier

Briefly, the externally heated fluidized bed gasifier (FBG) consisted in a Hastelloy X pipe (404-mm-long, 23.8 mm internal diameter) (PID ENG&Tech, Spain). After the FBG the produced gas pass through a series of filters and condensers in order to remove particulates and condense water and tars. A control system that allows continuous operation and the recording of the main process parameters (temperature, flow and pressure in different points) completes the experimental system. In this study a modification was included in the original rig. In order to determine the concentration of HCl, NH_3, HCN and H_2S, a fraction of the producer gas was collected (after the hot filter), in a Tedlar gas-sampling bag. Further details of the experimental setup and experimental procedure can be found elsewhere [13].

Gasification was performed under air atmosphere, with an equivalence ratio (ER) between 0.25 and 0.35 and four different temperatures (700, 750, 800 and 850 ºC). The used flows resulted in a fluidizing gas velocity between five and six times the bed material minimum fluidization velocity (U_{mf}), i.e. residence times in the reactor of 2.7-3.3 s. Mass balances were calculated taking into account the mass of gases produced (gas balance) and the mass of obtained tar and unconverted solid particles. Adequate mass balance closures (≥ 95 %) were obtained for all the conducted tests.

4.2.3 Gas and tar analysis

An online micro GC (Agilent 490) was used to quantify the major components (H_2, O_2, N_2, CO, CO_2, CH_4 and saturated and unsaturated C_1 to C_5

hydrocarbons) in the fuel gas during the experiments. Further details of the gas analysis system can be found elsewhere.[13]

The analysis of H_2S, HCN, NH_3 and HCl was carried out by means of ion selective electrodes (ISE, Metrohm). The producer gas, previously collected in a tedlar bag, was pumped sequentially through a series of impingers containing specific solutions to retain the ions (S_2^-, CN^-, Cl^- and NH_4^+). The gas was pumped at a constant flow of 1 LN min^{-1} during 5 min for each measured compound.

Previously to their analysis by ISE, about 0.1 mL of Total Ionic Strength Adjustment Buffer (TISAB) was added to each sample solution in order to adjust its ionic strength and pH value. Afterwards, the ion analyses of the bubbled solutions were performed with a 905 Titrando and an 814 USB Sample Processor (Metrohm) equipped with tiamo™ software for direct potentiometry. The setup consisted of a specific ISE and an Ag/AgCl reference electrode containing electrolyte solution (i.e. KCl 3M). In addition, the temperature and pH were controlled with a PT1000 temperature sensor and pH glass electrode respectively, and a rod stirrer assured a continuous stirring of the samples. Table 4.2 gathers the information about the absorbing solution, reference electrolyte and TISAB solution used for the analysis of each ion. The electrodes were calibrated using four solutions prepared from a standard stock (1000 ppm) in order to obtain a linear calibration curve for each ion concentration determination.

Table 4.2 Characteristics of the Ion Selective Electrode measurements

ISE	Absorbing solution (mL)	Calibration solutions (ppm)	Ag/AgCl reference electrolyte	TISAB solution	pH range
S^{2-}	50 % Milli-Q water + 50 % SAOB	0.1, 1, 10 and 100	KCl 3 M	NaOH 10 M	2-12
CN^-	100 % NaOH 0.1 M	0.2, 2, 20 and 100	KCl 3 M	NaOH 10 M	10-14
Cl^-	100 % Milli-Q water	1.8, 10, 50 and 100	KNO_3 1 M	$NaNO_3$ 5 M	0-14
NH_4^+	100 % Milli-Q water	0.1, 5, 50 and 100	-	NaOH 10 M	11-14

Tar structural features were compared by Fourier transform infrared (FT-IR) spectroscopy using a Bruker Vertex 70 spectrometer equipped with Platinum diamond ATR unit. Spectra were collected at room temperature (range 400-4000 cm^{-1}) by co-addition of 32 scans at a nominal resolution of 4 cm^{-1}. The background spectrum was set with an empty cell at ambient conditions.

4.3 Results and discussion

4.3.1 Product yields and syngas composition

Table 4.3 lists the operating conditions (i.e. temperature and ER) of all the performed tests, together with the main experimental results. These results include the gas, tar and char yields obtained under different experimental conditions. The product yields are calculated as the percentage of mass of compound per mass of dry fuel. As a result of using this basis the sum of gas, tar and char yields results above 100%, since products are formed due to the reaction with the gasification agent (air).

4.3.1.1 Effect of gasification temperature

The obtained results showed an increase in gas yield at higher gasification temperatures, together with a decrease in tar and char yields. In general higher temperatures enhanced the gasification reactions; in the range 700-750 ºC the effect of the increase in the initial devolatilization step could be noticed, with an increase in gas yield and a decrease in char yield. On the other hand higher temperatures (800-850 ºC) provoked an increase of the rates of the char gasification reactions (Boudouard and water-gas reaction), leading again to higher gas and lower char yields. Temperature also affected the evolution of tar yield, mainly related to the tar cracking towards gas products.

The effect of temperature on gas composition evolution is presented in Figure 4.1. At a constant ER (~0.31), the H_2 content in the producer gas increased with temperature in all the studied range with a steep increment in the range 800 to 850 ºC (from 5.3 to 10.8 % vol.). This rise could be explained by the increase of the rates of char steam gasification, the mechanisms of PAH growing, which lead to larger production of hydrogen and the shift of

methanation equilibrium [14-18]. CO and CO_2 concentration presented opposite trends. In the interval from 700 to 800 ºC, CO_2 concentration experienced a slight increase together with a diminishment of CO. At 850 ºC, a clear increase of CO concentration was observed whereas CO_2 concentration remained almost constant. This effect could be related to char gasification reactions (Boudouard and water-gas reaction) and the evolution of methanation equilibrium [15].

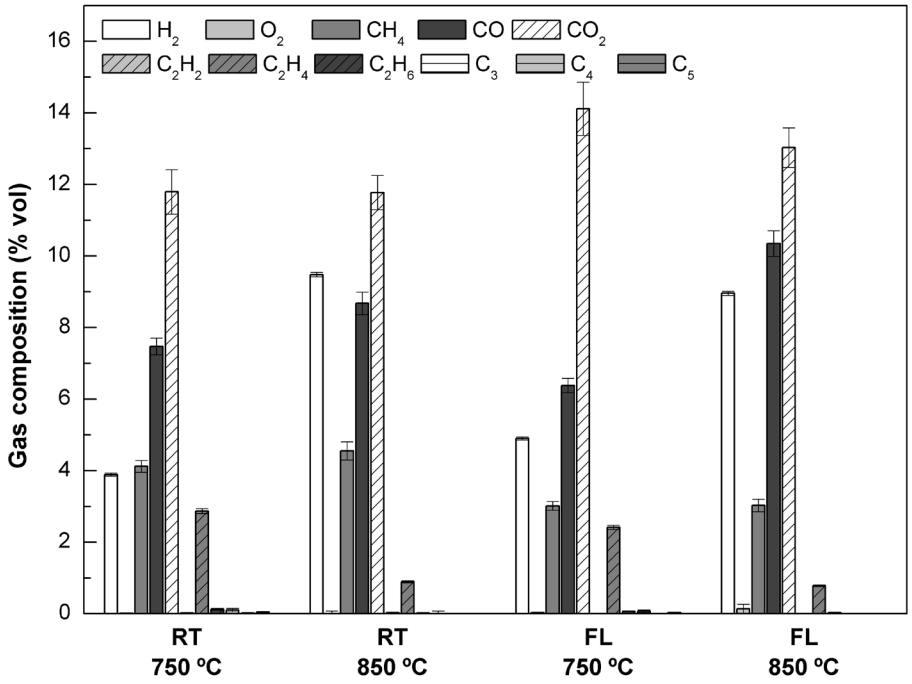

Figure 4.1 Effect of gasification temperature on producer gas composition (ER ~ 0.31)

On the other hand CH_4 concentration increased when gasification temperature varied from 700 to 800 ºC whereas a lower concentration (4.6 % vol.) was observed at 850 ºC. The initial growth with temperature can be explained since temperature favours the de-alkylation of tertiary aromatic tars and cracking of aliphatic hydrocarbons towards methane. At higher temperature (850 ºC), methane shifted towards H_2 and CO due to the exothermic character of methanation equilibrium [19].

Other hydrocarbons (C_2-C_5) were produced in lower concentration than the rest of the gas species, with the exception of ethylene that presented a concentration in the order of 1 to 3% vol. These hydrocarbons, which probably derived from the plastic fraction of the feedstock [17], showed a general decrease with temperature. On the one hand, heavier hydrocarbons (C_4-C_5) only

appeared in a representative level at 700 and 750 ºC, showing a marginal presence in the gas produced at higher temperatures. On the other hand C_2H_4 suffered an important depletion from 800 to 850 ºC. These trends are related to the higher rates of cracking and reforming of hydrocarbons at higher temperature together with the fact that these compounds could be involved in the formation of tertiary tar and PAHs, a process enhanced at high temperature (800-850 ºC) [14,17].

4.3.1.2 Effect of equivalence ratio:

The equivalence ratio presented a clear effect on gas yield, which increased almost linearly in the whole studied range. In contrast, tar and char yields decreased with increasing ER. An increase of ER implies a larger amount of oxygen available and therefore a greater extension of partial oxidation reactions. Figure 4.2 shows the effect of equivalence ratio on syngas composition.

The content of hydrogen, methane and C_2-C_5 hydrocarbons decreased as the equivalence ratio increased. For instance H_2 concentration dropped from 5.2% vol. to 3.9% vol. when the ER increased from 0.22 to 0.35. Similarly, CH_4 concentration decreased from 5.8 to 3.7 % vol. under the same experimental conditions. As stated previously, this reduction with ER was justified by the enhancement of the oxidation reactions. CO and CO_2 concentrations remained substantially unchanged as a consequence of the opposite effect of Boudouard reaction and CO partial oxidation, with a slight decrease with the equivalence ratio [19]. This reduction was the result of N_2 dilution (as larger flows of air were introduced to increase ER levels) rather than a lesser extension of oxidation reactions. In fact the concentration of CO and CO_2 in a hypothetic N_2-free syngas would present a sustained growth with ER, whereas the rest of combustible gases would show the opposite trend.

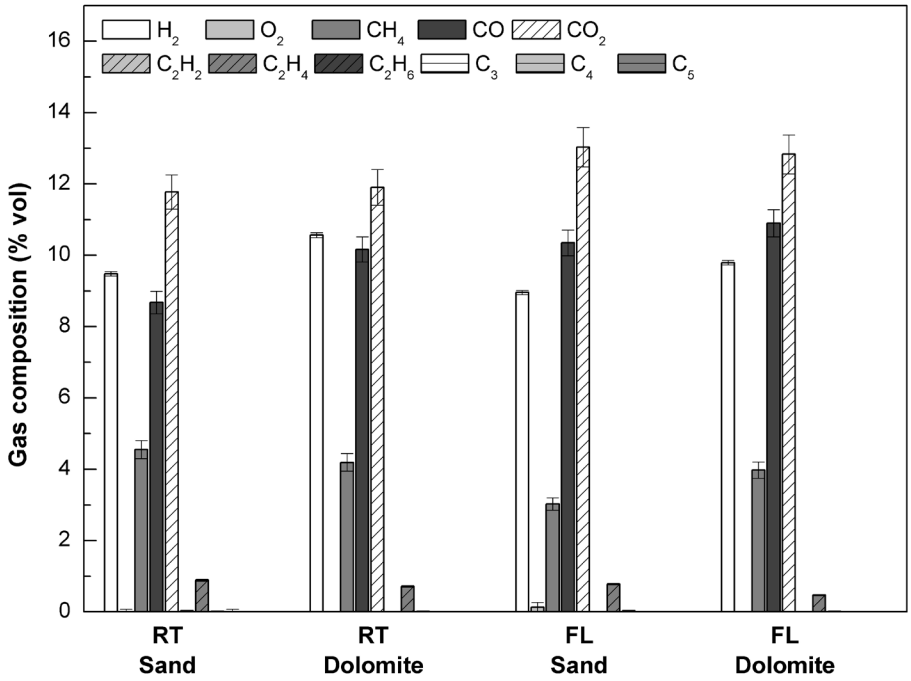

Figure 4.2 Effect of ER on producer gas composition (T 750 ºC)

4.3.2 Tar concentration

The results of tar content in the dry produced gas (expressed as g Nm^{-3}) appear displayed in Figure 4.3. The data showed a reduction in tar content as the temperature and ER increased. This decrease was more marked in the interval of ER from 0.22 to 0.25 and almost linear at higher ER values, while tar content decreased linearly with temperature in all the studied range. The influence of temperature and equivalence ratio on tar content is directly related to the larger extent of the tar cracking and oxidation reactions under these conditions. Notice that the values of tar concentration reported here are in accordance with the results reported in previous studies of air gasification in FBG of different SRF, both in laboratory and pilot plant scale [5-9]. However the levels of tar concentration for SRF are considerably higher than those obtained for biomass under similar conditions [14-18], and therefore additional strategies and cleaning steps should be considered for an adequate conditioning of the producer gas.

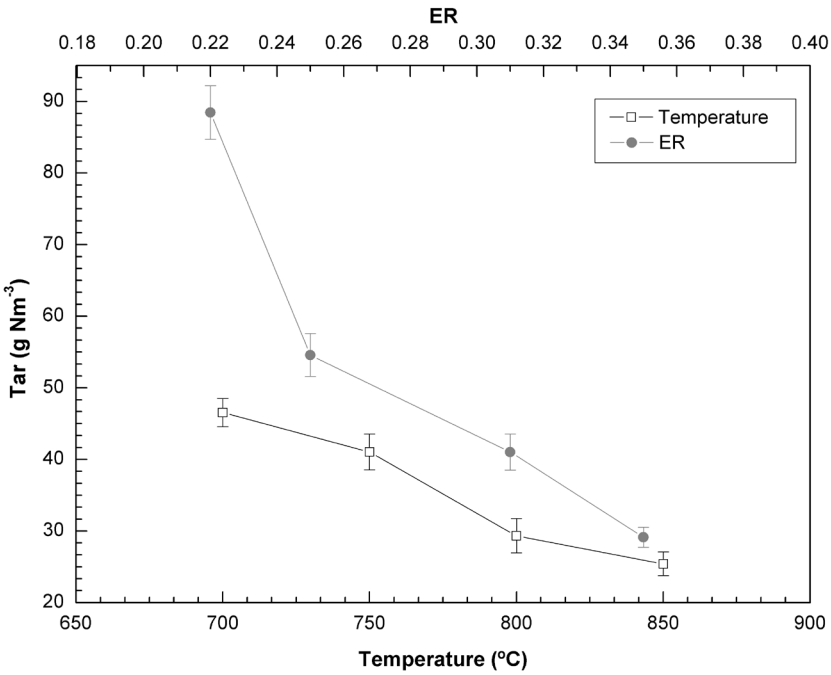

Figure 4.3 Effect of gasification temperature (ER 0.31) and ER (T 750 ºC) on tar content

In addition, an initial evaluation of the tar structural parameters of the obtained tars by Fourier transform infrared spectroscopy is presented in Figure 4.4. The assignment of the IR absorption bands to the functional groups of greatest relevance to tars can be found elsewhere [20,21]. The obtained spectra showed a decrease in the aliphatic band (2990 cm^{-1}) together with an increase in the signal of the different aromatic band region as gasification temperature and ER increased. Additionally, an increase of the ratio between the absorbance due to aliphatic C-H stretching (2920 cm^{-1}) and aromatic C-H stretching (3040 cm^{-1}) was also observed. The evolution of the oxygenated functionalities was less evident. In general, the intensity of the peaks related to these compounds (C=O structures, broad band at 1715 cm^{-1}- 1650 cm^{-1}, methoxyl groups, 1265 cm^{-1} and C-O bands, 1035 cm^{-1}) was higher for the tars obtained at lower temperature and ER, although the differences were minor.

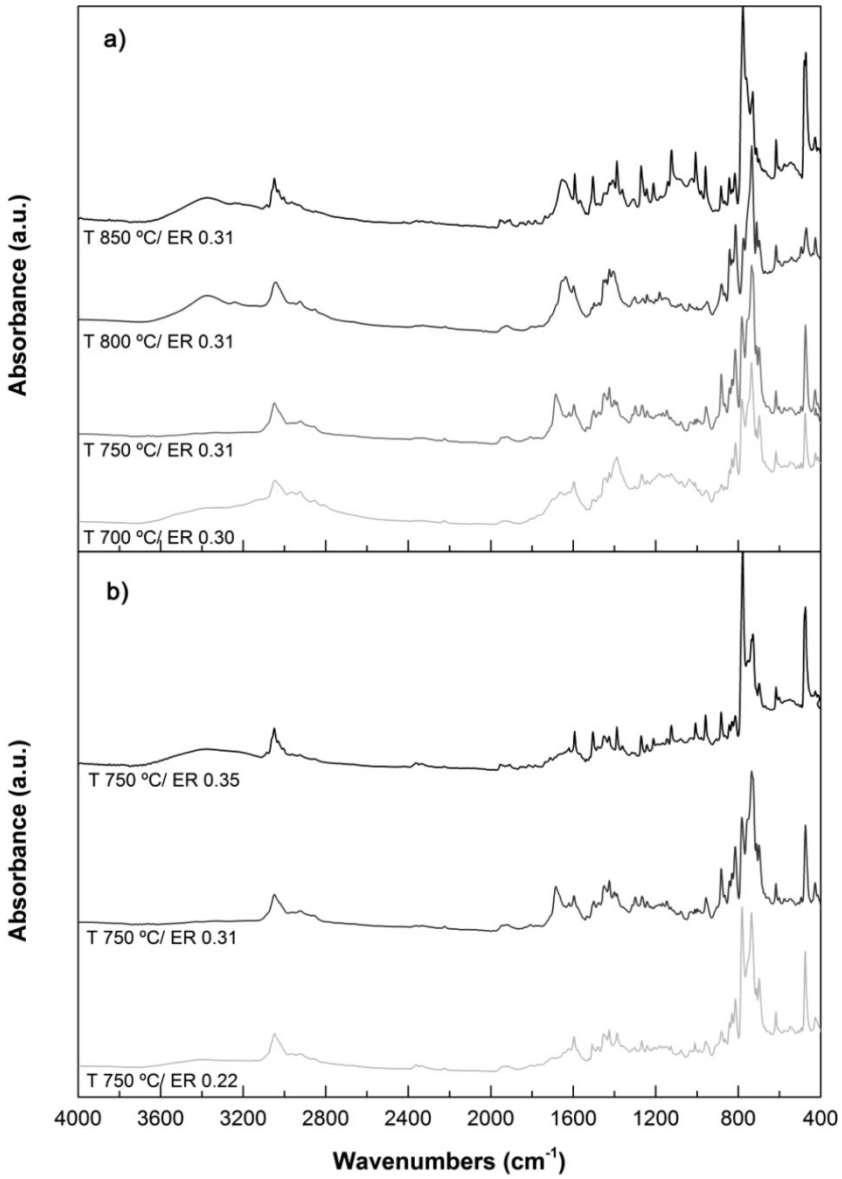

Figure 4.4 FTIR spectra of tars obtained in a FBG: influence of: a) gasification temperature and b) ER

These results indicated that higher gasification temperatures led to the cracking and oxidation of the aliphatic and olefinic compounds formed from the plastic content of the feedstock, together with a larger degree of aromatization for the tars obtained at higher gasification temperatures, in particular for gasification temperatures above 750-800 ºC. These data support the hypothesis of polymerization of the tars towards polycyclic aromatic hydrocarbon [22].

4.3.3 Evolution of HCl, HCN, NH_3 and H_2S in the producer gas

The minor contaminants analysed in the syngas were hydrogen chloride (HCl), hydrogen cyanide (HCN), hydrogen sulphide (H_2S) and ammonia (NH_3). As previously stated, the analysis was carried out by means of ion selective electrodes after retaining the ions in specific solutions. Notice that the detection limits for the analytical procedure were 1.0, 0.16, 2 10^{-3} and 1.2 mg Nm^{-3} for HCl, HCN, H_2S and NH_3 respectively.

The preliminary results showed that HCl and HCN were dominant among the analysed minor contaminants. The effect of gasification temperature (from 700 to 850 ºC) on the evolution of the studied minor contaminants is shown in Figure 4.5. HCl concentration in the producer gas decreased a 73% as gasification temperature increased, from 450 mg Nm^{-3} at 700 ºC to 123 mg Nm^{-3} at 850 ºC. This reduction was not linear in the studied range, and a plateau around 300 mg Nm^{-3} was observed at the intermediate gasification temperatures (750 and 800 ºC). The chlorine nature in SRF is dual, organic from chlorinated polymers (e.g. PVC) and inorganic, for instance salts (NaCl and/or KCl) from food waste [23]. Organic and inorganic chlorine partially transforms into HCl during thermal processes; PVC almost totally decomposes at 550 ºC [24]. On the other hand, the inorganic salts volatilize at higher temperatures (above 800 ºC) and partly evolve towards HCl or remain in the sand bed due to sintering effects [24]. Several studies indicated that the evolution of HCl in the producer gas are affected by a series of parameters, and related the decrease of HCl in the gas phase with the equilibrium among Cl and alkaline metals [25-29]. The studies also suggested that the increase of KCl in the gas with temperature was not just related to the KCl/HCl equilibrium, but more significantly to the amount of potassium available in the reaction media. At temperatures below 700 ºC, the formation of alkaline carboxylates is favoured, and Cl would mainly form HCl. At higher temperatures, the carboxylates degrade and the alkaline metals become available more easily, causing the decrease of the HCl in the gas [25]. Despite the fact the cited studies used different biomasses and thermal processes, the results are in concordance with the current study, providing a qualitative explanation for HCl evolution. Regarding the study of HCl release, a SRF air gasification work by Dunnu et al. [9] reported a decrease in HCl concentration in the producer gas with temperature (700 – 800 ºC) from 56.8

mg Nm^{-3} to 37.6 mg $\cdot$ Nm^{-3}. The trend is similar to the one presented in the current study, with a reduction of about 35% in the interval from 700-800 ºC, although the actual figures differed in a large extent.

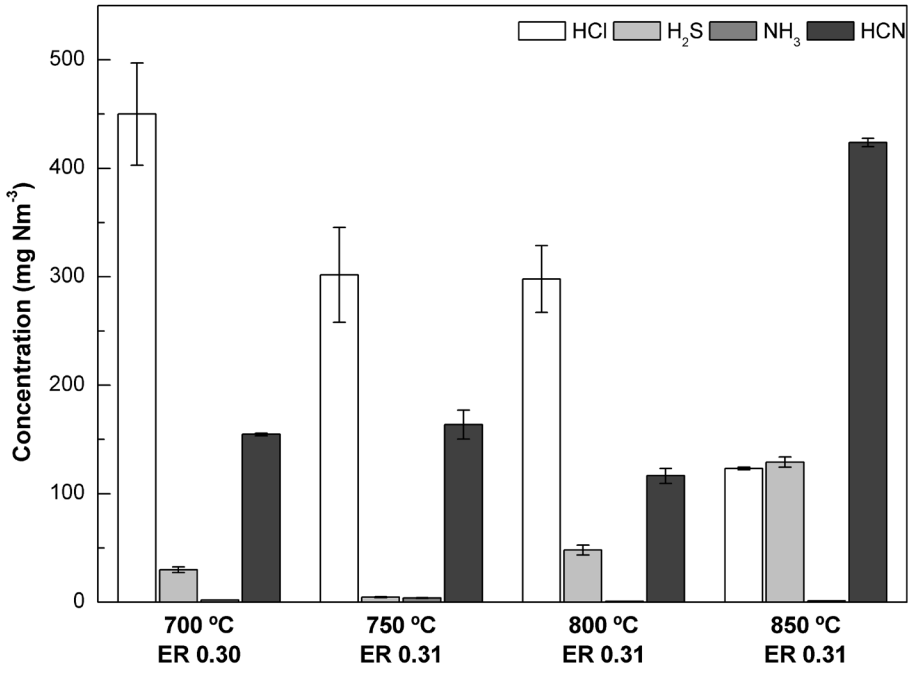

Figure 4.5 Effect of gasification temperature on minor contaminants concentration in producer gas

The evolution of the studied minor contaminants containing N (NH_3 and HCN) with gasification temperature is also presented in Figure 4.5. These compounds have been selected to trace N evolution in the gas phase, as they have been identified as the main nitrogen gas compounds in pyrolysis and gasification processes [30]. In all the studied range HCN appeared in a higher concentration in comparison to NH_3, whose presence was always below 4 mg Nm^{-3}. HCN concentration remained at an almost stable level around 155 mg Nm^{-3} in the temperature range from 700 to 800 ºC, showing a steep increase at the maximum gasification temperature up to 424 mg Nm^{-3}. These figures imply that in the temperature interval from 700 to 800 ºC about 3% (9% at 850 ºC) of the nitrogen contained in the fuel ended up in the producer gas as NH_3 and HCN under the presented experimental conditions. Although the mechanisms for the formation of nitrogen compounds during pyrolysis/gasification are still not well understood [31], especially in the case of biofuels, a series of studies give insight into the results here presented. Among the factors affecting the fuel-

N conversion (i.e. type of fuel, nitrogen functionality, initial oxygen concentration, reactor temperature, residence time, heating rate, particle size, bed material, etc.), chemical composition of the fuel and fuel nitrogen functionalities are key in the initial product distribution [28,31]. Generally speaking, the main nitrogen-containing pyrolysis product is expected to be HCN when nitrogen fuel is present in pyrrolic and pyridinic forms whereas NH_3 will appear when fuel-N is present in amino-groups [30-32]. This fact would explain the higher level of NH_3 detected during biomass gasification, in comparison to the present study. Biomass has mainly protein nitrogen, which would evolve mainly towards NH_3 under gasification conditions [29]. On the other hand, the main source of nitrogen in SRF samples are polymers used as textiles (polyamides, polyacrylonitriles, etc), which preferentially decompose at high temperatures towards HCN, particularly under high heating rate conditions [30,33].

The evolution of biomass N-fuel with temperature has also been described [28], showing an important increase of conversion towards HCN with temperature. This can be linked to the secondary reactions of tar and volatile [28,34,35]. The evolution of primary volatiles, produced during the pyrolysis of N-containing polymers [33], such as cyclic amides and nitriles, would explain the observed trend in Figure 4.5 at temperatures above 800 ºC. In addition, other authors [30,36]. hypothesize that NH_3 formation takes mainly place in solid phase in reactions involving char thermal cracking, and would be favoured at low temperature, low heating rates and large particle size [28,30]. Therefore, this argument supports the high HCN/NH_3 ratio presented in Figure 4.5, as the experimental conditions used in the study include high temperatures (in the range 700 – 850 ºC), high heating rates of the fuel (> 1000 ºC s^{-1}), and small particle size (250-500 μm). Another aspect worth mentioning is that the percentage of the nitrogen contained in the fuel ending up in the producer gas (as NH_3 and HCN) was much lower than the reported values for different biomasses (20-60%). This fact can be related to the presence of alkali and alkaline earth metals in the fuel ashes (Table 4.1), as the presence of calcium, potassium and iron may catalyse the conversion for N-fuel, leading to the formation of N_2 [28,37]. Notice that the level of ashes in SRF, and in particular

in the fuel used in the present study, is much higher than that in typical biomass.

H_2S has been traced as the main sulphur compound in the syngas (Figure 4.5). Several studies have reported that under gasification conditions, the release of sulphur into syngas happens mainly as H_2S, whereas other sulphur compounds (COS, CS_2 or thiophene), appear in much lower concentration (30 times smaller or less) [11,28,38,39]. The evolution of hydrogen sulphide concentration in the syngas suffered an overall increase from 30 mg Nm^{-3} to 129 mg Nm^{-3} in the range 700-850 ºC, with a minimum around 750 ºC. Similarly to other heteroatoms, several factors affect the sulphur release during thermal treatments of solid [28]. Concerning the effect of temperature, organic sulphur in biomass is generally released at low temperatures during the volatilization stage. On the other hand, inorganic sulphates present higher stability, remaining in the solid char unless high temperatures are reached and gasification/combustion reactions of char occur in a large [28]. In addition to the sulphur release from the fuel, the effect of temperature on H_2S release might be also related to the presence of some elements in the fuel ashes (mainly Ca and K) [28,40]. Several works [28,41] have reported the influence of ash composition in the evolution of H_2S in gas phase. In particular, Knudsen et al. [41] reported the sulphur propensity to react with potassium; however at temperatures above 700 ºC, Cl and Si would compete to react with the available K resulting in higher levels of H_2S release. This observation is consistent with the H_2S evolution shown in Figure 4.5 and the information about ash composition presented in Table 4.1. Nevertheless, a full characterization of the char and bed material may be necessary to validate this assumption.

Regarding the effect of ER (Figure 4.6), the analysis of the minor contaminants revealed that the lower the equivalence ratio the higher the concentrations of all the analysed species, especially HCl. HCl level dropped an 85% (from 2268 to 342 mg Nm^{-3}) upon increasing ER (0.22-0.35). The rest of contaminants (H_2S, HCN, and NH_3) barely decreased in the interval 0.22-0.25; nevertheless a remarkable decline appeared at ER 0.31, and HCl was the only compound detected above 30 mg Nm^{-3} at ER 0.35. Contrasting to other studies, Pinto et al. [11] reported H_2S contents below 500 ppmv [759 mg Nm^{-3}] during the gasification of a SRF in a bubbling fluidized bench-scale reactor at 800 ºC

and ER 0.2. The ER increase from 0.2 to 0.4 decreased the H_2S concentration about 31% as oxidations reactions were favoured. The ER increase also seemed to promote the nitrogen release resulting in higher NH_3 levels (from 2700 ppmv [2049 mg Nm^{-3}] to 5200 ppmv [3947 mg Nm^{-3}] approximately) [11]. Arena and Di Gregorio [5] performed the air gasification of a SRF in a FBG at 850-930 ºC with equivalence ratios ranging from 0.25 to 0.33. Given the autothermal operation of the gasifier ER and temperature are couple, making the study of the evolution of HCl, H_2S and NH_3 compositions challenging, in fact the reported data did not show clear trends while varying the experimental conditions. The highest levels of HCl (117.5 mg Nm^{-3}), NH_3 (134 mg Nm^{-3}) and H_2S (39.1 mg Nm^{-3}) in the producer gas were reported at temperatures around 870-880 ºC and equivalence ratios between 0.27-0.30.

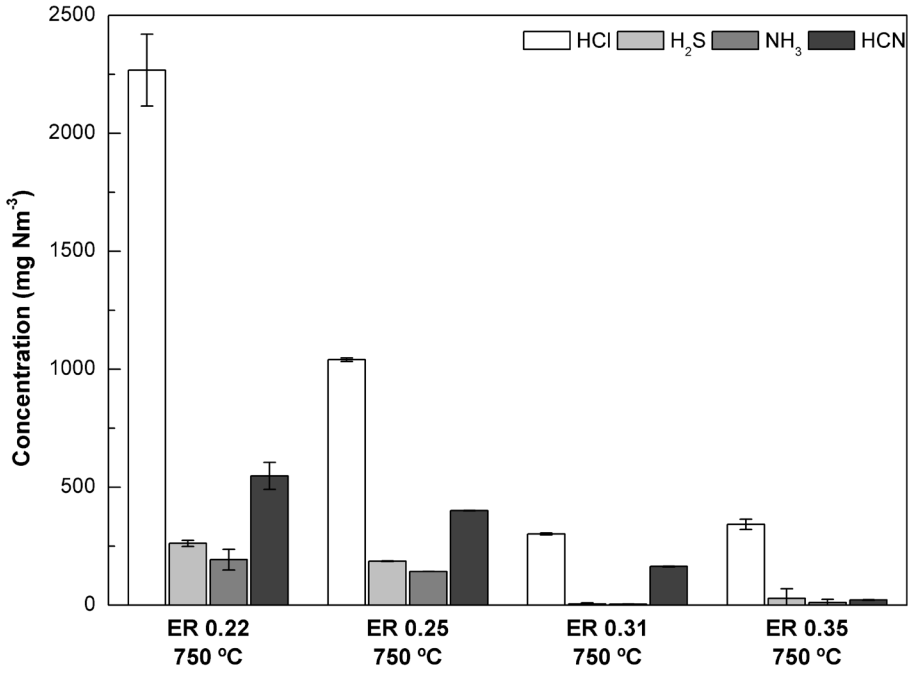

Figure 4.6 Effect of ER on minor contaminants concentration in producer gas

The literature review denotes that the different studies on refuse derived fuels (RDF), SRF and biomass gasification present discrepancies on the influence of equivalence ratio on the evolution of these minor contaminants. Following the discussion on the influence of temperature on the release of HCl, NH_3, H_2S and HCN, it could be expected larger amounts of these compounds as ER increases, since the combustion and gasification reactions of char are

enhanced under these conditions, favouring the release of Cl, N or S retained in the char. Nevertheless several hypotheses support the decrease of the analysed compounds. N and S could evolve towards NO_x and SO_x at higher ER (compounds not identified in the current studies). Furthermore, Broer et al. [42] also hypothesized that increasing ER and temperature favoured the conversion of NH_3 towards N_2 against other NH_3 release pathways, leading to lower NH_3 yields. Their work showed not only a reduction of NH_3 concentration from 7590 to 4402 mg Nm^{-3} (about 50-32% less) but also a HCN concentration drop (from 3014 to 530 mg Nm^{-3}) when ER increased (0.21-0.38). In addition to these hypotheses, the influence of ash composition might also have an important effect on the evolution of the studied contaminants. The evolution of HCl could be explained taking into account that part of the alkali compounds could not be accessible at the lower equivalence ratios (as they may be still imbibed in the char matrix), while the chlorine, mainly coming from the decomposition of different chlorinated polymers, is almost completely released at much lower temperatures. As equivalence ratio increases, the alkali compounds could be more accessible, reacting with chlorine and reducing the HCl concentration in the gas.

4.3.4 Effect of experimental parameters on gasification performance

This section gathers a series of parameters providing additional information that can be combined with the results of tar and minor contaminants content in the syngas in order to assess the more adequate conditions for performing the gasification of the studied material. It is important to notice that these parameters are presented as qualitative information and are not directly applicable to industrial gasifiers. Nevertheless the main trends and conclusions can be useful for further evaluation of SRF gasification.

4.3.4.1 H_2/CO ratio in the producer gas

Table 4.3 shows the evolution of these ratios with the gasification temperature and ER. This ratio ranged between 0.4 and 1.0, increasing with gasification temperature, and presented a slight decrease (from 0.7 to 0.5) with ER. Several factors affected the H_2/CO ratio, on the one hand H_2 production

increased with gasification temperature and slightly decreased as ER rose (due to the enhancement of oxidation reactions). On the other hand CO concentration also increased with gasification temperature (based on the CO/CO_2 equilibrium), although to a lower extent than the one reported for H_2. CO composition remained almost constant in all the investigated ER range. The observed levels of H_2/CO were comparable to those of air gasification of biomass [18,19], however this ratio is far from the optimum for any subsequent fuel catalytic synthesis. The results depicted that the higher the temperature and the lower the ER the higher the H_2/CO, although these two parameters are not completely independent in an industrial autothermal gasifier; the results suggest that the gasification temperature should be close to 800-850 ºC.

4.3.4.2 Carbon conversion efficiency (X_C)

This parameter describes the performance of gasification process, defining the conversion of carbon into gaseous products. This value (see Table 4.3) was determined as the ratio of carbon leaving the gasifier as gaseous products over the carbon in the feedstock. Both, temperature and ER, presented a similar influence on carbon conversion efficiency, with an increase in this parameter as gasification temperature and ER increased. The larger tar and char conversion at higher temperatures and ER (due to enhancement of char gasification and oxidation and tar cracking reactions) would explain this fact [13,18].

4.3.4.3 Syngas heating value

Another important parameter for the syngas use is the heating value of the producer gas, presented in Table 4.3 as lower heating value (LHV).

The calculated syngas LHV values ranged between 4.8 and 6.4 MJ Nm^{-3}, presenting different trends as a function of temperature and ER. An increase of gasification temperature led to an initial decrease of the LHV (from 700 to 750 ºC), remaining practically constant at 800 ºC, and decreasing again at 850 º C. This trend is directly related to the gas composition, and the opposite effect of gasification temperature on H_2 (increased with gasification temperature), CH_4 (increased in the range 700- 800 ºC), and the rest of hydrocarbons (decreased from 700 to 850 ºC). The increase of H_2 would provoke an increase of LHV of

the syngas with gasification temperature; however the reduction of hydrocarbons in the syngas surpassed the contribution of H_2 to the LHV.

The effect of ER on the syngas LHV was more evident; the greater extension of partial oxidation reactions at higher ER provoked a reduction in the main combustible gases. This effect led to a reduction in the LHV of syngas in the studied ER range. Another remarkable fact is the more distinct decrease of LHV in the range from 700 to 800 ºC, remaining almost constant at higher temperatures. As previously stated, this is related to the diminishment of the hydrocarbon content in the syngas and mainly the decrease of ethylene content. It is important to notice that the evolution of syngas LHV may be slightly different to the one reported for syngas from biomass gasification. In the case of SRF gasification, the presence of hydrocarbons in the producer gas and their contribution to the LHV of the gas was more significant. These hydrocarbons, and in particular ethylene, derive from the plastic fraction of the original SRF. The evolution of these hydrocarbons with the temperature influences the LHV of the syngas in a different way to the one observed for biomass samples.

4.4 Conclusions

This work reports experimental results of gasification of a SRF sample, carried out in a fluidized bed reactor in order to determine the influence of temperature and equivalence ratio on gasification performance and the release of minor contaminants.

An increase of gasification temperature and ER resulted in an increase of gas yield, together with lower tar and char yields. Although the influence of both parameters on product yields was similar, the causes differ. Increasing temperatures enhanced the cracking of hydrocarbons and the gasification reactions of the produced chars, whereas higher ER led to a larger extent of partial oxidation reactions due to the higher oxygen availability. Additionally, the analysis of the obtained tars corroborated that the increase in temperature and ER led to lower tar levels, but aromaticity of the obtained tar increased, especially at higher temperatures.

Increasing temperature made the produced gas composition shift towards higher H_2, CH_4 and CO content, while heavier hydrocarbon (C_2-C_5) levels decreased. Regarding the effect of equivalence ratio, the higher levels of oxygen

in the gasification agent resulted in a decrease in almost all the combustible gases (H_2, CH_4 and hydrocarbons) while CO and CO_2 concentration remained practically constant.

In addition, the paper also presents the evolution of minor contaminants (HCl, HCN, NH_3 and H_2S) in the producer gas. Among the most relevant results a clear diminishment of HCl concentration with gasification temperature and ER is reported. In addition H_2S and HCN presence increased with temperature, and the release of N as HCN was predominant over NH_3 under the studied experimental conditions. The observed trends in the current study have been contrasted with studies under similar conditions and different feedstocks. This comparison, together with the information of the current work has derived in a qualitative explanation, according to the experimental conditions and the influence of ash composition, for the release of the minor contaminants.

The presented results suggest that gasification temperatures around 800-850 ºC and equivalence ratios between 0.30 and 0.35 could be appropriate conditions for SRF gasification in order to reduce the tars and trace contaminants concentration without compromising to a large extent other gasification performance parameters such as carbon conversion efficiency or syngas heating value.

4.5 References

[1] Schneider, D.R.; Ragossnig, A.M.; *Waste Manage. Res.* 2013, 31, 339-340. http://dx.doi.org/10.1177/0734242x13482228.

[2] Arena, U. Gasification: An Alternative Solution for Waste Treatment with Energy Recovery. *Waste Manag.* 2011, *31*, 405–406. http://dx.doi.org/10.1016/j.wasman.2010.12.006.

[3] H Arafat, H. A.; Jijakli, K. Modeling and Comparative Assessment of Municipal Solid Waste Gasification for Energy Production. *Waste Manag.* 2013, *33*, 1704–1713. http://dx.doi.org/10.1016/j.wasman.2013.04.008.

[4] Stiegel, G. J.; Maxwell, R. C. Gasification Technologies: The Path to Clean, Affordable Energy in the 21st Century. *Fuel Process. Technol.* 2001, *71*, 79–97. http://dx.doi.org/10.1016/s0378-3820(01)00138-2.

[5] Arena, U.; Di Gregorio, F. Gasification of a Solid Recovered Fuel in a Pilot Scale Fluidized Bed Reactor. *Fuel* 2014, *117*, 528–536. http://dx.doi.org/10.1016/j.fuel.2013.09.044.

[6] Tijmensen, M. Exploration of the Possibilities for Production of Fischer Tropsch Liquids and Power via Biomass Gasification. *Biomass and Bioenergy* 2002, *23*, 129–152. http://dx.doi.org/10.1016/s0961-9534(02)00037-5.

[7] Galadima, A.; Muraza, O. Waste to Liquid Fuels: Potency, Progress and Challenges. *Int. J. Energy Res.* 2015, *39*, 1451–1478. http://dx.doi.org/10.1002/er.3360.

[8] Kim, K.; Kim, Y.; Yang, C.; Moon, J.; Kim, B.; Lee, J.; Lee, U.; Lee, S.; Kim, J.; Eom, W.; et al. Long-Term Operation of Biomass-to-Liquid Systems Coupled to Gasification and Fischer–Tropsch Processes for Biofuel Production. *Bioresour. Technol.* 2013, *127*, 391–399. http://dx.doi.org/10.1016/j.biortech.2012.09.126.

[9] Dunnu, G.; Panopoulos, K. D.; Karellas, S.; Maier, J.; Touliou, S.; Koufodimos, G.; Boukis, I.; Kakaras, E. The Solid Recovered Fuel Stabilat??: Characteristics and Fluidised Bed Gasification Tests. *Fuel* 2012, *93*, 273–283. http://dx.doi.org/10.1016/j.fuel.2011.08.061.

[10] Pinto, F.; Franco, C.; André, R. N.; Miranda, M.; Gulyurtlu, I.; Cabrita, I. Co-Gasification Study of Biomass Mixed with Plastic Wastes. *Fuel* 2002, *81*, 291–297. http://dx.doi.org/10.1016/s0016-2361(01)00164-8.

[11] Pinto, F.; André, R. N.; Carolino, C.; Miranda, M.; Abelha, P.; Direito, D.; Perdikaris, N.; Boukis, I. Gasification Improvement of a Poor Quality Solid Recovered Fuel (SRF). Effect of Using Natural Minerals and Biomass Wastes Blends. *Fuel* 2014, *117*, 1034–1044. http://dx.doi.org/10.1016/j.fuel.2013.10.015.

[12] Tanigaki, N.; Manako, K.; Osada, M. Co-Gasification of Municipal Solid Waste and Material Recovery in a Large-Scale Gasification and Melting System. *Waste Manag.* 2012, *32*, 667–675. http://dx.doi.org/10.1016/j.wasman.2011.10.019.

[13] Berrueco, C.; Recari, J.; Güell, B. M.; Alamo, G. Del. Pressurized Gasification of Torrefied Woody Biomass in a Lab Scale Fluidized Bed. *Energy* 2014, *70*, 68–78. http://dx.doi.org/10.1016/j.energy.2014.03.087.

[14] Berrueco, C.; Montané, D.; Matas Güell, B.; del Alamo, G. Effect of Temperature and Dolomite on Tar Formation during Gasification of Torrefied Biomass in a Pressurized Fluidized Bed. *Energy* 2014, *66*, 849–859. http://dx.doi.org/10.1016/j.energy.2013.12.035.

[15] Kitzler, H.; Pfeifer, C.; Hofbauer, H. Pressurized Gasification of Woody Biomass-Variation of Parameter. *Fuel Process. Technol.* 2011, *92*, 908–914. http://dx.doi.org/10.1016/j.fuproc.2010.12.009.

[16] Lv, P. M.; Xiong, Z. H.; Chang, J.; Wu, C. Z.; Chen, Y.; Zhu, J. X. An Experimental Study on Biomass Air-Steam Gasification in a Fluidized Bed. *Bioresour. Technol.* 2004, *95*, 95–101. http://dx.doi.org/10.1016/j.biortech.2004.02.003.

[17] Mastral, J. F.; Berrueco, C.; Ceamanos, J. Pyrolysis of High-Density Polyethylene in Free-Fall Reactors in Series. *Energy and Fuels* 2006, *20*, 1365–1371. http://dx.doi.org/10.1021/ef060007n.

[18] Narváez, I.; Orío, A.; Aznar, M. P.; Corella, J. Biomass Gasification with Air in an Atmospheric Bubbling Fluidized Bed. Effect of Six Operational Variables on the Quality of the Produced Raw Gas. *Ind. Eng. Chem. Res.* 1996, *35*, 2110–2120. http://dx.doi.org/10.1021/ie9507540.

[19] Higman, C.; van der Burgt, M.; *Gasification, 2nd ed.*, Gulf Professional Publishing, Burlington, 2003.

[20] Blanco, P. H.; Wu, C.; Onwudili, J. A.; Williams, P. T. Characterization of Tar from the Pyrolysis/Gasification of Refuse Derived Fuel: Influence of Process Parameters and Catalysis. *Energy & Fuels* 2012, *26*, 2107–2115. http://dx.doi.org/10.1021/ef300031j.

[21] Casal, M. D.; Díez, M. A.; Alvarez, R.; Barriocanal, C. Primary Tar of Different Coking Coal Ranks. *Int. J. Coal Geol.* 2008, *76*, 237–242. http://dx.doi.org/10.1016/j.coal.2008.07.018.

[22] Font Palma, C. Modelling of Tar Formation and Evolution for Biomass Gasification: A Review. *Appl. Energy* 2013, *111*, 129–141. http://dx.doi.org/10.1016/j.apenergy.2013.04.082.

[23] Ma, W.; Hoffmann, G.; Schirmer, M.; Chen, G.; Rotter, V. S. Chlorine Characterization and Thermal Behavior in MSW and RDF. *J. Hazard. Mater.* 2010, *178*, 489–498. http://dx.doi.org/10.1016/j.jhazmat.2010.01.108.

[24] Lu, H.; Purushothama, S.; Hyatt, J.; Pan, W.-P.; Riley, J. T.; Lloyd, W. G.; Flynn, J.; Gill, P. Co-Firing High-Sulfur Coals with Refuse-Derived Fuel. *Thermochim. Acta* 1996, *284*, 161–177. http://dx.doi.org/10.1016/0040-6031(96)02864-x.

[25] M Bläsing, M.; Zini, M.; Müller, M. Influence of Feedstock on the Release of Potassium, Sodium, Chlorine, Sulfur, and Phosphorus Species during Gasification of Wood and Biomass Shells. *Energy and Fuels* 2013, *27*, 1439–1445. http://dx.doi.org/10.1021/ef302093r.

[26] Corella, J.; Toledo, J. M.; Molina, G. Performance of CaO and MgO for the Hot Gas Clean up in Gasification of a Chlorine-Containing (RDF) Feedstock. *Bioresour. Technol.* 2008, *99*, 7539–7544. http://dx.doi.org/10.1016/j.biortech.2008.02.018.

[27] Kuramochi, H.; Wu, W.; Kawamoto, K. Prediction of the Behaviors of H2S and HCl during Gasification of Selected Residual Biomass Fuels by Equilibrium Calculation. *Fuel* 2005, *84*, 377–387. http://dx.doi.org/10.1016/j.fuel.2004.09.009.

[28] Tchapda, A.; Pisupati, S. A Review of Thermal Co-Conversion of Coal and Biomass/Waste. *Energies* 2014, *7*, 1098–1148. http://dx.doi.org/10.3390/en7031098.

[29] Wei, X.; Schnell, U.; Hein, K. R. G. Behaviour of Gaseous Chlorine and Alkali Metals during Biomass Thermal Utilisation. *Fuel* 2005, *84*, 841–848. http://dx.doi.org/10.1016/j.fuel.2004.11.022.

[30] Hansson, K. M.; Samuelsson, J.; Tullin, C.; Åmand, L. E. Formation of HNCO, HCN, and NH3 from the Pyrolysis of Bark and Nitrogen-Containing Model

Compounds. *Combust. Flame* 2004, *137*, 265–277. http://dx.doi.org/10.1016/j.combustflame.2004.01.005.

[31] Vriesman, P.; Heginuz, E.; Sjöström, K. Biomass Gasification in a Laboratory-Scale AFBG: Influence of the Location of the Feeding Point on the Fuel-N Conversion. *Fuel* 2000, *79*, 1371–1378. http://dx.doi.org/10.1016/s0016-2361(99)00278-1.

[32] Calvo, L. F.; Gil, M. V; Otero, M.; Morán, A.; García, A. I. Gasification of Rice Straw in a Fluidized-Bed Gasifier for Syngas Application in Close-Coupled Boiler-Gasifier Systems. *Bioresour. Technol.* 2012, *109*, 206–214. http://dx.doi.org/10.1016/j.biortech.2012.01.027.

[33] Leichtnam, J. N.; Schwartz, D.; Gadiou, R. Behaviour of Fuel-Nitrogen during Fast Pyrolysis of Polyamide at High Temperature. *J. Anal. Appl. Pyrolysis* 2000, *55*, 255–268. http://dx.doi.org/10.1016/s0165-2370(00)00075-9.

[34] Becidan, M.; Skreiberg, Ø.; Hustad, J. E. NOx and N2O Precursors (NH3 and HCN) in Pyrolysis of Biomass Residues. *Energy & Fuels* 2007, *21*, 1173–1180. http://dx.doi.org/10.1021/ef060426k.

[35] Tian, F. J.; Yu, J.; McKenzie, L. J.; Hayashi, J. I.; Li, C. Z. Conversion of Fuel-N into HCN and NH3 during the Pyrolysis and Gasification in Steam: A Comparative Study of Coal and Biomass. *Energy and Fuels* 2007, *21*, 517–521. http://dx.doi.org/10.1021/ef060415r.

[36] Yu, Q. Z.; Brage, C.; Chen, G. X.; Sjöström, K. The Fate of Fuel-Nitrogen during Gasification of Biomass in a Pressurised Fluidised Bed Gasifier. *Fuel* 2007, *86*, 611–618. http://dx.doi.org/10.1016/j.fuel.2006.08.007.

[37] Glarborg, P. Fuel Nitrogen Conversion in Solid Fuel Fired Systems. *Prog. Energy Combust. Sci.* 2003, *29*, 89–113. http://dx.doi.org/10.1016/s0360-1285(02)00031-x.

[38] Jazbec, M.; Sendt, K.; Haynes, B. S. Kinetic and Thermodynamic Analysis of the Fate of Sulphur Compounds in Gasification Products. *Fuel* 2004, *83*, 2133–2138. http://dx.doi.org/10.1016/j.fuel.2004.06.017.

[39] Kaufman-Rechulski, M. D.; Schildhauer, T. J.; Biollaz, S. M. a. Sulfur containing organic compounds in the raw producer gas of wood and grass gasification. *Fuel.* 2014, *128*, 330-339. http://dx.doi.org/10.1016/j.fuel.2014.02.038.

[40] Bläsing, M.; Nazeri, K.; Müller, M. Release of Alkali Metal, Sulphur and Chlorine Species during High-Temperature Gasification and Co-Gasification of Hard Coal, Refinery Residue, and Petroleum Coke. *Fuel* 2014, *126*, 62–68. http://dx.doi.org/10.1016/j.fuel.2014.02.042.

[41] Knudsen, J. N.; Jensen, P. A.; Lin, W.; Frandsen, F. J.; Dam-Johansen, K. Sulfur Transformations during Thermal Conversion of Herbaceous Biomass. *Energy & Fuels* 2004, *18*, 810–819. http://dx.doi.org/10.1021/ef034085b.

[42] Broer, K. M.; Woolcock, P. J.; Johnston, P. A.; Brown, R. C. Steam/oxygen Gasification System for the Production of Clean Syngas from Switchgrass. *Fuel* 2015, *140*, 282–292. http://dx.doi.org/10.1016/j.fuel.2014.09.078.

5. GASIFICATION OF TWO SOLID RECOVERED FUELS (SRFs): EFFECT OF EXPERIMENTAL CONDITIONS

Abstract

This paper studied the gasification of two solid recovered fuels (SRF) in a laboratory scale fluidized bed reactor. The gasification performance and syngas quality were assessed under the influence of: gasification temperature (750 ºC and 850 ºC), SRF feedstock (RT or FL), bed material (sand or dolomite) and gasification agent (air or O_2/H_2O). One of the parameters to evaluate the gasification performance was the concentration of minor contaminants (tar, N, S and Cl compounds) in the syngas. High temperature (850 ºC) and the use of calcined dolomite as bed material improved gas quality (increasing H2/CO ratio, carbon conversion and reducing tar content) during SRF gasification. The use of O_2/H_2O also enhanced gas composition (i.e. higher calorific value), although further research is needed to fully understand the release of minor contaminants under these conditions. The results indicated that the presence of minor contaminants in the syngas was strongly affected by the composition of the SRF itself, the composition of the ash fraction and the bed material, and provided valuable information to assess the most adequate conditions for SRF gasification.

This chapter is based on the following research article:

Recari J, Berrueco C, Abelló S, Montané D, Farriol X. Gasification of two solid recovered fuels (SRFs) in a lab-scale fluidized bed reactor: Influence of experimental conditions on process performance and release of HCl, H2S, HCN and NH3. Fuel Process Technol 2016;142:107–14. doi:10.1016/j.fuproc.2015.10.006.

5.1 Introduction

Generation of municipal solid waste (MSW) is increasing yearly worldwide as the living standards of wide groups of population in developing nations improve and their consumption patterns evolve accordingly. Following to a recent report by the World Bank [1] by the year 2025 about 2.2 billion tonnes MSW per year will be produced, doubling the estimates of 2010. In the European Union (EU) roughly 23% of total waste (excluding major mineral wastes) is subjected to landfill [2], provoking diverse environmental problems [3], and the consequent loss of energy and primary resources contained in the waste. The introduction of waste directives (i.e. Landfill Directive 1999/31/EC) and technical documents have encouraged the exploration of new concepts of waste-to-energy, including modifications in the market and the classification of fuels from MSW. In this scenario, those wastes that cannot be conveniently recycled because of economic inefficiency [4] can be subjected to stringent quality criteria to prepare a solid recovered fuel (SRF), that is a potential feedstock for thermal applications with energy recovery [CEN/TC 343]. Although current waste-to-energy valorization is mainly based on incineration with energy recovery, accounting a 4% of total waste generated in the 28 state members of the EU [2], other technologies have been proposed in the last decades. Among them, waste gasification is a promising pathway to convert carbonaceous materials into valuable end products through different synthesis routes [5], besides the efficient production of power and useable heat. Coal and biomass gasification has been extensively studied in the last decades [6-10] as well as waste gasification [3, 11, 12], whereas SRF is one of the main topics in waste gasification nowadays [13-15]. Some limitations in gasification still need to be tackled, especially when dealing with contaminants in the syngas, such as tar, H_2S, HCl, NH_3 and other species. Due to their nature, the levels of chlorine, sulphur, and heavy metals in SRF are significantly higher than those in woody biomass [16]. The problems that appear during plant operation due to the presence of those contaminants are fouling, corrosion in pipes and downstream units, besides poisoning of catalysts [17-19]. Hence these impurities must be reduced to safe levels in order to assure a continuous operation in industrial applications. For instance, tar level should reach levels as low as 100 mg Nm^{-3} for syngas applications in internal combustion engines, and the allowed levels of

sulphur, nitrogen or halides in gas turbines are around 20, 50 and 1 mL Nm^{-3} respectively, being these limits even lower for the use of the syngas in catalytic processes [19]. A way to reduce the release of these species is the use of low cost natural minerals like dolomite or olivine during gasification, which has shown promising results on removing tar and minor contaminants and achieving better syngas compositions. [14, 20-23]. Nonetheless, few studies [10] have assessed the evolution of minor contaminants concentration in the syngas as a function of experimental conditions.

In this study two SRF (RT and FL) were gasified in an atmospheric lab-scale fluidized bed reactor. The aim was to assess the influence of several parameters on the gasification performance and the quality of the synthesis gas: gasification temperature (750 and 850 ºC), bed material (sand or dolomite) and fluidizing agent (air or a mixture of oxygen and steam). Furthermore, special attention was devoted to the evolution of minor contaminants (tar, H_2S, HCN, HCl and NH_3) in the syngas. Notice that the information here presented has been obtained in a lab-scale gasifier, and therefore the actual numbers could differ from the ones in industrial scale gasifiers. Nevertheless, the main trends and conclusions of the present study can be useful to give insight to the gasification of SRF.

5.2 Materials and methods

5.2.1 SRF samples preparation and characterisation

The two SRF used as gasification feedstocks (hereinafter referred as RT and FL) were obtained from local waste management companies [24]. RT was produced by Ambiensys (Spain) after an active hygienization process (GeiserBox®) of unsorted waste streams. The composition of this fraction was mainly plastics and textiles with a low content of biomass and paper. On the other hand, FL derived from mixed domestic waste streams provided by Griñó Ecològic (Spain). This feedstock presented a significant content of biomass, waste paper and non-recyclable post-consumer plastics. Both fuels were grounded and sieved to a particle size of 1 mm in a cutting mill (Retsch SM-300) operated at slow speed rate to avoid overheating of the feedstock. The characterisation of samples (Table 5.1) was performed following standard

methods for solid recovered fuels. The proximate analysis was conducted using a LECO Thermogravimetric analyser (TGA 701) according to the EN-15402:2011 and EN-15403:2011 standard methods. The ultimate analysis was performed in a LECO TruSpec CHN-S analyser following the EN-15407:2011 standard method. The lower heating value was determined in an isoperibolic LECO automatic calorimetric bomb (AC 600), according to the EN-15400:2011 standard method. Halogens (HCl, HF, HBr), recovered from the calorimetric bomb with Milli-Q® water, were analysed by ionic chromatography (Dionex ICS-1100) following the EN-15408:2011 standard method. The chemical composition of the feedstock ashes was determined by inductively coupled plasma-optical emission spectroscopy (ICP-OES) in a Spectro Arcos 165 spectrophotometer. A homogeneous batch of each ash was prepared by burning several batches of the samples in a dedicated furnace under controlled temperature profiles, following the EN-15403:2011 standard method. The prepared ash samples were digested in microwave system (Berghof Speedwave 4), following the EN-15410:2006 and EN-15411:2006 standard methods. Table 5.1 shows the characterisation results of both feedstocks. All the analyses were carried out by triplicate, and the uncertainties of the obtained values were estimated at a 95% probability level.

5.2.2 Bed materials

Sand (J.T.Baker) and dolomite (Minelco GmbH) sieved to particle size range of 150-200 μm were used as bed materials. Previous to the gasification experiments, dolomite was calcined in static air at 900 ºC for 4 hours.

5.2.3 Experimental setup and procedure

The experimental setup consisted in a fluidized bed reactor (404 mm long and 23.8 mm internal diameter) made of Hastelloy X. The reactor, capable of operating at temperatures up to 900º C and pressures up to 20 bar (PID ENG&Tech, Spain), was externally heated using an electrical furnace and was fully equipped with a control system (i.e. flow, pressure, temperature and feeding control). The solid fuel was fed into the bed reactor at feed rates from 0.25 to 0.5 g min^{-1} with the help of a controlled inlet of nitrogen (~50 NmL min^{-1}, Praxair, Inc.). Fluidizing agent varied between air (~125 NmL min^{-1}, Praxair,

Inc.) or oxygen/steam (O_2: 226 NmL min^{-1}, Praxair, Inc.; $H_2O_{(l)}$ 0.41 mL min^{-1}). The flue gas released from the gasification tests firstly flowed through a hot filter (40 µm stainless steel, Classic Filters Ltd.) and two condensers in order to remove particulates and condense water and tars. A fraction of the syngas was collected in a 25 L Tedlar® gas sampling bag coupled after the hot filter (in air gasification runs) or after the cold trap (in steam gasification conditions) for the analysis of minor contaminants. Overall and carbon mass balance closures for all conducted experiments were ≥ 95 %. Further details of the experimental setup and experimental procedure can be found elsewhere [6].

Table 5.1 Main characteristics of feedstock (as received basis)

		RT	FL
Proximate analysis (wt.%)	**Moisture**	1.13±0.12	2.60±0.02
	Volatiles	86.20±0.90	70.15±0.27
	Fixed carbon	2.51±0.11	8.30±0.23
	Ash	10.15±0.31	18.95±0.51
Ultimate analysis (wt.%)	**C**	66.78±1.01	51.73±0.04
	H	10.70±0.46	8.15±0.14
	O (by difference)	10.68±1.12	19.03±0.54
	N	0.76±0.12	1.22±0.09
	S	0.23±0.018	0.20±0.003
	F	< 0.01	< 0.01
	Cl	0.70±0.0001	0.70±0.06
LHV (MJ/kg)		26.99±0.69	20.26±0.19
Ash composition (mg/kg_{fuel})	**Aluminium as Al_2O_3**	18029±429	33324±1705
	Calcium as CaO	24453±452	42459±707
	Chrome as Cr	<50	<50
	Iron as Fe_2O_3	3051±60	7086±404
	Lead as Pb	<50	<50
	Magnesium as MgO	2359±115	5236±358
	Manganese as MnO	<50	<50
	Nickel as Ni	<50	<50
	Phosphorus as P_2O_5	3749±116	3811±157
	Potassium as K_2O	1973±80	4948±427
	Silicon as SiO_2	19597±609	42477±923
	Sodium as Na_2O	2881±115	6392±492
	Titanium as TiO_2	3693±131	3623±149
	Vanadium as V	<50	<50
	Zinc as Zn	224±11	183±24

5.2.4 Gas and minor contaminants analyses

The main components of the producer gas (H_2, O_2, N_2, CO, CO_2, CH_4 and hydrocarbons up to C_5) were analysed using a micro GC (Agilet 490). Further information can be obtained in previous studies [6]. The inorganic traces (H_2S, HCN, HCl and NH_3) were analysed in liquid state from the syngas collected in the sampling bag by means of ion-selective electrodes (ISE, Metrohm). For this purpose, firstly the syngas was pumped sequentially through a series of impingers containing specific solutions to retain the ions (S_2^-, CN^-, $Cl^-$and NH_4^+) respectively. The gas flowed (1 NL min^{-1}) for 5 minutes per compound. Prior the ion determination, the ionic strength and pH of the solutions were adjusted adding a small quantity (0.1 mL) of a buffer solution. After this step, the ion concentrations were determined with a 905 Titrando and an 814 USB Sample Processor (Metrohm) equipped with tiamo™ software for direct potentiometry. The setup employed the specific ISE and an Ag/AgCl reference electrode containing electrolyte solution (i.e. KCl 3M). Additionally, temperature and pH were monitored with a PT1000 temperature sensor and pH glass electrode respectively, and a rod stirrer assured a continuous stirring of the samples. All ISE were calibrated using four solutions prepared from a standard stock (1000 ppm) in order to obtain a linear calibration curve for each ion concentration determination. Table 5.2 gathers the main characteristics for the ion measurements.

Table 5.2 Ion selective electrodes characteristics

ISE	Absorbing solution (mL)	Calibration solutions (ppm)	Ag/AgCl reference electrolyte	TISAB solution	pH range
S^{2-}	50 % Milli-Q water + 50 % SAOB	0.1, 1, 10 and 100	KCl 3 M	NaOH 10 M	2 - 12
CN^-	100 % NaOH 0.1 M	0.2, 2, 20 and 100	KCl 3 M	NaOH 10 M	10 - 14
Cl^-	100 % Milli-Q water	1.8, 10, 50 and 100	KNO_3 1 M	$NaNO_3$ 5 M	0 - 14
NH_4^+	100 % Milli-Q water	0.1, 5, 50 and 100	-	NaOH 10 M	11 - 14

5.3 Results and discussion

5.3.1 SRF characterisation and classification

Both solid recovered fuels (RT and FL) were analysed in terms of proximate and ultimate analysis and heating value. The results listed in Table 5.1 showed lower contents of fixed carbon (< 8.5%) and moisture (ranging from 1-3%), and higher ash contents (> 10%) for both samples when compared to typical biomass values [6, 10, 25] but in the range of waste-derived fuels [13-15]. The RT feedstock contained lesser amount of paper and biomass, and therefore presented lower fixed carbon (2.51%) and ash contents (10.15%) than FL (8.30 and 18.95%, respectively). The elemental composition as well showed differences in C (66.78% for RT and 51.73% for FL) and H contents (10.70 % for RT and 8.15 % for FL). Regarding the contaminants precursors (N, S, Cl), similar values were obtained for sulphur (~0.20%) and chlorine (0.70%) while nitrogen appeared in higher levels for the FL sample (1.22%) in comparison to RT (0.76%). The lower heating value (LHV) results were also consistent with the SRF composition. Approximately, RT had a LHV that was a 25 % higher (26.99 MJ kg^{-1}) when compared to FL, mainly due to the presence of synthetic polymers and lower ash content.

5.3.2 Product yields

The results gathered in Table 5.3 show the yields of gas, tar and char from the gasification tests under different experimental conditions. The yields were calculated in terms of percentage as the product mass per mass of dry SRF, and therefore the total yield percentage results above 100%, because of the incorporation of oxygen from air or O_2/H_2O, to form CO and CO_2.

Table 5.3 Experimental conditions and product yields for the gasification of SRF samples

Effect	SRF	T (ºC)	ER	Bed material	Gasification agent	Yield (g/100 g dry SRF)			H_2/CO	Syngas LHV (MJ Nm^{-3} dry)	Xc	Tar content (g Nm^{-3} dry)
						Gas	Tar	Char[a]				
SRF	RT	750	0.31	Sand	Air	127.1±0.6	13.1±0.8	3.6±0.2	0.52±0.02	4.81±0.23	75.6±1.5	41.03±2.57
	RT	850	0.31	Sand	Air	140.4±0.8	9.3±0.5	1.7±0.2	1.09±0.04	4.34±0.24	76.2±1.6	26.01±1.65
	FL	750	0.30	Sand	Air	96.5±0.8	10.8±0.4	9.6±1.3	0.77±0.02	4.01±0.16	67.4±1.5	46.62±1.67
	FL	850	0.30	Sand	Air	107.1±0.7	8.8±0.5	4.5±0.4	0.87±0.03	3.91±0.14	70.8±1.6	34.81±1.80
Bed material	RT	850	0.31	Sand	Air	140.4±0.8	9.3±0.5	1.7±0.2	1.09±0.04	4.34±0.24	76.2±1.6	26.01±1.65
	RT	850	0.31	Dolomite	Air	148.0±0.7	2.6±0.1	11.0±0.3	1.04±0.04	4.45±0.16	79.3±1.9	7.06±0.36
	FL	850	0.30	Sand	Air	107.1±0.6	8.8±0.5	4.5±0.4	0.87±0.03	3.91±0.14	70.8±1.6	34.81±1.80
	FL	850	0.31	Dolomite	Air	115.2±0.7	2.7±0.1	7.5±0.4	0.90±0.03	4.24±0.15	77.0±1.8	10.10±0.52
Gasification agent	RT	850	0.31	Dolomite	Air	148.0±0.7	2.6±0.1	11.0±0.3	1.04±0.04	4.45±0.16	79.3±1.9	7.06±0.36
	RT	850	0.30	Dolomite	O_2/H_2O[b]	171.1±1.8	2.2±0.1	2.43±0.2	1.09±0.04	10.02±0.77	90.2±1.9	13.04±0.67

[a] Ash free. Ash content ~ 10.27 g/100 g dry RT and ~ 19.46 g/100 g dry FL

[b] Steam/SRF ratio ~ 1

5.3.2.1 Effect of SRF

In this section the yields of gasification products of both feedstocks (RT and FL) are compared at two gasification temperatures (750 and 850 ºC).

The effect of rising gasification temperature on RT resulted in an increase of gas yields and a decrease on the tar and char yields due to an enhancement of gasification reactions (devolatilization, together with char and tar cracking reactions) [26]. The gas yields for the gasification experiments of RT (127.1-140.4%) were higher in comparison to those of FL (96.5-107.1 %) at both temperatures. The rising of gasification temperature from 750 ºC to 850 ºC increased the gas production a 10.4 % and a 10.9 % for RT and FL, respectively. Tar yields were similar for both SRF (around 9-13 %) although slightly higher for RT experiments. The decrease of tar at the studied temperatures was a 28.7 % using RT and 18.8 % with FL. Concerning char yield, some differences were observed, presumably derived from the feedstock composition; the higher fixed carbon levels in FL led to 2.7 times higher char yields (4.5-9.6 %) than the obtained with RT (1.7-3.6 %).

5.3.2.2 Effect of bed material

The gasification experiments performed to evaluate the influence of the bed material (silica sand or calcined dolomite) in the product yields were set at a gasification temperature of 850 ºC and at a constant equivalence ratio (ER) ~0.31. The use of dolomite in the bed reactor exhibited a positive effect on the production of syngas, increasing gas yield from 140.4 to 148.0 % (growth of ~5.4 %) and from 107.1 to 115.2 % (~7.6 % higher) for RT and FL experiments, respectively. Also char yield suffered a rise for the dolomite experiments, more pronounced for RT than for FL. Concerning the tar yield, the presence of dolomite favoured cracking reactions (consequently increasing gas yield) leading to a reduction of tar for both feedstocks. In the case of RT the decrease was around 72.4 % (from 9.3 to 2.6 %) and 69.0 % (8.8 to 2.7 %) for FL. To summarize, the catalytic effect of dolomite promoted tar cracking and polymerization reactions leading to an increase of gas and char yields [26].

5.3.2.3 Effect of gasification agent

Considering the results from the previous experiments, a test at 850 ºC with RT as feedstock and dolomite as bed material was performed using O_2/H_2O as gasification agent. The results were then compared to those obtained when air was used as gasification agent at the same conditions. Gasification with O_2/H_2O showed higher gas yield (from 148.0 to 171.1 %) and lower tar and char yields. Tar yield decreased by 13.2 % (from 2.6 to 2.2 %) and char yield by 77.9 % (from 11.0 to 2.4 %) as a result of promoting tar steam reforming and char steam gasification reactions. The rise of gas yield with the addition of O_2/H_2O is in agreement with the diminishment of char and tar yields.

5.3.3 Gas composition

This section presents the effect of experimental conditions on the produced gas. The gas compositions (dry basis) are plotted in Figures 5.1-5.3 whereas the other discussed values are listed in Table 5.3.

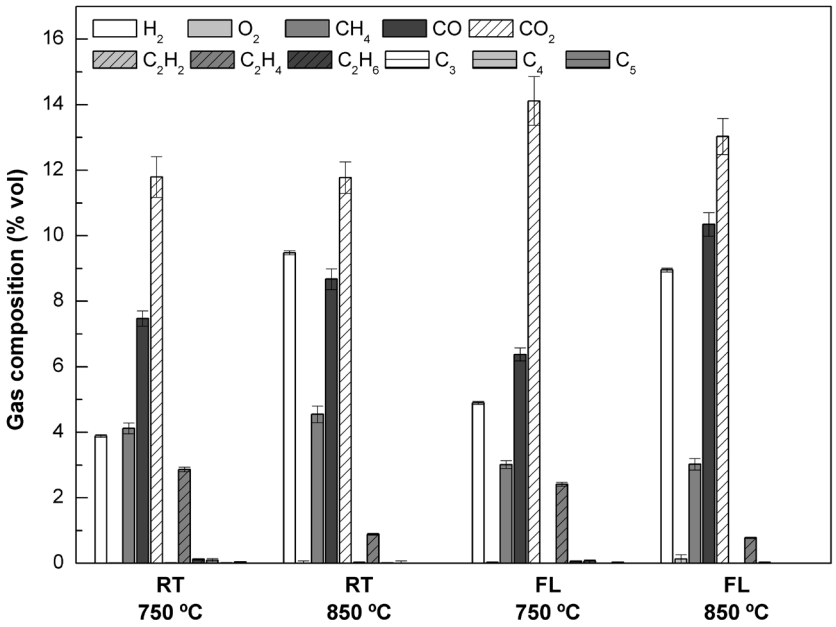

Figure 5.1 Gas composition. Effect of SRF (RT and FL) with gasification temperature (750 and 850 ºC)

5.3.3.1 Effect of SRF

Figure 5.1 presents the influence of SRF (RT and FL) and gasification temperature (750 and 850 ºC) on gas composition. For the experiments

performed with RT there was an increase in H_2 and CO concentrations when temperature varied from 750 to 850 ºC, from 3.9 % to 9.5 % for H_2 and from 7.5 % to 8.7 % for CO. Thus, the H_2/CO ratio was doubled at 850 ºC, reaching a value of 1.09. The CO/CO_2 ratio increased from 0.63 to 0.74. These trends can be related to an enhancement of gasification reactions rates together with the influence of the water gas shift reaction and the more intense cracking of the hydrocarbons present in the gas [6, 25, 27]. The temperature increase also provoked a slight diminishment on CO_2 concentration (related to Boudouard and water-gas shift reactions) and sharply decreased the concentration of hydrocarbons (C_2-C_5), due to cracking reactions.

As regards FL gasification, practically all compounds appeared in a lower concentration compared to those of RT gasification, although they presented resembling qualitative trends (Figure 5.1). H_2/CO and CO/CO_2 ratios increased with temperature from 0.77 to 0.87 and from 0.45 to 0.79, respectively. Additionally, meanwhile in RT gasification CH_4 barely rose (from 4.1 to 4.6 %) in FL gasification it remained constant (3.0 %). During the gasification of both materials at 750 ºC the concentration of hydrocarbons (C_2-C_5) was below 0.1 % with the exception of ethylene (2.4 to 2.9 %). This compound was acutely reduced (below 1 %) at the highest gasification temperature for both SRF as a consequence of higher levels of cracking and reforming reactions. In addition to the cracking reactions, ethylene might also play a key role in the formation of tertiary tars and polycyclic aromatic hydrocarbons (PAHs) at high temperature [26].

5.3.3.2 Effect of bed material.

Figure 5.2 displays the effect of varying the type of bed material (silica sand or calcined dolomite) on gas composition. The experiments were carried out at a gasification temperature of 850 ºC with air as fluidizing agent.

H_2 concentration in the gas produced for both SRF suffered a slight rise in presence of dolomite, from 9.5 % to 10.6 % (RT) and from 9.0 % to 9.8 % (FL). The concentration of CO when RT was gasified was 10.2 % and 10.9 % in the case of FL. In both cases CO concentration increased in comparison to the experiments performed with sand as bed material, but in a lesser extent for FL. Regarding the evolution of H_2/CO and CO/CO_2 ratios, RT gasification using

dolomite in the bed material led to a relevant increase of CO concentration (~17.1 %) probably promoted by char gasification reactions (Boudouard and water-gas shift), and tar cracking and reforming reactions. Dolomite led to an increase of CO/CO_2 ratio (from 0.74 to 0.85) and a slight decrease of H_2/CO ratio (from 1.09 to 1.04). On the other hand, the effect of dolomite on FL gasification was less significant concerning the increase of CO yield. The obtained levels of CH_4 presented opposite trends, meanwhile for RT gasification there was a small decrease (7.9 %), CH_4 increased from 3.0 to 4.0 % with FL. This difference could be related to the activity of calcined dolomite as catalysts, and the more marked decrease of other hydrocarbons (mainly C_2H_4) for the experiments carried out with FL.

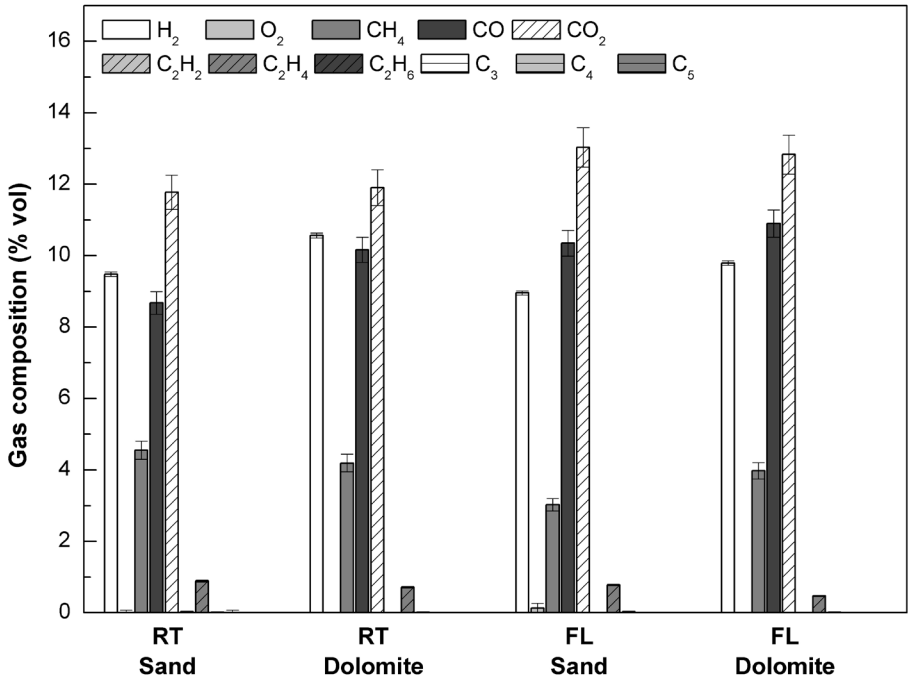

Figure 5.2 Gas composition. Effect of SRF (RT and FL) with bed material (sand and dolomite)

5.3.3.3 Effect of gasification agent

As previously discussed, the use of a different gasification agent (O_2/H_2O) was compared with air gasification of RT (850 ºC, ER ~ 0.3 and dolomite).

Figure 5.3 evidences the sharp increase of hydrogen and carbon monoxide production when using O_2/H_2O as gasification media. This fact is explained, on one side by the addition of steam, enhancing water-gas, steam reforming and

water gas shift reactions [28]. On the other side, there is an additional effect due to the non-dilution with N_2, and therefore the concentration of the main gases (H_2, CH_4, CO, CO_2, C_2H_6 and especially C_2H_2) increased. This effect was also noticeable in the increase of the gas calorific value, which reached values close to 10 MJ Nm^{-3} for the experiment with O_2/H_2O versus the 4-4.5 MJ Nm^{-3} obtained with air.

The H_2/CO and CO/CO_2 ratios pointed to a higher production of both main syngas species. The H_2/CO ratio barely increased from 1.04 to 1.09 and CO/CO_2 ratio went from 0.85 to 1.00. Steam in the gasification medium might promote hydrocarbons reduction by steam reforming reactions, favouring H_2, CO and CO_2 release [15]. However, in the present study an increase of some light hydrocarbons (C_2H_6, C_2H_4 and C_2H_2) under steam gasification conditions was observed with respect to air gasification. It has been reported that the use of oxygen and steam enhances char combustion and gasification reactions together with tar cracking [11, 29-31]. Therefore the higher level of hydrocarbons like C_2H_4 could be originated from tar cracking of heavier hydrocarbons in the gasifier freeboard.

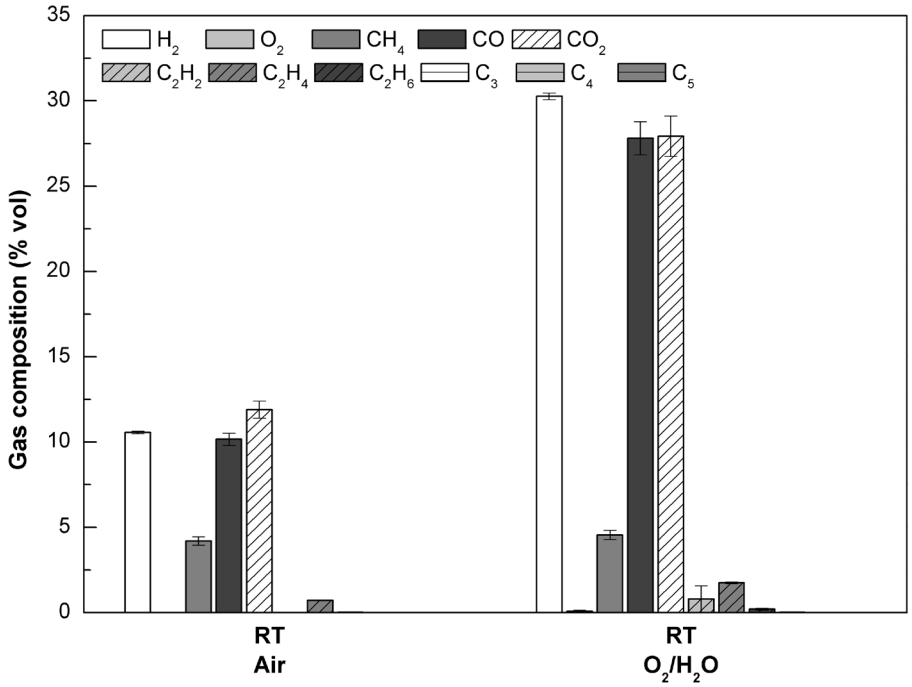

Figure 5.3 Gas composition. Effect of RT with gasification agent (air or oxygen/steam)

5.3.4 Tar content

The concentration of tar (Table 5.3) in the dry producer gas is also an important parameter for the design of syngas cleaning. In accordance to tar yield, increasing the gasification temperature from 750 ºC to 850 ºC provoked a larger extent of tar cracking reactions which considerably reduced (around 25-36 %) the mass of tar in the producer gas. Considering both fuels, FL gasification released 34.8 g Nm^{-3} and RT 26.0 g Nm^{-3} at 850 ºC. These results are much higher than values reported for biomass gasification [6, 32] but are in accordance with other air gasification experiments of SRF [13, 14]. On the other hand, the depletion of tar was significant with dolomite in the bed. The catalytic activity of dolomite resulted in minimum tar values, 7.1 g Nm^{-3} and 10.1 g Nm^{-3} for the gasification of RT and FL, respectively. Under these conditions, the tar concentrations got closer to levels showed in biomass gasification with and without catalyst [26, 33-35]. Notice that the higher tar contents with O_2/H_2O in RT gasification were a result of the N_2 diluting effect. In fact, results in N_2 free basis showed the expected decline in tar content (about 25.6%), from 18.8 g Nm^{-3} for the air experiment to 14.0 g Nm^{-3} for the O_2/H_2O test.

5.3.5 Evolution of minor contaminants (HCl, H_2S, HCN and NH_3) in the syngas

This section discusses the evolution of minor contaminants concentration in the synthesis gas under different experimental conditions. It is generally accepted that the reducing atmosphere of the gasification conditions prevents the formation of nitrogen and sulphur species in their oxidized forms (i.e. SO_2, NOx). Thus, the S and N species appear in the producer gas mainly as NH_3 (but also HCN) and H_2S (with lesser amounts of COS). As well, a predominant halide in biomass and waste-derived samples is chlorine, which is rapidly vaporized at high temperatures and reacts with water vapour to form HCl [19]. Therefore the evolution of these compounds has been tracked under different experimental conditions.

5.3.5.1 Effect of SRF

Figure 5.4a displays a comparison of the contaminants concentration in the gas produced during RT and FL gasification experiments at 750 and 850 ºC. The results showed that, among the studied contaminants, HCl and HCN were dominant for these particular fuels.

The most remarkable difference between both feedstocks was the much higher levels of HCl obtained for the experiments carried out using FL in comparison to those performed with RT. In addition, the evolution of HCl with temperature presented a different trend for both feedstocks. The diminishment of chlorine concentration in the experiments with RT was presumably the result of alkaline metal and carboxylates degradation causing the decrease of HCl in the gas phase KCl/HCl equilibrium [36]. However the increase of HCl concentration with temperature when using the FL sample could be related to the volatilization of inorganic chloride, salts (NaCl and KCl) derived from kitchen food/waste, at temperatures over 800 ºC that partially transform into HCl [36]. In fact, this fuel comes from domestic waste and contains a higher content of inorganic chlorine [24]. This evolution is consistent as well with the ash composition (Table 5.1), since FL exhibited higher levels of sodium (Na) and potassium (K).

The increase of gasification temperature led to a general increase in HCN concentration, particularly in the fuel richer in plastics and textiles (RT). The nitrogen-containing polymers (i.e. nitriles, cyclic amides) decomposes at high temperatures towards HCN rather than NH_3, especially under high heating conditions [12, 37, 38]. Along the same lines, the FL sample with a lower content of plastics and textiles, led to a smaller release of HCN at the highest gasification temperature in comparison to RT, although both fuels presented similar levels (around 160 mg Nm^{-3}) at the less severe conditions (750 ºC). Ammonia was hardly detected in these experiments; the concentration range was below 4 mg Nm^{-3} for RT and 1.5 mg Nm^{-3} for FL, supporting the assumption that fuel-N is released preferentially as HCN despite the higher biomass content in the FL sample [12].

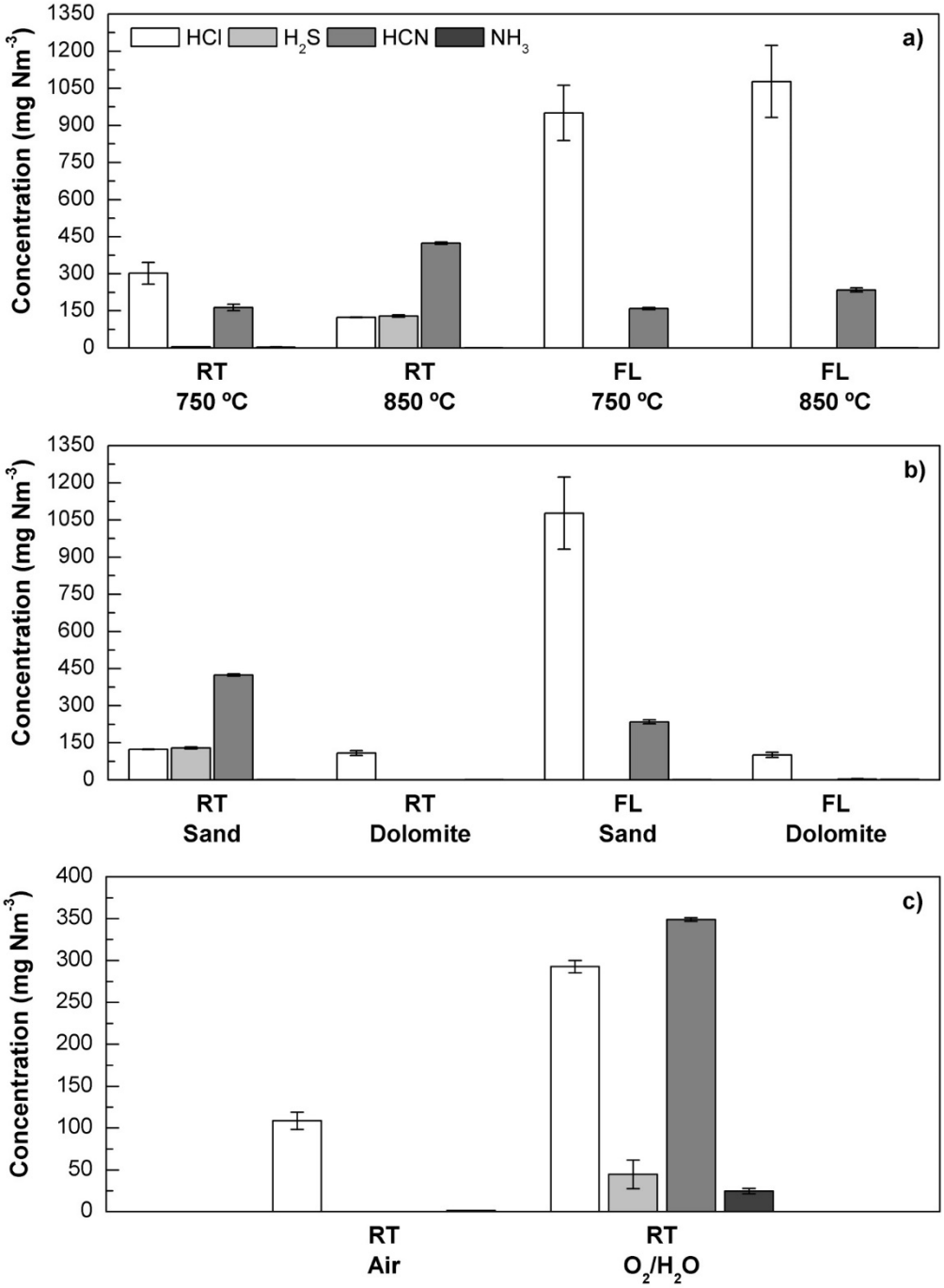

Figure 5.4 Minor contaminants release. Effect of SRF (RT and FL) with: a) gasification temperature (ER 0.3 and sand as bed material), b) bed material (T 850 ºC and ER 0.3), c) gasification agent (T 850 ºC, ER 0.3 and dolomite as bed material)

The presence of H_2S in the syngas was only detectable for the experiments performed with RT, where an increase from 5 to 129 mg Nm^{-3} appeared from the lowest to the highest gasification temperature. The mechanisms of release of sulphur species are complex, influenced by many factors, particularly by the presence of inorganic sulphates or other elements in the fuel ash [10, 12]. Among

these elements K and Ca have a significant effect. The release of H_2S has been reported to be highly dependent on the affinity between potassium and sulphur, however the competition with Cl and silicon (Si) at temperatures above 700 ºC may prevent the formation of the K_2S in solid form and therefore favours H_2S release [12]. The higher levels of Ca and K in FL ash sample would support the lower H_2S release for this particular material in comparison to RT.

5.3.5.2 Effect of bed material.

The modification of bed material (sand or dolomite) affected the minor contaminants concentration in the syngas as illustrated in Figure 5.4b. The results were obtained from air gasification experiments performed at a gasification temperature of 850 ºC, with alike ER (~0.31) for both SRF.

RT gasification with sand presented similar levels of HCl and H_2S (around 125 mg Nm^{-3}), a high concentration of HCN (425 mg Nm^{-3}) and low levels of NH_3 (< 2 mg Nm^{-3}). However the influence of dolomite as bed material showed not only a pronounced reduction in H_2S concentration leading to undetectable sulphur in the form of H_2S, but also a huge decline in HCN, achieving very low concentrations (< 0.15 mg Nm^{-3}) in the producer gas. The results of H_2S diminishment are similar to those presented by Pinto et al. [15]. This decrease can be related to the presence of calcium in the bed, which favours the formation of CaS that would probably remain in the solid phase. Furthermore, other alkali (K), alkaline earth metals (Mg) and Fe present in ashes may catalyse N-fuel conversion ending up with lower HCN concentration [12].

In addition, the level of HCl dropped a 12 %, probably due to the larger amount of Ca and Mg available in the dolomite bed [10, 19]. The air gasification of FL using dolomite as bed material led to similar trends to those observed during RT gasification using dolomite. In particular similar levels of minor contaminants were obtained for both studied fuels. This fact gives an idea of the influence of dolomite on minor contaminant evolution, being partially independent of the feedstock. For example the level of HCl obtained during FL gasification test using sand as bed material was as high as 1075 mg Nm^{-3} while the value obtained for RT gasification test was around 125 mg Nm^{-3}. In presence of dolomite, those values dropped up to 100 mg Nm^{-3} in both cases. Additionally, HCN also dropped for both materials from 425 and 234 mg Nm^{-3}

(for RT and FL respectively) to very low concentrations (0.15 and 4 mg Nm^{-3}), probably linked to the presence of alkali and alkaline metals under the gasification conditions [12, 39]. In general, the use of dolomite as bed material resulted in a producer gas with less contaminant levels than the experiments with sand.

5.3.5.3 Effect of fluidizing agent

The levels of contaminants obtained in air RT gasification were compared to the results from O_2/H_2O RT gasification under the same conditions (gasification temperature of 850 C, ER ~0.31, and dolomite as the bed material).

The results using O_2/H_2O as gasification medium showed an abrupt increase for all the analysed minor contaminants (Figure 5.4c). This steep increase could be related to the absence of N_2 diluting effect or the higher level of char and tar conversion. Our previous results in air gasification reported almost inexistent levels of NH_3 (1.7 mg Nm^{-3}), HCN (0.13 mg Nm^{-3}) and H_2S (not detected) and concentrations of HCl close to 100 mg Nm^{-3}. However when O_2/H_2O was used as gasification agent, HCl and HCN concentrations were around 293 and 350 mg Nm^{-3}, respectively, while H_2S (~45 mg Nm^{-3}) and NH_3 (~25 mg Nm^{-3}) contents increased in a lesser extent. The presence of steam clearly caused a lager consumption of the produced char, and therefore promoted the release of S, Cl and specially N. A similar increase was also reported in previous studies with coal, biomass and waste-derived fuels [15, 40-43].

In order to discern between the effect of N_2 dilution and gasification agent reactivity on the minor contaminants evolution, their concentration in inert basis were compared (not shown). This comparison indicated that the rise of HCl was mainly due to the non N_2 diluting effect. However H_2S and HCN (and NH_3 in a lesser extent) concentrations appeared to be influenced by the use of O_2/H_2O as gasification agent. On the one hand, the presence of steam promoted H_2S release during coal gasification due to the influence of steam in the CaS-CaO equilibrium [42]. On the other hand, several parameters can influence the N-conversion but for steam gasification the quantity of steam, residence time, nitrogen functionalities of the fuel and its feeding position are apparently the

most critical aspects [43]. For a better understanding of the release mechanisms of these compounds during SRF gasification, more detailed research is still necessary.

5.4 Conclusions

This paper studied the gasification of two SRF in a laboratory scale fluidized bed reactor, assessing the influence of varying the feedstock (RT or FL), bed material (sand or dolomite) and gasification agent (air or O_2/H_2O) on the gasification performance and syngas quality. The evolution of minor contaminants concentration in the syngas (H_2S, HCN, HCl and NH_3) was determined by means of ion selective electrodes.

The composition of both feedstocks influenced the results but similar trends were observed regarding the product yields. Increasing gasification temperature (750-850 ºC) resulted in a higher gas yield together with lower char and tar yields due to an enhancement of gasification reactions and hydrocarbons cracking. As well the use of dolomite and O_2/H_2O promoted the increase of gas yield and decreased tar and char production in relation to the experiments performed with sand and air.

Both SRF experiments carried out at 850 ºC showed an increase in H_2 and CO contents and a decrease in hydrocarbons (C_2-C_5), although RT presented slightly better characteristics as gasification feedstock with respect to FL. The replacement of sand with dolomite favoured tar cracking reactions showing a significant diminishment on tar content and some increment in H2 and CO levels for both feedstocks. Although FL seemed to be more influenced by the presence of catalyst in the bed, RT achieved an overall better gasification performance. The study of gasification of RT with O_2/H_2O and dolomite showed the best gasification performance among the studied conditions (highest gas yield, LHV gas, carbon conversion and lowest tar content) due to the enhancement of steam reactions (char gasification, homogeneous and tar reforming reactions).

The results indicated that the presence of minor contaminants in the syngas was strongly affected by the composition of the SRF itself, the composition of the ash fraction and the bed material. HCl and HCN concentrations were dominant for these particular fuels, nonetheless their levels

were severely reduced in air gasification (850 ºC and ER ~0.3) when dolomite was used as the bed material. At these conditions, HCl was the only compound detected (~100 mg Nm^{-3}) for both feedstocks. On the other hand, the change to O_2/H_2O as gasification agent increased the concentration of all the contaminants, especially HCN (~350 mg Nm^{-3}) and H_2S, NH_3 and HCl in a lower extent.

The results indicated that higher temperatures (850 ºC) and calcined dolomite in the bed would be appropriate experimental conditions for SRF gasification. The introduction of O_2/H_2O could also enhance the characteristics of the syngas but more research is needed on the release of minor contaminants under these conditions.

5.5 References

[1] Hoornweg DB-T, Perinaz. What a Waste : A Global Review of Solid Waste Management. Washington D.C.: World Bank; 2012.

[2] Eurostat. Energy, transport and environment indicators - 2013 edition. 2013.

[3] Lee U, Chung JN, Ingley HA. High-temperature steam gasification of municipal solid waste, rubber, plastic and wood. Energy Fuels 2014;28:4573-4587. http://dx.doi.org/10.1021/ef500713j.

[4] Nasrullah M, Vainikka P, Hannula J, Hurme M. Elemental balance of SRF production process: Solid recovered fuel produced from commercial and industrial waste. Fuel 2015;145:1-11. http://dx.doi.org/10.1016/j.fuel.2014.12.071.

[5] Schneider DR, Ragossnig AM. Biofuels from waste. Waste Manage. Res. 2013;31:339-340. http://dx.doi.org/10.1177/0734242x13482228.

[6] Berrueco C, Recari J, Güell BM, Alamo GD. Pressurized gasification of torrefied woody biomass in a lab scale fluidized bed. Energy 2014;70:68-78. http://dx.doi.org/10.1016/j.energy.2014.03.087.

[7] Hanaoka T, Inoue S, Uno S, Ogi T, Minowa T. Effect of woody biomass components on air-steam gasification. Biomass Bioenergy 2005;28:69-76. http://dx.doi.org/10.1016/j.biombioe.2004.03.008.

[8] Karatas H, Olgun H, Akgun F. Coal and coal and calcined dolomite gasification experiments in a bubbling fluidized bed gasifier under air atmosphere. Fuel Process. Technol. 2013;106:666-672. http://dx.doi.org/10.1016/j.fuproc.2012.09.063.

[9] Prins MJ, Ptasinski KJ, Janssen FJJG. From coal to biomass gasification: Comparison of thermodynamic efficiency. Energy 2007;32:1248-1259. http://dx.doi.org/10.1016/j.energy.2006.07.017.

[10] Bläsing M, Zini M, Müller M. Influence of feedstock on the release of potassium, sodium, chlorine, sulfur, and phosphorus species during gasification of wood and biomass shells. Energy Fuels 2013;27:1439-1445. http://dx.doi.org/10.1021/ef302093r.

[11] Guan Y, Luo S, Liu S, Xiao B, Cai L. Steam catalytic gasification of municipal solid waste for producing tar-free fuel gas. Int. J. Hydrogen Energy 2009;34:9341-9346. http://dx.doi.org/10.1016/j.ijhydene.2009.09.050.

[12] Tchapda AH, Pisupati SV. A review of thermal co-conversion of coal and biomass/waste. Energies 2014;7:1098-1148. http://dx.doi.org/10.3390/en7031098.

[13] Arena U, Di Gregorio F. Gasification of a solid recovered fuel in a pilot scale fluidized bed reactor. Fuel 2014;117:528-536. http://dx.doi.org/10.1016/j.fuel.2013.09.044.

[14] Dunnu G, Panopoulos KD, Karellas S, Maier J, Touliou S, Koufodimos G, et al. The solid recovered fuel Stabilat®: Characteristics and fluidised bed gasification tests. Fuel 2012;93:273-283. http://dx.doi.org/10.1016/j.fuel.2011.08.061.

[15] Pinto F, André RN, Carolino C, Miranda M, Abelha P, Direito D, et al. Gasification improvement of a poor quality solid recovered fuel (SRF). Effect of using natural minerals and biomass wastes blends. Fuel 2014;117:1034-1044. http://dx.doi.org/10.1016/j.fuel.2013.10.015.

[16] Roddy DJ, Manson-Whitton C. Biomass gasification and pyrolysis. In: Earth and Planetary Sciences; 2012, p. 133-153.

[17] Dou B, Zhang M, Gao J, Shen W, Sha X. High-temperature removal of NH3, organic sulfur, HCl, and tar component from coal-derived gas. Ind. Eng. Chem. Res. 2002;41:4195-4200.

[18] Torres W, Pansare SS, Goodwin Jr JG. Hot gas removal of tars, ammonia, and hydrogen sulfide from biomass gasification gas. Cat. Rev. - Sci. Eng. 2007;49:407-456. http://dx.doi.org/10.1080/01614940701375134.

[19] Woolcock PJ, Brown RC. A review of cleaning technologies for biomass-derived syngas. Biomass Bioenergy 2013;52:54-84. http://dx.doi.org/10.1016/j.biombioe.2013.02.036.

[20] Arena U, Di Gregorio F, De Troia G, Saponaro A. A techno-economic evaluation of a small-scale fluidized bed gasifier for solid recovered fuel. Fuel Process. Technol. 2015;131:69-77. http://dx.doi.org/10.1016/j.fuproc.2014.11.003.

[21] Luo S, Zhou Y, Yi C. Syngas production by catalytic steam gasification of municipal solid waste in fixed-bed reactor. Energy 2012;44:391-395. http://dx.doi.org/10.1016/j.energy.2012.06.016.

[22] Mayerhofer M, Mitsakis P, Meng X, de Jong W, Spliethoff H, Gaderer M. Influence of pressure, temperature and steam on tar and gas in allothermal fluidized bed gasification. Fuel 2012;99:204-209. http://dx.doi.org/http://dx.doi.org/10.1016/j.fuel.2012.04.022.

[23] Wang J, Cheng G, You Y, Xiao B, Liu S, He P, et al. Hydrogen-rich gas production by steam gasification of municipal solid waste (MSW) using NiO supported on modified dolomite. Int. J. Hydrogen Energy 2012;37:6503-6510. http://dx.doi.org/10.1016/j.ijhydene.2012.01.070.

[24] Montané D, Abelló S, Farriol X, Berrueco C. Volatilization characteristics of solid recovered fuels (SRFs). Fuel Process. Technol. 2013;113:90-96. http://dx.doi.org/10.1016/j.fuproc.2013.03.026.

[25] Lv P, Yuan Z, Wu C, Ma L, Chen Y, Tsubaki N. Bio-syngas production from biomass catalytic gasification. Energy Convers. Manage. 2007;48:1132-1139. http://dx.doi.org/10.1016/j.enconman.2006.10.014.

[26] Berrueco C, Montané D, Matas Güell B, del Alamo G. Effect of temperature and dolomite on tar formation during gasification of torrefied biomass in a pressurized fluidized bed. Energy 2014;66:849-859. http://dx.doi.org/10.1016/j.energy.2013.12.035.

[27] Kitzler H, Pfeifer C, Hofbauer H. Pressurized gasification of woody biomass-Variation of parameter. Fuel Process. Technol. 2011;92:908-914. http://dx.doi.org/10.1016/j.fuproc.2010.12.009.

[28] Lv P, Yuan Z, Ma L, Wu C, Chen Y, Zhu J. Hydrogen-rich gas production from biomass air and oxygen/steam gasification in a downdraft gasifier. Renewable Energy 2007;32:2173-2185. http://dx.doi.org/10.1016/j.renene.2006.11.010.

[29] He M, Xiao B, Liu S, Guo X, Luo S, Xu Z, et al. Hydrogen-rich gas from catalytic steam gasification of municipal solid waste (MSW): Influence of steam to MSW ratios and weight hourly space velocity on gas production and composition. Int. J. Hydrogen Energy 2009;34:2174-2183. http://dx.doi.org/10.1016/j.ijhydene.2008.11.115.

[30] Rapagnà S, Jand N, Kiennemann A, Foscolo PU. Steam-gasification of biomass in a fluidised-bed of olivine particles. Biomass Bioenergy 2000;19:187-197. http://dx.doi.org/10.1016/s0961-9534(00)00031-3.

[31] Wei L, Xu S, Zhang L, Liu C, Zhu H, Liu S. Steam gasification of biomass for hydrogen-rich gas in a free-fall reactor. Int. J. Hydrogen Energy 2007;32:24-31. http://dx.doi.org/10.1016/j.ijhydene.2006.06.002.

[32] Narváez I, Orío A, Aznar MP, Corella J. Biomass gasification with air in an atmospheric bubbling fluidized bed. Effect of six operational variables on the quality of the produced raw gas. Ind. Eng. Chem. Res. 1996;35:2110-2120.

[33] Gil J, Caballero MA, Martín JA, Aznar MP, Corella J. Biomass gasification with air in a fluidized bed: Effect of the in-bed use of dolomite under different operation conditions. Ind. Eng. Chem. Res. 1999;38:4226-4235.

[34] Han J, Kim H. The reduction and control technology of tar during biomass gasification/pyrolysis: An overview. Renewable and Sustainable Energy Reviews 2008;12:397-416. http://dx.doi.org/10.1016/j.rser.2006.07.015.

[35] Meng X, de Jong W, Fu N, Verkooijen AHM. Biomass gasification in a 100 kWth steam-oxygen blown circulating fluidized bed gasifier: Effects of operational conditions

on product gas distribution and tar formation. Biomass Bioenergy 2011;35:2910-2924. http://dx.doi.org/10.1016/j.biombioe.2011.03.028.

[36] Ma W, Hoffmann G, Schirmer M, Chen G, Rotter VS. Chlorine characterization and thermal behavior in MSW and RDF. J. Hazard. Mater. 2010;178:489-498. http://dx.doi.org/10.1016/j.jhazmat.2010.01.108.

[37] Hansson KM, Samuelsson J, Tullin C, Åmand LE. Formation of HNCO, HCN, and NH3 from the pyrolysis of bark and nitrogen-containing model compounds. Combust. Flame 2004;137:265-277. http://dx.doi.org/10.1016/j.combustflame.2004.01.005.

[38] Leichtnam JN, Schwartz D, Gadiou R. Behaviour of fuel-nitrogen during fast pyrolysis of polyamide at high temperature. J. Anal. Appl. Pyrolysis 2000;55:255-268. http://dx.doi.org/10.1016/s0165-2370(00)00075-9.

[39] Vriesman P, Heginuz E, Sjöström K. Biomass gasification in a laboratory-scale AFBG: influence of the location of the feeding point on the fuel-N conversion. Fuel 2000;79:1371-1378. http://dx.doi.org/10.1016/s0016-2361(99)00278-1.

[40] Corella J, Orío A, Aznar P. Biomass gasification with air in fluidized bed: Reforming of the gas composition with commercial steam reforming catalysts. Ind. Eng. Chem. Res. 1998;37:4617-4624.

[41] McKenzie LJ, Tian FJ, Guo X, Li CZ. NH3 and HCN formation during the gasification of three rank-ordered coals in steam and oxygen. Fuel 2008;87:1102-1107. http://dx.doi.org/10.1016/j.fuel.2007.07.004.

[42] Tanner J, Bläsing M, Müller M, Bhattacharya S. The temperature-dependent release of volatile inorganic species from Victorian brown coals and German lignites under CO2 and H2O gasification conditions. Fuel 2015;158:72-80.

http://dx.doi.org/10.1016/j.fuel.2015.04.071.

[43] Wilk V, Hofbauer H. Conversion of fuel nitrogen in a dual fluidized bed steam gasifier. Fuel 2013;106:793-801. http://dx.doi.org/10.1016/j.fuel.2012.12.056.

6. OXYGEN/STEAM GASIFICATION OF TWO SOLID RECOVERED FUELS (SRFs): EFFECT OF BED MATERIAL

Abstract

The goal of this study is to assess the release of contaminants during the oxygen-steam gasification of two waste-derived fuels using three different bed materials. The solid recovered fuels (SRFs) were tested at 850 ºC in a bench-scale fluidized bed reactor with sand, dolomite and olivine as bed material. The effect of the experimental conditions was assessed based on the gasification performance (product yields, carbon conversion, etc.) and the presence of tar, including polycyclic aromatic hydrocarbons (PAHs), and minor contaminants (HCl, H_2S, HCN and NH_3) in the producer gas. The results show higher gas yields with the use of catalysts, particularly with dolomite, and a lower catalytic activity of olivine towards tar abatement. The presence of contaminants precursors (Cl, S and N) together with the concentration of metals from both catalysts and waste fuel ashes appeared to influence the evolution of contaminants. In general, dolomite was more efficient than olivine in reducing tar compounds and most of minor contaminants but NH_3, whereas olivine mainly exhibited ability to reduce light PAHs and nitrogenous compounds (HCN and NH_3) in the producer gas.

This chapter is based on the following research article:

Recari J, Berrueco C, Abelló S, Montané D, Farriol X. Effect of bed material on oxygen/steam gasification of two solid recovered fuels (SRFs) in a bench-scale fluidized bed reactor. Energy & Fuels n.d. doi:Submitted to journal.

6.1 Introduction

Gasification is a thermochemical process that can convert a carbonaceous material into a synthesis gas (syngas). This gas mixture is formed by H_2, CO among other compounds (CO_2, CH_4 and higher hydrocarbons), and it may be directly used as gaseous fuel to produce electricity, synthetic liquid fuels and chemicals [1]. Historically, coal and biomass have been considered the preferred carbonaceous feedstocks for gasification, but in recent years the use of waste materials has been gaining attention [2–6].

Waste materials such as municipal solid waste (MSW) are abundant and have a high content of carbon (up to 50%). Nowadays, incineration is the dominant process to reduce the amount of landfilled waste, however gasification is a promising alternative to handle waste disposal with efficient energy recovery [6]. Although incineration can be coupled with an energy recovery system, only 4.4% of waste in the European Union is treated in this way [7]. The high costs of traditional incineration plants are usually related to the flue gas treatment units required to abate atmospheric emissions of toxic contaminants formed during combustion (dioxins, furans, and nitrous and sulphur oxides) [8]. This suggests that gasification may have potential advantages over waste combustion [9].

Gasification in a fluidized bed is a well-established technology that allows a good control of the gasification temperature and has flexibility to process different types of solid fuels. However, the main disadvantage of waste gasification is the lack of experience handling such heterogeneous feedstocks. Contrary to biomass, waste contains a considerable amount of ash, nitrogen, sulphur and chlorine, which may induce operational problems like bed sintering and agglomeration, and the presence of trace contaminants in the syngas [10]. This implies that the syngas cleaning and conditioning stage for this kind of feedstock will be more complex than those developed for biomass gasification. Catalysts are commonly used during gasification and syngas conditioning in order to improve the syngas quality and abate contaminants [11,12]. Mineral catalysts such as dolomite and olivine are cheap compared to supported metallic catalysts, and both types have been extensively used in gasification [3,13–16]. Although dolomite presents higher efficiencies for tar reforming during biomass gasification [15,16], olivine is still the preferred bed material due to its higher

mechanical resistance against attrition [11,17]. The choice of gasification medium (air, oxygen, steam, etc.) is also important and influences the quality and concentration of contaminants in the producer gas. Unlike gasification with oxygen/steam, air gasification produces a syngas highly diluted in nitrogen. Notice that the production of some biofuels such as Bio-SNG (Synthetic Natural Gas) through gasification, a topic that has received increasing attention in the last years, requires of a nitrogen-free syngas [18]. Few studies have focused on oxygen/steam gasification of waste-derived fuels [19–23] and especially the presence of minor contaminants in the syngas (i.e. HCl, H_2S, HCN and NH_3). Therefore a better understanding of oxygen/steam gasification of waste materials in the presence of catalytic materials and its influence on syngas quality is needed to fully develop the potential of this resource.

The present paper deals with the oxygen/steam gasification of two solid recovered fuels (SRFs) in a lab-scale fluidized bed reactor. The experimental conditions were chosen based on the results of a previous gasification study with SRFs [23], which revealed that a gasification temperature of 850 ºC and equivalence ratio (ER) around 0.3 were the most adequate conditions for the gasification of the studied SRFs. This work explores the influence of the use of different bed materials (sand, dolomite and olivine) on the release of contaminants (tar compounds and traces such as HCl, H_2S, HCN and NH_3) during the oxygen steam gasification of two different SRFs.

6.2 Experimental

6.2.1 SRF samples characterization and bed materials

Two MSW fractions categorized as SRFs were employed as feedstocks during the gasification experiments. The SRFs, provided by local waste management companies, were obtained after different mechanical treatments: one SRF consists in the fraction rejected by trommel (RT) from unsorted waste streams and the other is a fluff type (FL) derived from mixed domestic waste streams. In RT predominated textiles and plastics whereas FL contained higher presence of paper, biomass and as well post-consumer plastics. Both SRFs had little organic matter. Further information for these solid fuels can be found

elsewhere [23–25]. For analytical and gasification purposes the materials were grounded and sieved to a particle size of 1 mm.

A summary of the main techniques, equipment and methods used for the characterization of SRFs are listed as follows:

- Proximate analysis in a LECO Thermogravimetric (TGA 701), according to EN-15402:2011 and EN-15403:2011 standard methods.
- Ultimate analysis in a LECO TruSpec CHN-S analyser following the EN-15407:2011.
- Heating value conducted in a LECO calorimeter (AC-600) according to the EN-15400:2011 standard method.
- Halogens (Cl, F and Br) content analysed by ionic chromatography (Dionex ICS-1100) following the EN-15408:2011 standard method.
- Ash composition determined in Spectro Arcos 165 spectrophotometer after ash samples digestion in a microwave system (Berghof Speedwave 4), according to the EN-15410:2006 and EN-15411:2006 standard methods.

Table 1 gathers the characterization results performed by triplicate with uncertainties estimated at a 95% probability level.

The bed materials tested during the gasification experiments were quartz sand (J.T.Baker), dolomite (Productos Dolomíticos de Málaga S.A.) and olivine (Sibelco Hispania); all sieved to particle size range of 150-200 μm and calcined in a furnace at 900 ºC for 4 hours.

6.2.2 Experimental setup and procedure

The bench-scale fluidized bed gasifier (PID ENG&Tech, Spain) consisted in a Hastelloy X reactor (450 mm long and 23.8 mm internal diameter) externally heated by an electrical furnace and equipped with a control system (flow, temperature and feeder control). The experimental rig was able to operate up to 900 ºC and 20 bar.

Gasification experiments were performed at 850 ºC and atmospheric pressure using a mixture of oxygen and steam (O_2/H_2O) as gasification agent (O_2: ~200 NmL/min and $H_2O_{(l)}$: 0.4 mL/min) with a ratio of steam/SRF around 1 and equivalence ratio (ER) of ~0.3. These operational flows lead to a bubbling fluidized bed regime and a gas residence time in the reactor of about 3 s.

The tested bed material (50 g of sand or olivine, or 30 g of dolomite) was placed inside the gasifier, and after all the parts were connected, the reactor was heated up to the desired temperature. Once temperature was reached, the fluidization gas was switched to the mixture O_2/steam, and the SRF was continuously fed by means of a screw feeder at rates ranging from 0.3-0.5 g/min. The generated gas exited the reactor passing through a cleaning system formed by a hot filter to remove particulates, and condensers to collect water and tar products. A fraction of the producer gas was collected in a Tedlar® gas bag for the minor contaminants assessment whereas the rest was analysed in an on-line micro gas chromatograph (micro GC). Total mass and carbon balances closed higher than 95% in all conducted experiments. A more accurate explanation of the experimental setup and procedure can be found elsewhere [23,25,26].

6.2.3 Analyses of gas composition, tar and minor contaminants

The Agilent 490 micro GC quantified the main components of the syngas (H_2, O_2, N_2, CO, CO_2, CH_4 and hydrocarbons up to C_5) whereas the ion-selective electrodes (ISEs, Metrohm) assessed the concentration of the inorganic traces (HCl, H_2S, HCN and NH_3) in aqueous solution. For this purpose, the gas collected in the gas bag was pumped through a series of impingers filled with solutions to retain specific ions (S_2^-, CN^-, Cl^- and NH_4^+). Additionally, due to the use of steam as gasification agent, the liquid collected in the condensers was also analysed since it may have retained part of the inorganic compounds of the gas. In this case, samples of 1 mL of the liquid from the condensers were filtered with a syringe filter (CHROMAFIL® Xtra. PTFE-45/25) and diluted into 50 mL of Milli-Q water. Therefore, the amounts of minor contaminants reported in this work comprise the sum of those sampled from gas bags and the condenser liquids. The solutions were conditioned and tested with adequate ISEs by direct potentiometric analysis on a 905 Titrando (Metrohm) using the Tiamo™ software. Further details, such as the trap solutions and conditioning procedures, were reported in our previous studies [23,25].

Characterization of the aromatic hydrocarbons present on tar samples was carried out in a Hewlett Packard 6850 GC-FID (gas chromatograph with a flame ionization detector) using an automatic sampler (7683B). The column configuration and methodology was also described elsewhere [26].

6.3 Results and discussion

6.3.1 SRFs characterization

The two solid recovered fuels used in this study (RT and FL) were used in previous works [23–25]. However, a new characterization was carried out in order to evaluate minor changes due to sample ageing (in the case of RT) and the use of a new sample batch (for FL).

RT has a high quantity of textiles, fabrics and plastics and fewer cellulosic materials than FL, meanwhile the latter comprises more paper and biomass albeit having also a diverse sort of polymers (i.e. non-recyclable post-consumer plastics) as it is a mixture of domestic waste.

Table 6.1 presents the characterization results of the SRFs in terms of proximate and ultimate analysis, lower heating value (LHV) and ash composition. The differences in the characterization results are in agreement to their composition.

First of all, it is noticeable that these SRFs present higher ash content (> 8.6%) and lower fixed carbon (< 5.8%) in comparison to many biomass samples such as wood, corn cobs or walnut shells [26,27]. The FL feedstock presented levels of ash (13.2%) and fixed carbon (5.8%) 1.5 times higher than those of RT (8.6% and 3.9%, respectively). This might result from the higher proportion of paper and biomass in FL. On the other hand, both solid fuels showed a high content of volatiles (ranging from 73-86%) similarly to biomass samples.

The composition of the fuels affected as well the ultimate analysis, with larger carbon values for the RT fuel (66%) than for FL (46%). Concerning nitrogen, sulphur and chlorine (precursors of minor contaminants), both feedstocks presented similar values (below 1%). However, FL had slightly more nitrogen (0.66%) and chlorine (0.59%) than RT (0.41% and 0.35%, respectively). The calorific content expressed as LHV was higher for RT, presumably due to the lower moisture and ash content, and the presence of polymers (plastic fraction) in its composition (28 MJ/kg for RT and 23 MJ/kg for FL). Regarding the ash composition, the analysis of both SRFs revealed aluminium, calcium, phosphorous and silicon as main trace elements, although in slightly higher proportion in the FL sample.

Table 6.1 Characterization of SRFs (as received basis)

		RT	FL
Proximate analysis (wt.%)	**Moisture**	1.83±0.73	8.39±0.41
	Volatiles	85.68±1.15	72.58±0.86
	Fixed carbon	3.92±0.20	5.78±0.44
	Ash	8.59±0.75	13.24±1.01
Ultimate analysis (wt.%)	**C**	65.99±0.07	46.03±0.54
	H	9.48±0.02	7.49±0.02
	O (by difference)	14.86±0.56	31.71±0.55
	N	0.41±0.10	0.66±0.06
	S	0.32±0.05	0.26±0.01
	F	<0.01	<0.02
	Cl	0.35±0.11	0.59±0.06
LHV (MJ/kg)		28.44±0.13	23.29±0.22
Ash composition (mg/kg$_{fuel}$)	**Aluminium as Al_2O_3**	15670±250	30754±584
	Calcium as CaO	23534±221	39541±539
	Chrome as Cr	114±14	143±20
	Iron as Fe_2O_3	3108±157	4094±214
	Lead as Pb	91±11	642±17
	Magnesium as MgO	2012±95	4319±573
	Manganese as MnO	155±3	241±8
	Nickel as Ni	77±6	87±7
	Phosphorus as P_2O_5	9630±301	13385±541
	Potassium as K_2O	1391±34	2162±126
	Silicon as SiO_2	17276±521	20262±837
	Sodium as Na_2O	1916±117	4104±183
	Titanium as TiO_2	3236±242	2436±357
	Vanadium as V	<50	<50
	Zinc as Zn	288±20	631±80

6.3.2 Product yields

Table 6.3 lists the yields of gas, tar and char, together with the carbon conversion and H_2/CO and CO/CO_2 ratios of the producer gas, its LHV and tar content.

Table 6.2 Product yields of oxygen/steam gasification experiments (T= 850 ºC, Equivalence Ratio (ER) ~0.3 and Steam/SRF ~ 1)

SRF	ER	Bed material	Yield (g/100 g dry SRF)			H_2/CO	CO/CO_2	Gas LHV (MJ/Nm³ dry)	X_c	Tar content (g/Nm³ dry)
			Gas	Tar	Char*					
RT	0.31	Sand	142.5±1.3	4.5±0.4	4.1±0.4	1.5±0.07	0.41±0.04	10.72±0.77	75.3±1.6	33.65±2.72
RT	0.34	Dolomite	165.8±1.5	1.5±0.1	3.7±0.4	2.68±0.12	0.22±0.02	11.07±0.79	87.5±1.9	9.85±0.80
RT	0.29	Olivine	151.5±1.3	4.0±0.3	2.9±0.3	2.34±0.11	0.25±0.02	10.45±0.75	78.3±1.7	29.26±2.37
FL	0.30	Sand	105.9±0.9	11.9±0.8	6.7±0.7	1.49±0.07	0.45±0.04	12.28±0.80	74.9±1.6	116.93±9.45
FL	0.31	Dolomite	115.2±1.0	6.9±0.6	3.6±0.4	2.75±0.12	0.27±0.02	14.44±0.94	86.3±1.8	60.24±4.87
FL	0.30	Olivine	113.9±1.0	11.4±0.8	5.0±0.5	2.04±0.09	0.34±0.03	11.47±0.75	76.9±1.6	103.31±8.35

* Ash free. Ash content ~ 8.75 g/100 g dry RT and ~ 14.45 g/100 g dry FL.

Notice that product yields (g/100 g of dry SRF) are above 100% as the oxygen from the gasification agent (O_2/H_2O) reacts with the feedstock during gasification to form products such as CO and CO_2.

In general, RT produced higher gas yields and lower tar and char yields than FL. The use of catalytic materials in the bed instead of sand caused the gas yield to increase by 2-12%. During RT gasification, gas yield raised from 143% with sand as bed material to 166% and 152% with dolomite and olivine, respectively. On the other hand, with the FL material, gas yields increased from 106% with sand to around 115% with both catalysts. A common fact observed during gasification of RT and FL was that dolomite made tar yield to decrease about 2 times the value obtained with sand (~4% for RT and ~12% for FL) whereas this effect was less significant when olivine was used as bed material. Experiments with olivine in the bed resulted in tar yields of the same order as those reported for sand. Concerning char yield, it always dropped when a catalyst was used, probably due to the promotion of water gas reactions under these conditions [28].

These results indicate that the catalysts promoted tar cracking and char gasification reactions resulting in an increase of gas yield at expense of lower tar and char yields. Among the catalysts tested in this work, dolomite showed in general greater tar and char yields reductions than olivine for both SRFs.

6.3.3 Gas composition

Figure 6.1 presents the composition (% vol.) of the gas produced during gasification of two SRFs using sand, dolomite and olivine as bed material. High levels of hydrogen (H_2), carbon monoxide (CO) and dioxide (CO_2) were expected under oxygen/steam (O_2/H_2O) gasification conditions; on the one hand the gas is not diluted in nitrogen (N_2) as occurs when using air as gasification agent, and on the other hand steam enhances reactions such as water gas and steam reforming, which favour the production of gaseous compounds.

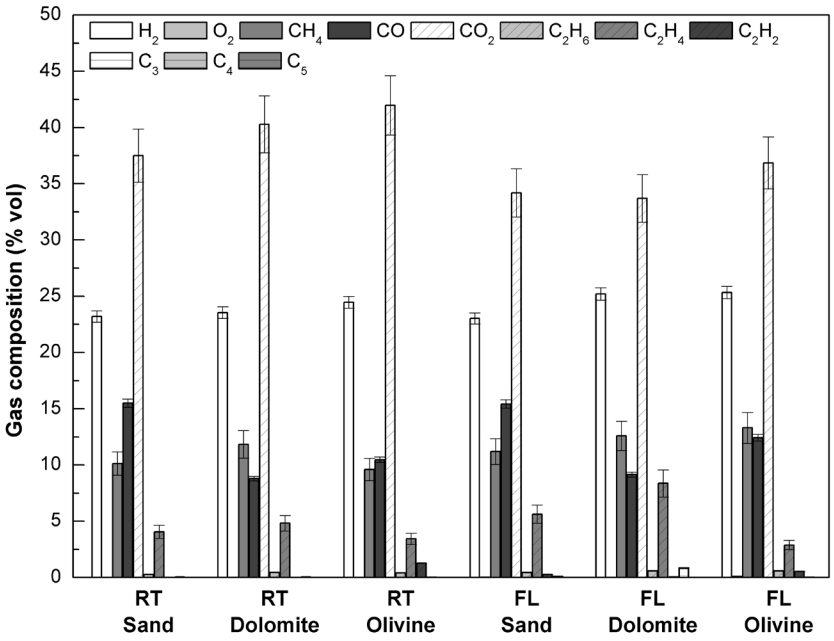

Figure 6.1 Gas composition (dry basis) of oxygen/steam gasification experiments (T=850 C, ER ~0.3, Steam/SRF ~1; two SRFs (RT and FL) and three bed materials (sand, dolomite and olivine)

H_2 concentration in the producer gas (~ 24% vol.) increased with the use of catalyst for both SRFs. This rise was less noticeable during RT gasification (growth around 5%) than with FL (around 9%) regardless of the catalytic bed material. CO concentration followed an equivalent but decreasing trend, diminishing from 15% vol. with sand up to 9% vol. with dolomite and olivine for both solid fuels. The evolution of these gases affected the H_2/CO and CO/CO_2 ratios. For the experiments with sand, H_2/CO and CO/CO_2 ratios were around 1.5 and 0.4, respectively, however in catalytic tests H_2/CO ratios increased > 2.0 and CO/CO_2 ratios decreased to levels around 0.3. Gasification tests with dolomite presented the highest H_2/CO ratios for both SRF (~2.7) meanwhile the ratios with olivine were < 2.4. Opposite to these trends, the levels of CO/CO_2 ratios were slightly higher with olivine than with dolomite. The concentration of CH_4 and light hydrocarbons (C_2H_2, C_2H_4 and C_2H_6) was higher in the syngas obtained during gasification of the FL material (which contained more post-consumer plastics) particularly when dolomite was used as bed material. The increase of these compounds when using catalysts could be due to the cracking of tar and larger hydrocarbons [29]. However, when using olivine, CH_4 concentrations were closer to those obtained with sand as bed

material. This may indicate a different catalytic effect between olivine and dolomite on tar cracking (discussed in more detail in the following section). Another important parameter is the LHV of the syngas. Initially the calorific content of the RT feedstock was higher than FL; however, the producer gas of the latter material resulted in a higher LHV. An interesting point is that the gas calorific value was scarcely affected by the bed material in RT gasification (~11 MJ/Nm^3), but the effect of catalysts was relevant in FL gasification tests. For instance, in comparison to sand experiments, dolomite improved the calorific value from 12 to 14 MJ/Nm^3, which corresponds to an increase of 18%, while the calorific content decreased by 7% with olivine. As stated in a previous work [25], apart from H_2, hydrocarbons (particularly C_2H_4) play an important role on gas LHV produced from SRFs. The degree of tar cracking induced by the catalyst may be relevant to explain the changes in the concentration of hydrocarbons. The catalytic effect of olivine led to a lower C_2H_4 concentration. This reduction was not compensated by the increase in H_2 production, causing a diminishment of the syngas calorific content. Thus, during both SRF gasification experiments, olivine decreased the gas heating value when compared to dolomite. Regarding carbon conversion (X_c), although both catalysts increased this parameter from the lowest 75% up to > 86%, dolomite always showed the highest carbon conversion (88% for RT and 86% for FL) in contrast to olivine (78% for RT and 77% for FL).

6.3.4 Tar characterization

6.3.4.1 Tar content

Table 3 reports tar concentration in the producer gas. Tar content was 32 g/Nm^3 for RT and 117 g/Nm^3 for FL gasification when sand was used as bed material. These levels dropped when using catalysts, resulting in the lowest tar contents when dolomite was used (10 and 60 g/Nm^3 for RT and FL, respectively). On the contrary, olivine hardly reduced tar concentration leading to similar values to those obtained with sand. This fact corroborates the lower activity of olivine in comparison to dolomite towards tar decomposition [13,15,16].

6.3.4.2 GC-FID analysis

Tar samples were analysed by GC with a flame ionization detector (GC-FID) to quantify the presence of polycyclic aromatic hydrocarbons (PAHs). These compounds are relevant pollutants appearing in tars formed at high gasification temperature, and considered to be carcinogenic [13,26,30]. A standard of 16 PAHs (EPA 610 PAH Mix) was used for the identification and quantification of the compounds present in the tar samples; nonetheless three additional compounds (assigned as 1a, 1b and 1c) were easily recognized and hence added to the calibration database. Figure 6.2 shows an example of a tar chromatograph with the list of the identified hydrocarbons. All samples were analysed by triplicate, and the results were normalized to grams of tar per gram of dry SRF.

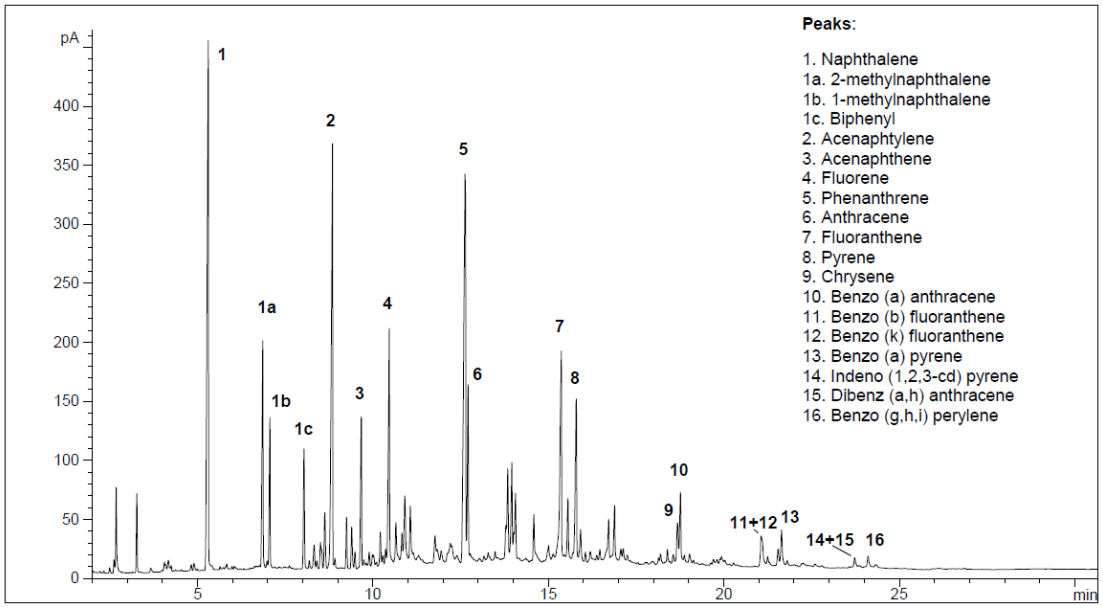

Figure 6.2 Example of a GC-FID tar chromatograph with detected peaks

As already explained and observed in Table 3, the amount of tar produced when feeding FL was significantly higher than the one obtained with RT as feedstock (see Figure 6.3). However, the relative amounts of PAHs were equivalent in both feedstocks at the same gasification conditions. For instance, when sand was used as bed material around 2.7 g PAHs/100 g dry SRF were produced during RT gasification, whilst 7.0 g PAHs were quantified with the FL feedstock; these values represented a 60% in terms of mass percentage between PAHs and total tar content. Following the trends discussed above, the

presence of olivine barely changed the quantity of PAHs (2.2 g with RT and 7.0 g with the FL material) compared to results with sand as bed material.

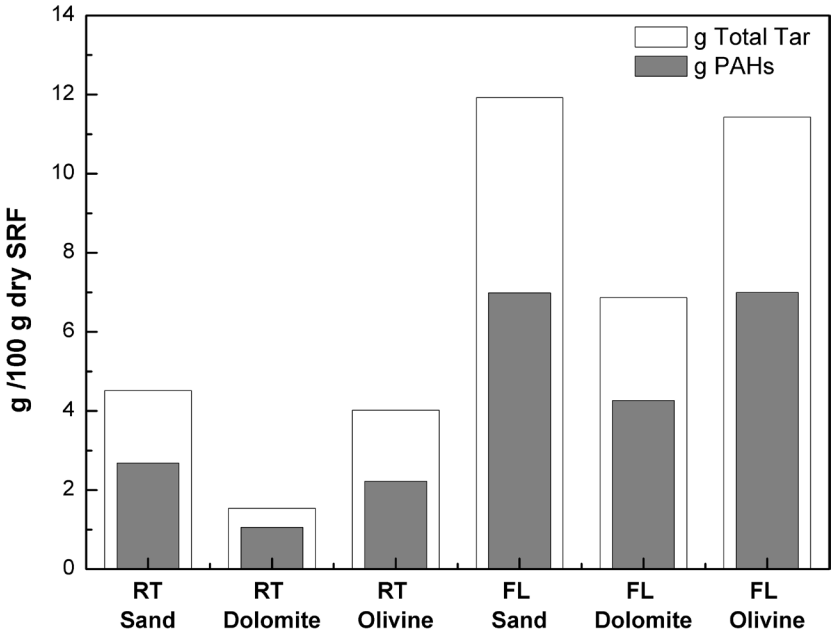

Figure 6.3 Total tar and PAHs yields in oxygen/steam gasification experiments (T=850 ºC, ER ~0.3, Steam/SRF ~1)

A more detailed evaluation of the PAHs composition (Figure 6.4) shows that naphthalene ($C_{10}H_8$), acenaphtylene ($C_{12}H_8$) and phenanthrene ($C_{14}H_{10}$) were the major PAH compounds present in tar samples. Acenaphtylene predominated in tars obtained during RT gasification with sand (maximum of 0.5 g/100g dry RT) and olivine (0.4 g) as bed material, whilst naphthalene stood out in RT tests with dolomite and all FL experiments (maximum of 1.45 g/100 g dry FL). Regarding RT gasification, dolomite just reduced naphthalene by 7% whereas larger aromatic hydrocarbons were reduced between 60-86%. The reduction of these compounds with dolomite indicates the role of this catalyst in the polymerization pathway of hydrocarbons, cracking larger aromatics and hindering the formation of heavier PAHs [31,32]. On the contrary, the use of olivine reduced naphthalene by 41% but the drop of other tar species was almost negligible (in the range of 0-11%). Only fluorene, phenanthrene, fluoranthene and pyrene decreased about 22%. Considering FL as gasification feedstock, the effect of catalysts on PAHs formation showed a few differences. A common trend was the effectiveness of dolomite to break tars

down; an average reduction of 40% in PAHs was achieved (even with naphthalene). Nevertheless, olivine scarcely had an effect on tar composition. Naphthalene experienced a drop of about 20%, but the rest of compounds remained constant or slightly increased (i.e. phenanthrene, anthracene, pyrene, etc.). These results suggest the lower activity of olivine towards tar cracking.

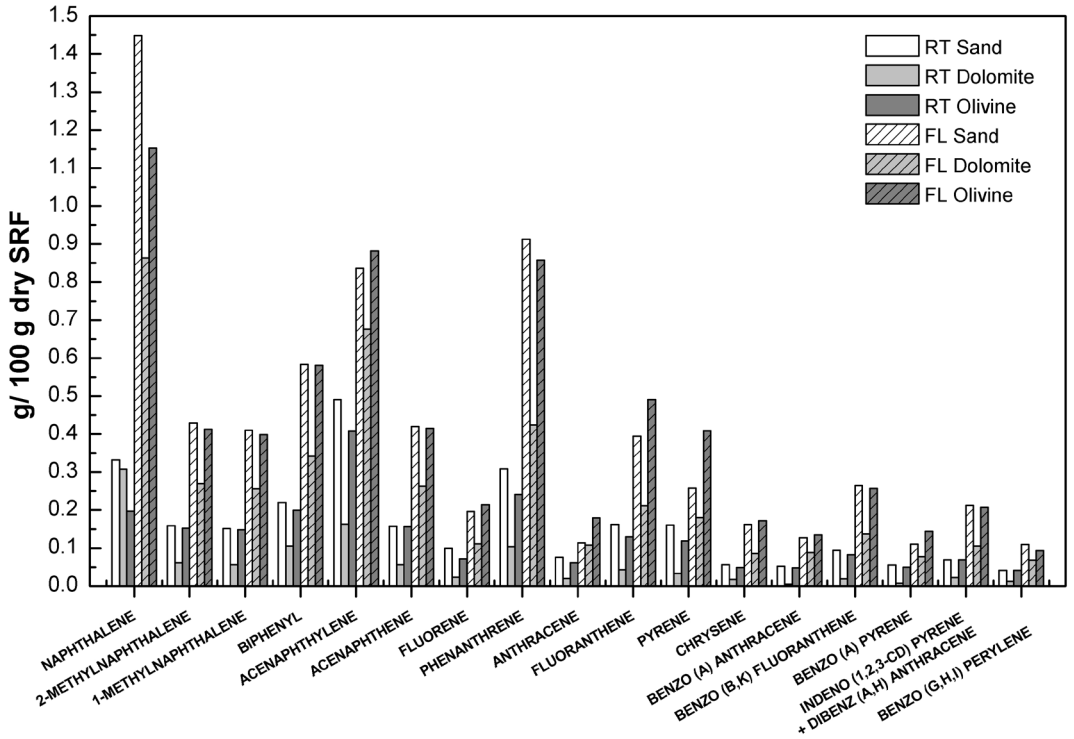

Figure 6.4 Tar composition in oxygen/steam gasification experiments (T=850 ºC, ER ~0.3, Steam/SRF ~1)

Other studies have reported the higher activity of dolomite in comparison to olivine during gasification of biomass [3,16,33,34]. In particular, Devi et al. [16] studied the activity of dolomite and olivine for tar destruction in syngas during biomass gasification at laboratory scale. Tar concentration decreased from 4 g/m^3 to 1.5 g/m^3 and 2.2 g/m^3 with dolomite and olivine, respectively. At a temperature of 900 ºC calcined dolomite decreased total heavy PAHs to a greater extent than olivine and sand. Calcined dolomite was therefore more reactive than untreated olivine. The authors pointed out the lower porosity and iron content of olivine as the causes of its moderate activity compared to calcined dolomite. However in that study olivine was not pretreated, and thus the calcination of olivine could improve the activity of this catalyst. In another

study Arena et al [3] indicated that magnesium and iron present in olivine promoted a series of reactions enhancing the formation of molecular hydrogen and coke. However this coke formed through carbonization reactions could deposit on the external surface of the catalyst masking the iron active sites. An interesting work carried out by Mastellone and Zaccariello [29] which can be relevant for SRF gasification studies, reported the rapid and irreversible deactivation of olivine during gasification of polyolefins (also present on the plastic fraction of SRF samples). The authors stated that this deactivation was related not just to the coke deposition, but more importantly, to the loss of metals due to detachment of coke from the olivine surface. Another explanation for the limited influence of olivine on tar depletion could be the more prominent effect of elements like sulphur and chlorine on its catalytic activity. These compounds could poison the ferrous active sites of olivine due to the formation of a film of sulphide or chloride [3,35].

The results presented in the current study support the idea that dolomite is a more effective material than olivine for tar abatement during SRF gasification. It is evident that olivine presents a certain catalytic effect and provokes a decrease in some tar species (mainly light PAHs), but in general the reduction, both in total tar and PAHs contents, is less remarkable than the obtained with dolomite. On the other hand, the effect of dolomite is not limited to the cracking of light PAHs but has an even more relevant effect on depletion of heavier PAHs.

6.3.5 Minor contaminants

This section discusses the release of minor contaminants (HCl, H_2S, HCN and NH_3) in the producer gas.

Fig. 5 plots the concentration of the minor contaminants determined in collected gas and condensed water. In general, the levels of most of contaminants (HCl, HCN and NH_3) produced during RT gasification were generally lower than those detected when feeding FL. The relative amounts of minor contaminants found in the gas are in agreement with their concentrations in the feedstocks (Table 6.1). RT contains in mass percentage half the chlorine (0.35%) than FL (0.59%), and therefore a lower release of HCl from this fuel should be expected. HCl concentration during RT gasification with sand as bed

material was close to 3000 mg/Nm³ whereas hydrogen chloride level was around 7500 mg/Nm³ for FL. The higher presence of inorganic chlorine in the FL sample, which can be partially released as HCl at temperatures over 800 ºC [25], derives from the presence of chloride salts (sodium and potassium) in the domestic waste. The higher amount of both compounds (Na and K) detected in FL ash (Table 6.1) confirms this hypothesis. Furthermore, the larger concentration of aluminium (Al) and silicon (Si) present in ash from FL may provoke a reaction between these compounds and chloride salts (i.e. KCl) releasing higher amounts of HCl [36]. Another explanation is that most of HCl comes from dechlorination of polymers (e.g. PVC) released during the pyrolysis stage [37] in the gasification process.

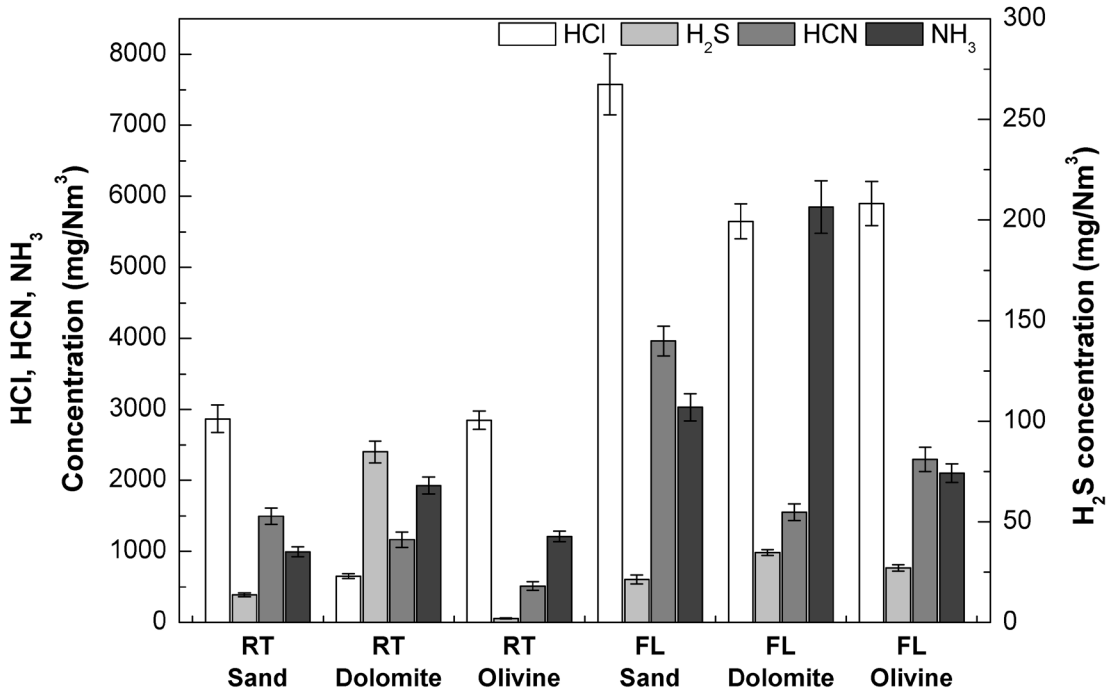

Figure 6.5 Minor contaminants in oxygen/steam gasification experiments (T=850 ºC, ER ~0.3, Steam/SRF ~1)

The presence of nitrogen-containing compounds (HCN and NH_3) was dominant in the syngas from SRFs. Regarding gasification of RT with sand as bed material, NH_3 and HCN levels ranged 1000-1500 mg/Nm³, whereas FL, which contained higher levels of nitrogen in its composition, reported larger values (3000-4000 mg/Nm³). In a previous work dealing with gasification of these SRFs [23] it was observed that under similar gasification conditions

nitrogen was released preferentially as HCN. However, in this study the presence of NH_3 is also relevant. The difference lies in the analysis of the condensed water, which contained almost all the ammonia and part of the hydrogen chloride. Several factors could affect the fuel-N conversion mechanism (i.e., type of fuel, nitrogen functionality, oxygen concentration, temperature, residence time, heating rate, particle size, bed material, etc.). Among them, chemical composition of the fuel and fuel nitrogen functionalities are key [38]. The presence of nitrogen as pyrrolic and pyridinic forms in the parent fuel would lead to the formation of HCN, whereas the amino-groups would evolve towards NH_3 [25]. The results suggested that the source of nitrogen in SRF samples is dual, polymers used as textiles (polyamides, polyacrylonitriles, etc.) which preferentially evolved toward HCN, and protein nitrogen, similar to that of biomass, which could form NH_3 [25].

Hydrogen sulphide was barely detected (< 90 mg/Nm^3) in the producer gas of all gasification tests, with the highest value of 85 mg/Nm^3 measured with the RT feedstock in combination with dolomite. The evolution of H_2S might be explained by competitive reactions with some elements present in the ashes, such as alkali (K) and alkaline earth metals (Ca). As both sulphur and chlorine are prone to react with potassium, the equilibrium between KCl and HCl has to be considered [25]. A decrease of HCl concentration could be produced due to larger formation of KCl, thus lowering the availability of K in the media to react with H_2S, preventing the formation of K_2S and subsequently causing a higher release of H_2S to the gas. In fact, the experimental results with a decreasing trend of HCl showed higher concentrations of H_2S, for instance in the gasification experiments with dolomite as bed material. In addition, the release of H_2S may be influenced by the presence of calcium (Ca) and silicon (Si) introduced with the bed materials like dolomite (a calcium magnesium carbonate) and olivine (a magnesium iron silicate). These species have been reported to have an effect on H_2S release [38,39].

The substitution of sand for dolomite or olivine provoked the decrease of the concentration of most contaminants. In the case of RT, dolomite reduced HCl concentration by 77% (to 650 mg/Nm^3) and HCN by 22% (to 1165 mg/Nm^3). However NH_3 and H_2S concentrations rose up to 2000 mg/Nm^3 and 85 mg/Nm^3, respectively. These trends were also observed for FL gasification

with dolomite, showing a decline in HCl and HCN levels but an increase in NH_3 and H_2S; (in a lesser extent to H_2S, which was scarcely detected in the syngas although a slight rise was observed). The drop of HCl concentration could be related to the larger amount of Ca and Mg available in the dolomite bed [1,40]. Regarding NH_3 and HCN trends, Corella et al. [15] reported higher ammonia content in air gasification of biomass when using dolomite instead of olivine. The authors suggested that higher tar cracking would release higher amounts of the nitrogen contained in the tar compounds and therefore generate more NH_3. On the other hand, Leppälahti et al.[41] studied the catalytic effect of various materials on the presence of nitrogenous compounds in the gas. They concluded that dolomite did not decompose ammonia but reduced hydrogen cyanide content, which is in agreement with the results obtained in the present study. Those results were also confirmed by Tchapda and Pisupati [38] which reported the catalytic effect of some alkali (K), alkaline earth metals (Mg) and Fe on N-fuel conversion leading to lower HCN concentration as observed in the present study when using catalytic beds. For instance, FL gasification with olivine in the bed decreased HCN by 42% (to 2300 mg/Nm3) in contrast to the level obtained with sand. However, the studied catalysts had different effects depending on the minor contaminant. During FL gasification, the rise of ammonia concentration observed with dolomite was the opposite with olivine; NH_3 levels decreased to 2100 mg/Nm^3 but remained similar to those obtained with sand (3000 mg/Nm^3) as occurred in RT gasification. A lower release of ammonia is probably due to a lower conversion of tar and char with olivine, and thus, more nitrogen-containing organics will remain in these products. The iron content of olivine also may cause the reduction of NH_3 when compared to dolomite [41,42]. Our results also suggest that olivine could promote HCN destruction. Thus, the choice of bed material has a great importance since it affects the rates of char conversion, tar abatement, and the release of nitrogenous compounds. All these issues, together with the bed material deactivation rate, due to the presence of chlorine and sulphur, should be taken into account during the selection of the most suitable bed material.

6.4 Conclusions

The release of tar and minor contaminants during the oxygen/steam gasification of two SRFs (RT and FL) was evaluated with different bed materials (sand, dolomite and olivine) at selected operating conditions (T=850 ºC, ER ~0.3, Steam/SRF=1).

Gas composition was similar for the experiments carried out with both SRFs and followed equivalent trends when replacing the bed material from sand to catalyst. The most remarkable difference was the effect of bed material on tar cracking and the subsequent production of CH_4 and C_2 hydrocarbons.

The use of mineral catalysts promoted tar cracking and char reaction; however, dolomite was far more efficient than olivine on tar abatement, which could be partially related to the rapid deactivation of the catalytic activity of olivine in presence of chlorine and sulphur. The obtained results showed that olivine was active on naphthalene cracking, whereas dolomite also caused a steep decrease of larger PAHs (> 2 aromatic rings).

RT, the feedstock with lower levels of heteroatoms (N, Cl and S) and ash, led to lower concentrations of minor contaminants (HCl, H_2S, HCN and NH_3) in comparison to FL. Regarding the effect of bed material, dolomite promoted the conversion of nitrogen-containing organics to NH_3 and diminished HCN concentration; meanwhile olivine seemed to be more effective in reducing nitrogen compounds, probably due to iron content of the mineral. Fuel ash levels and its composition (alkali and alkaline earth metals) also could play an important role in the competing reactions involving the release of minor contaminants in the producer gas. Overall, results showed a clear depletion of contaminants with dolomite at expense of higher NH_3 levels, probably as a result of the higher conversion of char and tar when using dolomite as bed material.

The presented results showed similar effects of the different evaluated bed materials regardless of the SRF. The differences observed from a quantitative point of view can be partially related to the SRF characteristics and composition. This could be a start point for developing a method to predict the behaviour of SRFs as gasification feedstocks from an initial characterization.

6.5 References

[1] Woolcock PJ, Brown RC. A review of cleaning technologies for biomass-derived syngas. Biomass and Bioenergy 2013;52:54–84. doi:10.1016/j.biombioe.2013.02.036.

[2] Luo S, Zhou Y, Yi C. Syngas production by catalytic steam gasification of municipal solid waste in fixed-bed reactor. Energy 2012;44:391–5. doi:10.1016/j.energy.2012.06.016.

[3] Arena U, Zaccariello L, Mastellone ML. Fluidized bed gasification of waste-derived fuels. Waste Manag 2010;30:1212–9. doi:10.1016/j.wasman.2010.01.038.

[4] Couto N, Silva V, Rouboa A. Municipal solid waste gasification in semi-industrial conditions using air-CO2 mixtures. Energy 2016;104:42–52. doi:10.1016/j.energy.2016.03.088.

[5] Zheng X, Chen C, Ying Z, Wang B. Experimental study on gasification performance of bamboo and PE from municipal solid waste in a bench-scale fixed bed reactor. Energy Convers Manag 2016;117:393–9. doi:10.1016/j.enconman.2016.03.044.

[6] Ng WPQ, Lam HL, Varbanov PS, Klemeš JJ. Waste-to-Energy (WTE) network synthesis for Municipal Solid Waste (MSW). Energy Convers Manag 2014;85:866–74. doi:10.1016/j.enconman.2014.01.004.

[7] Eurostat. Energy, transport and environment indicators. 2016. doi:10.2785/260003.

[8] García-Pérez J, Fernández-Navarro P, Castelló A, López-Cima MF, Ramis R, Boldo E, et al. Cancer mortality in towns in the vicinity of incinerators and installations for the recovery or disposal of hazardous waste. Environ Int 2013;51:31–44. doi:10.1016/j.envint.2012.10.003.

[9] Arena U. Gasification: An alternative solution for waste treatment with energy recovery. Waste Manag 2011;31:405–6. doi:10.1016/j.wasman.2010.12.006.

[10] Bartels M, Lin W, Nijenhuis J, Kapteijn F, van Ommen JR. Agglomeration in fluidized beds at high temperatures: Mechanisms, detection and prevention. Prog Energy Combust Sci 2008;34:633–66. doi:10.1016/j.pecs.2008.04.002.

[11] Anis S, Zainal Z a. Tar reduction in biomass producer gas via mechanical, catalytic and thermal methods: A review. Renew Sustain Energy Rev 2011;15:2355–77. doi:10.1016/j.rser.2011.02.018.

[12] Rownaghi AA, Huhnke RL. Producing hydrogen-rich gases by steam reforming of syngas tar over CaO/MgO/NiO catalysts. ACS Sustain Chem Eng 2013;1:80–6. doi:10.1021/sc300042e.

[13] Miccio F, Piriou B, Ruoppolo G, Chirone R. Biomass gasification in a catalytic fluidized reactor with beds of different materials. Chem Eng J 2009;154:369–74. doi:10.1016/j.cej.2009.04.002.

[14] Abdoulmoumine N, Adhikari S, Kulkarni A, Chattanathan S. A review on biomass gasification syngas cleanup. Appl Energy 2015;155:294–307. doi:10.1016/j.apenergy.2015.05.095.

[15] Corella J, Toledo JM, Padilla R. Olivine or dolomite as in-bed additive in biomass gasification with air in a fluidized bed: Which is better? Energy and Fuels 2004;18:713–20. doi:10.1021/ef0340918.

[16] Devi L, Ptasinski KJ, Janssen FJJG, Van Paasen SVB, Bergman PC a, Kiel JH a. Catalytic decomposition of biomass tars: Use of dolomite and untreated olivine. Renew Energy 2005;30:565–87. doi:10.1016/j.renene.2004.07.014.

[17] Rapagnà S, Jand N, Kiennemann a., Foscolo PU. Steam-gasification of biomass in a fluidised-bed of olivine particles. Biomass and Bioenergy 2000;19:187–97. doi:10.1016/S0961-9534(00)00031-3.

[18] Gröbl T, Walter H, Haider M. Biomass steam gasification for production of SNG - Process design and sensitivity analysis. Appl Energy 2012;97:451–61. doi:10.1016/j.apenergy.2012.01.038.

[19] Pinto F, André RN, Carolino C, Miranda M, Abelha P, Direito D, et al. Gasification improvement of a poor quality solid recovered fuel (SRF). Effect of using natural minerals and biomass wastes blends. Fuel 2014;117:1034–44. doi:10.1016/j.fuel.2013.10.015.

[20] Guan Y, Luo S, Liu S, Xiao B, Cai L. Steam catalytic gasification of municipal solid waste for producing tar-free fuel gas. Int J Hydrogen Energy 2009;34:9341–6. doi:10.1016/j.ijhydene.2009.09.050.

[21] Lee U, Chung JN, Ingley H a. High-temperature steam gasification of municipal solid waste, rubber, plastic and wood. Energy and Fuels 2014;28:4573–87. doi:10.1021/ef500713j.

[22] Galvagno S, Casu S, Casciaro G, Martino M, Russo A, Portofino S. Steam gasification of refuse-derived Fuel (RDF): Influence of process temperature on yield and product composition. Energy and Fuels 2006;20:2284–8. doi:10.1021/ef060239m.

[23] Recari J, Berrueco C, Abelló S, Montané D, Farriol X. Gasification of two solid recovered fuels (SRFs) in a lab-scale fluidized bed reactor: Influence of experimental conditions on process performance and release of HCl, H2S, HCN and NH3. Fuel Process Technol 2016;142:107–14. doi:10.1016/j.fuproc.2015.10.006.

[24] Montané D, Abelló S, Farriol X, Berrueco C. Volatilization characteristics of solid recovered fuels (SRFs). Fuel Process Technol 2013;113:90–6. doi:10.1016/j.fuproc.2013.03.026.

[25] Berrueco C, Recari J, Abelló S, Farriol X, Montané D. Experimental investigation of solid recovered fuel (SRF) gasification: Effect of temperature and equivalence ratio on process performance and release of minor contaminants. Energy & Fuels 2015;29:7419–27. doi:10.1021/acs.energyfuels.5b02032.

[26] Berrueco C, Recari J, Güell BM, Alamo G Del. Pressurized gasification of torrefied woody biomass in a lab scale fluidized bed. Energy 2014;70:68–78. doi:10.1016/j.energy.2014.03.087.

[27] Vassilev S V., Baxter D, Andersen LK, Vassileva CG. An overview of the composition and application of biomass ash. Fuel 2013;105:19–39. doi:10.1016/j.fuel.2012.10.001.

[28] He M, Hu Z, Xiao B, Li J, Guo X, Luo S, et al. Hydrogen-rich gas from catalytic steam gasification of municipal solid waste (MSW): Influence of catalyst and temperature on yield and product composition. Int J Hydrogen Energy 2009;34:195–203. doi:10.1016/j.ijhydene.2008.09.070.

[29] Mastellone ML, Zaccariello L. Metals flow analysis applied to the hydrogen production by catalytic gasification of plastics. Int J Hydrogen Energy 2013;38:3621–9. doi:10.1016/j.ijhydene.2012.12.111.

[30] Van Caneghem J, Brems A, Lievens P, Block C, Billen P, Vermeulen I, et al. Fluidized bed waste incinerators: Design, operational and environmental issues. Prog Energy Combust Sci 2012;38:551–82. doi:10.1016/j.pecs.2012.03.001.

[31] Berrueco C, Montané D, Matas Güell B, del Alamo G. Effect of temperature and dolomite on tar formation during gasification of torrefied biomass in a pressurized fluidized bed. Energy 2014;66:849–59. doi:10.1016/j.energy.2013.12.035.

[32] Font Palma C. Modelling of tar formation and evolution for biomass gasification: A review. Appl Energy 2013;111:129–41. doi:10.1016/j.apenergy.2013.04.082.

[33] Rapagnà S, Spinelli G. Biomass gasification with dolomite and olivine particles as a bed inventory in presence of catalytic ceramic filter. Chemical Engineering Transactions 2015;52:64100. doi:10.3303/CET1652049.

[34] Abu El-Rub Z, Bramer EA, Brem G. Experimental comparison of biomass chars with other catalysts for tar reduction. Fuel 2008;87:2243–52. doi:10.1016/j.fuel.2008.01.004.

[35] Huang Q, Tang Y, Wang S, Chi Y, Yan J. Effect of Cellulose and Polyvinyl Chloride Interactions on the Catalytic Cracking of Tar Contained in Syngas. Energy and Fuels 2016;30:4888–94. doi:10.1021/acs.energyfuels.6b00432.

[36] Chen H, Chen X, Qiao Z, Liu H. Release and transformation behavior of Cl during pyrolysis of torrefied rice straw. Fuel 2016;183:145–54. doi:10.1016/j.fuel.2016.06.031.

[37] Wu CH, Chang CY, Lin JP, Liang Y. Effects of hydrogen chloride on the pyrolysis of polyethylene: Pyrolysis kinetics. J Hazard Mater 1998;58:195–205. doi:10.1016/S0304-3894(97)00131-3.

[38] Tchapda AH, Pisupati S V. A review of thermal co-conversion of coal and biomass/waste. Energies 2014;7:1098–148. doi:10.3390/en7031098.

[39] Bläsing M, Nazeri K, Müller M. Release of alkali metal, sulphur and chlorine species during high-temperature gasification and co-gasification of hard coal, refinery residue, and petroleum coke. Fuel 2014;126:62–8. doi:10.1016/j.fuel.2014.02.042.

[40] Bläsing M, Zini M, Müller M. Influence of feedstock on the release of potassium, sodium, chlorine, sulfur, and phosphorus species during gasification of wood and biomass shells. Energy and Fuels 2013;27:1439–45. doi:10.1021/ef302093r.

[41] Leppälahti J, Simell P, Kurkela E. Catalytic conversion of nitrogen compounds in gasification gas. Fuel Process Technol 1991;29:43–56. doi:http://dx.doi.org/10.1016/0378-3820(91)90016-6.

[42] Pinto F, Lopes H, André RN, Gulyurtlu I, Cabrita I. Effect of catalysts in the quality of syngas and by-products obtained by co-gasification of coal and wastes. 1: Tars and nitrogen compounds abatement. Fuel 2008;87:1050–62. doi:10.1016/j.fuel.2007.06.014.

Chapter 6

7. GASIFICATION OF A TORREFIED SOLID RECOVERED FUEL (SRF)

Abstract

This work studies the torrefaction of a solid recovered fuel (SRF) and its effect on the fuel properties as gasification feedstock. The SRF (namely FL) was torrefied at two temperatures (290 ºC and 320 ºC) in a pilot auger reactor (capacity of up to 100 kg/h) and evaluated as fuel for gasification. This evaluation included the characterization of the obtained torrefied materials (FL290 and FL320) and several gasification tests in a bench-scale fluidized bed reactor. These tests were performed with different gasification agents (air and oxygen/steam) and bed materials (sand, dolomite and olivine) at similar experimental conditions (T=850 ºC and ER ~0.3). The evaluation of the gasification performance was presented in terms of product yields and gas composition together with the release of contaminants. Tar species and minor contaminants (H_2S, HCl, HCN and NH_3) were analysed by gas chromatography and ion-selective potentiometry, respectively. Additionally the process efficiency (gasification and its combination with torrefaction) was presented according to the energy content in the producer gas. The results indicated that the torrefaction process improved the SRF gasification parameters (lower tar, higher H_2/CO ratio, carbon conversion, etc.) and strongly affected the presence of HCl in the producer gas.

This chapter is based on the following research article:

Recari J, Berrueco C, Puy N, Alier S, Bartrolí J, Farriol X. Torrefaction of a solid recovered fuel (SRF) to improve the fuel properties for gasification processes. Appl Energy n.d. doi:Submitted to journal

7.1 Introduction

Municipal solid waste (MSW) is not only one of the main by-products of human society, but also a potential energy source that has attracted increasing attention over the years [1]. Among various waste-to-energy technologies, gasification is recognized as a promising method [1,2]. Gasification is usually defined as a partial oxidation of the fuel, which is treated in substoichiometric conditions, leading to the production of a syngas and a series of by-products. The potential benefits of gasification over traditional combustion of solid wastes are mainly related to the advantages of handling (and burning) a gas versus a solid waste [2]. In addition, gasification presents a high level of efficiency and the produced syngas can be used in different application, such as generation of electricity, fuels and chemicals.

At present, biomass is acting as the primary renewable source for gasification [3,4]. However, municipal solid waste (MSW) and related fractions (i.e. Solid Recovered Fuels, SRFs) have the potential to become an interesting alternative [5]. The high availability of waste and its continuous generation assures an almost inexhaustible source for thermal conversion routes as a way for energy recovery. However, waste gasification has still to overcome some problems related to gas quality and the release of contaminants. In this scenario, one possible route, scarcely explored with SRFs, is the use of thermal pretreatments such as torrefaction. These pretreatments have potential to improve the properties of biomass and SRFs making them better feedstocks for conversion into fuels and chemicals [6–9].

Biomass torrefaction involves heating the feedstock at temperatures between 200-300 ºC in inert atmosphere, resulting in a hydrophobic product with less moisture, which prevents the biomass from decomposing, and higher energy density for subsequent thermochemical applications [6,10,11].

Considering the energy efficiency, the overall efficiency of a process that combines torrefaction and gasification has been reported to improve or to be slightly lower than the direct biomass gasification [10,12], depending on the process configuration. Several strategies can be adopted, such as include the heat integration of the torrefaction and gasification processes [13] or reinject the volatiles produced in the torrefaction step downstream the gasification unit [12]. Biomass torrefaction also presents positive effects on the gasification process

from an operational point of view [6]. Various studies have reported lower storage and transportation costs, together with increasing syngas yields and lower tar levels and acid contents [6,8,14,15] when comparing gasification of torrefied and original biomasses.

Nevertheless, the mentioned advantages of torrefaction may differ for a highly heterogeneous material as waste, composed by different sorts of residues: plastic, paper, cardboard, food waste, glass, etc. As observed with biomass, it is important to explore this route with waste fractions as it can lead to a more homogenous material and attenuate the release of pollutants during the energy valorization of the torrefied materials.

Few investigations have addressed waste torrefaction, such waste from food, kitchen and agricultural waste [11,16–21]. Yuan et al. [19] studied the properties of MSW samples torrefied at various temperatures (250-450 ºC). They concluded that in the temperature range of 250-350 ºC the calorific values were higher and chlorine contents decreased in the torrefied MSW. Another work by Poudel et al. [16] investigated the effects of torrefaction temperature and time on food waste, concluding that 290-330 ºC was the optimum torrefaction region due to a high energy yield (> 90%) and high heating value (which increased > 10%). Manatura et al. [21] presented an exergetic evaluation of the gasification process of torrefied rice husk, an agricultural waste. The reported results depicted the contradictory effects of torrefaction on the gasification efficiency. On the one hand the increase of chemical energy (exergy) of syngas due to lower O/C and H/C in the torrefied material led to higher exergy efficiencies. On the other hand, the release of volatiles during torrefaction, more pronounced at higher torrefaction temperatures, provoked a decrease in overall efficiency. The authors reported that this adverse effect became dominant at a torrefaction temperature of 350 ºC, whereas a torrefaction temperature close to 250 ºC improved the biomass properties and resulted in enhanced gasification performance and energy efficiency. In contrast to gasification of torrefied biomass or torrefied agricultural waste, there is no published data of torrefied MSW as gasification feedstock.

This work studies the torrefaction of a solid recovered fuel (SRF) and its effect on the fuel properties as gasification feedstock. The evaluated SRF was a fluff material (referred as FL) with high moisture (> 8%) and chlorine content

(0.6%). In order to upgrade its properties as fuel, the FL sample was torrefied at two temperatures (290 and 320 ºC) in a pilot auger reactor. The assessment of the torrefied materials as gasification feedstock was carried out through the materials characterization and a series of gasification tests. Gasification experiments were carried out in a laboratory scale fluidized bed reactor at fixed operation conditions (gasification temperature of 850 ºC and equivalence ratio of 0.3) but varying the fluidizing agent (air or a mixture of oxygen/steam) and the bed material (sand, dolomite or olivine). The evaluation of the influence of torrefaction on the gasification performance was one of the key aspects of the work, focusing on the evolution of main compounds (H_2, CO, CO_2, CH_4…) and minor contaminants (tar, H_2S, HCl, HCN and NH_3) in the producer gas.

7.2 Experimental

7.2.1 SRF sample preparation and characterization

The studied SRF was a fluff material (namely FL) provided by a local waste management company. FL was obtained from a mechanical process of mixed domestic waste streams, composed by diverse fractions of paper, biomass and polymers (post-consumer plastics and textiles). More details about this fuel can be found elsewhere [22,23]. This SRF was subjected to a torrefaction pretreatment (see section 7.2.2) in order to obtain two torrefied batches (referred as FL290 and FL320) to be used as gasification feedstock. The parent SRF was grounded and sieved to a particle size of 8 mm for the torrefaction process and then all samples were milled to 1 mm for characterization and gasification purposes. A list of the main techniques and equipments used is shown as follows:

- Proximate analysis in a LECO Thermogravimetric (TGA 701), according to EN-15402:2011 and EN-15403:2011 standard methods.
- Ultimate analysis in a LECO TruSpec CHN-S analyser following the EN-15407:2011.
- Heating value conducted in a LECO calorimeter (AC-600) according to the EN- 15400:2011 standard method.
- Halogens (Cl, F and Br) content analysed by ionic chromatography (Dionex ICS-1100) following the EN- 15408:2011 standard method.

- Ash composition determined in Spectro Arcos 165 spectrophotometer after ash samples digestion in a microwave system (Berghof Speedwave 4), according to the EN-15410:2006 and EN-15411:2006 standard methods.

Table 7.1 presents the characterization results. Each analysis was performed by triplicate with uncertainties estimated at a 95% probability level.

Table 7.1 Characterization and torrefaction yields of studied samples (as received basis)

		FL	FL290	FL320
Torrefaction yield (g/100g SRF fed)		100	90.9	83.5
Proximate analysis (wt.%)	**Moisture**	8.39±0.41	0.91±0.14	1.12±0.10
	Volatiles	72.58±0.86	74.10±0.67	71.47±0.05
	Fixed carbon	5.78±0.44	10.42±0.28	11.55±0.24
	Ash	13.24±1.01	14.57±0.33	15.86±0.17
Ultimate analysis (wt.%)	**C**	46.03±0.54	57.55±0.90	53.68±0.53
	H	7.49±0.02	7.07±0.15	6.55±0.07
	O (by difference)	31.71±0.55	19.31±0.92	22.28±0.54
	N	0.66±0.06	0.75±0.06	0.85±0.01
	S	0.26±0.01	0.31±0.02	0.27±0.02
	F	< 0.02	< 0.02	< 0.02
	Cl	0.59±0.06	0.42±0.04	0.49±0.04
LHV (MJ/kg)		23.29±0.22	25.44±0.38	23.06±0.18
Ash composition (mg/kg_{fuel})	**Aluminium as Al_2O_3**	30754±584	30802 ± 556	33659 ± 1226
	Calcium as CaO	39541±539	40107 ± 1214	43436 ± 2041
	Chrome as Cr	143±20	205 ± 23	192 ± 8
	Iron as Fe_2O_3	4094±214	4586 ± 102	7699 ± 443
	Lead as Pb	642±17	520 ± 23	733 ± 21
	Magnesium as MgO	4319±573	4667 ± 122	4947 ± 236
	Manganese as MnO	241±8	275 ± 5	277 ± 8
	Nickel as Ni	87±7	120 ± 11	119 ± 2
	Phosphorus as P_2O_5	13385±541	13709 ± 583	15272 ± 554
	Potassium as K_2O	2162±126	2498 ± 272	2708 ± 44
	Silicon as SiO_2	20262±837	24780 ± 620	25585 ± 128
	Sodium as Na_2O	4104±183	4299 ± 72	4750 ± 70
	Titanium as TiO_2	2436±357	3347 ± 211	3637 ± 170
	Vanadium as V	< 50	< 50	< 50
	Zinc as Zn	631±80	669 ± 21	670 ± 23

7.2.2 Torrefaction process

The FL sample was torrefied at two final temperatures (290 and 320 ºC) using a pilot auger reactor. The torrefaction and pyrolysis pilot plant comprises six main parts: the feeding system, a drying reactor, the torrefaction reactor, a cooling screw, the vessel for solids collection and the condensing system (see Figure 7.1). The drying and torrefaction reactors, together with the cooling screw, consisted in a horizontal pipe (i.d.:160 mm) with a screw conveyor that allowed a precise control of residence time of the different stages (varying the conveyor rotation speed). The drying and torrefaction reactors were temperature controlled using electrical heating elements whereas the last conveyor was cooled using a water jacket. Drying and cooling conveyors had a length of 3000 mm and the torrefaction reactor was 4000 mm long. The reactor, capable of operating at temperature of up to 600 ºC, had a capacity up to 100 kg/h of biomass and/or wastes in size range of 1-10 mm.

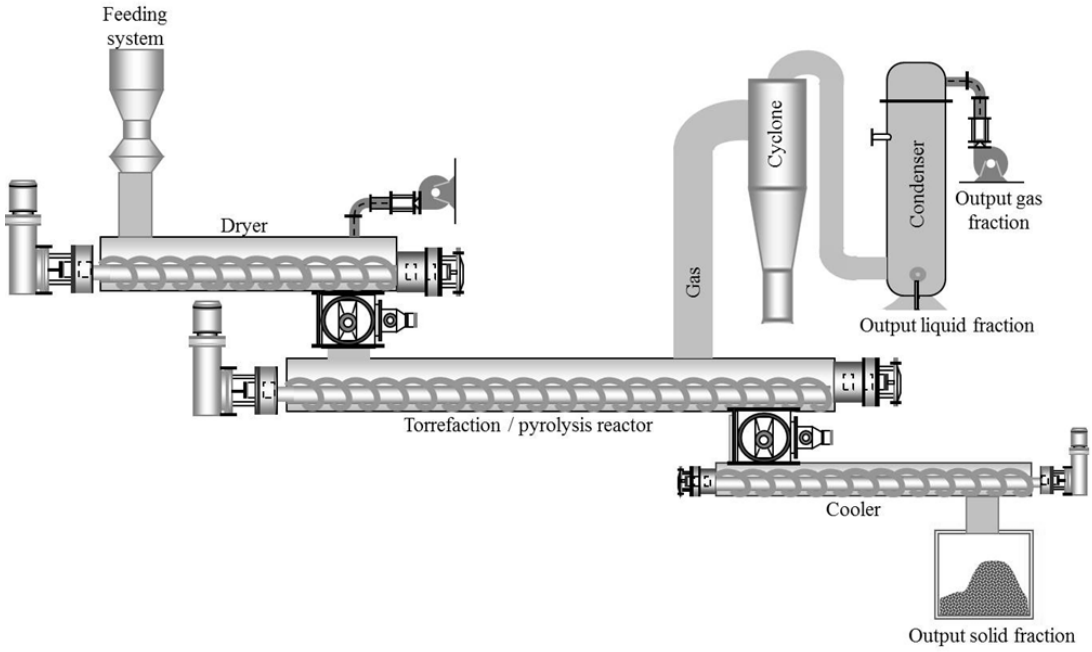

Figure 7.1 Scheme of torrefaction process

The SRF was fed into the feeding system, moved along the drying reactor and followed to the torrefaction reactor where the conversion took place. The solid fraction was collected after exiting through a cooling screw. The gas fraction was led to the cyclone to remove particles and followed to a condenser, where the condensable gas was collected as liquid fraction.

In order to ensure inert conditions and remove the volatiles, each part of the reactor was purged with a nitrogen flow of about 8 NL/min. Feeder and screws were driven by individual motors allowing for basically independent setting of mass flow (feeder setting) and residence time (screw setting). Notice that the material was transferred between conveyors using rotary valves.

The process was carried out continuously, with a total mass flow rate of about 13 kg/h, and a torrefaction residence time of about 15 min in all the cases. A drying temperature of 125 ºC was applied, whereas the final torrefaction temperature varied from 290 to 320 ºC for the different tests. Apart from the temperature control system, temperature profiles along the different conveyors were measured and recorded using several thermocouples.

7.2.3 Gasification setup and procedure

The fluidized bed gasifier (PID ENG&Tech, Spain) consisted in a Hastelloy X reactor (450 mm long and 23.8 mm internal diameter) externally heated by an electrical furnace. The experimental rig was equipped with a control system (gas flow, feeding system, temperature and pressure) and was able to operate up to 900 ºC and 20 bar.

The experiments were conducted at a gasification temperature of 850 ºC and atmospheric pressure. Two gasification agents were tested (air and oxygen/steam) maintaining an equivalence ratio (ER) around 0.3 and employing three bed materials. ER is defined as the moles of oxygen available for gasification divided by the total moles of oxygen required for stoichiometric combustion. The selection of the conditions for the gasification process was based in our previous works of SRF gasification, evaluating the effect of the gasification parameters on the process performance, and the usual conditions in commercial fluidized bed gasifiers [23]. The temperature level (850 ºC) was selected to promote steam reforming and steam gasification reactions (especially under O_2/H_2O conditions).

The operation flows, 795 NmL/min of air and ~200 NmL/min of O_2 and 0.4 mL/min of $H2O_{(l)}$ in the case of air and oxygen/steam experiments respectively, provided afluidizing gas velocity five to six times the minimum fluidization velocity (U_{mf}), corresponding to gas residence time in the reactor of between 2-3 s.

The tested bed materials included quartz sand (J.T.Baker), dolomite (Productos Dolomíticos de Málaga S.A.) and olivine (Sibelco Hispania); all sieved to particle size range of 150-200 μm and calcined in a furnace at 900 ºC for 4 hours. The sample (FL290 or FL320) was placed in the hopper and introduced continuously into the reactor through a screw feeder at rates from 0.40 to 0.47 g/min.

The producer gas was cleaned prior to gas analysis by passing through a hot filter to remove particulates and a condenser system (Peltier and ice tar trap) to collect liquids and tar products. A Tedlar® gas bag was used to collect a fraction of the gas for the minor contaminants assessment whereas the rest was analysed in an on-line micro gas chromatograph. Overall mass and carbon balances of conducted tests closed higher than 95 %. Further details of the experimental setup and procedure can be found in previous studies [15,22,23].

7.2.4 Gas, tar and minor contaminants analyses

Syngas composition (H_2, O_2, N_2, CO, CO_2, CH_4 and hydrocarbons up to C_5) was analysed using a micro GC (Agilent 490) whereas the determination of contaminants (tar compounds and minor contaminants) followed different techniques. The quantification of polyaromatic hydrocarbons of the tar samples was carried out in a Hewlett Packard 6850 GC-FID (gas chromatograph with a flame ionization detector). The column configuration and methodology is described in a previous work [24].

Minor contaminants (HCl, H_2S, HCN and NH_3) were quantified by potentiometry through ion-selective electrodes (ISEs, Metrohm). For the assessment of these inorganic traces, a fraction of the gas was collected in a Tedlar® gas bag and afterwards it was pumped into a series of impingers filled with solutions to retain specific ions (Cl^-, S_2^-, CN^-, and NH_4^+). The aqueous solutions were analysed by ISEs. Additionally, in steam gasification experiments the condenser liquids were also analysed. All solutions were conditioned (adjusting ionic strength and pH) prior the ion determination on a 905 Titrando (Metrohm). A detailed procedure was described elsewhere [22,23].

7.3 Results and discussion

7.3.1 Characterization of raw and torrefied samples

Table 7.1 gathers the characterization results of the raw FL and torrefied samples (FL290 and FL320), together with the mass yield of the torrefaction process under the studied conditions.

The parent material (FL) contained a moisture level of 8.4%, which predictably enough, decreased after torrefaction at 290 and 320 ºC up to ~1%. As well, during torrefaction there was a change in volatiles levels with an initial increase at 290 ºC from 72% to 74% followed by a decrease at 320 ºC (71%). This variation in dry basis corresponded to a loss of volatiles from 79% for raw FL to 75% and 72% for FL290 and FL320, respectively. The content of ashes remained ca. 15%, observing a slight and steady augment as torrefaction level increased. Fixed carbon content rose from 5.8% to 10.4-11.6% with the increase of torrefaction temperature. This increment of fixed carbon can also be related to the increase of carbon content in the sample. The ultimate analysis reflects that C content raised 1.25 times up to 57.6% for FL290. On the other hand, the loss of moisture and some oxygenated volatiles provoked a steep decrease of oxygen, ranging between 19.3-22.3% for the torrefied samples versus the 31.7% of FL. H scarcely decreased from 7.5% to 7.0% and 6.6% for FL290 and FL320, respectively. The content of minor components also changed with torrefaction. N rose by 14-22% with the torrefaction severity, however Cl decreased from 0.6% to < 0.5%. Regarding the percentage of S, this parameter slightly oscillated around 0.3% in both torrefied samples. The calorific content improved only in the torrefied sample at 290 ºC, i.e. the sample with higher carbon content and less moisture. Apparently, higher temperatures provoked a substantial loss of volatiles and a consequent increase of ash content, affecting the calorific content of the sample. Regarding ash composition, the major compounds detected were aluminium, calcium, phosphorous and silicon. In general, the compounds concentration seemed to increase with the torrefaction temperature but taking into account the levels of ashes, some elements were preferentially released during the torrefaction pretreatment (i.e. calcium, lead, etc.) whereas others slightly increased (i.e. silicon, potassium, etc.).

7.3.2 Gasification tests

7.3.2.1 Product yields

Table 7.2 presents the product yields of the gasification experiments in terms of gas, tar and char. The sum of the yields is above 100% as the oxygen introduced with the gasification agent (air and oxygen/steam) reacts with the feedstock to form compounds as CO and CO_2 during gasification.

Table 7.2 Product yields of torrefied SRFs gasification experiments. (T= 850 ºC and Steam/SRF ~ 1)

SRF	Gasification agent	ER	Bed material	Yield (g/100 g dry SRF)		
				Gas	Tar	Char*
FL290	Air	0.29	Sand	104.5±0.8	7.9±0.3	3.9±0.1
FL290	Air	0.31	Dolomite	110.8±0.8	3.5±0.1	5.3±0.2
FL320	Air	0.29	Sand	96.9±0.7	5.7±0.2	6.4±0.2
FL320	Air	0.29	Dolomite	99.5±0.7	3.0±0.1	7.2±0.2
FL290	O_2/H_2O	0.32	Sand	132.6±1.3	3.3±0.7	3.7±0.6
FL290	O_2/H_2O	0.32	Dolomite	138.7±1.4	2.0±0.4	2.5±0.4
FL320	O_2/H_2O	0.30	Sand	127.9±1.0	3.1±0.6	5.9±1.0
FL320	O_2/H_2O	0.31	Dolomite	133.5±1.0	1.5±0.3	4.2±0.7
FL320	O_2/H_2O	0.31	Olivine	130.3±1.0	2.9±0.6	1.0±0.2

* Residual char given in ash free basis. Ash content ~ 14.70 g/100g dry FL290 and ~ 16.04 g/100g dry FL320.

Considering the results from air gasification tests with sand, both torrefied feedstocks showed similar gas yields ranging from 96.9%-110.8% but slightly lower gas levels for the material torrefied at the highest temperature. FL320 also yielded lower tar and higher char than FL290, which is consistent with the proximate analysis results (lower volatiles and higher fixed carbon content). The use of dolomite as bed material exhibited a positive effect on the gasification performance. There was a significant reduction of all tar yields (2 times lower than with sand) due to the promotion of tar cracking and polymerization reactions, leading to a slight increase of gas and char yields.

The use of O_2/H_2O as gasification agent resulted in an increase of gas yields ranging between 127.9-138.7% whereas tar results were similar to those obtained with air and dolomite (~ 3%). The presence of oxygen and steam in

the gasification media promoted a general decrease of char due to char combustion and steam gasification reactions. In addition, the replacement of sand with catalyst (dolomite or olivine) in the bed also improved the gasification (gas yields above 130% and the lowest tar and char yields). Comparing the catalytic activity of both dolomite and olivine, dolomite decreased significantly tar yield, however olivine reported similar tar yields as those obtained with sand as bed material. This lower efficiency of olivine for tar depletion, in comparison to dolomite, was recently reported in a previous work [25]. In that paper the effect of both catalysts was studied under oxygen/steam gasification of two SRFs.

7.3.2.2 Gas composition

This section discusses the evolution of the gas composition produced from gasification of two torrefied SRFs (FL290 and FL320) at a gasification temperature of 850 ºC and ER ~0.3. Sand or catalyst (dolomite, olivine) were used as bed material and air or oxygen/steam as gasification agent. Figures 7.2 and 7.3 plot the main components of the producer gas with different gasification mediums (air and oxygen/steam, respectively).

Both feedstocks produced a similar gas composition (Figure 7.2), under air gasification conditions and sand as bed material. However, the most torrefied fuel presented a slightly better gas quality, with higher volumetric composition (% vol.) of H_2 than the obtained with FL290 (8.5% for FL320 and 7.9% for FL290). On the other hand, the concentration of CO with FL290 was 9.3% compared to the 8.5% of FL320. These variations in the main gas compounds resulted in the H_2/CO and CO/CO_2 ratios displayed in Table 7.3. H_2/CO ratios were 0.85 for FL290 and 0.99 for FL320 whereas CO/CO_2 ratios were 0.80 and 0.69, respectively. The reported H_2/CO increase with torrefaction level is consistent with the results presented in previous studies of gasification of torrefied biomass [8,26,27]. This effect can be related to the reduction of oxygenated volatiles during the torrefaction process (that would rapidly evolve towards CO), and the formation of a slightly less reactive char, declining the effect of char steam reforming towards CO and H_2. Additionally, in the case of SRFs, the reactions of pyrolysis of polymers are also relevant, leading to the formation of H_2 as final product [28].

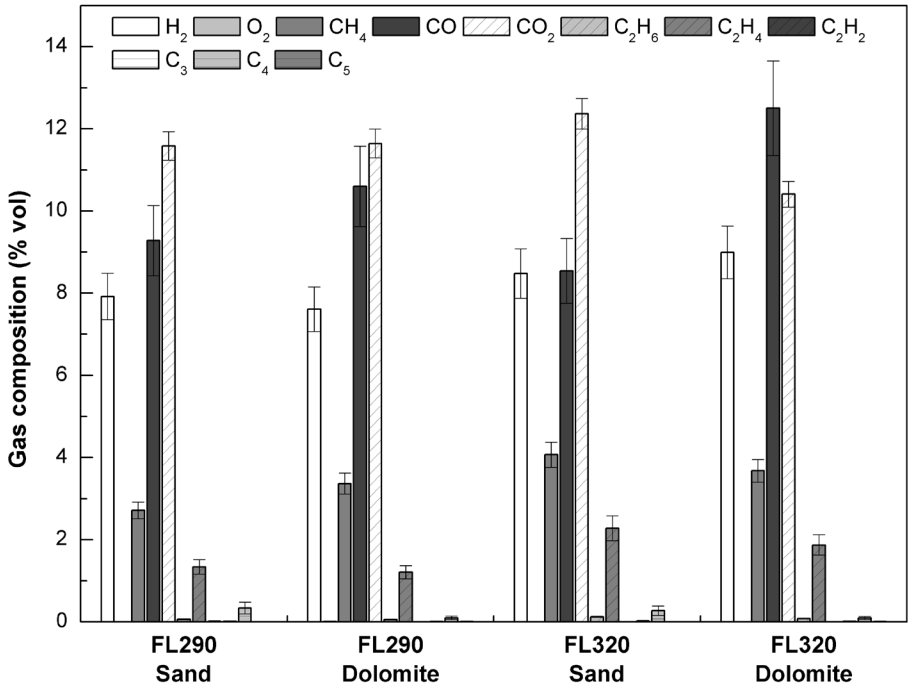

Figure 7.2 Gas composition (dry basis) in air gasification experiments (T= 850 ºC, ER ~0.3)

Other evaluated parameters were carbon conversion and gas heating value (Table 7.3). The higher levels of hydrocarbons (CH_4, C_2H_4, C_2H_6...) present in the gas produced from FL320 gasification resulted not only in a higher gas calorific value in contrast to FL290 (~5 versus ~4 MJ/Nm^3, respectively) but also in a higher carbon conversion (69.1 and 66.5%, respectively). The substitution of sand by dolomite resulted in different trends in the gas compositions but a similar response on the overall gasification performance. Both fuels exhibited a drop of H_2/CO ratio (to values close to 0.7) and an increase of CO/CO_2 mainly due to the rise of CO concentration (to a greater extent for FL320). The presence of calcined dolomite might have promoted char gasification reactions (Boudouard and water gas) leading to an increase of CO [29]. As well hydrocarbons (CH_4, C_2H_4, C_2H_6 and higher) presented a marked decrease attributed to the enhancement of cracking reactions. Despite the reduction of olefins with high heating value, the gas LHV remained almost constant and carbon conversion increased by 5%.

Figure 7.3 shows the results of gas composition of the experiments performed with oxygen/steam as gasification agent. Compared to Figure 7.2, the concentration of the main gas compounds increased due to the absence of N_2

from air in the producer gas. In air gasification experiments, N_2 accounted for about 60% of the volumetric composition meanwhile in O_2/H_2O tests, it was lower than 10%. This percentage of nitrogen stem from a small inlet of N_2 (50 NmL/min) in the hopper to facilitate the continuous feeding. Furthermore, the use of pure oxygen and steam enhanced the production of H_2 associated to steam reforming, water gas and shift reactions [30].

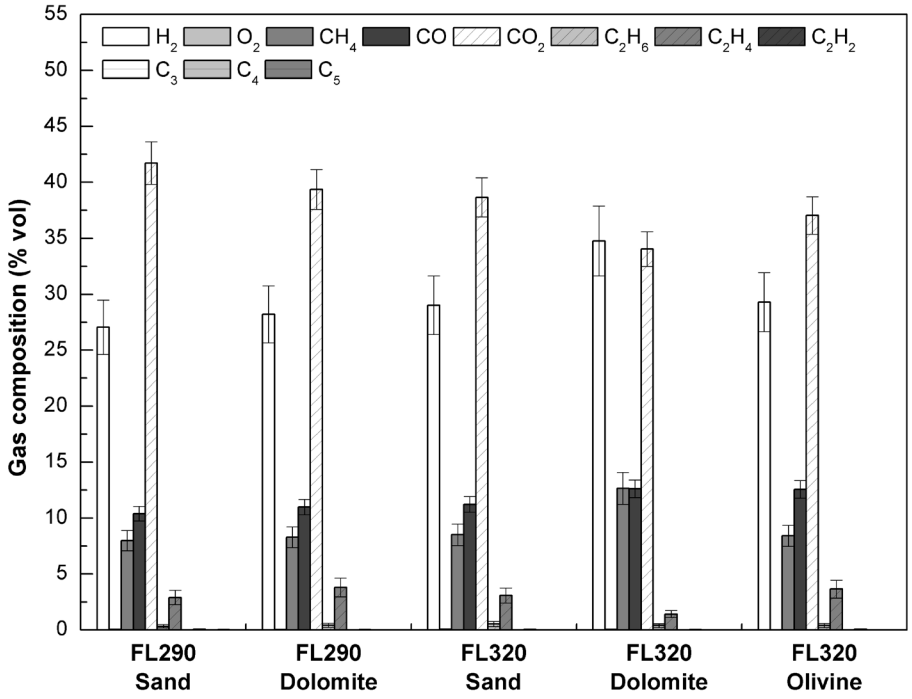

Figure 7.3 Gas composition (dry basis) in oxygen/steam gasification experiments (T= 850 ºC, ER ~0.3 and Steam/SRF ~ 1)

In comparison to air gasification results, H_2/CO ratio rose above 2.0, CO/CO_2 ratio ranged between 0.2-0.4 and LHV levels were doubled. The obtained results were also useful to assess the effect of varying the bed material (sand or catalyst). In general, the combination of catalyst and steam reinforced tar cracking and steam tar reforming reactions, which consumed the heaviest hydrocarbons to produce lighter hydrocarbons such as C_2 and CH_4. Hydrogen and carbon monoxide rose and CO_2 concentration diminished when dolomite was used as bed material. The small changes observed in CO and CO_2 percentages in the case of FL290, might be linked to a slight higher equivalence ratio (i.e. larger degree of oxidation) in this test. Among all evaluated conditions, gasification of FL320 with dolomite led to the most satisfactory

conditions. H_2/CO ratio was around 2.8, the gas calorific value reached a value about 11.0 MJ/Nm^3 and carbon conversion was close to 85%. These results corroborated the positive effect of combining torrefaction and gasification using dolomite as bed material. The effect of an additional bed material was tested using olivine, a common bed material in biomass gasification processes. The use of calcined olivine as bed material hardly raised H_2 and CO concentrations nor barely reduced tar content in comparison to sand tests. The values of gas LHV and carbon conversion were in between the results obtained with sand and dolomite.

Summarizing, the producer gas from FL320 presented higher calorific content and lower tar levels than FL290 both with air and oxygen/steam as gasification agents. These results were enhanced with the use of catalyst, especially with dolomite.

7.3.2.3 Tar characterization

Tar content: Tar content results (Table 7.3) are in agreement with the evolution of the discussed tar yields. In air gasification experiments with sand as bed material, tar concentration in the dry producer gas ranged between 25-30 g/Nm^3, however it experienced a drastic decrease of 50 % with dolomite in the bed. The obtained values under these conditions (around 13 g/Nm^3) are similar to other air gasification tests with SRFs [22,23,31–33] and closer to those obtained in biomass gasification [34,35]. Even though when comparing air experiments to those with O_2/H_2O could seem that the implementation of O_2/H_2O as gasification agent barely reduced tar content, in this case it is convenient to express the content in N_2 free basis (note that N_2 represents about 60% of gas composition in air experiments). As an example of N_2 diluting effect, the tar content of the syngas obtained with FL320 decreased from 34 g/Nm^3 (with dolomite and air) to 11.3 g/Nm^3 (dolomite and O_2/H_2O) when expressed in N_2 free basis. Besides, among the two torrefied SRFs, the syngas produced with FL320 showed the lowest tar concentration (10.9 g/Nm^3 or 11.3 g/Nm^3 inert free basis).

Table 7.3 Gasification parameters of experiments. (T= 850 ºC and Steam/SRF ~ 1)

SRF	Gasification agent	Bed material	H_2/CO	CO/CO_2	Gas LHV (MJ/Nm³ dry)	Xc	Tar content (g/Nm³ dry)	Tar content (g/Nm³ dry N_2 free)
FL 290	Air	Sand	0.85±0.04	0.80±0.12	4.08±0.10	66.5±1.8	29.61±1.65	89.49±4.98
FL 290	Air	Dolomite	0.72±0.03	0.91±0.14	4.21±0.10	70.8±1.9	13.07±0.73	37.84±2.11
FL 320	Air	Sand	0.99±0.04	0.69±0.11	5.09±0.13	69.0±1.9	24.65±1.37	68.46±3.81
FL 320	Air	Dolomite	0.72±0.03	1.20±0.19	5.14±0.13	71.6±1.9	12.79±0.71	34.01±1.89
FL 290	O2/H2O	Sand	2.60±0.07	0.25±0.03	9.18±0.75	76.0±1.7	26.33±4.27	29.09±4.72
FL 290	O2/H2O	Dolomite	2.57±0.07	0.28±0.03	9.95±0.82	81.8±1.9	14.84±2.41	16.29±2.64
FL 320	O2/H2O	Sand	2.58±0.07	0.29±0.03	9.83±0.81	80.1±1.8	24.36±3.95	26.74±4.34
FL 320	O2/H2O	Dolomite	2.75±0.08	0.37±0.04	10.99±0.90	85.1±1.9	10.88±1.76	11.34±1.84
FL 320	O2/H2O	Olivine	2.33±0.06	0.34±0.04	10.25±0.84	83.1±1.9	22.20±3.60	24.28±3.94

Additionally, olivine was tested as bed material only for FL320 gasification under oxygen/steam conditions. However, in line with a previous work [25], olivine just decreased tar content by 9% in comparison with sand (from 24.4 to 22.2 g/Nm^3). Therefore, tar and gas composition results reinforced the argument that dolomite might be a suitable catalyst for this type of fuels and gasification conditions.

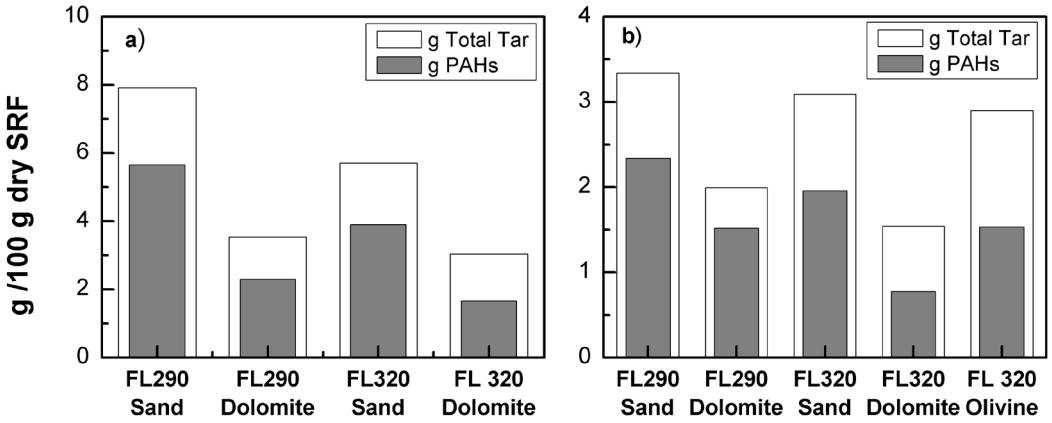

Figure 7.4 Total tar and PAHs yields in: a) air and b) oxygen/steam gasification experiments. (T=850 ºC, ER ~0.3 and Steam/SRF ~ 1)

GC-FID analysis: The characterization of tar samples was carried out in a GC with flame ionization detector (GC-FID) to determine the presence of polynuclear aromatic hydrocarbons (PAHs). A standard of 16 PAHs (EPA 610 PAH Mix) was used for the identification of these hydrocarbons. Three additional compounds (1- and 2-menthylnaphtalene, and biphenyl) were also identified and quantified [25].

Figure 7.4 compares the total amount of tar and PAHs produced by 100 g dry FL (torrefied at 290 and 320 ºC) during gasification experiments under different gasification agents and bed materials. As previously commented, tar yields were higher when air was used as gasification agent in comparison with oxygen/steam experiments. This fact may be attributed to a higher extent of tar cracking reactions with steam and the higher reactivity of oxygen. Similarly to the results observed for torrefied biomass [8,15], a greater degree of torrefaction in FL samples showed lower tar production. Therefore, torrefaction level favoured tar depletion. Despite the observed decrease on tar yield, PAH compounds represented on average the 65% of total tar for both torrefied

materials. When dolomite was used as bed material, tar yields decreased by 50% and PAHs yields by 60%.

Figures 7.5 and 7.6 plot the yield of the studied PAHs on tars obtained from air and oxygen/steam gasification experiments, respectively. In all cases, naphthalene, acenaphtylene and phenanthrene were the three main PAH compounds, and among them naphthalene was the dominant aromatic compound. The increase of the torrefaction level led to a clear decrease of naphthalene together with a reduction, to a lesser degree, of the other PAH species, for both studied gasification agents.

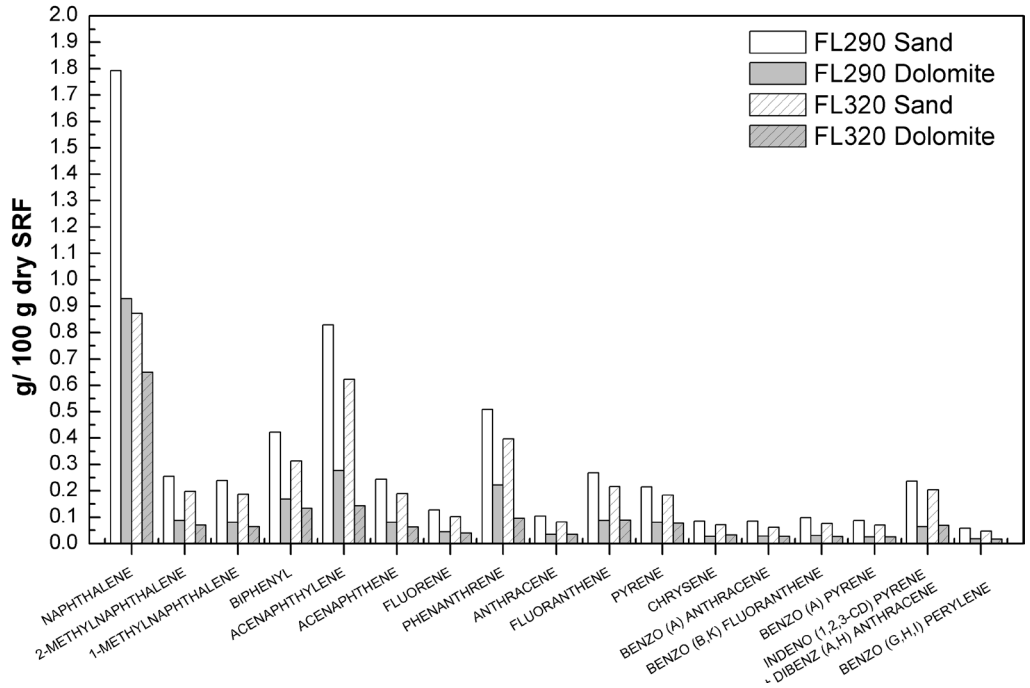

Figure 7.5 Tar composition of FL290 and FL320 air gasification experiments (T=850 ºC, ER 0.3 and bed materials: sand and dolomite)

The substitution of bed material from sand to dolomite also presented a positive effect on tar depletion. There was a substantial decrease of tar compounds with this catalyst; practically all tar species halved their yield. These trends were similar for both gasification agents, although dolomite seemed more active for tar cracking under steam rather than under air gasification conditions [36]. An additional test to evaluate the effect of another mineral catalyst (calcined olivine) with FL320 was performed. The use of olivine reduced PAHs but could not reach the levels obtained with dolomite, in

particular with the main PAHs compounds (naphthalene, acenaphtylene and phenanthrene). This lower efficiency of olivine on tar cracking was also reported in other works with waste-derived fuels and biomass [25,37] under similar gasification conditions. It is also worth mentioning that in that previous study [25], oxygen/steam gasification of raw FL produced larger amounts of tars (> 60 g/Nm^3) than the torrefied feedstocks (< 30 g/Nm^3).

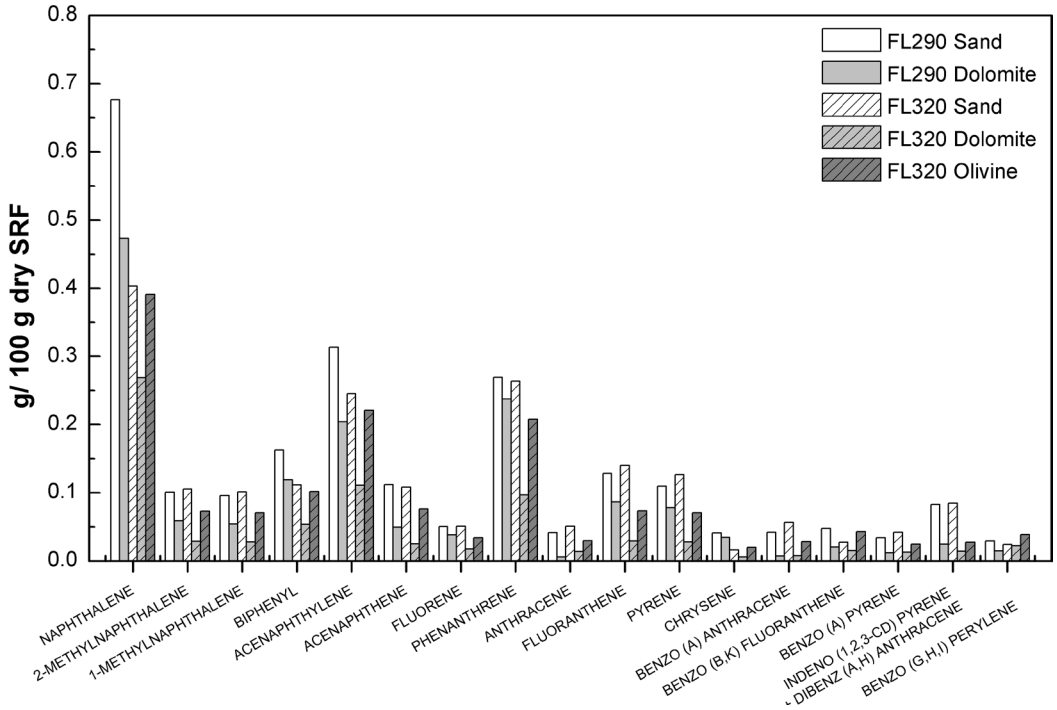

Figure 7.6 Tar composition of FL290 and FL320 oxygen/steam gasification experiments (T= 850 ºC, ER ~0.3, bed materials: sand, dolomite and olivine)

7.3.2.4 Minor contaminants

This section presents the evolution of the concentration of minor contaminants in the producer gas from gasification experiments with torrefied FL (FL290 and FL320), two gasification agents (air and oxygen/steam) and different bed materials (sand, dolomite or olivine) Additionally, previous results obtained with the parent FL [23,25], have been included to facilitate the discussion. The studied minor contaminants determined through ISEs were hydrogen chloride (HCl), hydrogen sulphide (H_2S), hydrogen cyanide (HCN) and ammonia (NH_3).

Air gasification experiments: Figure 7.7 displays the minor contaminants concentration produced in air gasification of FL [23], FL290 and FL320 tests with two bed materials (sand and dolomite). In contrast to previous air gasification experiments with raw FL under similar conditions (T=850 ºC and ER 0.3) [23] there was a steep diminishment on HCl release after the torrefaction pretreatment, especially at 290 ºC (< 50 mg/Nm³). This fact indicates a relevant positive effect of torrefaction (discussed in more detail in the next section).

Comparing both torrefied fuels, HCN and H_2S were the dominant minor contaminants released in the gas. The gasification experiments performed with FL320 showed higher concentration of all contaminants even when dolomite was used as bed material. This fact can be connected to the higher level of tar cracking for the most torrefied material. The heteroatoms (S and N) contained in the tar compounds could evolve towards HCN, NH_3 or H_2S, when tar cracking is more severe [23].

The influence of dolomite on contaminants release was more relevant in some cases depending on the level of torrefaction, but in general the reduction of contaminants followed equivalent trends. HCN levels decreased from ca. 1350 mg/Nm³ to 450 mg/Nm³ on FL290 gasification, whilst the decrease with FL320 was much less remarkable (from 1635 to 1510 mg/Nm³). The presence of metals like Fe and alkaline earth metals (Mg) in dolomite may catalyse N-fuel conversion ending up with lower HCN concentration [22,23].

The emissions of HCl with FL320 was higher than with FL290, this can be related to the larger amount of aluminium (Al) and silicon (Si) in ashes from FL320. The mentioned compounds may react with alkali chlorides (i.e. KCl) to form HCl [38]. In addition, it should be noted that the concentration of elemental chlorine (in mass percentage) was slightly higher in this feedstock.

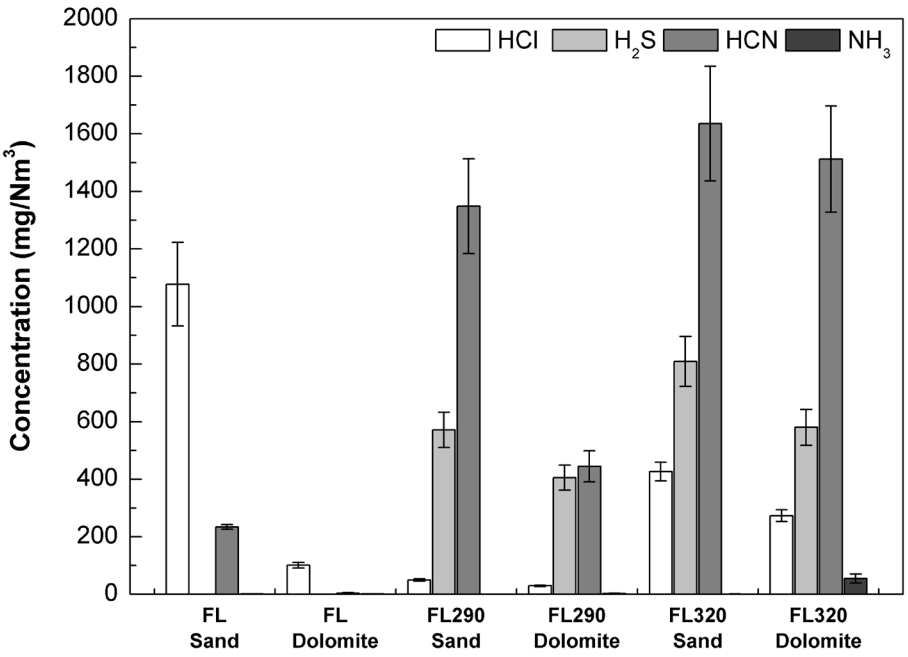

Figure 7.7 Minor contaminants in air gasification experiments (T=850 C and ER~0.3). Data for FL experiments from [16]

In addition, use of dolomite seemed to slightly favour the production of ammonia. NH_3 was hardly produced (< 1 mg/Nm^3) in the experiments performed with sand but increased on those with dolomite (3 and 55 mg/Nm^3 for FL290 and FL320, respectively). This effect might be related to the decrease of HCN, as dolomite may favour the release of the fuel-N, forming preferentially NH_3 [39] instead of HCN.

Moreover, this study shows an important increase of H_2S in the gas from torrefied samples in comparison to the original feedstock where hydrogen sulphide was scarcely detected. The mechanisms of release of sulphur species are complex and can influenced by many factors, for instance by the presence of inorganic sulphates or other elements in the fuel ash [40,41]. The release of H_2S has been reported to be highly dependent on the affinity between potassium and sulphur, however the competition with Cl and Si at temperatures above 700 ºC may prevent the formation of K_2S in solid phase and therefore favour H_2S release [40]. The lower levels of the Ca/Si ratio of the torrefied samples in comparison to the parent SRF may partially explain the observed results. Other plausible explanation is the evolution of the chlorine derived from the dechlorination of PVC. Part of the released Cl could have reacted with the Ca and K of the fuel ash, making these compounds unavailable for sulphur, leading

to the release of H_2S. Another fact that supports the hypothesis of the reaction of the released Cl during torrefaction with the SRF ash compounds, is the drop in HCl concentration when dolomite is used as bed material, due to the larger amounts of Ca and Mg available in the dolomite bed. This reduction was about 36-40% for both torrefied materials. The utilization of dolomite reduced H_2S concentration by 30% for both FL290 and FL320 (final values of 405 and 580 mg/Nm^3, respectively). The results of H_2S diminishment are similar to those presented by Pinto et al. [32], and can be related to the presence of Ca available in the bed, which favours the formation of CaS that would probably remain in the ashes [22,23].

Oxygen/steam gasification experiments: Figure 7.8 plots the contaminants concentration produced in oxygen/steam gasification of raw FL and torrefied samples at equivalent experimental conditions (T=850 ºC, ER 0.3). In this case an additional bed material (olivine) was tested with the FL320 sample. The contaminants released in higher level were HCN and NH_3 for both torrefied samples. Contaminants concentration increased with tar cracking, especially increasing NH_3 and decreasing HCN concentration.

Concerning the experiments with sand, HCN was the major contaminant released with concentration values around 2200 mg/Nm^3 for FL290 and the double for FL320. As observed in air gasification experiments (Figure 7.7), the replacement of sand with dolomite produced a reduction of hydrogen cyanide together with a rise of ammonia more marked in the FL290 sample. In fact, that increase of NH_3 (2860 mg/Nm^3) surpassed the levels of HCN (1470 mg HCN/Nm^3). These results may confirm that the presence of steam together with dolomite clearly have promoted the conversion of the fuel-N to NH_3. In particular, the important decrease of tar could provoke the release of part of the nitrogen present in the tar compounds as ammonia. This trend was also observed in a previous work [25] regarding the oxygen/steam gasification of the parent fuel FL (results included in Figure 7.8). In that study the concentration of NH_3 increased with dolomite for two different SRFs. On the other hand, H_2S content was reduced by 75-95% ranging between 40-140 mg/Nm^3. In fact, the most remarkable difference was the low formation of HCl detected for the tests performed with torrefied FL compared to the data obtained with the parent FL

(HCl levels > 5000 mg/Nm^3). As commented in the air gasification section, this fact manifests the positive effect of torrefaction, reducing the release of chlorine in the gas phase to a range of 90-230 mg/Nm^3. This reduction seemed to be in contradiction with the slight decrease of chlorine content in the torrefied samples, in comparison to the parent fuel. However, the results pointed out that most of the chlorine released as HCl in the producer gas in the experiments with the FL sample stem from some polymers (in the polymer formulation or as additives) and would be released during the torrefaction process. On the other hand, inorganic chlorine present in salts would remain as ashes under the gasification conditions [42,43]. Therefore, although the reduction of chlorine between FL and torrefied samples is limited, the effect of the torrefaction process on HCl release is key. Lower levels of HCl in the producer gas would reduce the risk of corrosion, affecting not only to the design of the syngas conditioning process, but the materials selection for the gasification and syngas cleaning sections.

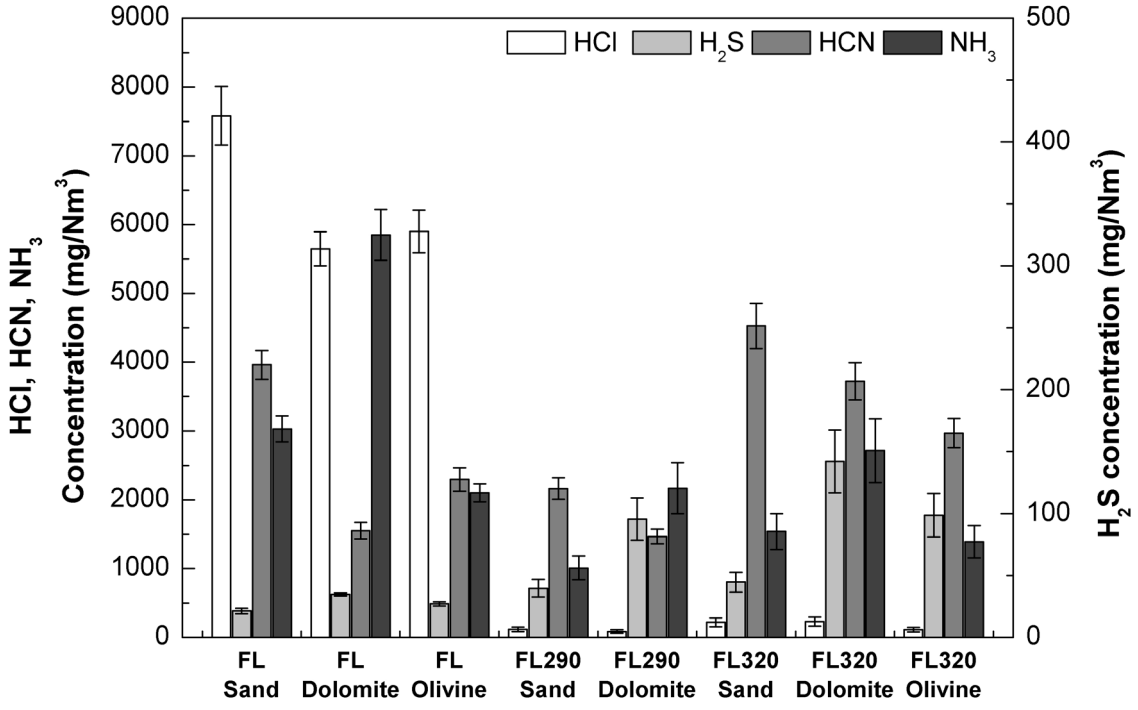

Figure 7.8 Minor contaminants in oxygen/steam gasification experiments. (T=850 C, ER~0.3 and Steam/SRF~1). (T=850 C and ER~0.3). Data for FL experiments from [25]

Gasification of FL320 led generally to higher concentrations of minor contaminants than FL290 experiments. One possible explanation for this result is related to the higher level of tar cracking (lower level of tar yields) during the gasification of FL320. The tar produced during MSW derived fuels gasification can contain N and S compounds that would evolve towards H_2S, NH_3 and/or HCN during tar cracking reactions, increasing the release of these contaminants. Apart from the use of dolomite, another catalyst (olivine) was tested with the most torrefied FL. According to our previous study [25], olivine reduced nitrogenous contaminants in a higher extent than dolomite. In this study olivine also resulted in a diminishment of HCN concentration compared to the utilization of sand as bed material, and similar ammonia levels. On the other hand, HCl diminished (to 113 mg/Nm^3) and H_2S slightly increased (to 99 mg/Nm^3). Usually the decrease of hydrogen chloride led to an increase of hydrogen sulphide due to the interaction of ash constituents (mainly K), under oxygen/steam gasification conditions [13].

7.3.3 Overall efficiency. Torrefaction combined with gasification

The overall efficiency of the process (torrefaction and gasification) was determined as the energy content (calculated as LHV) in the producer gas in relation to energy content of the raw feedstock [25] (Eq. 7.1). Figure 7.9 displays a diagram that explains the mass and energy balances of the overall process. Notice that efficiency is evaluated at 25 ºC and does not take into account the sensible heat of the gas at the gasifier exit.

$$\eta_{LHV}(\%) = 100\left(\frac{LHV_{producer\ gas}[MW]}{LHV_{raw\ feedstock}[MW]}\right) \qquad \text{Eq. 7.1}$$

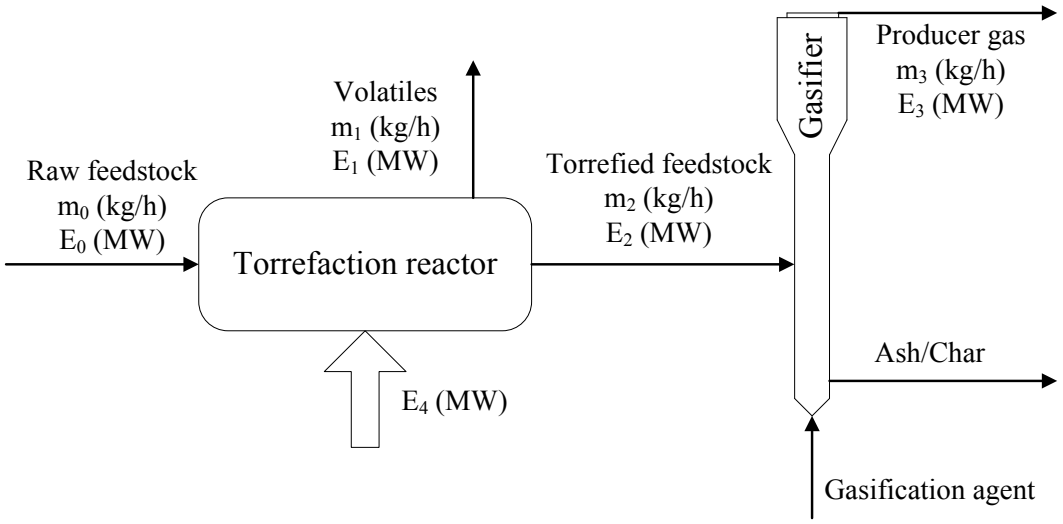

Figure 7.9 Scheme of the mass and energy balances for the combination of torrefaction and gasification

The efficiency values (η_{LHV}) displayed in Table 7.4 varied in the range of 42 to 44% for air gasification experiments. There was a slight decrease of the overall efficiency with the level of torrefaction. This reduction could be attributed to the loss of volatiles (from plastic fractions of FL) during torrefaction, causing a smaller gas production. However the efficiency results were close for both torrefaction levels. Under oxygen/steam conditions η_{LHV} increased up to a range of 45-55%. The lower formation of tar and the steady increase of carbon conversion and gas LHV could explain this fact. The efficiencies at these conditions also decreased with the torrefaction severity but for the combination of FL320 with dolomite. This experiment led to higher gas LHV than the obtained with FL290, probably linked to lower degree of oxidation (i.e. lower equivalence ratio). Additionally, η_{LHV} values for experiments with the parent material (FL) were calculated using data from a previous work [23]. The obtained results varied in the range of 47-55% for air gasification tests, slightly higher values than those obtained with the torrefied samples. Tests with oxygen/steam resulted in higher efficiencies (49-65%), especially when using dolomite as bed material (with an efficiency peak of 65%).

In order to evaluate the gasifier performance, the cold gas efficiency (CGE) of the gasification process has been included in Table 7.4. CGE is calculated according to the energy in the gas (as LHV) in relation to the energy of feedstock introduced in the gasifier (Eq. 7.2).

$$CGE_{LHV}(\%) = 100\left(\frac{LHV_{producer\ gas}[MW]}{LHV_{gasifier\ feedstock}\,[MW]}\right) \quad \text{Eq. 7.2}$$

CGE results ranged between 42-52% for air and between 45-67% for oxygen/steam experiments of torrefied materials. In general, CGE values with the FL320 material led to higher efficiencies due to the lower LHV of the feedstock compared to FL290. This fact could be related to the loss of hydrocarbons from the partial pyrolysis of polymers during torrefaction at 320 ºC. As commented for air experiments, the use of catalyst increased the producer gas LHV and hence cold gas efficiency. Contrasting these results with calculated CGE for experiments with FL [25], they followed similar trends to air experiments. Note that part of energy present in the volatiles of the torrefaction process could be reintroduced in the process and therefore improve the overall efficiency.

7.4 Conclusions

This paper studies the torrefaction of a solid recovered fuel (SRF) and its influence on the fuel properties for gasification purposes. The SRF was torrefied at two temperatures (290 ºC and 320 ºC) in a pilot auger reactor and evaluated as gasification feedstock. The torrefied materials (FL290 and FL320) were characterised and gasified in a bench-scale fluidized bed reactor. Gasification tests were carried out with different gasification agents (air and oxygen/steam) and bed materials (sand, dolomite and olivine) at similar experimental conditions (gasification temperature of 850 ºC and equivalence ratio of 0.3). The evaluation of the gasification performance was presented in terms of product yields and gas composition together with the release of contaminants. Tar species and minor contaminants (H_2S, HCl, HCN and NH_3) were analysed by gas chromatography and ion-selective potentiometry, respectively. Additionally the gasification efficiency (including the combination of torrefaction and gasification) was assessed according to the energy content in the producer gas.

The torrefaction pretreatment provoked the reduction of moisture and the increase of fixed carbon content in the torrefied samples. Regarding minor contaminants precursors, contents of N and S increased with the torrefaction severity whereas Cl experienced a slight decrease. The calorific value just

improved in FL290 probably due to the lower ash and higher volatiles content than in FL320.

Gasification performance was similar for both torrefied materials although FL320 generally performed better in terms of gas and tar production. FL320 yielded higher H_2/CO ratio, gas LHV and carbon conversion. Dolomite as bed material reduced tar content (2 times lower than with sand) in air experiments. These results were enhanced with O_2/H_2O as gasification agent. The lowest tar yields were obtained with dolomite in the bed rather than with olivine. Olivine seemed to be less effective in tar cracking, yielding similar tar levels as those obtained in experiments with sand. Characterization of tar samples revealed naphthalene, acenaphtylene and phenanthrene as the major polycyclic aromatic hydrocarbons.

Regarding the formation of minor contaminants in the producer gas, the main species when using air were HCN and H_2S whereas NH_3 and HCN dominated under oxygen/steam conditions. Generally, FL320 showed the highest concentration of contaminants. The results are in accordance with the higher levels of N and S reported for the FL320 sample. In addition, ash levels and its composition (potassium, silicon, etc.) affected the release of some species together with the larger consumption of char and tar cracking due to the presence of catalysts. Dolomite seemed to favour the formation of NH_3 formation and decrease the rest of contaminants meanwhile olivine (less effective on tar cracking) led to fewer nitrogenous compounds. A remarkable finding is the important reduction of HCl release for the O_2/steam gasification tests performed with the torrefied samples in comparison to those with the parent fuel, despite the slight variation of chlorine content among the samples. The release of chlorine attached to different polymers during the torrefaction process, rather than the inorganic chlorine present as salts, would explain this fact. The reduction of HCl levels in the producer gas would lead to a reduction in the gasification process cost, related not only to the syngas conditioning train, but more importantly to the selection of construction materials (due to the lower risk of corrosion). Taking into account the energy content in the producer gas, torrefaction severity usually diminished the efficiency of both gasification and combined process (torrefaction and gasification). However, these are preliminary results, and the use of additional strategies, such as the

reintroduction of the volatiles from the torrefaction process after conditioning for HCl removing, could improve the presented values.

The torrefaction pretreatment in the range of 290-320 ºC improved the gasification of the SRF (lower tar, higher H_2/CO ratio, carbon conversion, etc.) at expense of increasing the release of some minor contaminants (H_2S and NH_3). However, a relevant fact is that HCl concentration was greatly reduced from > 5000 mg/Nm^3 for oxygen/steam gasification of raw FL to values below 250 mg/Nm^3 for torrefied feedstocks, showing an additional benefit of torrefaction pretreatment for this type of feedstock.

7.5 References

[1] Zhang Q, Wu Y, Dor L, Yang W, Blasiak W. A thermodynamic analysis of solid waste gasification in the Plasma Gasification Melting process. Appl Energy 2013;112:405–13. doi:10.1016/j.apenergy.2013.03.054.

[2] Arena U. Process and technological aspects of municipal solid waste gasification. A review. Waste Manag 2012;32:625–39. doi:http://dx.doi.org/10.1016/j.wasman.2011.09.025.

[3] Alimuddin Z, Zainal B, Lahijani P, Mohammadi M, Rahman A. Gasification of lignocellulosic biomass in fluidized beds for renewable energy development : A review. Renew Sustain Energy Rev 2010;14:2852–62. doi:10.1016/j.rser.2010.07.026.

[4] Ahmad AA, Zawawi NA, Kasim FH, Inayat A, Khasri A. Assessing the gasification performance of biomass: A review on biomass gasification process conditions, optimization and economic evaluation. Renew Sustain Energy Rev 2016;53:1333–47. doi:10.1016/j.rser.2015.09.030.

[5] Arena U. Gasification: An alternative solution for waste treatment with energy recovery. Waste Manag 2011;31:405–6. doi:10.1016/j.wasman.2010.12.006.

[6] Sarkar M, Kumar A, Tumuluru JS, Patil KN, Bellmer DD. Gasification performance of switchgrass pretreated with torrefaction and densification. Appl Energy 2014;127:194–201. doi:10.1016/j.apenergy.2014.04.027.

[7] Arnsfeld S, Senk D, Gudenau HW. The qualification of torrefied wooden biomass and agricultural wastes products for gasification processes. J Anal Appl Pyrolysis 2014;107:133–41. doi:10.1016/j.jaap.2014.02.013.

[8] Dudyński M, van Dyk JC, Kwiatkowski K, Sosnowska M. Biomass gasification: Influence of torrefaction on syngas production and tar formation. Fuel Process Technol 2015;131:203–12. doi:10.1016/j.fuproc.2014.11.018.

[9] Chew JJ, Doshi V. Recent advances in biomass pretreatment–Torrefaction fundamentals and technology. Renew Sustain Energy Rev 2011;15:4212–22. doi:http://dx.doi.org/10.1016/j.rser.2011.09.017.

[10] Huang Y-F, Cheng P-H, Chiueh P-T, Lo S-L. Leucaena biochar produced by microwave torrefaction: Fuel properties and energy efficiency. Appl Energy 2017. doi:10.1016/j.apenergy.2017.03.007.

[11] Chen WH, Lu KM, Tsai CM. An experimental analysis on property and structure variations of agricultural wastes undergoing torrefaction. Appl Energy 2012;100:318–25. doi:10.1016/j.apenergy.2012.05.056.

[12] Prins MJ, Ptasinski KJ, Janssen FJJG. More efficient biomass gasification via torrefaction. Energy 2006;31:3458–70. doi:10.1016/j.energy.2006.03.008.

[13] Kirsanovs V, Zandeckis A. Investigation of Biomass Gasification Process with Torrefaction Using Equilibrium Model. Energy Procedia 2015;72:329–36. doi:10.1016/j.egypro.2015.06.048.

[14] Chen W-H, Peng J, Bi XT. A state-of-the-art review of biomass torrefaction, densification and applications. Renew Sustain Energy Rev 2015;44:847–66. doi:10.1016/j.rser.2014.12.039.

[15] Berrueco C, Recari J, Güell BM, Alamo G Del. Pressurized gasification of torrefied woody biomass in a lab scale fluidized bed. Energy 2014;70:68–78. doi:10.1016/j.energy.2014.03.087.

[16] Poudel J, Ohm T-I, Oh SC. A study on torrefaction of food waste. Fuel 2015;140:275–81. doi:10.1016/j.fuel.2014.09.120.

[17] Benavente V, Fullana A. Torrefaction of olive mill waste. Biomass and Bioenergy 2015;73:186–94. doi:10.1016/j.biombioe.2014.12.020.

[18] Liu S, Qiao Y, Lu Z, Gui B, Wei M, Yu Y, et al. Release and Transformation of Sodium in Kitchen Waste during Torrefaction. Energy & Fuels 2014;28:1911–7. doi:10.1021/ef500066b.

[19] Yuan H, Wang Y, Kobayashi N, Zhao D, Xing S. Study of Fuel Properties of Torrefied Municipal Solid Waste. Energy & Fuels 2015:150728062838002. doi:10.1021/ef502277u.

[20] Ahmed II, Gupta AK. Pyrolysis and gasification of food waste: Syngas characteristics and char gasification kinetics. Appl Energy 2010;87:101–8. doi:10.1016/j.apenergy.2009.08.032.

[21] Manatura K, Lu J-H, Wu K-T, Hsu H-T. Exergy analysis on torrefied rice husk pellet in Fluidized Bed gasification. Appl Therm Eng 2016;111:1016–24. doi:10.1016/j.applthermaleng.2016.09.135.

[22] Berrueco C, Recari J, Abelló S, Farriol X, Montané D. Experimental investigation of solid recovered fuel (SRF) gasification: Effect of temperature and equivalence ratio on process performance and release of minor contaminants. Energy & Fuels 2015;29:7419–27. doi:10.1021/acs.energyfuels.5b02032.

[23] Recari J, Berrueco C, Abelló S, Montané D, Farriol X. Gasification of two solid recovered fuels (SRFs) in a lab-scale fluidized bed reactor: Influence of experimental

conditions on process performance and release of HCl, H2S, HCN and NH3. Fuel Process Technol 2016;142:107–14. doi:10.1016/j.fuproc.2015.10.006.

[24] Berrueco C, Montané D, Matas Güell B, del Alamo G. Effect of temperature and dolomite on tar formation during gasification of torrefied biomass in a pressurized fluidized bed. Energy 2014;66:849–59. doi:10.1016/j.energy.2013.12.035.

[25] Recari J, Berrueco C, Abelló S, Montané D, Farriol X. Effect of bed material on oxygen/steam gasification of two solid recovered fuels (SRFs) in a bench-scale fluidized bed reactor. Energy & Fuels 2017. doi:Submitted to journal/Unpublished results.

[26] Woytiuk K, Campbell W, Gerspacher R, Evitts RW, Phoenix A. The effect of torrefaction on syngas quality metrics from fluidized bed gasification of SRC willow. Renew Energy 2017;101:409–16. doi:10.1016/j.renene.2016.08.071.

[27] Couhert C, Salvador S, Commandré JM. Impact of torrefaction on syngas production from wood. Fuel 2009;88:2286–90. doi:10.1016/j.fuel.2009.05.003.

[28] Mastral JF, Berrueco C, Ceamanos J. Pyrolysis of high-density polyethylene in free-fall reactors in series. Energy and Fuels 2006;20:1365–71. doi:10.1021/ef060007n.

[29] He M, Hu Z, Xiao B, Li J, Guo X, Luo S, et al. Hydrogen-rich gas from catalytic steam gasification of municipal solid waste (MSW): Influence of catalyst and temperature on yield and product composition. Int J Hydrogen Energy 2009;34:195–203. doi:10.1016/j.ijhydene.2008.09.070.

[30] Hwang IH, Kobayashi J, Kawamoto K. Characterization of products obtained from pyrolysis and steam gasification of wood waste, RDF, and RPF. Waste Manag 2014;34:402–10. doi:10.1016/j.wasman.2013.10.009.

[31] Dunnu G, Panopoulos KD, Karellas S, Maier J, Touliou S, Koufodimos G, et al. The solid recovered fuel Stabilat®: Characteristics and fluidised bed gasification tests. Fuel 2012;93:273–83. doi:10.1016/j.fuel.2011.08.061.

[32] Pinto F, André RN, Carolino C, Miranda M, Abelha P, Direito D, et al. Gasification improvement of a poor quality solid recovered fuel (SRF). Effect of using natural minerals and biomass wastes blends. Fuel 2014;117:1034–44. doi:10.1016/j.fuel.2013.10.015.

[33] Arena U, Di Gregorio F. Gasification of a solid recovered fuel in a pilot scale fluidized bed reactor. Fuel 2014;117:528–36. doi:10.1016/j.fuel.2013.09.044.

[34] Miccio F, Piriou B, Ruoppolo G, Chirone R. Biomass gasification in a catalytic fluidized reactor with beds of different materials. Chem Eng J 2009;154:369–74. doi:10.1016/j.cej.2009.04.002.

[35] Campoy M, Gómez-Barea A, Ollero P, Nilsson S. Gasification of wastes in a pilot fluidized bed gasifier. Fuel Process Technol 2014;121:63–9. doi:10.1016/j.fuproc.2013.12.019.

[36] Abdoulmoumine N, Adhikari S, Kulkarni A, Chattanathan S. A review on biomass gasification syngas cleanup. Appl Energy 2015;155:294–307. doi:10.1016/j.apenergy.2015.05.095.

[37] Devi L, Ptasinski KJ, Janssen FJJG, Van Paasen SVB, Bergman PC a, Kiel JH a. Catalytic decomposition of biomass tars: Use of dolomite and untreated olivine. Renew Energy 2005;30:565–87. doi:10.1016/j.renene.2004.07.014.

[38] Chen H, Chen X, Qiao Z, Liu H. Release and transformation behavior of Cl during pyrolysis of torrefied rice straw. Fuel 2016;183:145–54. doi:10.1016/j.fuel.2016.06.031.

[39] Jeremiáš M, Pohořelý M, Bode P, Skoblia S, Beňo Z, Svoboda K. Ammonia yield from gasification of biomass and coal in fluidized bed reactor. Fuel 2014;117:917–25. doi:10.1016/j.fuel.2013.10.009.

[40] Tchapda AH, Pisupati S V. A review of thermal co-conversion of coal and biomass/waste. Energies 2014;7:1098–148. doi:10.3390/en7031098.

[41] Bläsing M, Zini M, Müller M. Influence of feedstock on the release of potassium, sodium, chlorine, sulfur, and phosphorus species during gasification of wood and biomass shells. Energy and Fuels 2013;27:1439–45. doi:10.1021/ef302093r.

[42] Montané D, Abelló S, Farriol X, Berrueco C. Volatilization characteristics of solid recovered fuels (SRFs). Fuel Process Technol 2013;113:90–6. doi:10.1016/j.fuproc.2013.03.026.

[43] Ma W, Hoffmann G, Schirmer M, Chen G, Rotter VS. Chlorine characterization and thermal behavior in MSW and RDF. J Hazard Mater 2010;178:489–98. doi:10.1016/j.jhazmat.2010.01.108.

8. Techno-economic analysis of liquid fuel plants via biomass and SRF gasification

Abstract

This work estimates capital and production costs of liquid fuel plants based on gasification, followed by Fischer-Tropsch synthesis and hydroprocessing. An interesting part of this study is the integration of torrefaction during the pretreatment stage, taking into account their consequences on the process performance. Four gasification feedstocks were considered: a lignocellulosic biomass, a solid recovered fuel (SRF) and their torrefied samples. The syngas production was modelled using an Aspen simulation based on experimental results in a bench-scale fluidized bed reactor. All biomass and SRF scenarios showed high investment costs (about 600 M€$_{2015}$), slightly higher for SRF scenarios; however the combination of torrefaction and gasification proved to reduce costs ascribed to process improvements. The product value (PV) of liquid fuels (diesel and gasoline) was estimated to be about 1700 €/tonnes (1.25 €/liter gasoline equivalent) and 1200 €/tonnes (0.87 €/liter gasoline equivalent) for biomass and SRF scenarios, respectively. A sensitivity analysis performed to assess influential parameters on the fuel PV revealed that economic parameters, such as capital investment, were the largest contributors, whereas other costs, such as the catalyst, price were the least.

This chapter is based on the following research article:

Recari J, Berrueco C, Farriol X. Techno-economic assessment of Fischer-Tropsch liquid fuel production plants based on biomass and waste gasification. Energy Convers Manag n.d. doi:To be submitted.

8.1 Introduction

Currently, liquid transportation fuels derive primarily from petroleum, however, due to global warming effect and fossil fuels depletion there is an increasing demand for the production of clean and renewable fuels. Some of those alternatives are second generation biofuels such as biomass-based fuels [1]. Biomass is a renewable energy source that can be exploited for energy production through two main pathways: biological (i.e. anaerobic digestion) and thermochemical (i.e. pyrolysis and gasification). Gasification is one of the most attractive platforms for the conversion of biomass into a synthesis gas (syngas) with multiple end uses, including chemicals and fuels production. A possible route is through the Fischer-Tropsch (FT) process, that can convert the syngas into liquid fuels such as diesel, gasoline and kerosene [2–5]. Numerous plants have produced FT liquids from coal and natural gas [4–7], however, biomass-to-liquid (BTL) has still commercial limitations ascribed to high investment costs [5,8].

Several techno-economic analyses have been reported for a variety of conversion pathways with different feedstocks and end products. Regarding BTL studies, Swanson et al. [9] stated that a corn stover gasification plant (input of 2000 dry tonnes/day) required a total capital investment (TCI) of $500-600 million. The authors claimed that the product value (PV) would range between 1-1.32 $/liter gasoline equivalent. In another study, the production costs of FT fuels was 0.88-1.39 $/liter gasoline equivalent for forest residues gasification plants with capacities of 2000 dry tonnes/day [10]. A 50 MWth input BTL plant resulted in a fuel cost of 1.25 €/L whereas the increase of the plant capacity up to 8500 MWth led to values about 0.53 €/liter [8]. Another study [11] was more optimistic reporting a PV as low as 0.19 $/liter gasoline equivalent for a switchgrass gasification plant of 227 ML/year. Hamelinck et al. [12] estimated, for a 400 $MWth_{HHV}$ input plant, that FT diesel would cost 0.69 €/liter gasoline equivalent (16 €/GJ), and even could decrease to half in the future. Therefore, there is a diversity of cost estimations depending on the applied methodologies and the selected hypothesis. This situation presents an interesting opportunity for developing economic studies using other feedstocks and more realistic assumptions.

Municipal solid waste (MSW) acts as a potential resource for waste-to-energy (WTE) purposes. Despite of the promotion of waste management practices, most of MSW is still disposed to landfills and dump sites, while a small portion is recycled or used in WTE plants [13]. Waste incineration for electricity and heat production is the most common WTE route [14]. Nevertheless, other approaches must be implemented to contribute the WTE concept, for instance the development of waste-to-liquid (WTL) plants. In this sense, investigations concerning MSW gasification are currently being carried out [13,15–20]. Furthermore, economic studies have been reported for MSW gasification plants [15,21–23]. However, to our knowledge, there is no published works for WTL plants based on gasification.

This work aims to fill this gap by reporting a techno-economic assessment of biomass- and waste-to liquids plants. This study estimates the capital investment and production costs of four liquid fuel plants based on gasification. The four scenarios included the gasification of: one woody biomass, one solid recovered fuel (SRF) derived from MSW, and their torrefied subproducts (torrefied biomass and torrefied SRF). Torrefaction was integrated during the pretreatment stage and their consequences on the gasification feedstock were considered during gasification and syngas cleaning. A sensitivity analysis illustrates the effect of economic and process parameters on the fuel product value.

8.2 Materials and methods

This section presents the methodology followed to perform the techno-economic assessment (TEA) of a liquid fuel production plant. Gasification was the technology studied for the production of the syngas used in the catalytic Fischer-Tropsch (FT) synthesis followed by hydroprocessing. The integration of torrefaction as a pretreatment stage was considered for each type of gasification feedstock (biomass and waste). Four scenarios were selected based on published lab-scale gasification experiments. Two woody biomasses (VW and VW-LT) [24] and two solid recovered fuels (FL and FL320) [25,26].

Equipment and unit costs were evaluated using the output of an Aspen simulation model and literature data.

8.2.1 Biomass- and waste-to-liquids via gasification

The gasification plant capacity was set to be 2000 dry tonnes per day to be consistent with other studies for biomass gasification [10,27,28] and facilitate the comparison of results. The same plant capacity was assumed for SRF gasification.

Figure 8.1 shows a schematic representation of the liquid fuel production plant based on gasification. The following sections describe the plant process including the assumptions taken in each area (additional assumptions can be found in section 8.2.2.1).

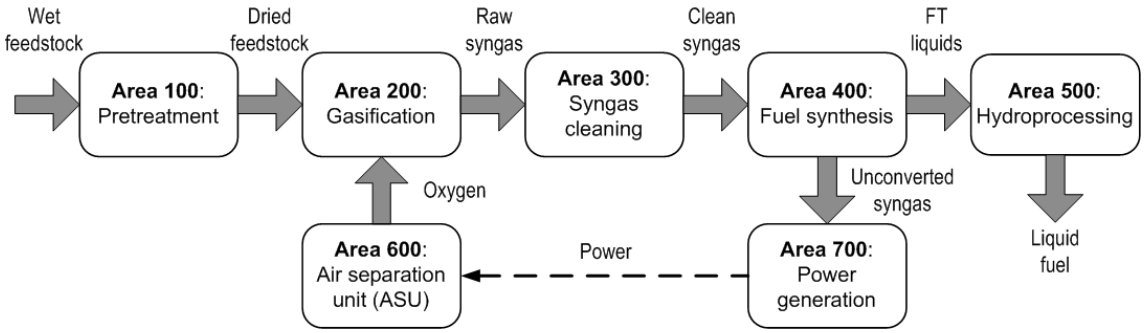

Figure 8.1 Plant flow diagram for all scenarios

8.2.1.1 Area 100: Pretreatment

The pretreatment area prepared the feedstock for the gasification process. This area included chopping, grinding, magnetic separator (to remove any metal) and drying. The feedstock was fed in wet basis (assumed 30% wt. moisture), then dried and grounded to a suitable particle size for gasification (~30 mm). The drying process was assumed to be a belt dryer and the initial moisture content is reduced to the levels reported in Table 8.1.

8.2.1.2 Area 200: Gasification

In the gasification area took place the production of the synthesis gas (syngas) in an atmospheric bubbling fluidized bed reactor operating at 850 ºC and using oxygen/steam as gasification agent. After the gasification stage, cyclones (a train of high efficient separators) were used to remove solids (ash and uncombusted char) from the syngas.

The gasification of feedstocks (biomass and solid recovered fuels) was modelled by Aspen Plus process engineering software (Aspen Plus® V8.4). The

thermodynamic equilibrium model for gasification was developed using the Gibbs minimizing method to predict and adjust the composition of product gas to the results obtained in lab-scale experimental tests [25,26]. The following assumptions [29] were considered in the gasification model:

a) Operation at steady state and at atmospheric pressure (~1 bar).
b) Pressure drops and heat losses were neglected.
c) Gases behaved ideally.
d) Ash was assumed to be inert.
e) Char was assumed to be 100% solid carbon (C).
f) Tar formation was not considered.

Table 8.1 Characterization of feedstocks (as received basis) as reported by [24,26]

		VW	VW-LT	FL	FL320
Proximate analysis (wt.%)	**Moisture**	5.03±0.01	3.45±0.01	8.39±0.41	1.12±0.10
	Volatiles	77.15±0.12	77.44±0.04	72.58±0.86	71.47±0.05
	Fixed carbon	17.46±0.12	18.70±0.05	5.78±0.44	11.55±0.24
	Ash	0.36±0.02	0.42±0.01	13.24±1.01	15.86±0.17
Ultimate analysis (wt.%)	**C**	47.20±0.17	48.86±0.48	46.03±0.54	53.68±0.53
	H	6.21±0.10	6.08±0.13	7.49±0.02	6.55±0.07
	O	46.18±0.30	44.57±0.55	31.71±0.55	22.28±0.54
	N	0.02±0.02	0.05±0.02	0.66±0.06	0.85±0.01
	S	0.03±0.002	0.03±0.002	0.26±0.01	0.27±0.02
	F	< 0.002	< 0.002	<0.02	<0.02
	Cl	< 0.002	< 0.002	0.59±0.06	0.49±0.04
HHV (MJ/kg)		19.10±0.09	19.59±0.04	24.91±0.23	24.46±0.19
LHV (MJ/kg)		17.74±0.09	18.26±0.04	23.29±0.22	23.06±0.18

The Peng-Robinson equation of state was selected as the property method to estimate all physical properties of the conventional components. The gasification feedstock and ash were defined as non-conventional components, thus the enthalpy and density model were specified in the HCOALGEN and DCOALGIST property method. The feedstock heat of combustion (HCOMB) was selected as a user-specified value by introducing the high heating value (HHV).

A general Aspen Plus flowsheet of gasification is illustrated in Figure 8.2. The feedstock stream (FEED) was defined as a non-conventional stream by

introducing the proximate and ultimate analysis in dry basis given in Table 8.1. A yield reactor (RYield titled DECOMP) was used to simulate the decomposition of the feed stream at a temperature of 500 ºC and 1 bar. The mass yields of the RYield reactor were set using a calculator block (with a FORTRAN subroutine) to convert the non-conventional components into conventional including carbon, hydrogen, oxygen, nitrogen, chlorine, sulphur and ash.

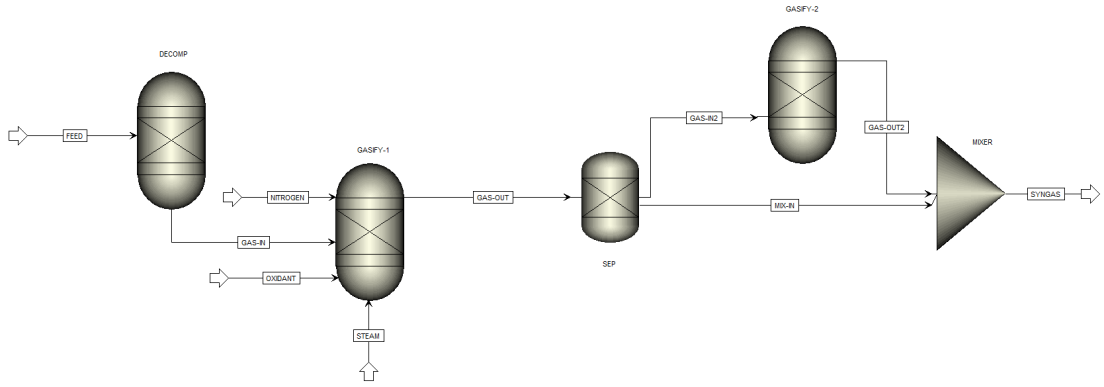

Figure 8.2 Aspen Plus flowsheet of gasification model

The gasification reactor (GASIFY-1) was an RGibbs reactor set to calculate phase and chemical equilibrium at the operating conditions (850 ºC and 1 bar) and identify the possible products of the gas (major and minor compounds). Major compounds included H_2, CO, CO_2, O_2, N_2, H_2O, CH_4, C_2H_2, C_2H_4, C_2H_6 and C_3H_8 while minor compounds included H_2S, HCl, NH_3 and HCN. There were other three inlet streams into the gasifier which corresponded to the gasification agent (OXIDANT and STEAM streams) and the nitrogen (NITROGEN) used in the experiments to facilitate the feeding. The mole fraction of the OXIDANT stream was specified as 0.95 O_2 and 0.05 N_2. These streams were set to 400 ºC and 1 bar and mass flow rates were calculated by a design specification block according to the values for equivalence ratio (ER) and steam to feedstock ratio for each scenario (Table 8.2). The ER is defined as the actual oxygen to fuel ratio divided by the stoichiometric oxygen to fuel ratio required for complete combustion [30]. The steam/feedstock ratio is defined as the ratio of flow rates between steam (from process and feedstock moisture) and the feedstock (in dry basis).

In order to adjust the composition of the product gas (GAS-OUT) to match the obtained experimental data, the steam-methane reforming (R1) and the water-gas shift (R2) reactions were used.

$$CH_4 + H_2O \leftrightarrows CO + 3H_2 \quad (R1)$$

$$CO + H_2O \leftrightarrows CO_2 + H_2 \quad (R2)$$

For this purpose the main components involved in the reactions (H_2, H_2O, CO, CO_2 and CH4) were separated (SEP) and sent to a second RGibbs reactor (GASIFY-2). The block is set to restrict the chemical equilibrium by specifying reactions R1 and R2 and temperature approach values (Table 8.2). These temperature approach values reflect the deviation from the equilibrium and ensure that the model reproduces the reported experimental gas composition. This type of modelling based on an equilibrium approach was used in recent studies [29,31,32]. Finally, a mixer block mixed the gas streams (MIX-IN, GAS-OUT2) to obtain the final syngas stream (SYNGAS). The obtained composition can be observed in Table 8.2. Afterwards, other Aspen Plus equipment (i.e. separators, compressors, heat exchangers, etc.) could be used in the model to reproduce the stream conditions for upgrading the syngas

Table 8.2 Operational conditions, simulation and experimental results

	VW	**VW-LT**	**FL**	**FL320**
ER	0.22	0.23	0.30	0.30
Steam/Feedstock	1.60	1.6	1.0	1.0
R1 temp. approach	-330	-310	-370	-350
R2 temp. approach	300	280	180	-120
Simulation results: Syngas composition (% vol. dry)	H_2 (35.4) CH_4 (8.2) CO (20.2) CO_2 (27.1) N_2 (9.1)	H_2 (40.2), CH_4 (6.3), CO (22.5), CO_2 (26.8), N_2 (4.3)	H_2 (23.6), CH_4 (19.6), CO (15.8), CO_2 (31.1), N_2 (9.4)	H_2 (28.7), CH_4 (16.3), CO (11.1), CO_2 (34.6), N_2 (9.0)
H_2/CO	1.76	1.78	1.49	2.57
Experimental results: Syngas composition (% vol. dry)	H_2 (36.3) CH_4 (5.2) CO (20.6) CO_2 (27.8) N_2 (10.0)	H_2 (39.4), CH_4 (5.0), CO (22.1), CO_2 (29.2), N_2 (4.0)	H_2 (23.0), CH_4 (11.2), CO (15.4), CO_2 (34.2), N_2 (9.7)	H_2 (29.0), CH_4 (8.5), CO (11.2), CO_2 (38.7), N_2 (8.9)
H_2/CO	1.76	1.78	1.49	2.58

8.2.1.3 Area 300: Syngas cleaning

In this stage the syngas still could contain some particulate (fly ash) and other contaminants in the form of tar (condensable hydrocarbons higher than benzene), hydrogen sulphide (H_2S), ammonia (NH_3), hydrogen cyanide (HCN) and hydrogen chloride (HCl). A direct water quench cooled the syngas down to condense tar and absorbe most of ammonia and ammonium chloride [9]. First the syngas cooler decreased the gas temperature to 200 ºC and then a scrubber system cleaned the syngas up, reducing the temperature to about 40 ºC. Some studies such as Swanson et al. [9] removed the CO_2 after an acid gas removal system using monoethanolamine, however the CO_2 removal units are not significantly important in terms of carbon and energy efficiencies, or annual net cash flows of the process [33]. Besides an adequate catalyst for the Fischer-Tropsch (FT) process could sufficiently improve the FT selectivity to liquids. For this reason, in this study the CO_2 removal was not considered but the CO_2 dilution of the syngas was taken into account. Finally, the syngas was directly cleaned and polished for sulphur and trace contaminants (contaminants must be below 200 ppb H_2S and 10 ppm NH_3) using zinc oxide (ZnO) and activated carbon.

8.2.1.4 Area 400: Fischer-Tropsch synthesis

Fischer-Tropsch (FT) synthesis requires pressures between 25-60 bar and two possible temperature ranges: 200-250 ºC and 300-350 ºC for low and high temperature synthesis, respectively [10]. In this study, and similarly to [9], a low temperature synthesis was considered as it favours the formation of liquid products such as diesel and wax. First the cleaned syngas was compressed to 25 bar. Before FT synthesis there was a syngas conditioning stage. In order to reduce the amounts of methane and ethane, a steam methane reforming (SMR) reactor operating at 850 ºC was included. An optimal ratio of H_2/CO for FT synthesis is 2.1 [9], therefore a water gas shift (WGS) reactor was required to increase this ratio. Just before the FT reactor, a pressure swing adsorption (PSA) unit separated some hydrogen for the hydroprocessing (Area 500). Afterwards, the syngas reacted in a fixed-bed FT reactor at 200 ºC and 25 bar in presence of a cobalt-based catalyst according to reaction 3.

$$CO + 2.1H_2 \rightarrow -(CH_2)- + H_2O \quad \text{(R3)}$$

The output gas was cooled down (45 ºC) and separated into liquid hydrocarbons (~8% wt.), water (~16% wt.) and unconverted syngas (~77% wt.). Finally, a fraction of the unconverted syngas (70% wt.) was recycled back into the FT reactor, whereas the other gas fraction (30% wt.) was sent to the power generation system (Area 700). The product distribution was obtained following the approach of Swanson et al. [9], considering the differences in syngas composition and a CO per pass conversion of 40%.

8.2.1.5 Area 500: Hydroprocessing

The Fischer-Tropsch liquids were hydrocracked with hydrogen from the PSA unit in a hydroprocessing unit. The product distribution by weight was 62% diesel, 26% gasoline and 12% flue gas (gaseous hydrocarbons with an assumed composition of 30% wt. methane and 70% wt. propane) [9]. The flue gas was sent to the gas turbine in Area 700.

8.2.1.6 Area 600: Air separation unit

The Air separation unit (ASU) provided the oxygen (95% purity) for the gasification area. This area consumed a significant amount of power which was provided by Area 700.

8.2.1.7 Area 700: Power generation

A gas turbine and steam turbine provide the required power for the plant. Unconverted syngas from Fischer-Tropsch synthesis (Area 400) and fuel gas from hydroprocessing (Area 500) are combusted in a gas turbine to produce power and heat recovered in a steam generator. Electric generators for both gas and steam turbines produce electricity with an efficiency of 50% of gas energy for the gas turbine and 25% for steam turbine (the remaining 25% were losses).

8.2.2 Economic analysis

The total capital investment (TCI) and the cost of fuel production (or product value, PV) were calculated for the four considered scenarios.

Literature data and Aspen Plus model results were used to calculate stream flows and other operating conditions to perform the economic analysis. The facility cost was assumed to be the *n*th plant for 20 years with a 90% annual availability (7884 hours per year). Total purchased equipment cost (TPEC) was estimated by the factored estimation method [12,34] scaling the unit costs from base equipment in the literature [12,35]. The scaled cost was calculated using the Eq. 1. $Cost_0$ is the base equipment cost and $Cost_1$ is the new equipment cost. $Size_1$ and $Size_0$ are the capacity of base and new equipment, respectively. Cost escalation was applied using the scaling factor (n), typically ranging between 0.6-0.8 depending on the equipment type. Currency conversion factors and the Chemical Engineering Plant Cost Index (CEPCI) [36] adjusted the final costs to €$_{2015}$ (CEPCI$_{2015}$ = 556.8). Table 8.3 gathers the equipment costs in million €$_{2015}$.

$$Cost_1 = Cost_0 \cdot \left(\frac{Size_1}{Size_0}\right)^n \qquad \text{Eq. 8.1}$$

A balance of plant (BOP) cost (i.e. piping, electrical systems, instrumentation and controls) was added after determining the cost of areas 100-700. BOP was assumed to be 11% of TPEC [9]. Table 8.4 lists the assumptions followed to determine the indirect costs and total capital cost. Indirect costs (IC) were calculated as 89% of TPEC (32% for engineering and supervision, 34% for construction expenses, and 23% for legal and contractor's fees) according to Peters et al. [34]. Total direct and indirect costs (TDIC) were the sum of TIC and IC. The fixed capital investment (FCI) included the project contingency calculated as 20% of TDIC [9]. The assumed contingency was higher than the one used in other studies (5-15%) [34], as the current work does not include a thorough list of equipment. Finally total capital investment (TCI) was calculated including working capital (WC) as 15% of FCI and land use as 6% of TPEC [28].

Table 8.5 shows the operating costs including feedstock, utilities, chemicals and disposal prices. The values were obtained from manufacturers and literature [9,34,37].

Variable costs included natural gas to produce power in the gas turbine during starting and backup periods (assumed to be 5% of annual operating time and 100% of plant power usage), sand as the bed material for the fluidized bed reactor (assumed to be needed 1% of feedstock mass flow rate), steam used in the process, disposal costs for solids (removal of ash and char) and wastewater (applied to water produced during direct syngas quench and catalysts for main units (SMR, WGS and FT reactor). Catalysts costs were estimated on annual basis according to the volume flow rate fed in each unit and assuming a gas hourly space velocity (2600 h^{-1} for SMR, 1000 h^{-1} for WGS and 100 h^{-1} for FT reactor). The catalysts replacement period was 3 years.

Fixed costs included salaries (50 employees with gross salary of 45000 €/employee), overhead (60% of salaries), maintenance and insurance (both 2% of TIC) [27,37].

The plant power usage was determined based on the power requirements (Table 8.6) for the main unit equipment from values reported by Swanson et al [9] and results from Aspen Plus.

The fuel cost (product value, PV) was calculated as the minimum selling price taking into account the total costs and revenues. Total costs included operating costs (OC), return on investment (ROI) and income tax (IT). A 10% of discount rate and 28% of income tax were assumed. Eq. 8.2 shows the calculation for ROI, where the plant life (PL) was 20 years and TCI was the total capital investment.

$$ROI = \frac{DR \cdot (1+DR)^{PL}}{(1+DR)^{PL}-1} \cdot TCI \qquad \text{Eq. 8.2}$$

Table 8.3 Base costs for major equipment

Unit	Base capacity	Base cost (M€$_{2015}$)	Scale factor	Installation factor*	Reference
Area 100: Pretreatment					
Conveyers	132.5 wet t/h	0.58	0.8	1.51	[35]
Grinder	132.5 wet t/h	0.39	0.6	3.02	[35]
Chopper	132.5 wet t/h	0.015	0.7	2.72	[35]
Magnetic separator	132.5 wet t/h	1.19	0.7	1.26	[35]
Dryer	18.5 t H_2O evap/h	4.90	0.8	2.40	[35]
Area 200: Gasification					
Feeding system	92.6 dry t/h	1.01	1.0	2.49	[35]
FBR gasifier	92.6 dry t/h	7.76	0.7	1.93	[35]
Cyclone	128 m^3 gas/s	0.17	0.7	2.81	[35]
Area 300: Syngas cleaning					
Syngas cooler	138.1 MWth	11.40	0.6	1.84	[12]
Scrubbers	12.1 m^3 gas/s	4.22	0.7	2.00	[12]
Guard beds (ZnO and active C)	8.0 m^3_{NTP} gas/s	0.03	1.0	3.00	[12]
Area 400: FT synthesis					
Syngas booster compressor	1 MWe	1.43	0.85	1.20	[35]
SMR reactor	7.1 m^3 gas/s	1.28	0.6	3.02	[35]
WGS reactor	2585 kmol CO+H_2/h	0.11	0.6	3.02	[35]
PSA Unit and compressor	167 kmol feed/h	2.58	0.7	2.21	[35]
FT reactor	11400 kmol feed/h	7.38	0.72	3.60	[35]
Area 500: Hydroprocessing					
FT product upgrading	69.4 kmol FT liquids/h	6.13	0.65	3.02	[35]
Area 600: Air separation unit					
Air separation unit (95% O_2 purity)	562 t O_2/day	9.61	0.75	1.57	[35]
Area 700: Power generation					
Gas turbine	21.0 MWe	23.15	0.7	1.20	[35]
Steam turbine	10.4 MWe	6.66	0.7	1.20	[35]

* Installation factors were consistent with those recommended by Peters et al. [34] and used by other authors [9,12]

Table 8.4 Methodology for capital cost estimation

Parameter	**Assumption**
Total purchased equipment cost (TPEC)	Aspen Plus output and literature (Table 8.3)
Total installed cost (TIC)	TPEC × installation factor (Table 8.3)
Indirect cost (IC)	89% of TPEC
Engineering	32% of TPEC
Construction	34% of TPEC
Legal and contractors fee	23% of TPEC
Total direct and indirect costs (TDIC)	TIC+IC
Contingency	20% of TDIC
Fixed capital investment (FCI)	TDIC+Contingency
Working capital (WC)	15% of FCI
Land use	6% of TPEC
Total capital investment (TCI)	FCI+WC+ Land use

Table 8.5 Material costs and assumptions ($€_{2015}$)

Variable	**Cost**	**Source**
Feedstocks		
Biomass (VW and VW-LT)	57.5 €/dry tonne	Manufacturer
SRF (FL and F320)	-15 €/dry tonne	Manufacturer
Natural gas	50 €/MWh	Manufacturer
Sand	110 €/t	Manufacturer
Steam	9 €/t	[9]
Solids disposal	20 €/t	Manufacturer
Wastewater disposal	0.2 €/m^3	Manufacturer
Catalysts		
SMR catalyst (nickel-aluminium)	30 €/kg (density: 1121 kg/m^3)	[9]
WGS catalyst (copper-zinc)	15 €/kg (density: 900 kg/m^3)	[9]
FT catalyst (cobalt)	30 €/kg (density: 1025 kg/m^3)	[9]
Electricity	60 €/MWh	Manufacturer

Table 8.6 Power requirements for main units

Unit	**Power requirement***
A100. Chopper	4.5 kW/(wet tonne/h)
A100. Grinder	5 kW/(wet tonne/h)
A200. Feeding system (lockhopper system)	2 kW/(dry tonne/h)
A400. Syngas booster compressor	From Aspen Plus model
A400. PSA compressor	From Aspen Plus model
A500. Hydroprocessing area	48 kW/(kmol FT liquids/h)
A600. ASU compressors (both air and oxygen)	18 kW/(t O_2/d)

*Energy requirements and power consumption were estimated from values reported by Swanson et al [9]

The income tax (IT) was calculated according to Eq. 8.3 by assuming a tax rate (TR) of 28%. Depreciation cost (DC) was estimated based on a Double-Declining Balance method, assuming a zero salvage value and depreciation periods of 7 and 20 years for general plant and power generation unit, respectively [28,38].

$$IT = TR \cdot (FSR + ESR - OC - DC) \quad \text{Eq. 8.3}$$

Total revenues accounted for electricity sales revenue (ESR) and fuel sales revenue (FSR). ESR was calculated from electricity sold to grid whereas FSR was calculated at the breakeven point, where total revenues should be equal to total costs (Eq. 8.4)

$$ESR + FSR = OC + ROI + IT \quad \text{Eq. 8.4}$$

By solving equations Eq. 8.3 and Eq. 8.4, the FSR could be calculated and the PV was determined by dividing the FSR into the total fuel output (annual tonnes of gasoline and diesel).

8.2.2.1 Assumptions made for the economic assessment

A compilation of additional assumptions for the TEA are listed as follows:

- Only major equipment was considered for the estimation of total purchased equipment cost. Other equipment, such as pumps or small heat exchangers, was not taken into account.
- Energy requirements and power consumption were estimated from values reported by Swanson et al [9]. Energy consumption for grinding was calculated for a final size of 30 mm using adapted correlations by Mani et al. [39].
- The basis of the drier was set in tonnes of water evaporated per hour, which reproduces properly the investment costs of a torrefaction reactor [40] depending on the torrefaction severity.
- The final costs of the gasification unit (Area 200) and syngas cleaning (Area 300) were reduced or increased based on what is expected to occur in a real

gasification plant, according to the levels of tar and minor contaminants in the syngas. For the torrefied biomass scenario (VW-LT), the final cost of the cleaning stage (Area 300) was reduced by 10% compared to the VW scenario due to a lower tar production with this feedstock [24]. Tar content decreased from 2.6 g/Nm^3 (0.52 g/100 g dry biomass) for VW gasification to 0.9 g/Nm^3 (0.18 g/100 g dry biomass) for VW-LT gasification. This tar reduction of 65% would reduce costs in gas cleanup units. For SRFs scenarios different assumptions were considered. The gasification stage (Area 200) was assumed to be 10% more expensive when using FL ascribed to the presence of chlorine (i.e. corrosion might affect the type of material used in the gasifier). In addition, the cost of syngas cleaning was increased by 15% as a consequence of higher levels of tar and minor contaminants compared to biomass gasification. In FL gasification, tar content was up to 23 times higher (60 g/Nm^3 and 12 g/100g dry FL), as well as a rather high presence of minor contaminants (for instance > 5000 mg HCl/Nm^3) [25]. On the other hand, as the torrefaction of FL would potentially decrease the level of contaminants in the syngas (i.e. tar, chlorine) [26], for FL320 scenario the cost of the gasification area was slightly increased by 5%, whereas the cost of the cleaning area was not varied in comparison to basis case. In line with this, Recari et al. [26] reported values of tar below 24 g/Nm^3 and HCl concentration below 450 mg/Nm^3 during gasification of FL320, still far from acceptable limits for FT synthesis but significantly lower than those obtained during FL gasification.

- This study considered the reduction of tar and minor contaminants to acceptable limits for FT synthesis.
- Solids disposal were calculated with ash and char yields of the feedstocks reported elsewhere [24,26].
- WGS reactor was not necessary for syngas obtained during FL320 gasification as the H_2/CO ratio was already higher than 2.1.
- Other studies considered the combustion of char collected in the cyclones or the utilization of unconverted syngas from the fuel synthesis to provide heat for the drying process [9,28]; however this case was not considered in the study.
- Feedstock price included cost of transportation.

- Costs of other utilities such as cooling water were not included.
- Construction period and storage costs were not accounted.
- Fuel densities were assumed to be 737 kg/m^3 for gasoline and 840 kg/m^3 for diesel. The liters of gasoline equivalent were calculated taking into account that a liter of diesel has 114% of the energy of one liter of gasoline (1 liter gasoline equivalent = liter of diesel × 1.14).

Table 8.7 Sensitivity parameters

Parameter	**Favourable**	**Baseline**	**Unfavourable**
Discount rate (%)	5	10	15
Total Capital Investment, TCI (%)	75	100	125
Annual production (% of tonnes FT fuels)	110	100	90
Biomass cost (%)	75	100	125
SRF cost (%)	125	100	75
Availability (%)	95	90	85
Electricity price (%)	125	100	75
Catalyst life (years)	5	3	1
Catalyst cost (%)	50	100	150

8.2.3 Sensitivity analysis

The sensitivity analysis considered the influence of one parameter at a time on the product value (PV). The parameters shown in Table 8.7 involved changes associated to uncertainties estimated in this study (such as capital expenditures and plant capacity) affecting the estimated PV. Baseline sensitivity parameters were the values assumed in this study, whereas favourable sensitivity parameters included the reduction of the total capital investment (TCI) and the increase of annual fuel production. In contrast, unfavourable sensitivity parameters reflected the increase of costs and a lower efficiency of the plant.

8.3 Results and discussion

8.3.1 Aspen model results

The simulation model for gasification was validated using reported experimental data of both biomasses and SRFs gasification experiments in a

lab-scale fluidized bed reactor [25,26]. Table 8.2 displays the simulation model and experimental results.

The gas composition (% vol. dry) obtained in the model simulation was in good agreement with the syngas obtained experimentally. In all scenarios the percentage of error was below 2% for H_2 and CO. This led to almost identical H_2/CO ratios. Other compounds such as CO_2 and CH_4 presented higher percentage of error but concentrations were in the same order of magnitude. In fact, CH_4 concentration led to the greatest deviation in SRFs gasification as these materials produce other lighter hydrocarbons (C_2H_2, C_2H_4 and C_2H_3 and C_3) not accurately estimated by the model. Nevertheless, these hydrocarbons represented about 5% of gas composition and this deviation did not compromise the results for the goal of this study. Therefore this simulation could be used to obtain a representative syngas composition for developing the economic assessment.

8.3.2 Economic results

The main economic results for the four liquid fuel production plants are gathered in Table 8.8.

Biomass scenarios (VW and VW-LT) produced higher daily fuel outputs compared to SRFs (FL and FL320). The estimated total fuel production of gasoline and diesel was 265 tonnes/day for VW and 268 tonnes/day for VW-LT. SRFs scenarios followed similar trends with a lower but close fuel output: 259 and 261 for FL and FL320, respectively. Therefore, torrefied samples raised the fuel production as an effect of the higher carbon conversion efficiency and syngas production (i.e. higher gas yield). Along with the higher fuel output the power usage increased especially for torrefied materials. The main contributions were the compressors power requirements in the FT and ASU areas. The syngas needed to be compressed from 1 bar to 25 bar and also torrefied samples required larger amounts of oxygen fed in the gasifier to maintain the equivalence ratio at the same value. Regarding power consumption for raw materials (VW and FL), the lower gas yield and differences in the gas composition led to less unconverted syngas and fuel gas for turbines in the power generation area. Thus, VW and FL scenarios generated around 66 MW and the torrefied samples (VW-LT and FL320) ranged between 67-71 MW.

These results follow logical trends according to the process conditions. The excess of electricity was sold to grid, resulting in higher electricity sales for VW-LT (22 MW) and FL (19 MW) scenarios.

Table 8.8 Main plant process and economic results

Scenario	**VW**	**VW-LT**	**FL**	**FL320**
Fuel output ($t_{liquid\ fuels}$/d)	265	268	259	261
Power usage (MW)	48.0	49.5	47.1	50.7
Power generated (MW)	65.6	71.4	66.5	67.2
Total installed equipment cost (M€)	281	283	286	284
Total capital investment (M€)	599	606	611	606
Product Value (€/$t_{liquid\ fuels}$)	1697	1680	1178	1164
Product Value (€/$L_{gasoline\ equivalent}$)	1.25	1.24	0.87	0.86

The installed equipment cost (TIEC) was > 280 M€ for all scenarios, especially with higher equipment expenditure in SRFs scenarios due to more conservative assumptions (section 8.2.2.1). Along with the raise of TIEC, total capital investment (TCI) as well increased. TCI for VW and VW-LT scenarios were 599 and 606 M€ meanwhile FL and FL320 scenarios accounted for 611 and 606 M€, respectively. In the case of torrefied biomass plant, the implementation of torrefaction increased the TIEC, although with SRFs was the opposite. The torrefaction of the gasification feedstock improved significantly the gas quality resulting in a less problematic upgrading through FT synthesis. This can be observed in the breakdown of costs by area shown in Table 8.9. Syngas cleaning (A300) and FT synthesis (A400) contributed to about 15 and 25% of installed cost, respectively. Therefore an strategy leading to a process optimization and costs reduction should be focused on these particular areas. As well, the power generation isle (A700) was responsible of more than 20% of final cost, mainly due to the purchase cost of compressors. This was the case for syngas booster compressor in A400 and compressors for both air and oxygen in A600. The other units (A100, A200 and A500) accounted less than 10% and BOP was assumed to be 11%. Table 8.9 also includes the breakdown costs for TCI.

Figure 8.3 depicts the breakdown of annual operating costs for biomass and SRFs scenarios.

Table 8.9 Capital investment breakdown costs for plant scenarios

Area	VW		VW-LT		FL		FL320	
	M€	%	M€	%	M€	%	M€	%
Area 100: Pretreatment	22	8	23	8	21	7	24	8
Area 200: Gasification	18	6	18	6	18	6	17	6
Area 300: Syngas cleaning	45	16	41	14	43	15	44	16
Area 400: FT synthesis	72	26	73	26	74	26	65	23
Area 500: Hydroprocessing	17	6	17	6	17	6	17	6
Area 600: Air separation unit	16	6	17	6	22	8	24	8
Area 700: Power generation	60	21	63	22	60	21	61	21
Balance of plant (BOP)	31	11	31	11	31	11	31	11
Total installed cost (TIC)	281		283		286		284	
Indirect cost (IC)	147		149		149		148	
Total direct and indirect costs (TDIC)	427		432		435		432	
Contingency	85		86		87		86	
Fixed capital investment (FCI)	513		519		522		518	
Working capital (WC)	77		78		78		78	
Land use	10		10		10		10	
Total capital investment (TCI)	599		606		611		606	

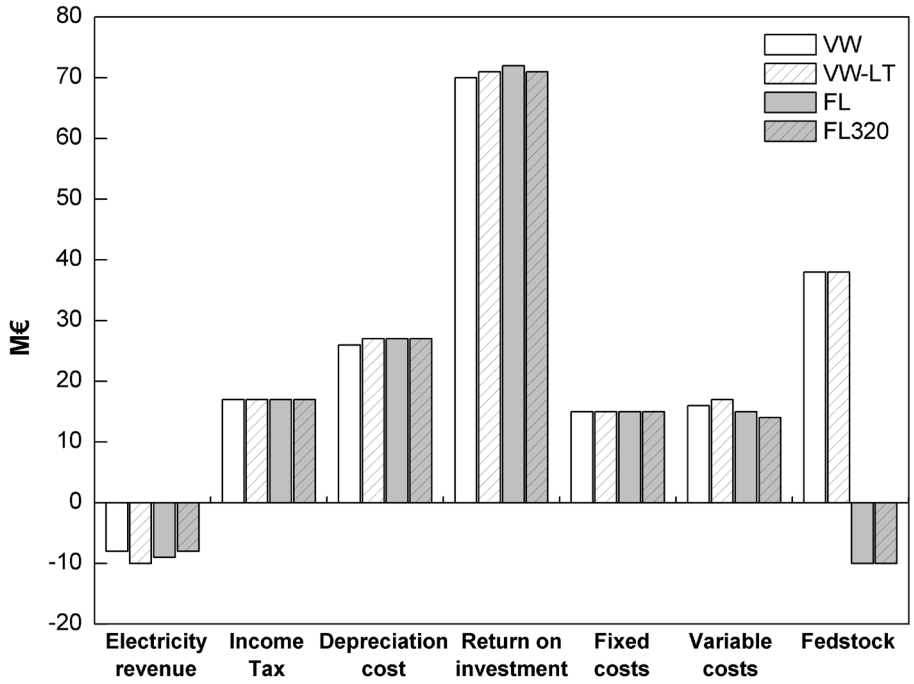

Figure 8.3 Annual operating costs (in million €2015) for biomass and SRF scenarios

Economic parameters (return on investment, income tax or capital depreciation) proved to have the largest impact on the annualized capital costs. Particularly, return on investment (ROI) was the largest contributor (> 70 M€). Those economic parameters were consequently higher in the scenarios with

higher capital expenditures (VW-LT and FL). Apart from ROI, the feedstock cost contributed significantly in biomass scenarios (about 38 M€). The difference when dealing with waste was that the feedstock cost is assumed to generate revenue for treating waste. Revenues are shown as negative entries in the chart, for instance the income for SRF feedstocks (FL and FL320) was estimated to be 10 M€. Electricity revenues were generated by selling the surplus electricity from A700, resulting in an income of about 9 M€ for all scenarios. Variable costs were slightly higher in VW-LT and FL scenarios ascribed to the higher steam flow rates and catalyst use.

Based on annual investment costs and revenues, the fuel product value (PV) was estimated for the plant scenarios as shown in Table 8.8. The PV was slightly lower for torrefied biomass (1683 €/t) compared to raw biomass (1700 €/t). In terms of annual production in liters of gasoline equivalent, the values would be around 1.25 €/L for both scenarios. The FL and FL320 scenarios reflected lower product prices. The PV was 1181 €/t (0.87 €/L) for FL and 1167 €/t (0.86 €/L) for FL320 scenario.

8.3.3 Sensitivity analysis results

Figures 8.4-8.5 illustrate the sensitivity of the product value (PV) according to the studied parameters in Table 8.7 in the order of favourable, baseline, and unfavourable. In the charts the PV is presented in € (adjusted in the year 2015) per tonnes of FT fuels (diesel and gasoline) produced annually.

The results show that the PV ranged between 1327-2104 €/t (0.98-1.55 €/liter gasoline equivalent) for biomass scenarios (Figure 8.4) and between 803-1604 €/t (0.59-1.18 €/liter gasoline equivalent) for SRF scenarios (Figure 8.5). The most sensitive parameters for all scenarios were the discount rate (DR) and total capital investment (TCI). The economic parameters had a strong influence in the PV as they affect the cash flow (in this study the calculation of the breakeven price). As commented in the previous section, the return on investment (ROI) represented a significant amount of the annual operating costs, and ROI was affected by both DR and TCI parameters. TCI influenced the calculation of ROI, depreciation cost (DC) and income tax (IT). It should be noted that DR depended on several external factors (i.e. fluctuation of the market and directives) but TCI could be reduced by an optimization of the

plant, the choice of optimal operating conditions and an accurate economic assessment.

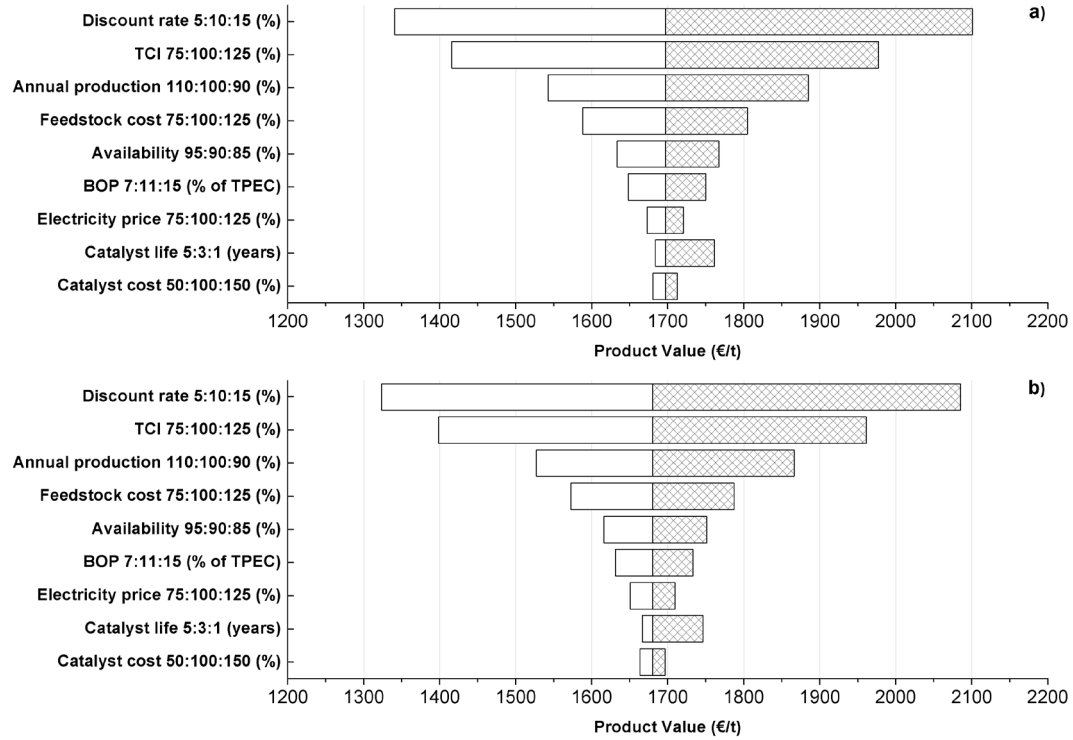

Figure 8.4 PV sensitivity analysis for the scenarios: a) VW and b) VW-LT

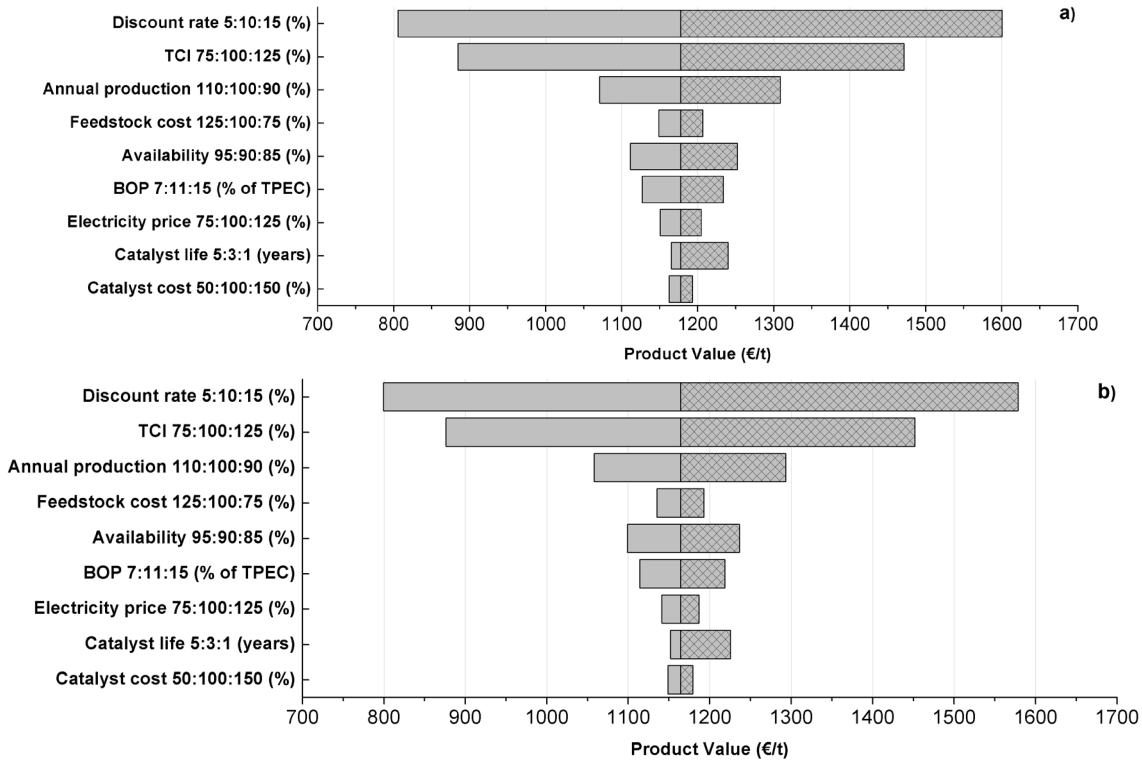

Figure 8.5 PV sensitivity analysis for the scenarios: a) FL and b) FL320

For biomass scenarios (Figure 8.4a and 8.4b), the DR varied the PV in a range of ±380 €/t (±0.28 €/L) meanwhile for SRFs (Figures 8.5a and 8.5b) the range was slightly larger ±394 €/t (±0.29 €/L). When the TCI was varied (reduction or increase of 25% to the baseline value) the PV range was ±281 €/t for biomass scenarios and ±291 €/t for SRF scenarios which corresponded to approximately ±0.21 €/L for all scenarios. Therefore, DR and TCI changed the PV in a range of 0.21-0.29 €/L. The PV proved to be sensitive to the total annual production. The variation of the fuel yield (±10%) influenced the PV in a range of ±171 €/t and ±119€/t for biomass and SRF scenarios, respectively (or ±0.13 €/L and ±0.09 €/L, respectively). In the case of biomass scenarios, the feedstock cost represented a significant portion of the annual operating costs and therefore was another important contributor. When the biomass cost varied between 43 and 72 € per dry tonne purchased, the PV showed a variation of ±108 €/t (±0.08 €/L). However, in SRF scenarios the purchase cost was considered negative (as an income) and ranged between -18.75 and -11.75 € per dry tonne. Thus, the PV just varied ±29 €/t (±0.02 €/L), being one of the parameters with lower influence in the PV. These parameters included the electricity price, catalyst life and catalyst cost, which affected the PV less than ±70€/tonne or ±0.08 €/L for all scenarios. Nonetheless, the PV increased significantly when the catalyst life was reduced to 1 year rather than replacing the catalyst in 5 years. For these reasons, there was room to utilise a more expensive and effective catalyst to improve the fuel yield and subsequently decrease the fuel PV.

8.3.4 Comparison to other studies

Table 8.10 gathers previous techno-economic studies for biofuel production through FT synthesis. The fuel prices remain in the original monetary units (some authors have not specified the year of the currency for conversion) but the results were also presented in terms of liters per gasoline equivalent. The fuel cost based on biomass gasification would range between 0.20-1.30 €/liter of gasoline equivalent. Note that these numbers depend on several assumptions such as plant capacity, technology and feed-to-fuel efficiency. Additionally the steep escalation of plant and inflation were responsible for the cost differences. This study shows higher capital investment and fuel costs than other studies

due to more conservative assumptions such as higher contingency (20% instead of 10-15%) or a lower fuel product distribution. However the presented fuel cost from biomass scenarios (1.25€/L) fitted in the range of those reported by other authors. In contrast, economical assessments for waste-to-liquids based on gasification have not been reported yet as MSW gasification plants are still being developed [15,16]. Nevertheless, there are TEA about waste-to-energy, including waste incineration and gasification [16,21–23], generation of biogas for combined heat and power (CHP), biogas for transport fuels [23] and electricity production [15,22]. The studies showed promising results but the viability of these facilities is still limited and restricted to waste regulations and strategies, such as incentives from governments to produce energy from renewable sources. Moreover, further process improvements are required to reduce high capital costs associated to waste-to-energy technologies.

Table 8.10 Capital costs for BTL plants based on gasification and FT synthesis

Feedstock	**Size/Technology**	**TCI**	**Fuel cost**	**Reference**
Corn stover	2000 dry t/d input (389 MWth input)	498M$$_{2007}$$	4.83 $$_{2007}$$/GGE. (1.28 $$_{2007}$$/$$L_{gasoline\ equivalent}$$)	[9]
Forest residues	2000 dry t/d input (RENUGAS-based plant)	-	1.53 $/kg (1.22 $/$L_{diesel}$ or 1.39 $/$L_{gasoline\ equiv.}$)	[10]
Forest residues	2000 dry t/d input (SilvaGas-based plant)	-	0.97 $/kg (0.77 $/$L_{diesel}$ or 0.88 $/$L_{gasoline\ equiv.}$)	[10]
Woody biomass	50-8500 MWth input	1800 M$ for 34000 bbld BTL plant (52000 $/bbld)	1.1-0.55€/L_{diesel} (1.25-0.63 €/$L_{gasoline\ equivalent}$)	[8]
Willow wood	400 $MWth_{HHV}$ input	286 M€	16 €/GJ_{HHV} (0.69 €/$L_{gasoline\ equiv.\ HHV}$	[12]
Switchgrass	60 Mgal/year (or 227 Mliters/year)	216 M$	0.71$/gallon diesel (or 0.19$/$L_{gasoline\ equivalent}$)	[11]

GGE= gallon of gasoline equivalent; bbld=barrels oil per day

Note that the methodology presented in this economic assessment resulted in conservative results but led to promising figures for biomass and waste to liquids fuel production plant. Although this TEA was performed for a *n*th plant,

a pioneer plant (first-of-its-kind plant) would have higher investment costs. Swanson et al. [9] concluded that capital costs in a pioneer plant could increase about 120% whereas PV might increase by approximately 60-90%. Nevertheless, the final costs could potentially decrease by applying a more detailed economic assessment together with the optimization of both process and simulation model.

8.4 Conclusions

This study presents the economic assessment of liquid fuel plants based on four gasification scenarios. These scenarios included gasification of two woody biomasses and two solid recovered fuels (SRFs) derived from municipal waste. An interesting point of this work is the integration of torrefaction in the pretreatment stage and their consequences in both gasification performance and economic analysis. Literature data and an Aspen simulation model were used for the plant cost analysis.

This study estimated the capital and operating costs together with the fuel product value (PV) of biomass- and waste-to-liquids plants. All scenarios showed capital costs close to 600 M€$_{2015}$ for a feedstock input of 2000 dry tonnes/day. SRF gasification scenarios presented higher capital costs (> 610 M€$_{2015}$) compared to biomass-to-liquid plants. However total costs could be reduced to values comparable to biomass scenarios when integrating torrefaction as pretreatment. Torrefaction is assumed to improve gasification performance and produce a cleaner gas to be used in the Fischer-Tropsch synthesis, especially when dealing with SRFs. Plant scenarios combining torrefaction are expected to produce not only higher amount of liquid fuel (diesel and gasoline) but also higher electricity surplus which would reduce the fuel PV. For biomass scenarios the fuel PV was estimated to be 1700 €/tonnes of liquid fuels (1.25 €/liter of gasoline equivalent) whereas for SRF scenarios the PV decreased to 1200 €/t (0.87 €/L). Note that these are conservative results which might not be directly comparable due to differences in the operational conditions and other assumptions. For this reason a sensitivity analysis was performed to show the most influential parameters on PV. Economic parameters (i.e discount rate and total capital investment) were the largest contributors to the fuel PV. Other key factors affecting the PV were the plant efficiency (i.e. annual fuel

production) and the feedstock price. On the other hand, catalyst cost proved to affect PV in a lesser extent, offering the opportunity to use more expensive and effective catalysts in the process. In general, fuel PV would range between 1320-2100 €/t (0.98-1.55 €/L) for biomass scenarios and between 800-1600 €/t (0.59-1.18 €/L) for SRF scenarios. Despite the complexity of dealing with waste in a FT liquids plant, final fuel costs could be less expensive in SRF scenarios compared to biomass scenarios due to the negative cost of these feedstocks, which is a primary source of revenues. However, further studies are required to optimize the process in waste-to-liquid plants, including waste regulations and technological improvements that could decrease the final costs.

Nomenclature

ASU	Air separation unit
BOP	Balance of plant
BTL	Biomass-to-liquid
CHP	Combined heat and power
DC	Depreciation cost
ER	Equivalence ratio
ESR	Electricity sales revenue
FL	Fluff (a SRF sample)
FL320	FL torrefied at 320 ºC
FSR	Fuel sales revenue
FT	Fischer-Tropsch
HHV	Higher heating value
IC	Indirect cost
IT	Income tax
LHV	Lower heating value
MSW	Municipal solid waste
PL	Plant life
PSA	Pressure swing adsorption
PV	Product value
ROI	Return on investment

SMR	Steam methane reforming
SRF	Solid recovered fuel
TCI	Total capital investment
TDIC	Total direct and indirect costs
TEA	Techno-economic assessment
TIEC	Total installed equipment cost
TPEC	Total purchased equipment cost
TR	Tax rate
VW	VW (a biomass sample)
VW-LT	VW lightly torrefied at 225 ºC
WC	Working capital
WGS	Water gas shift
WTE	Waste-to-energy
WTL	Waste-to-liquid

8.5 References

[1] Tunå P, Hulteberg C. Woody biomass-based transportation fuels - A comparative techno-economic study. Fuel 2014;117:1020–6. doi:10.1016/j.fuel.2013.10.019.

[2] Tijmensen MJ a, Faaij a. PC, Hamelinck CN, Van Hardeveld MRM. Exploration of the possibilities for production of Fischer Tropsch liquids and power via biomass gasification. Biomass and Bioenergy 2002;23:129–52. doi:10.1016/S0961-9534(02)00037-5.

[3] Hanaoka T, Inoue S, Uno S, Ogi T, Minowa T. Effect of woody biomass components on air-steam gasification. Biomass and Bioenergy 2005;28:69–76. doi:10.1016/j.biombioe.2004.03.008.

[4] van Vliet OPR, Faaij APC, Turkenburg WC. Fischer-Tropsch diesel production in a well-to-wheel perspective: A carbon, energy flow and cost analysis. Energy Convers Manag 2009;50:855–76. doi:10.1016/j.enconman.2009.01.008.

[5] Rafati M, Wang L, Dayton DC, Schimmel K, Kabadi V, Shahbazi A. Techno-economic analysis of production of Fischer-Tropsch liquids via biomass gasification: The effects of Fischer-Tropsch catalysts and natural gas co-feeding. Energy Convers Manag 2017;133:153–66. doi:10.1016/j.enconman.2016.11.051.

[6] Sudiro M, Bertucco A. Production of synthetic gasoline and diesel fuel by alternative processes using natural gas and coal: Process simulation and optimization. Energy 2009;34:2206–14. doi:10.1016/j.energy.2008.12.009.

[7] Steynberg AP, Nel HG. Clean coal conversion options using Fischer-Tropsch technology. Fuel 2004;83:765–70. doi:10.1016/j.fuel.2003.09.023.

[8] Boerrigter H. Economy of Biomass-to-Liquids (BTL) plants An engineering assessment 2006:29.

[9] Swanson RM, Platon A, Satrio JA, Brown RC. Techno-economic analysis of biomass-to-liquids production based on gasification. Fuel 2010;89:S11–9. doi:10.1016/j.fuel.2010.07.027.

[10] Sarkar S, Kumar A, Sultana A. Biofuels and biochemicals production from forest biomass in Western Canada. Energy 2011;36:6251–62. doi:10.1016/j.energy.2011.07.024.

[11] Martín M, Grossmann IE. Process optimization of FT-diesel production from lignocellulosic switchgrass. Ind Eng Chem Res 2011;50:13485–99. doi:10.1021/ie201261t.

[12] Hamelinck CN, Faaij APC, den Uil H, Boerrigter H. Production of FT transportation fuels from biomass; technical options, process analysis and optimisation, and development potential. Energy 2004;29:1743–71. doi:10.1016/j.energy.2004.01.002.

[13] Recari J, Berrueco C, Abelló S, Montané D, Farriol X. Gasification of two solid recovered fuels (SRFs) in a lab-scale fluidized bed reactor: Influence of experimental conditions on process performance and release of HCl, H2S, HCN and NH3. Fuel Process Technol 2016;142:107–14. doi:10.1016/j.fuproc.2015.10.006.

[14] Tabasová A, Kropáč J, Kermes V, Nemet A, Stehlík P. Wast e-to-energy technologies: Impact on environment. Energy 2012;44:146–55. doi:10.1016/j.energy.2012.01.014.

[15] Luz FC, Rocha MH, Lora EES, Venturini OJ, Andrade RV, Leme MMV, et al. Techno-economic analysis of municipal solid waste gasification for electricity generation in Brazil. Energy Convers Manag 2015;103:321–37. doi:10.1016/j.enconman.2015.06.074.

[16] Arafat H a., Jijakli K. Modeling and comparative assessment of municipal solid waste gasification for energy production. Waste Manag 2013;33:1704–13. doi:10.1016/j.wasman.2013.04.008.

[17] Couto N, Silva V, Rouboa A. Municipal solid waste gasification in semi-industrial conditions using air-CO2 mixtures. Energy 2016;104:42–52. doi:10.1016/j.energy.2016.03.088.

[18] Campoy M, Gómez-Barea A, Ollero P, Nilsson S. Gasification of wastes in a pilot fluidized bed gasifier. Fuel Process Technol 2014;121:63–9. doi:10.1016/j.fuproc.2013.12.019.

[19] Luo S, Zhou Y, Yi C. Syngas production by catalytic steam gasification of municipal solid waste in fixed-bed reactor. Energy 2012;44:391–5. doi:10.1016/j.energy.2012.06.016.

[20] Berrueco C, Recari J, Abelló S, Farriol X, Montané D. Experimental investigation of solid recovered fuel (SRF) gasification: Effect of temperature and

equivalence ratio on process performance and release of minor contaminants. Energy & Fuels 2015;29:7419–27. doi:10.1021/acs.energyfuels.5b02032.

[21] Arena U, Di Gregorio F, Amorese C, Mastellone ML. A techno-economic comparison of fluidized bed gasification of two mixed plastic wastes. Waste Manag 2011;31:1494–504. doi:10.1016/j.wasman.2011.02.004.

[22] Yassin L, Lettieri P, Simons SJR, Germanà A. Techno-economic performance of energy-from-waste fluidized bed combustion and gasification processes in the UK context. Chem Eng J 2009;146:315–27. doi:10.1016/j.cej.2008.06.014.

[23] Murphy JD, McKeogh E. Technical, economic and environmental analysis of energy production from municipal solid waste. Renew Energy 2004;29:1043–57. doi:10.1016/j.renene.2003.12.002.

[24] Berrueco C, Recari J, Güell BM, Alamo G Del. Pressurized gasification of torrefied woody biomass in a lab scale fluidized bed. Energy 2014;70:68–78. doi:10.1016/j.energy.2014.03.087.

[25] Recari J, Berrueco C, Abelló S, Montané D, Farriol X. Effect of bed material on oxygen/steam gasification of two solid recovered fuels (SRFs) in a bench-scale fluidized bed reactor. Energy & Fuels 2017. doi:Submitted to journal/Unpublished results.

[26] Recari J, Berrueco C, Puy N, Alier S, Bartrolí J, Farriol X. Torrefaction of a solid recovered fuel (SRF) to improve the fuel properties for gasification processes. Appl Energy 2017. doi:Submitted to journal/Unpublished results.

[27] Swanson RM, Satrio JA, Brown RC, Platon A, Hsu DD. Techno-Economic Analysis of Biofuels Production Based on Gasification. 2010.

[28] Li Q, Zhang Y, Hu G. Techno-economic analysis of advanced biofuel production based on bio-oil gasification. Bioresour Technol 2015;191:88–96. doi:10.1016/j.biortech.2015.05.002.

[29] Doherty W, Reynolds a., Kennedy D. Aspen plus simulation of biomass gasification in a steam blown dual fluidised bed. Mater Process Energy 2013:212–20.

[30] Meng X, de Jong W, Fu N, Verkooijen AHM. Biomass gasification in a 100 kWth steam-oxygen blown circulating fluidized bed gasifier: Effects of operational conditions on product gas distribution and tar formation. Biomass and Bioenergy 2011;35:2910–24. doi:10.1016/j.biombioe.2011.03.028.

[31] Shehzad A, Bashir MJK, Sethupathi S. System analysis for synthesis gas (syngas) production in Pakistan from municipal solid waste gasification using a circulating fluidized bed gasifier. Renew Sustain Energy Rev 2016;60:1302–11. doi:10.1016/j.rser.2016.03.042.

[32] Carvalho L, Furusjö E, Kirtania K, Lundgren J, Anheden M, Wolf J. Techno-economic assessment of catalytic gasification of biomass powders for methanol production. 1st Int Conf Bioresour Technol Bioenergy, Bioprod Environ Sustain Sitges, Spain, 23-26 Oct 2016. doi:10.1016/j.biortech.2017.02.019.

[33] Rafiee A, Hillestad M. Techno-Economic Analysis of a Gas-to-Liquid Process with Different Placements of a CO2 Removal Unit. Chem Eng Technol 2012;35:420–30. doi:10.1002/ceat.201100418.

[34] Peters MS, Timmerhaus KO, West RE. Plant design and economics for chemical engineers. Boston [U.a.]: McGraw-Hill; 2003.

[35] Swanson RM, Satrio JA, Brown RC, Platon A, Hsu DD. Techno-Economic Analysis of Biofuels Production Based on Gasification. Golden, CO: National Renewable Energy Laboratory. Technical Report; 2010.

[36] Chemical Engineering Magazine n.d. http://www.chemengonline.com.

[37] Wright MM, Daugaard DE, Satrio JA, Brown RC. Techno-economic analysis of biomass fast pyrolysis to transportation fuels. Fuel 2010;89:S2–10. doi:10.1016/j.fuel.2010.07.029.

[38] Zhang Y, Brown TR, Hu G, Brown RC. Comparative techno-economic analysis of biohydrogen production via bio-oil gasification and bio-oil reforming. Biomass and Bioenergy 2013;51:99–108. doi:10.1016/j.biombioe.2013.01.013.

[39] Mani S, Tabil LG, Sokhansanj S. Grinding performance and physical properties of wheat and barley straws, corn stover and switchgrass. Biomass and Bioenergy 2004;27:339–52. doi:10.1016/j.biombioe.2004.03.007.

[40] Sermyagina E, Saari J, Kaikko J, Vakkilainen E. Integration of torrefaction and CHP plant: Operational and economic analysis. Appl Energy 2016;183:88–99. doi:10.1016/j.apenergy.2016.08.151.

Chapter 8

9. CONCLUSIONS AND FUTURE WORK

9.1 General conclusions

This doctoral thesis focuses on the **improvement of the synthesis gas for the production of liquid fuels** with a lower carbon footprint from the gasification of biomass and waste-derived fuels. One of the main challenges to overcome in gasification is the presence of contaminants in the syngas that must be reduced to certain limits before its use, especially in catalytic processes that converts the syngas into a wide range of chemicals and fuels such as ethanol, methanol, diesel, gasoline and olefins.

The completion of this work has provided insight into the **influence of torrefaction during gasification of biomass and solid recovered fuels (SRFs) and other key operating parameters** including gasification temperature, gasification agents and bed materials on gas composition of waste gasification. The information here reported can be useful for further development of gasification strategies, selecting adequate gasification conditions and combining torrefaction as pretreatment in order to reduce the emission of contaminants in the syngas. The production of a cleaner gas will improve the gasification performance and facilitate the syngas upgrading.

Torrefaction is known to be an effective pretreatment for upgrading the biomass properties, increasing the energy density of the feedstock, however the effect of torrefaction level during gasification has not been intensively studied. The influence of torrefaction level (225 ºC and 275 ºC) and pressure (1-10 bar) on biomass gasification was assessed in a laboratory-scale bubbling fluidized bed reactor. Two different sorts of woody biomasses were used as feedstocks for torrefaction and gasification. **Gasification tests of torrefied biomasses pointed out gas quality improvements** such as: an **increase of gas conversion**, higher H_2 yield, and a **significant reduction of tar concentration** about 3 times compared to non-torrefied biomass gasification. Differences on gasification performance among both torrefaction levels were not extremely relevant, however the higher the torrefaction severity, the lower unwanted products in the gas. Furthermore, the effect of pressurized gasification

was evaluated on product yields and composition. Pressure rose not only gas yield but also tar. **Contrary to torrefaction, pressure diminished gas quality** by decreasing both H_2 and CO levels and increasing tar concentration in the producer gas, which could be related to tar polymerization towards heavier aromatic compounds as stated after analysing the obtained tar samples. For further details of this work see Chapter 3.

Taking into account the adaptability of gasification and the seek of potential feedstocks for liquid fuels production, waste fractions derived from MSW was considered a possible resource. Nonetheless, waste-derived fuels such as SRFs are complex gasification feedstocks due to their heterogeneity and the higher contents of contaminants precursors that presumably will be released in the syngas. For this reason the **selection of adequate gasification conditions is decisive in waste gasification**. In this work, key gasification parameters such as temperature, equivalence ratio (ER), bed materials and gasification agents were studied, evaluating their influence on process performance and syngas composition from gasification of two supplied SRFs (namely RT and FL). To evaluate the concentration of expected minor contaminants in the syngas (i.e. HCl, H_2S, NH_3 and HCN), an analytical method by ion-selective potentiometry was developed (see Chapter 2, section 2.4.2.2). **Gasification results with a SRF stated that appropriate gasification conditions to reduce contaminants were relatively high temperatures (800-850 ºC) and ER ranging between 0.30-0.35**. Further details can be found in Chapter 4, section 4.3.

The suggested operating conditions (T=850 ºC and ER ~0.3) were corroborated with the gasification of an additional SRF and a catalytic bed material. **Air gasification of both SRFs indicated that higher temperatures (850 ºC) and the use of dolomite as bed material could improve the gasification performance** by increasing gas yield and carbon conversion. **Tar and minor contaminants content in the product gas significantly decreased under these conditions** leading to tar levels closer to those typically reported in biomass gasification (see Table 1.6 in Chapter 1), whereas HCl was the dominant minor contaminant (close to 100 mg/Nm^3). The shift of gasification agent from air to a mixture of oxygen and steam was initially tested with one SRF in order to enhance the gas production and reduce

tar content. However, despite the improvement of the gasification performance due to the promotion of steam gasification reactions, the concentration of minor contaminants showed a remarkable increment with levels around 300 mg/Nm^3 for HCl and HCN, and the detection of H_2S and NH_3 (below 50 mg/Nm^3); concluding that additional work was necessary under these conditions to fully understand the effect of this gasification agent. Chapter 5, section 5.3, provides the results of this research.

In Chapter 6, the **oxygen-steam gasification of SRFs was further investigated** focusing on the evolution of gas composition under the effect of common bed materials (sand, dolomite and olivine). The concentration of syngas compounds increased compared to experiments with air ascribed to the absence of nitrogen in the gasification agent. A clear depletion of tar and most of minor contaminants was observed with dolomite as bed material rather than with olivine. Collected tar samples were analysed for the quantification of aromatic hydrocarbons (i.e. PAHs). **Dolomite reduced tar content** by 50% and decreased the content of PAHs with more than 2-rings. On the other hand, **olivine hardly diminished tar**, **leading to similar tar levels as those obtained with sand** as bed material, although olivine was active on cracking naphthalene. In contrast to the preliminary investigation of oxygen-steam gasification in Chapter 5, the determination of minor contaminants under oxygen-steam conditions was improved by taking into account the condensed water during syngas cleaning, which retained NH_3 and HCl. The results pointed out that not only **both the fuel and ash composition played a major role in the release of minor contaminants** but also **the influence of catalysts was a key aspect**. Dolomite decreased most of minor contaminants at expense of NH_3 whereas olivine mostly decreased nitrogenous compounds (HCN and NH_3).

Apart from the change of gasification parameters such as gasification agents and bed materials, another strategy to improve the gasification performance of waste-derived fuels could be the application of a torrefaction as proved with biomass feedstocks in Chapter 3. With this purpose, in Chapter 7, **two torrefaction levels (290 and 320 ºC) were applied to a SRF** and the gasification of torrefied SRFs was studied under air and oxygen-steam conditions with different bed materials (sand, dolomite and olivine). **The**

thermal pretreatment within that range claimed to improve some of fuel properties for gasification, resulting in a **higher production of syngas with lower amounts of tar** compounds. Besides, this study allowed the comparison of gasification tests with torrefied and not pretreated SRFs. Concerning minor contaminants formation in the syngas, HCl content was abruptly diminished from > 5000 mg/Nm^3 for oxygen-steam gasification of parent SRF to values below 450 mg/Nm^3 for both torrefied SRFs. Although the concentration of other minor contaminants seemed to rise, this **significant reduction of HCl would imply less problems during operation of industrial gasification plants** mainly due to the reduction of risk of corrosion and catalyst deactivation. According to the results showed in section 7.3, gasification of **torrefied feedstocks would be recommended selecting oxygen-steam and dolomite as gasification agent and bed material**, respectively.

The experimental part of this thesis provided insights into the most adequate conditions for improving the syngas quality from gasification of biomass and SRFs. Consequently, the **experimental results of this thesis were the foundations for the development of a techno-economic study** (Chapter 8) of four Fischer-Tropsch liquid fuel plants based on gasification of biomass and SRF samples with a capacity of 2000 dry tonnes/day. The novelty lies in the integration of torrefaction as the pretreatment stage in the gasification process and the use of waste feedstocks. Literature data and Aspen simulation results were used to estimate capital and production costs. Despite the high capital investment for the evaluated plants (about 600 M€$_{2015}$), the figures showed **promising results when considering the combination of torrefaction and gasification**. **The product value of liquid fuels would be around 1700 €/t for biomass scenarios and 1200 €/t for SRF scenarios.** These values could be in the same order as current diesel and gasoline prices for final users in Europe. **Costs for liquid fuels from waste gasification were cheaper** than biomass-based fuels due to the negative cost paid for these feedstocks in waste processing facilities. In line with this, the sensitivity analysis of the study evidences that **economic parameters** (i.e. discount rate and total capital investment) **are key drivers when encouraging the production of liquid fuels** from renewables, in particular

from waste-derived fuels. Therefore **this work suggests that waste gasification would be a feasible route to produce liquid fuels**, provided that policy makers and competent authorities promote the exploitation of waste residues and further research in this line is carried out. More details of the obtained results are included in Chapter 8, section 8.3.

9.2 Future work

Based on the results obtained in this work a number of possible research lines are suggested:

- The application of torrefaction as a pretreatment for waste-derived fuels is promising and should be explored with additional feedstocks. The reduction of heavy metals, the preservation of most of the feedstock energy content and the energy integration between the torrefaction and gasification processes could be possible aspects to explorer. Future work should be also focused on release of volatiles during waste torrefaction. The results would be useful for explaining the evolution of minor contaminants (H_2S, HCl, HCN and NH_3).

- Further research is needed for fully understand the release of minor contaminants during gasification of heterogeneous feedstocks like waste-derived fuels. This information will be useful for the development of mechanisms that predict the evolution of contaminants according to waste composition and gasification conditions.

- An exhaustive economic study considering several gasification conditions would be necessary. For instance the use of air instead of oxygen-steam. This evaluation would be interesting as it could lead to reduction costs ascribed to the removal of the air separation unit. Furthermore, an optimization of the combined process (torrefaction and gasification) would potentially improve the whole process and hence the final costs for liquid fuels production. The integration of energy balances and detailed simulation should be explored in this domain.

Chapter 9

10. APPENDIX

10.1 Research articles

- Berrueco C, Recari J, Güell BM, Alamo G Del. Pressurized gasification of torrefied woody biomass in a lab scale fluidized bed. Energy 2014;70:68–78. doi:10.1016/j.energy.2014.03.087.
- Recari J, Berrueco C, Abelló S, Montané D, Farriol X. Effect of temperature and pressure on characteristics and reactivity of biomass-derived chars. Bioresour Technol 2014;170:204–10. doi:10.1016/j.biortech.2014.07.080.
- Berrueco C, Recari J, Abelló S, Farriol X, Montané D. Experimental Investigation of Solid Recovered Fuel (SRF) Gasification: Effect of Temperature and Equivalence Ratio on Process Performance and Release of Minor Contaminants. Energy & Fuels 2015;29:7419–27. doi:10.1021/acs.energyfuels.5b02032.
- Recari J, Berrueco C, Abelló S, Montané D, Farriol X. Gasification of two solid recovered fuels (SRFs) in a lab-scale fluidized bed reactor: Influence of experimental conditions on process performance and release of HCl, H2S, HCN and NH3. Fuel Process Technol 2016;142:107–14. doi:10.1016/j.fuproc.2015.10.006.
- Recari J, Berrueco C, Abelló S, Montané D, Farriol X. Effect of bed material on oxygen/steam gasification of two solid recovered fuels (SRFs) in a bench-scale fluidized bed reactor. Energy & Fuels n.d. doi:Submitted to journal.
- Recari J, Berrueco C, Puy N, Alier S, Bartrolí J, Farriol X. Torrefaction of a solid recovered fuel (SRF) to improve the fuel properties for gasification processes. Appl Energy n.d. doi:Submitted to journal
- Recari J, Berrueco C, Abelló S, Farriol X. Techno-economic assessment of Fischer-Tropsch liquid fuel production plants based on biomass and waste gasification. Energy Convers Manag n.d. doi:To be submitted.

10.2 Oral presentations

- J. Recari, C. Berrueco, D. Montané, X. Farriol, "Gasification of Solid Recovered Fuels in a Lab-Scale Fluidized Bed Reactor. Effect of Experimental Conditions on Process Performance and Syngas Quality", 23rd European Biomass Conference and Exhibition, EU BC&E 2015, Vienna, Austria, 1-4 June 2015.
- J. Recari, C. Berrueco, D. Montané, X. Farriol, "Gasification of solid recovered fuels: effect of experimental conditions on performance and syngas", 7th European Meeting on Chemical Industry and Environment, EMChIE-2015, Tarragona, Spain, 10-12 June 2015.

10.3 Poster presentations

- J. Recari, C. Berrueco, X. Farriol, "Improvement on the synthesis gas produced by thermal gasification of SRFs and biomass", 11th Doctoral Day, URV, Tarragona, Spain, 30th April 2014.
- J. Recari, C. Berrueco, S. Abelló, D. Montané, X. Farriol, "Production of char from woody biomass via pyrolysis: Effect of temperature and pressure", 22nd European Biomass Conference and Exhibition, EU BC&E 2014, Hamburg, Germany, 23rd-26th June 2014.
- J. Recari, C. Berrueco, X. Farriol, "Gasification of Solid Recovered Fuels (SRF): Effect of experimental conditions on performance and syngas quality", 11th Doctoral Day, URV, Tarragona, Spain, 20th May 2015.
- J. Recari, C. Berrueco, N. Puy, S. Alier, J. Bartrolí, X. Farriol, "Experimental investigation of torrefied Solid Recovered Fuel (SRF) gasification", 1st International Conference on Bioresource Technology for Bioenergy, Bioproducts & Environmental Sustainability, Biorestec, Sitges, Spain, 23rd-26th October 2016.